

Characterising Impaired Synaptic Plasticity and Network Function in a Mouse Model of Alzheimer's Disease in Down Syndrome

*A thesis submitted to University College London
for the degree of Doctor of Philosophy*

Amy Nick

*Department of Clinical and Experimental Epilepsy,
&
Department of Neurodegenerative Disease*

Institute of Neurology, University College London

2017

Declaration

I, Amy Nick, confirm that the work presented in this thesis is my own, and where information has been derived from other sources, I confirm that this has been indicated.

Abstract

Down syndrome (DS) results from an additional copy of human chromosome 21 (Hsa21). It is a leading cause of cognitive impairment, and hippocampal function appears to be specifically affected. Individuals with DS are at an elevated risk of childhood and late-onset seizure disorders, as well as early-onset Alzheimer's disease (AD). Duplication of the *APP* gene on Hsa21 is sufficient to cause early-onset AD in the absence of any other genetic abnormalities, but Hsa21 contains many other dosage-sensitive genes, and trisomy is associated with widespread transcriptional dysregulation. Therefore, other factors in addition to *APP* duplication are likely to modify the risk of AD and seizures in the DS population.

A double transgenic mouse model was used to investigate the interaction between trisomy of genes on Hsa21 and *APP* duplication. The Tc1 mouse model of DS contains a freely segregating copy of Hsa21, and is functionally trisomic for approximately 75% of Hsa21 genes, but critically, not for *APP*. This mouse model has been crossed with the J20 model of AD, which overexpresses mutant human *APP* (*APP_{Swe/Ind}*). Interactions between trisomy of Hsa21 and overexpressed *APP_{Swe/Ind}* have been shown to exacerbate cognitive deficits, and increase the risk of mortality in this model. The Dp1Tyb mouse model, which contains a duplication of the Hsa21 orthologous region of mouse chromosome 16 (Mmu16), was also investigated, in order to compare phenotypes across different models of DS.

Long-term potentiation (LTP) was recorded in the medial perforant pathway (MPP) of acute hippocampal slices. This pathway comprises the major input to the hippocampus and has been implicated in spatial memory. No changes in baseline synaptic transmission were observed in the Tc1, J20, or double transgenic mice, nor in the Dp1Tyb mice. Tc1 mice showed a deficit in stimulation induced LTP, but not chemical LTP. This deficit could not be

rescued by blocking GABA_AR-mediated inhibitory neurotransmission as has been reported previously in other DS models, suggesting a novel mechanism underlies the plasticity deficit observed in these animals. No deficits were observed in the J20 animals, and no interactions were observed between *APP_{Swe/Ind}* and trisomy of Hsa21. The exacerbation of cognitive deficits in these animals therefore does not appear result from greater impairment in synaptic plasticity in the MPP. Dp1tyb animals also showed a trend towards a deficit in LTP, although further data is required to determine the significance of this effect.

In addition, EEG was recorded from awake and freely moving animals from the Tc1 x J20 cross, and from Dp1Tyb animals and their wildtype littermates. Neither Tc1, nor Dp1tyb, animals experienced spontaneous seizures, and Hsa21 did not exacerbate seizures related to *APP* in J20 mice, suggesting changes in LTP and enhanced mortality were also not related to epileptic activity at 6-months of age. However, immunohistochemistry for NPY in Tc1 x J20 cross at 16-months of age indicates that Hsa21 may be associated with an exacerbation in seizures in later life.

Dedication

In memory of Laura Pulford

Your dedication to science and passion for life will always be an inspiration to all of us who has the privilege of working with you. This journey would not have been the adventure it was if you weren't part of it.

Acknowledgements

Firstly, I would like to thank my supervisors: Prof. Matthew Walker, Dr. Frances Wiseman, and Prof. Lizzy Fisher, for all their patience, guidance and support over the last 3 years.

I would also like to thank everyone in the Department of Clinical and Experimental Epilepsy, the Department of Neurodegenerative Disease, and the LonDownS Consortium. It has been a pleasure to work with you all.

Thanks in particular are due to Dr. Sue Noy for her expertise in histology; to Dr. Karen Cleverley and Matthew Rickman, for their assistance with imaging and genotyping; to Dr. Rob Wykes for his help with surgery and EEG analysis; and to Dr. Stephanie Schorge and Catherine Hills for all their hard work in setting up telemetry.

Further thanks are due to my colleagues and friends: Justin Tosh, Sophie Williams, Aytakin Khalil, Ramona Eckel, Eleonora Lugarà, Gareth Morris, Jenna Carpenter, Liz Nicholson, Claire King and Pishan Chang. I have been incredibly lucky to have the opportunity to work with you all. Thank you for the moral support and endless coffee. I would especially like to thank Xun Yu Choong; I would never have got this far without your help and support.

Outside of the lab, I would like to thank Ellie Andrews, Anna McEntire, Amy Dolan, Grant Lipszyc, Dee Norval, and Duo Zhang. Your friendship has been invaluable.

Most of all, I would like to thank my parents, Alison and Cecil, my sister Lisa, and my grandmother Bella, for all their encouragement and support.

Table of Contents

1	Introduction	18
1.1	Down syndrome	18
1.1.1	The Down syndrome phenotype	18
1.1.2	Genetics of Down syndrome.....	19
1.1.3	Mouse models of Down syndrome	21
1.1.4	Dosage sensitivity in Down syndrome	25
1.1.5	The ‘Down Syndrome Critical Region’	26
1.1.6	Transcriptional dysregulation in Down syndrome.....	28
1.1.7	Mechanisms of cognitive impairment in Down syndrome.....	30
1.2	Alzheimer’s disease.....	35
1.2.1	Pathophysiology of Alzheimer’s disease.....	35
1.2.2	The role of Amyloid- β in Alzheimer’s disease.....	36
1.2.3	Genetics of Alzheimer’s disease.....	38
1.2.4	The amyloid cascade hypothesis.....	40
1.2.5	Mouse models of Alzheimer’s disease.....	41
1.2.6	Synaptic dysfunction in Alzheimer’s disease.....	44
1.2.7	Genetic modifiers of Alzheimer’s disease in Down syndrome.....	48
1.2.8	Epilepsy in AD-DS	49
1.3	Modelling AD-DS phenotypes in mice	52
1.3.1	Hippocampal phenotypes in AD and DS	52
1.3.2	Long-term potentiation	53
1.3.3	Modelling hippocampal dysfunction in Down syndrome	55
1.3.4	Seizures in models of Alzheimer’s disease and Down syndrome.....	68
1.3.5	Tc1 \times J20 mouse cross.....	70
1.4	Thesis aims	73
1.4.1	Aims.....	73
1.4.2	Hypotheses.....	73
2	Materials and Methods.....	74
2.1	Animal husbandry	74
2.2	Hippocampal slice electrophysiology.....	75
2.2.1	Generation of isolated hippocampal slices	75
2.2.2	Solutions.....	77

2.2.3	Recording and stimulation.....	78
2.2.4	Analysis of LTP data.....	80
2.3	Electroencephalography.....	80
2.3.1	Implantation of subcutaneous EEG transmitters.....	80
2.3.2	EEG recording.....	83
2.3.3	Automated seizure detection.....	84
2.3.4	Power analysis.....	86
2.4	Histology.....	87
2.4.1	Perfusion for paraffin embedding.....	87
2.4.2	Tissue processing.....	87
2.4.3	IHC staining for NPY.....	88
2.4.4	Imaging and analysis of NPY immunohistochemistry.....	89
2.5	Genotyping.....	89
2.5.1	DNA extraction.....	89
2.5.2	PCR for Tc1 and J20.....	90
2.5.3	Genotyping for Dp1Tyb.....	91
2.6	Statistics.....	94
3	Synaptic function in AD-DS.....	95
3.1	Introduction.....	95
3.1.1	Synaptic transmission.....	95
3.1.2	The perforant path.....	96
3.1.3	The basis of extracellular postsynaptic field potentials.....	97
3.1.4	Paired pulse ratio and release probability.....	99
3.1.5	Synaptic dysfunction in models of AD-DS.....	101
3.2	Aims.....	102
3.3	Results.....	103
3.3.1	Baseline synaptic transmission in the Tc1 × J20 cross.....	103
3.3.2	Paired pulse ratio in the Tc1 × J20 cross.....	107
3.3.3Preliminary data on baseline synaptic transmission in the Dp1Tyb model.....	113
3.3.4	Paired pulse ratio in the Dp1Tyb model.....	116
3.4	Discussion.....	119
3.5	Conclusion.....	123
4	Synaptic plasticity in AD-DS.....	124
4.1	Introduction.....	124

4.1.1	Synaptic plasticity.....	124
4.1.2	Mechanisms underlying long-term potentiation	124
4.1.3	Post-tetanic potentiation	126
4.1.4	Mechanisms underlying long-term depression	127
4.1.5	Induction of LTP and LTD hippocampal slices.....	128
4.2	Aims.....	130
4.3	Results	131
4.3.1	Long-term potentiation in the Tc1 × J20 cross	131
4.3.2	Preliminary data on Long-term depression in the Tc1 × J20 cross	138
4.3.3	Preliminary data on LTP in the Dp1Tyb model at 6 months of age.....	144
4.4	Discussion	149
4.5	Conclusion.....	154
5	Mechanisms of impaired synaptic plasticity in AD-DS	155
5.1	Introduction	155
5.1.1	Impaired synaptic plasticity in DS and AD-DS	155
5.1.2	The role of inhibition in long-term potentiation.....	155
5.1.3	Inhibition in DS	157
5.1.4	Chemical LTP.....	161
5.2	Aims.....	162
5.3	Results	163
5.3.1	Blocking GABA _A Rs does not rescue LTP at 6 months of age in the Tc1 × J20 cross.....	163
5.3.2	Blocking GABA _A Rs has no effect on baseline synaptic transmission at 6 months of age	169
5.3.3	Preliminary data on the effect of PTX on LTP at 3 months of age in the Tc1 × J20 cross.....	171
5.3.4	Preliminary data on the effect of blocking GABA _A Rs on baseline synaptic transmission at 3 months of age.....	176
5.3.5	Chemical LTP in the Tc1 × J20 cross.....	178
5.4	Discussion	183
5.5	Conclusion.....	187
6	Synaptic plasticity and seizures in AD-DS.....	188
6.1	Introduction	188
6.1.1	Seizures in mouse models of AD and DS.....	188
6.1.2	The basis of EEG.....	189

6.1.3	EEG and seizures	191
6.1.4	Seizures and synaptic plasticity.....	191
6.1.5	Neuropeptide Y expression in epilepsy.....	195
6.1.6	Sudden death in epilepsy.....	196
6.2	Results	197
6.2.1	Frequency of seizures in the Tc1 × J20 cross.....	197
6.2.2	Interictal spikes in the Tc1 × J20 cross.....	199
6.2.3	Interictal spikes in the Dp1Tyb model	201
6.2.4	NPY staining at 6 months of age	201
6.2.5	NPY staining at 16 months of age	202
6.3	Power spectrum	205
6.4	Discussion	210
6.5	Conclusion.....	217
7	Discussion.....	218
7.1	Overview.....	218
7.2	Synaptic plasticity in AD-DS.....	219
7.3	Seizures in AD-DS	227
7.4	Modelling AD-DS	230
7.5	Conclusion.....	233

Table of Figures

Figure 1.1. <i>Nondisjunction in meiosis</i>	20
Figure 1.2 <i>Chromosome 21</i>	24
Figure 1.3 <i>Processing of APP via the amyloidogenic and non-amyloidogenic pathway</i>	37
Figure 1.4. <i>Tri-synaptic connectivity in a transverse section of the mouse hippocampus.</i>	52
Figure 1.5 <i>Illustration of the four genotypes produced by the Tc1×J20 cross</i>	70
Figure 1.6 <i>Aβ deposition in the Tc1×J20 cross</i>	71
Figure 1.7 <i>Behavioural phenotypes in the Tc1×J20 cross</i>	72
Figure 2.1 <i>Storage of slices</i>	76
Figure 2.2 <i>Location of recording and stimulation electrodes in the MPP</i>	77
Figure 2.3 <i>EEG transmitter implantation</i>	81
Figure 3.1 <i>Fibre volley</i>	98
Figure 3.2 <i>Input-output curves in the Tc1×J20 cross at 6 months of age</i>	105
Figure 3.3 <i>Example responses during input-output curves in the Tc1×J20 cross</i>	106
Figure 3.4 <i>Paired pulse ratio in the Tc1×J20 cross</i>	109
Figure 3.5 <i>Example traces showing paired pulse inhibition in the Tc1 × J20 cross</i>	112
Figure 3.6 <i>Paired pulse ratio in the Dp1Tyb model</i>	117
Figure 3.7 <i>Example traces showing paired pulse inhibition in the Dp1Tyb Model</i>	118
Figure 4.1 <i>LTP in the Tc1 × J20 cross</i>	134
Figure 4.2 <i>Paired pulse ratio during baseline, LTP and PTP in the Tc1×J20 cross</i>	135
Figure 4.3 <i>Example fEPSPs during LTP in the Tc1 × J20 cross</i>	136
Figure 4.4 <i>Superimposed average responses during tetanic stimulation</i>	137
Figure 4.5 <i>LTD in the Tc1 × J20 cross</i>	141
Figure 4.6 <i>Paired pulse ratio during baseline, LTD and STD in the Tc1×J20 cross</i>	142
Figure 4.7 <i>Example fEPSPs during LTD in the Tc1 × J20 cross</i>	143
Figure 4.8 <i>LTP in the MPP of the Dp1Tyb mice at 6 months of age</i>	146
Figure 5.1 <i>LTP following GABA_AR block in the MPP of the Tc1 × J20 cross at 6 months of age</i>	166
Figure 5.2 <i>Paired Pulse Ratio during LTP at 6 months of age with GABA_AR block</i>	167
Figure 5.3 <i>Examples of fEPSPs during LTP in the presence of PTX in the Tc1×J20 cross</i>	168
Figure 5.4 <i>Input-output curves following GABA_AR block in the MPP of the Tc1 × J20 cross at 6 months of age</i>	170

Figure 5.5 LTP following GABA _A R block in the MPP of the Tc1 × J20 cross at 3 months of age	173
Figure 5.6 Paired Pulse Ratio during LTP at 3-months of age with GABA _A R block.....	174
Figure 5.7 Examples of fEPSPs during LTP in the presence of PTX in the Tc1×J20 cross at 3 months of age.....	175
Figure 5.8 Input-output curves following GABA _A R block in the MPP of the Tc1 × J20 cross at 6 months of age.....	177
Figure 5.9 Chemical LTP in the MPP of the Tc1×J20 cross at 6 months of age	180
Figure 5.10 Paired Pulse Ratio during Chemical LTP.....	181
Figure 5.11 Examples of fEPSPs during Chemical LTP in the Tc1×J20 cross.....	182
Figure 5.12 Example outlying fEPSP from a wildtype animal.....	182
Figure 6.1 Examples of seizures from a J20 mice and a Tc1×J20 mouse	197
Figure 6.2 Seizures in the Tc1 × J20 cross.....	198
Figure 6.3 Examples of interictal activity taken from a Tc1×J20 mouse.....	199
Figure 6.4 Quantification of interictal spikes in the Tc1 × J20 cross.....	200
Figure 6.5 NPY immunoreactivity in the Tc1 × J20 cross at 6 months of age.....	202
Figure 6.6 NPY immunoreactivity in the Tc1 × J20 cross at 16 months of age	203
Figure 6.7 Normalised power spectrum across all EEG bands in the Tc1×J20 cross	206

Table of Tables

Table 1.1 <i>Examples of mouse models of DS</i>	62
Table 1.2 <i>Examples of mouse models of AD</i>	64
Table 1.3 <i>Hsa21 candidate genes implicated in neuronal dysfunction in DS</i>	65
Table 2.1 <i>Composition of aCSF</i>	78
Table 2.2 <i>Post-surgical outcomes</i>	83
Table 2.3 <i>NPY staining procedure (Provided by Dr. Susanna Noy)</i>	88
Table 2.4 <i>Solutions for DNA extraction</i>	90
Table 2.5 <i>PCR reaction</i>	92
Table 2.6 <i>Tc1 PCR Cycle</i>	92
Table 2.7 <i>J20 PCR Cycle</i>	92
Table 2.8 <i>Tc1 PCR Primers</i>	93
Table 2.9 <i>J20 PCR Primers</i>	93
Table 2.10 <i>Tc1 Primer Mix</i>	93
Table 2.11 <i>J20 Primer Mix</i>	93
Table 2.12 <i>qPCR primers and probes for Dp1Tyb</i>	93
Table 4.1 <i>Proportion of slices showing LTP in the Tc1×J20 cross</i>	133
Table 5.1 <i>Proportion of slices at 6 months of age showing LTP in the presence of PTX</i>	164
Table 5.2 <i>Proportion of slices at 3 months of age showing LTP in the presence of PTX</i>	171
Table 5.3 <i>Proportion of slices showing chemical LTP in the Tc1×J20 cross</i>	179

Annexes

Annex A:

ECP16V1 Metrics Script for Neuroachiver 101 (Tcl) (Kevan Hashemi)

Annex B:

Powerband Script for Neuroachiver 101 (Tcl) (Kevan Hashemi)

Annex C:

Power Analysis Script (Python 2.7)

Nomenclature

$\alpha 7$ nAChRs	<i>$\alpha 7$-nicotinic acetylcholine receptors</i>
A β	<i>Amyloid beta</i>
aCSF	<i>Artificial cerebrospinal fluid</i>
AD	<i>Alzheimer's disease</i>
AD-DS	<i>Alzheimer's disease in the Down syndrome population</i>
ADAM	<i>A disintegrin and metalloprotein</i>
AICD	<i>APP intracellular domain</i>
AMPA	<i>amino-3-hydroxy-5-methyl-4-isoxazolepropionic acid</i>
AMPAR	<i>amino-3-hydroxy-5-methyl-4-isoxazolepropionic acid receptor</i>
APP	<i>Amyloid Precursor Protein</i>
APOE	<i>Apolipoprotein E</i>
ATP	<i>Adenosine triphosphate</i>
BACE1	<i>β-secretase 1</i>
BDNF	<i>Brain-derived neurotropic factor</i>
CaMKII	<i>Calmodulin-dependent kinase II</i>
CA1	<i>Cornu ammonis area 1</i>
CA3	<i>Cornu ammonis area 3</i>
CSTB	<i>Cystatin B</i>
dup-APP	<i>duplication of the APP gene</i>
DS	<i>Down syndrome</i>
DG	<i>Dentate gyrus</i>
DNA	<i>Deoxyribose nucleic acid</i>
DSCR	<i>Down syndrome critical region</i>
DSCR1	<i>Down syndrome critical region gene 1</i>
DYRK1A	<i>Dual-specificity tyrosine phosphorylation-regulated kinase 1A</i>
EC	<i>Entorhinal cortex</i>
EEG	<i>Electroencephalography</i>
EOAD	<i>Early-onset Alzheimer's disease</i>
fEPSP	<i>Field excitatory postsynaptic potential</i>

GABA	<i>Gamma-aminobutyric acid</i>
GABA _A R	<i>Gamma-aminobutyric acid receptor type A</i>
GEDD	<i>Genome-wide dysregulation of gene expression domain</i>
GIRK	<i>G protein-coupled inwardly-rectifying K⁺ channel</i>
GluR1	<i>Glutamate receptor 1 (AMPA subunit)</i>
Hsa21	<i>Homo sapiens autosome 21</i>
IPSCs	<i>Induced pluripotent stem cells</i>
LEC	<i>Lateral entorhinal cortex</i>
LOMEDS	<i>Late -onset myoclonic epilepsy in Down syndrome</i>
LPP	<i>Lateral perforant pathway</i>
LTP	<i>Long-term potentiation</i>
LTD	<i>Long-term depression</i>
MEC	<i>Medial entorhinal cortex</i>
MF	<i>Mossy fibres</i>
mGluRs	<i>Metabotropic glutamate receptors</i>
mIPSC	<i>Miniature inhibitory postsynaptic current</i>
MPP	<i>Medial perforant pathway</i>
Mmu10	<i>Mus musculus chromosome 10</i>
Mmu16	<i>Mus musculus chromosome 16</i>
Mmu17	<i>Mus musculus chromosome 11</i>
MWM	<i>Morris water maze</i>
NFT	<i>Neurofibrillary tangle</i>
NMDA	<i>N-methyl-D-aspartate</i>
NMDAR	<i>N-methyl-D-aspartate receptor</i>
NMDG	<i>N-methyl-d-glucamine</i>
GluN1	<i>NMDA receptor subunit 1</i>
GluN2A	<i>NMDA receptor subunit 2A</i>
GluN2B	<i>NMDA receptor subunit 2B</i>
NPY	<i>Neuropeptide Y</i>
OLIG1	<i>Oligodendrocyte transcription factor 1</i>
OLIG2	<i>Oligodendrocyte transcription factor 2</i>
PDK	<i>Phosphoinositide-dependent kinase</i>

PKA	<i>Protein kinase A</i>
PKC	<i>Protein kinase C</i>
PP2B	<i>protein phosphatase 2B</i>
PPR	<i>Paired pulse ratio</i>
PPF	<i>Paired pulse facilitation</i>
PPI	<i>Paired pulse inhibition</i>
PSD-95	<i>Postsynaptic density protein 95</i>
PSEN1	<i>Presenilin 1</i>
PSEN2	<i>Presenilin 2</i>
PTP	<i>Post-tetanic potentiation</i>
PTX	<i>Picrotoxin</i>
PTZ	<i>Pentylentetrazol</i>
qPCR	<i>Quantitative polymerase chain reaction</i>
RNA	<i>Ribonucleic acid</i>
SL	<i>Stratum lucidum</i>
SC	<i>Schaffer collateral</i>
SM	<i>Stratum moleculare</i>
SR	<i>Stratum radiatum</i>
tgAPP	<i>Transgenic human APP</i>
AUC	<i>Area under the curve</i>

Chapter 1

Introduction

1.1 Down syndrome

1.1.1 The Down syndrome phenotype

Down syndrome (DS) is a developmental disorder resulting from a full or partial duplication of chromosome 21 (Hsa21). It is the most common genetic cause of intellectual disability, with an estimated incidence of between 1 in 650, and 1 in 1000, live births (Bittles and Glasson, 2004). DS was first described by John Langdon Down (Down, 1866), who noted common characteristics in a subset of the patients presenting at his clinic with intellectual disability. Almost a century later, Marthe Gautier and Jerome Lejeune observed that fibroblasts taken from patients with DS contained 47 chromosomes instead of the expected 46, and identified the additional chromosome as Hsa21 (Lejeune, Gauthier and Turpin, 1959).

Although DS is a highly heterogeneous condition, cognitive impairment is a ubiquitous feature, along with a characteristic craniofacial dysmorphism. Poor muscle tone, immunological and metabolic dysfunction, heart defects and an elevated risk of leukaemia are also common. Individuals with DS also have an increased susceptibility to seizures and an elevated risk of early-onset Alzheimer's disease (AD) (Roper and Reeves, 2006), and these features will be the focus of the work presented here.

Risk of aneuploidy (an abnormal number of chromosomes) increases with maternal age; consequently, an increase in the proportion of women choosing to postpone parenthood in Europe has led to an increase in the

number of conceptions affected by DS. Although prenatal testing is widely available, many women who receive a positive result elect to continue their pregnancy, and consequently the incidence of DS has remained stable over the past 20 years (Loane *et al.*, 2013). In addition, medical advances have prolonged the life expectancy of DS patients from an estimated 9 years in 1929 to over 60 currently (Bittles and Glasson, 2004), resulting in an increase in the prevalence of DS in the general population, and indicating that DS will remain a clinically significant problem for the foreseeable future (Resta, 2005; Morris and Alberman, 2009).

1.1.2 Genetics of Down syndrome

Hsa21 is the smallest human autosome. It contains an estimated 233 genes, 447 non-coding genes and 185 pseudogenes, accounting for 1-1.5% of the human genome (Ensembl, release 84). The low number of genes on Hsa21 may account for the comparatively mild phenotype of DS in contrast to other autosomal trisomies. Individuals with DS routinely survive into adulthood, and are often able to lead fulfilling and independent lives (Skotko, Levine and Goldstein, 2011); in contrast, the majority of non-Hsa21 trisomy cases result in infant mortality or spontaneous abortion (Menasha *et al.*, 2005).

The most common cause of DS is a nondisjunction error during meiosis, accounting for 92% of cases. Nondisjunction errors are maternal in origin in 95% of cases (Antonarakis, 1991), with 77.1% occurring during meiosis I and 22.9% during meiosis II (Antonarakis *et al.*, 1992). The remaining 8% of DS cases result from chromosomal rearrangements leading to partial translocations or duplications of disease-relevant regions of Hsa21, or from mosaic trisomy 21 due to mitotic nondisjunction errors (Owens *et al.*, 1983).

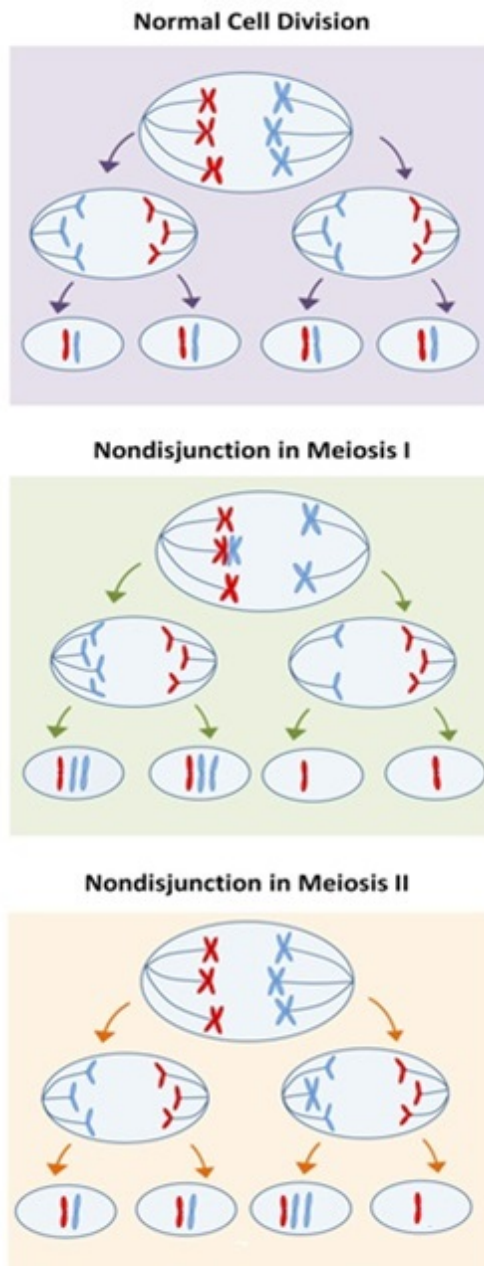


Figure 1.1. Nondisjunction in meiosis

Normal Cell Division:

Illustration of normal segregation of homologous chromosomes in meiosis I and normal segregation of sister chromatids in meiosis II, resulting in four gametes with the correct number of chromosomes.

Nondisjunction in meiosis I:

Illustration of nondisjunction in meiosis I, causing failure of homologous chromosomes to separate, resulting in an uneven distribution of chromatids in meiosis II, and producing two gametes with an additional copy of Hsa21 and two gametes missing Hsa21.

Nondisjunction in meiosis II:

Illustration of nondisjunction in meiosis II showing homologous chromosomes segregate normally during meiosis I, but sister chromatids fail to separate during meiosis II, resulting in one gamete with an additional copy of Hsa21, one gamete missing Hsa21, and two gametes with the correct number of chromosomes.

DS is a complex disorder, and a variety of mechanisms have been proposed to contribute to the pathogenic effect of trisomy of Hsa21. The most established of these is the ‘gene-dosage hypothesis’, which suggests that an increase in Hsa21 gene copy number leads to an increase in gene expression, and the resulting overexpression of dosage sensitive genes is responsible for the DS phenotype (Gardiner, 2004). However, additional copies of non-coding

regulatory regions on Hsa21 (Dekker, De Deyn and Rots, 2014); a non-specific stress response triggered by combined dosage increase in multiple genes (Santaguida and Amon, 2015); and the presence of a supernumerary chromosome itself (Letourneau *et al.*, 2014), have all been proposed to contribute to the DS phenotype. These mechanisms are unlikely to be mutually exclusive, and therefore unravelling the contribution they make to the DS phenotype may be critical in developing effective therapies for DS.

1.1.3 Mouse models of Down syndrome

One approach to investigating the pathophysiology of DS has been through the generation of genetically modified mice. Mouse models are of particular value in dissecting the DS phenotype, as they allow the contribution of individual genes and chromosomal regions to be dissociated from each other, and from the impact of a freely segregating supernumerary chromosome. A range of models of DS have been generated to date, including mice that are partially trisomic or monosomic for Hsa21 orthologous regions, overexpression and knockout models for DS-relevant candidate genes, and mice that are transchromosomic for Hsa21 itself. Although currently no single model is fully able to recapitulate the impact of trisomy, the combined use of these models provides a powerful tool for understanding genetic interactions and mapping DS phenotypes to specific genes or regions of Hsa21.

The genes on Hsa21 are syntenic with regions on three different mouse chromosomes, with the order and orientation of genes and non-coding sequences in each region conserved. The majority of Hsa21 orthologues are located on a 37 Megabase (Mb) region of mouse chromosome 16 (Mmu16). This region contains 224 genes between *Lipi* and *Zfp295*. Mouse chromosome 10 (Mmu10) carries a smaller 2.3 Mb orthologous region, consisting of 47

genes located between *Cstb* and *Prmt2*, and mouse chromosome 17 (Mmu17) carries an 1.1 Mb orthologous region with just 22 genes, located between *Umodl1* and *Hsf2bp* (Dierssen, Herault and Estivill, 2009). This dispersion of relevant genes has made modelling the DS phenotype in mice uniquely challenging.

To add to the challenge of modelling DS, not all Hsa21 genes are conserved between mice and humans, and of the genes that are conserved, differences in genetic sequence may significantly alter their capacity to cause disease. For example, while duplication of the human *APP* gene is linked to early-onset AD, overexpression of mouse *App* does not result in AD neuropathology (Yu, Li, *et al.*, 2010). Gardiner *et al.* (2003) report 164 protein-coding genes on Hsa21 to be highly conserved between humans and mice, 61 human genes to be minimally conserved in mice, and 111 putative genes which are human-specific, while Dierssen *et al.* (2009) identified just 293 murine homologs for over 430 Hsa21 genes. These figures suggest that a significant number of Hsa21 genes are not present in mice, and therefore any contribution made by these genes to the DS phenotype cannot be detected using mice with duplications of the murine Hsa21 syntenic regions. This may be of particular relevance for DS phenotypes relating to human-specific cognitive functions such as language.

The most extensively studied model of DS to date is the Ts65Dn model (Davisson *et al.*, 1993) which carries a freely segregating chromosome consisting of the distal portion of Mmu16, fused to the centromere of Mmu17. Ts65Dn mice are therefore functionally trisomic for the majority of the Hsa21 orthologues on Mmu16. However, they also overexpress a number of Mmu17 genes, which are not orthologous to Hsa21 and therefore have no relevance to the clinical phenotype of DS (Duchon *et al.*, 2011). In addition, the Ts65Dn mice do not overexpress any of the Hsa21 orthologous genes located on Mmu10 or Mmu17. Therefore, while this model demonstrates good face

validity for a number of DS phenotypes, the mechanistic validity of these phenotypes cannot be assumed. Consequently, further validation is required to ensure that the phenotypes observed in this model are of genuine clinical relevance.

An alternative approach has been the creation of a 'triple trisomic' model of DS, by generating three mouse strains, each with a duplication of one of the Hsa21 syntenic regions – Dp(10)1Yey, Dep(17)1Yey and Dp(16)1Yey – and crossing them to produce a mouse model containing all three regions (Yu, Li, *et al.*, 2010). This model represents the most complete genetic model of trisomy 21 to date. However, only approximately 3 out of every 100 progeny resulting from this cross are trisomic for all 3 regions, and these mice develop a number of adverse phenotypes, which cause severe welfare issues. Although this has limited the experimental utility of the 'triple trisomic' mice themselves, characterising the individual strains has proven valuable in mapping phenotypes to specific genetic regions.

Due to the number of Hsa21 orthologous genes present on Mmu16, a variety of Mmu16 segmental trisomy models have also been generated. Phenotyping of these models helps to elucidate the genetic interactions underlying complex phenotypes, by separating out the contributions of relevant genes or chromosomal regions. To further this approach, segmental monosomy models have also been created, which can be crossed into trisomic models to rescue trisomy of a selected region (Lana-Elola *et al.*, 2011). These models have been used to identify the regions of Hsa21 that are necessary, or sufficient, for particular DS phenotypes.

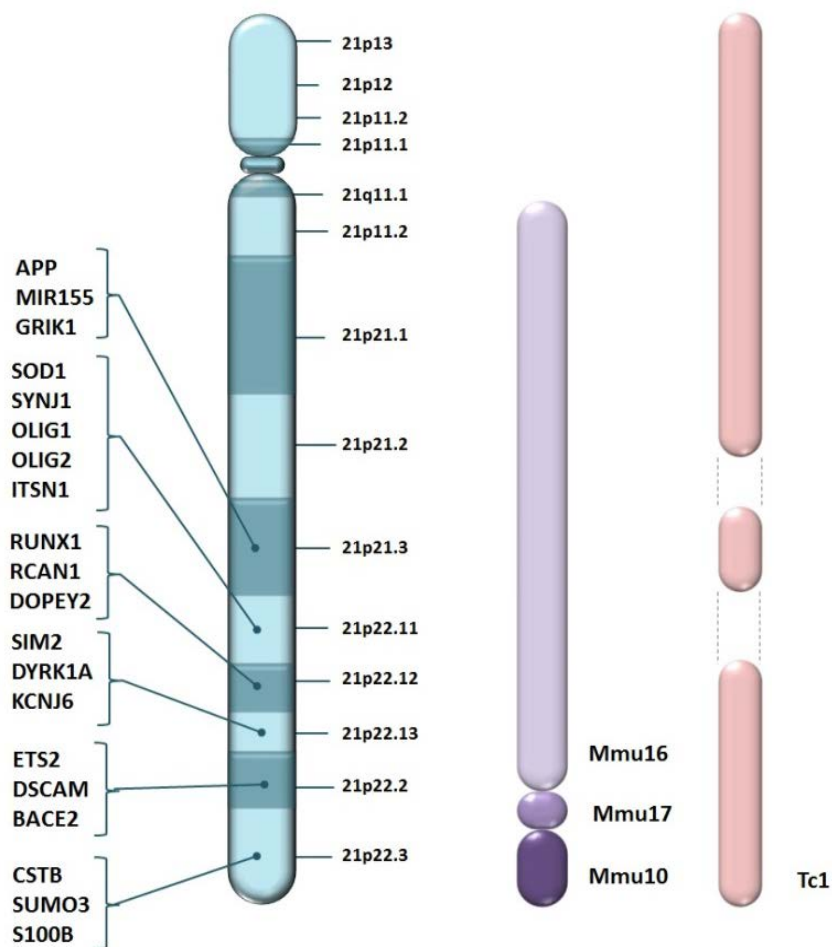


Figure 1.2 Chromosome 21

Illustration of Hsa21 (blue), showing the locations of DS candidate genes. Hsa21 orthologous regions on Mmu16, 17, and 10 (purple) and Hsa21 regions present in the Tc1 mouse (pink) are aligned. Two major regions of Hsa21 are deleted in the Tc1 model, including the genes SOD1, SYNJ1, OLIG1, OLIG2 and ISTN1. Although APP is not in this region, Tc1 mice do not have a functional copy of APP due to further chromosomal rearrangement. The Mmu16 orthologous region is duplicated in the Dp1Tyb model.

The work described in this thesis has been carried out in the Tc(Hsa21)1TybEmcf model (Tc1), which carries an extra copy of Hsa21 itself, thus eliminating the complications of combining multiple mouse chromosomal regions. The Tc1 mouse model is mosaic: approximately 60% of its cells contain Hsa21, and it is functionally trisomic for approximately 75% of Hsa21 genes (O'Doherty *et al.*, 2005). Crucially, due to chromosomal rearrangements, the Tc1 mouse is not functionally trisomic for the *APP* gene

(Gribble *et al.*, 2013), presenting a unique opportunity to model the interaction between trisomy of Hsa21 and *APP* overexpression. This has been achieved by crossing the Tc1 mouse with a mouse model of AD, and will be discussed further in **Section 1.3.5**.

1.1.4 Dosage sensitivity in Down syndrome

In support of the gene-dosage hypothesis, transgenic mouse models have also been used to identify phenotypic abnormalities resulting from the overexpression of individual Hsa21 genes, or their murine orthologues. One of the most frequently studied gene candidates for dosage sensitivity is *DYK1A*, a member of the dual specificity tyrosine-phosphorylation-regulated kinase family, which is known to phosphorylate a number of target proteins, including transcription factors, synaptic proteins, splicing factors and cell signalling molecules (reviewed by Park *et al.* 2009). Pleiotropic roles have been proposed for *DYRK1A* in neurodevelopment, cognitive function, and neurodegeneration. Both overexpression (Souchet *et al.*, 2014) and haploinsufficiency (Fotaki *et al.*, 2002) of the mouse *DYRK1A* homologue *Dyrk1a* are pathogenic in mice, and loss-of-function mutations in *DYRK1A* are associated with intellectual disability and craniofacial dysmorphism in patients, indicating that the tight regulation of *DYRK1A* level is critical for normal development.

Evidence for dosage sensitivity also exists for a number of other Hsa21 orthologues. For example, overexpression *Kcnj6*, which encodes the inwardly rectifying potassium channel GIRK2, has been linked to enhanced neuronal inhibition (Cramer *et al.*, 2010) and overexpression of *Ets2*, which encodes a transcription factor, has been implicated in skeletal and lymphocyte abnormalities, as well as in increased levels of neuronal apoptosis (Sumarsono *et al.*, 1996; Wolvetang *et al.*, 2003).

Furthermore, restoring individual dosage-sensitive genes to disomic levels has been shown to rescue a number of DS phenotypes in trisomic mice, suggesting that a small number of single genes may make a disproportionate contribution to the overall impact of trisomy. Reducing the activity of *Dyrk1a* in Ts65Dn mice using the inhibitor epigallocatechin-3-gallate improves a variety of electrophysiological and behavioural deficits (De la Torre *et al.*, 2014; Souchet *et al.*, 2014), and a similar rescue has been observed using RNA knockdown of *Dyrk1a* (Altafaj *et al.*, 2013). Additionally, normalising the gene dose of the transcription factors *Olig1* and *Olig2* in the Ts65Dn mouse by crossing them to *Olig1* and *Olig2* knockout mice (Chakrabarti *et al.*, 2010) rescues defects in neurogenesis, although the impact of overexpression of *Olig1* and *Olig2* isolation remains unknown.

Despite extensive evidence from mouse models indicating a pathogenic role for these Hsa21 genes, *APP* remains the only Hsa21 gene for which duplication has been directly linked to human disease. *APP* encodes amyloid precursor protein (APP), a primary component of the amyloid plaques which represent a major neuropathological hallmark of AD, and an additional copy of *APP* is sufficient to cause early-onset AD in the absence of any other chromosomal abnormalities (Cabrejo *et al.*, 2006; Sleegers *et al.*, 2006; Kasuga *et al.*, 2009). This will be discussed further in **Section 1.2**.

1.1.5 The 'Down Syndrome Critical Region'

Consistent with the results obtained from transgenic mice, cases of DS associated with partial trisomy of Hsa21 due to translocation indicate that Hsa21 gene duplication is sufficient to produce a clinically recognisable DS phenotype without a change in chromosome number. These cases have been used to attempt to identify a 'critical region' on Hsa21, containing all the genes necessary to produce the craniofacial dysmorphism and cognitive

impairment considered to be characteristic of DS. The existence of this putative 'Down Syndrome Critical Region' (DSCR) has proven controversial, in part because partial trisomy cases are rare, and the inherent variability of the DS phenotype, even in the context of full trisomy 21, makes phenotype-genotypes links difficult to resolve. Early analyses indicated that the duplication of a region located between 21q22.2–21q22.3 (Korenberg *et al.* 1990; Rahmani *et al.* 1989; Sinet *et al.* 1994) was sufficient to produce a DS phenotype. However, more detailed investigations of partial trisomy cases have subsequently called into question the concept that a single region of Hsa21 is common to all cases, suggesting instead that different DS phenotypes link to different susceptibility regions (Lyle *et al.*, 2009).

Furthermore, cases of DS involving partial trisomy of regions outside of the putative DSCR have since been reported (Korenberg *et al.*, 1994), casting further doubt on the suggestion that this region is critical. A systematic reanalysis of 125 cases of partial trisomy identified a 34 kb region common to all cases presenting with intellectual disability and craniofacial dysmorphism, and absent from all cases without them (Pelleri *et al.* 2016). However, the region identified does not contain any known genes, and consequently, how it may contribute to the DS phenotype has yet to be determined. It therefore remains unclear which, if any, regions of Hsa21 are essential in producing the clinically recognised DS phenotype.

Consistent with the complex role observed for the DSCR region in individuals with partial trisomy, Ts1Rhr mice, which carry a duplication of the DSCR orthologous region on Mmu16, display some, but not all, of the neurological phenotypes reported in mouse models of DS carrying larger duplications (Olson *et al.*, 2004; Belichenko *et al.*, 2009; Haas *et al.*, 2013). Interestingly, although the Ts1Rhr mice do not display the impairments in hippocampal function observed in the Ts65Dn mice, crossing the Ts65Dn mouse with a mouse strain that is monosomic for the DSCR orthologous region rescues

these impairments (Olson *et al.*, 2007), suggesting that the genes in this region are necessary but not sufficient to cause hippocampal dysfunction.

1.1.6 Transcriptional dysregulation in Down syndrome

Despite strong evidence for dosage sensitivity in DS, the picture is complicated by observations that the expression levels of Hsa21 genes in DS patients and DS mouse models are not reliably increased by 50%, reflecting the 50% increase in gene copy number. Analysis of gene expression in DS patient-derived lymphoblastoid cell lines indicated that only a small proportion of expressed Hsa21 genes were significantly upregulated, with some genes showing amplification of expression and others compensation (Aït Yahya-Graison *et al.*, 2007; Prandini *et al.*, 2007). Similar findings have been reported from the Ts65Dn mouse model, in which only 37% of duplicated genes analysed showed the expected 50% increase in expression (Lyle *et al.*, 2004).

Changes in expression levels of many non-Hsa21 genes have been also been reported, indicating that genome-wide transcriptional dysregulation contributes to the DS phenotype. In induced pluripotent stem cells (iPSCs) derived from a set of monozygotic twins discordant for trisomy 21, expression changes were noted in 1204 genes; 624 upregulated and 580 downregulated, and similar results have been observed in DS fibroblasts (Hibaoui *et al.*, 2014). These alterations are likely to represent a combination of primary pathological changes in gene expression, and secondary compensatory changes resulting from feedback mechanisms engaged to maintain homeostasis. Separating out the pathological changes from compensatory mechanisms is likely to be of great importance in determining appropriate therapeutic interventions.

Trisomy of Hsa21 may contribute to transcriptional dysregulation through several mechanisms: overexpression of transcription factors such as *RUNX1* and *ETS2*, and of transcriptional regulators such as *BRWD1*, may directly influence the transcription levels of their target genes. Increased levels of proteins mediating epigenetic modifications such as DNA methylation and histone acetylation will also alter levels of gene expression in the modified region. Candidate genes for such epigenetic modification on Hsa21 include the DNA methyltransferase *DNMT3L*, chromatin protein *HMGN-1* and the kinase *DYRK1A*. Consistent with the overexpression of epigenetic modifiers, genome-wide hypermethylation has been reported in DS patient lymphocytes (Pogribna *et al.*, 2001) and placental villi (Jin *et al.*, 2013), and differential methylation patterns have also been reported in buccal epithelial cells (Jones *et al.*, 2013).

Gene expression is also regulated at RNA level, and increased expression of Hsa21 microRNAs may result in an increase in silencing of target genes. 5 microRNAs have been identified on Hsa21, as well as a number of other small RNAs of unknown function. These effects would be highly dependent on genetic and epigenetic background, which may account for the extent of phenotypic variability in DS (Karmiloff-Smith *et al.*, 2016).

It has also been proposed that the presence of a supernumerary chromosome itself may disrupt gene expression. In foetal fibroblasts from the same set of monozygotic twins, domains of genome-wide dysregulation of gene expression (GEDDs) were observed (Letourneau *et al.*, 2014), suggesting that the presence of an extra chromosome within the cell is sufficient to alter gene expression systemically. However, although such changes may modify the presentation of DS, the fact that a DS phenotype is also observed in cases of partial trisomy caused by translocation suggests that the presence of an additional chromosome is unlikely to be a critical factor in the pathophysiology of DS. Furthermore, the results of Letourneau *et al.*, have

been called into question by a more recent publication (Do, Mobley and Singhal, 2015), in which the authors were unable to replicate their analysis on both the original dataset, and on a second dataset taken from the same set of twins reported in a different publication. They also failed to replicate the reports of GEDDs in a mouse model of DS, and therefore suggested that such regions of dysregulation may have been an analytical artefact. Further investigation is therefore required to resolve the discrepancy in results between the two groups.

Even if aneuploidy does not contribute to genome-wide dysregulation, it may still have a significant detrimental impact on the cell. Analysis of aneuploidy in yeast indicates the existence of a conserved 'aneuploidy-associated stress response', whereby small changes in the expression of multiple genes induces a stress response, even when overexpression of each individual gene has no effect (Santaguida and Amon, 2015). If an equivalent stress response exists in mammalian cells, it may make an important contribution to pathogenesis in cases of full trisomy of Hsa21.

This diversity of pathogenic mechanisms, and the complexity of the DS phenotype, means that DS has historically been perceived as intractable. However, recent developments in the capacity to model DS are challenging this perception, allowing the roles of individual genes and chromosomal regions to be dissected, and identifying the signalling pathways subject to dysregulation. This increased understanding has great potential to expand the scope for therapeutic intervention.

1.1.7 Mechanisms of cognitive impairment in Down syndrome

Cognitive deficits are a ubiquitous feature of DS, however the extent of intellectual disability is highly variable (Dierssen, 2012), with some individuals requiring extensive support to carry out basic daily tasks, while

others are able to live independently and maintain successful careers. The degree of transcriptional dysregulation in the trisomic brain indicates that neuronal dysfunction in DS results from a convergence of pathogenic mechanisms, which vary in their significance. The fact that DS is a systemic disorder may also be important; non-neurological phenotypes, including immune, endocrine and circulatory dysfunction, can also indirectly influence neuronal activity, exacerbating cognitive dysfunction.

Individuals with DS show a specific profile of cognitive deficits, with late developing structures such as the hippocampus and prefrontal cortex showing the greatest functional impairments (Edgin, Pennington and Mervis, 2010). Language deficits are also common in DS, with syntax showing greater impairment than vocabulary (Roberts, Price and Malkin, 2007). In contrast to explicit memory, implicit memory appears to be preserved (Vicari, Bellucci and Carlesimo, 2000), and verbal working memory shows greater impairment than visuospatial working memory (Lanfranchi, Cornoldi and Vianello, 2004). Interestingly, William syndrome shows an opposite profile of deficits to that observed in DS, suggesting that cognitive dysfunction in DS is syndrome specific, and not the result of generalised developmental retardation (Wang and Bellugi, 1994; Klein and Mervis, 1999).

The pattern of cognitive strengths and weaknesses in DS is complex, and contradictory results have been reported. Research has been confounded in childhood studies by differences in the developmental trajectories of DS children with respect to chronological-age or mental-age matched control groups, and in adult studies by the onset of undiagnosed early-stage dementia. For example, Pennington *et al.* (2013), report that school-aged children with DS exhibit a specific deficit on tests of hippocampal function in comparison to mental-age matched typically developing controls. However these syndrome specific impairments do not appear to be present in preschool children (Roberts and Richmond, 2015), indicating individuals

with DS may undergo a divergent developmental trajectory in early childhood. Furthermore, although Pennington *et al.* did not report deficits in executive function, Lanfranchi *et al.* (2010) observed broad deficits in executive tasks such as working memory, planning and inhibition in adolescents with DS in comparison to mental-age matched controls. Such differences may result from the methodology used for testing, or from the mental age of the participants, highlighting the difficulty in defining neurocognitive phenotypes in complex developmental disorders such as DS.

Both neuroimaging and post-mortem studies have indicated extensive structural abnormalities in the DS brain, including a reduction in total brain volume of approximately 18%, with a specific reduction in cerebellar volume (Pinter *et al.*, 2001), as well as brachycephaly, disordered cortical lamination, and simplified gyri (Dierssen, 2012). Reductions in hippocampal volume, and in frontal and temporal cortical grey matter, have also been described (White, Alkire and Haier, 2003), although not universally (Pinter *et al.*, 2001). This may once again be a reflection of the limitations of the methodology, or of the inherent heterogeneity of the DS population.

The number of cholinergic neurons in the Nucleus Basalis of Meynert is reduced, even before to the onset of dementia (Casanova *et al.*, 1985). However, other regions, such as the basal forebrain, amygdala, parietal and occipital lobes, and basal ganglia are preserved, at least prior to the onset of AD pathology (Lott and Dierssen, 2010). Regional grey matter density in DS patients has been associated with specific neurocognitive measures (Menghini, Costanzo and Vicari, 2011) suggesting that a direct connection between brain morphology and cognitive function exists in DS.

Impaired neurogenesis and an increase in neuronal apoptosis have both been reported in the DS foetal brain (Guidi *et al.*, 2008), which may contribute to the observed reduction in brain size. DS foetal neural progenitors show

reduced proliferative rates, increased apoptosis, and a shift towards glial fate (Lu *et al.*, 2011), and similar abnormalities have been noted in iPSCs generated from individuals with DS, including reduced neurogenesis and an increase in the ratio of glia to neurons (Hibaoui *et al.*, 2014).

These phenotypes have been replicated in a range of cell and animal models (Busciglio and Yankner, 1995; Contestabile *et al.*, 2007; Trazzi *et al.*, 2011); abnormalities in neurogenesis have been reported in the Ts65Dn, Ts1Cje and Ts2Cje models of DS, resulting in reduced neuronal number and structural abnormalities (Yamakawa, 2012). Data obtained from these models suggest such proliferative deficits may selectively impact on excitatory neurons, contributing to an increased ratio of excitation to inhibition in the DS brain (Chakrabarti *et al.*, 2010). This deficit in neurogenesis appears to continue throughout life, affecting adult neurogenesis in the sub-ventricular zone of the dentate gyrus (DG), which further contributes to hippocampal dysfunction (Llorens-Martín *et al.*, 2010).

The role of apoptosis in the DS phenotype however is less clear; although neuronal apoptosis is increased *in vitro* (Busciglio and Yankner, 1995) there is limited evidence supporting a role for increased apoptosis during development *in vivo* (Rueda, Flórez and Martínez-Cué, 2013).

In addition to the reduction in neuron number, post-mortem analysis of the brains of DS patients revealed decreased dendritic complexity throughout the cortex and hippocampus, a reduction in the number of dendritic spines, and abnormal dendritic spine morphology (Marin-Padilla, 1976; Suetsugu and Mehraein, 1980; Becker, Armstrong and Chan, 1986; Weitzdoerfer *et al.*, 2001). Dendritic spine loss appears to be progressive, with DS infants under the age of 6 months of age showing normal, or even enhanced, dendritic sprouting compared to typically developing infants. However, by 2 years of age, children with DS show a dramatic deficit in the number of dendritic

spines, indicating that the developmental process is derailed (Weitzdoerfer *et al.*, 2001). As the morphology of the dendritic tree plays a critical role in the computational properties of neurons, these dendritic abnormalities may have a significant impact on cognition. However, very little is currently known about the impairments in neuronal activity and network function corresponding to these morphological abnormalities, or what contribution they make to the observed cognitive deficits.

1.2 Alzheimer's disease

1.2.1 Pathophysiology of Alzheimer's disease

The presence of the *APP* gene on Hsa21 contributes to a dramatically elevated risk of AD in individuals with DS. AD is the most common form of dementia in the disomic population, and accounts for 50-70% of dementia cases (Fratiglioni, De Ronchi and Agüero-Torres, 1999). Incidence rates have been estimated as approximately 0.5% per year between ages 65–70, rising to approximately 6–8% per year for individuals over the age of 85 (Mayeux and Stern, 2012). In comparison, the risk of AD for individuals with DS is estimated to be 20% at age 50, rising to 45% at age 55, and reaching 80% age 65 (Mccarron *et al.*, 2014).

AD is characterised neuropathologically by the accumulation of extracellular plaques of Amyloid- β (A β) and intracellular neurofibrillary tangles (NFTs), composed of the microtubule associated protein, tau. AD neuropathology is universally present in the DS population by the age of 40 (Wisniewski *et al.*, 1985), and onset of pathology has been reported in individuals as young as 8 years old (Leverenz and Raskind, 1998).

Although plaque deposition correlates poorly with disease progression, tau pathology spreads throughout the hippocampus in a stereotyped way, reflecting disease severity. NFT formation is initiated in the entorhinal cortex and spreads throughout the hippocampal formation and subsequently into the neocortex (Braak and Braak, 1996). Consequently, in the initial stages, AD classically presents with impairment to hippocampal-dependent functions such as short-term memory loss, and disorientation. As the pathology spreads throughout the cortex, the memory impairments become more severe; language is affected, and patients may experience agitation, aggression and delusions. In late stage AD, cognitive function is lost almost

entirely, and motor function also becomes severely impaired (Tarawneh and Holtzman, 2012).

Contrary to the classic presentation of AD, in individuals with DS, personality and behavioural changes, such as apathy or increased impulsivity are frequently reported to precede memory problems in the early stages of disease (Holland *et al.*, 2000). These changes are often associated with a decline in executive function (Ball *et al.*, 2008; Adams and Oliver, 2010), suggesting that frontal lobe dysfunction may occur in the early stages of AD in DS patients (AD-DS). Although the entorhinal cortex and hippocampus remain focal points of AD neuropathology in DS (Mann *et al.*, 1986), pre-existing deficits in frontal lobe function may make it particularly susceptible to subtle changes in network activity. Individuals with AD-DS also show an increased incidence of non-cognitive neurological symptoms, such as postural and gait disturbances, and incontinence (Strydom *et al.*, 2010). Seizures are also a prominent feature of AD-DS, affecting up to 84% of individuals (Menéndez, 2005) and occurring early on in the disease progression; this is discussed in detail in **Section 1.2.8**.

1.2.2 The role of Amyloid- β in Alzheimer's disease

A β is formed through cleavage of Amyloid Precursor Protein (APP), a type 1 transmembrane protein encoded by the *APP* gene on Hsa21. Alternative splicing of APP produces three major isoforms: APP695, APP751 and APP770. The neuronal specific isoform, APP695, predominates in the brain. There are two major processing pathways for APP: an amyloidogenic pathway and a non-amyloidogenic pathway, although it is also a substrate for a number of other enzymes, such as caspases and lysosomal proteases. In the amyloidogenic pathway, APP is cleaved by a β -secretase, encoded by the gene

BACE1. This β -cleavage produces a soluble fragment, sAPP β , along with a membrane bound C-terminal fragment, β CTF.

In the non-amyloidogenic pathway, APP is cleaved by an α -secretase, to produce soluble sAPP α , and α CTF. The α -cleavage site is located within the A β domain, and consequently α -secretase cleavage precludes the formation of A β . Multiple members of the ADAM (A Disintegrin And Metalloproteinase) family demonstrate α -secretase activity; ADAM10 has been implicated in constitutive cleavage, and ADAM17 and ADAM9 in regulated cleavage.

Both α -CTF and β -CTF are subsequently cleaved by γ -secretase, with α -CTF generating a rapidly degraded fragment called p83, and β -CTF generating A β , in addition to amyloid precursor protein intracellular domain (AICD). The γ -secretase is comprised of multiple subunits, including Presenilin 1 and Presenilin 2, encoded by the genes *PSEN1* and *PSEN2* (Haass *et al.*, 2012) along with APH-1 and Nicastrin. γ -secretase cleavage initiates at variable locations, and cleavage occurs sequentially at multiple sites, separated by approximately 3 amino acids, giving rise to multiple species of A β between

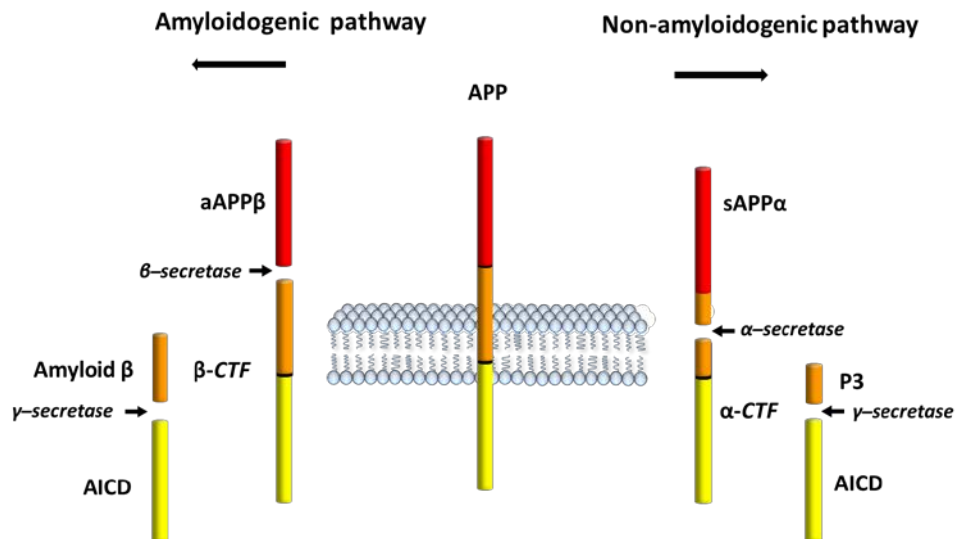


Figure 1.3 Processing of APP via the amyloidogenic and non-amyloidogenic pathway

37 and 43 amino acids in length (Haass *et al.*, 2012). The predominant species of A β is A β 40, however the ratio of A β 40 to the more aggregation-prone species A β 42 and A β 43 is an important factor in the pathogenesis of AD. In contrast to the toxic effects of A β , sAPP α appears to have a protective function, thus promoting α -cleavage over β -cleavage is likely to be of therapeutic value.

Despite being the subject of extensive research, neither the physiological function of the full-length APP protein, nor of its multiple cleavage products, have been fully defined, although APP has been implicated in synaptic function (Kamenetz *et al.*, 2003; Müller and Zheng, 2012). The exact role of APP in AD pathology is also yet to be established, however genetic evidence indicates a critical role for APP misprocessing in disease initiation (Hardy and Selkoe, 2002), and overexpression has been linked to epilepsy (Born *et al.*, 2014).

1.2.3 Genetics of Alzheimer's disease

Early-onset Alzheimer's Disease (EOAD), defined as disease onset prior to age 65 (Filley, Kelly and Heaton, 1986), has been linked to autosomal dominant mutations in three genes involved in the production of A β : *APP*, *PSEN1* and *PSEN2*. However, these mutations still only account for a small number of EOAD cases, with the majority remaining idiopathic (Sleegers and van Duijn, 2001). Pathogenic mutations in *APP* contribute to disease either by improving the affinity of APP for the β -secretase pathway, increasing A β production (Haass *et al.*, 1994), or by promoting the formation of the more amyloidogenic A β 42, altering the A β 40:A β 42 ratio and increasing the propensity of A β to aggregate (De Jonghe *et al.*, 2001). Mutations in *PSEN1* (Larner, 2013) and *PSEN2* (Cai, An and Kim, 2015) act through a similar mechanism, altering the processing of APP by γ -secretase, leading to

increased formation of A β 42, and other longer forms of the peptide. Conversely, a mutation that reduces the affinity of APP for β -secretase appears to have a protective effect, lowering the risk of AD in carriers (Jonsson *et al.*, 2012).

Consistent with a central role for A β in AD, EOAD is also associated with duplication of the *APP* locus (dup-*APP*), suggesting increased gene dosage of *APP* is sufficient to cause AD (Slegers *et al.*, 2006; Rovelet-Lecrux *et al.*, 2007; Hooli *et al.*, 2012). As *APP* is located on Hsa21, individuals with DS also have an additional copy of *APP*, however differences in presentation between AD-DS and dup-*APP* suggest that other genes on Hsa21 also modify disease (Wiseman *et al.*, 2015).

The vast majority of AD cases are sporadic and late-onset. A number of genes have been identified as risk factors for sporadic AD. These genes converge on three major pathways; cholesterol metabolism, endosomal vesicle recycling and immune function, suggesting that these pathways play a significant role in the pathogenesis of AD. The most significant risk gene is *APOE*, encoding Apolipoprotein E, which has been implicated in cholesterol metabolism and A β transport (Liu *et al.*, 2016). There are 3 major alleles of the *APOE* gene: *APOE* ϵ 2, *APOE* ϵ 3 and *APOE* ϵ 4. Individuals carrying two copies of the *APOE* ϵ 4 allele have up to 15 times greater risk of developing AD than those with two copies of *APOE* ϵ 3, while individuals with two copies of the *APOE* ϵ 2 have a 40% lower risk (Farrer *et al.*, 1997).

Other genes linked to an increased risk of AD include *TREM2*, *CR1*, *CD33*, which are implicated in microglial clearance of A β (Guerreiro *et al.*, 2014) and *SORL1* and *PICALM* which are involved in endosomal processing of APP (Rogaeva *et al.*, 2007; Xiao *et al.*, 2012). Although NFTs are a key feature of AD neuropathology, mutations in the *MAPT* gene, encoding the protein tau,

are not associated AD, but have been linked instead to frontotemporal dementia (Goedert, 2005).

Understanding the mechanisms through which these genes contribute to an increased risk of AD in disomic individuals may also provide insight into the disease modifying processes that occur in AD-DS, as many of the pathways identified as targets for AD risk genes are known to be dysregulated in trisomy. For example, several Hsa21 genes influence A β processing, while others play a role in tau phosphorylation, endosomal function, or the immune system.

1.2.4 The amyloid cascade hypothesis

The amyloid cascade hypothesis proposes that the deposition of A β in the brain is the initiating factor in AD (Hardy and Higgins, 1992), and that A β mediates NFT formation, synaptic dysfunction and neuronal loss. The link between *APP* mutations and EOAD provided strong initial support for the amyloid hypothesis. However, in the 25 years since it was published it has become clear that AD is a multifaceted and multifactorial disease, and many key aspects of AD pathogenesis remain unresolved.

Mutations in *APP*, *PSEN1* and *PSEN2* together account for less than 0.1% of all AD cases (Slegers and van Duijn, 2001), and the extent to which they share mechanistic similarities with sporadic disease is still unclear. The nature of the toxic species of A β also remains the subject of intense research; although A β deposition exerts a detrimental effect on synaptic function, and A β plaques are often associated with dystrophic dendrites and reactive microglia (Sasaki *et al.*, 1997), plaques do not appear to be the primary cause of neurotoxicity in the AD brain. Instead, a soluble form of oligomeric A β is likely to be the toxic species, although the exact identity of the species is disputed, and the mechanisms by which soluble A β oligomers contribute to

synaptic dysfunction, cell death, and NFT formation also remain controversial (Benilova, Karran and De Strooper, 2012). The role of oligomeric A β in synaptic dysfunction will be discussed further in **Section 1.2.6**.

Although attempts at restoring cognitive function in mouse models by reducing levels of oligomeric A β in the brain have shown promising results (Billings *et al.*, 2005; Kitazawa, Medeiros and Laferla, 2012), clinical trials in patients have had limited success. It has been proposed that this failure reflects inadequate drug development, or poor clinical trial design, rather than the invalidity of the amyloid hypothesis in sporadic AD (Karran, Mercken and De Strooper, 2011; De Strooper, 2014) Further investigation is therefore required to determine whether soluble A β could be a viable therapeutic target.

1.2.5 Mouse models of Alzheimer's disease

As is the case for DS, mouse models provide an opportunity to investigate the pathogenesis of AD, and offer insight into early cellular and molecular changes, which cannot be detected in AD patients. Although the vast majority of AD cases are sporadic, little is known about the aetiology of sporadic AD, so genetic approaches to generating AD mouse models have relied on modelling the processes underlying familial forms of disease. Currently, no model exists which is able to recreate the pathology of AD in its entirety. The predominant approach has been to create mice overexpressing human *APP*, containing one or more disease-linked mutations. The nature, timescale and severity of phenotypes varies between models, depending on the isoform of APP, the gene copy number, the type of mutation, the choice of promoter, and the background strain. In general, these models develop the amyloid pathology characteristic of AD, along with synaptic dysfunction and cognitive impairments, but do not exhibit NFTs or neuronal death.

Overexpression of wildtype human *APP* does not appear to be sufficient to induce plaque formation (Mucke *et al.*, 2000), despite being linked to disease. This may reflect the limited timescale over which the pathology must develop in mouse models to produce an experimentally tractable phenotype: the natural lifespan of a mouse is generally no more than three years, yet even the most aggressive forms of EOAD rarely present before the 3rd or 4th decade of life. Thus, a viable mouse model requires the natural disease progression to be greatly accelerated.

Most models have relied on the use of exogenous promoters, which express *APP* more strongly than its natural promoter. The most commonly used are Thy-1 and PDGF β , which are neuron-specific, and PrP which is expressed in both neurons and glia. These promoters differ in their strength, as well as in spatial and temporal regulation, resulting in differing phenotypes (Hall and Roberson, 2007). Recently, several knock-in models have been created, expressing versions of mutant humanised-*APP* under the mouse endogenous *APP* promoter. These mice also develop amyloid pathology, along with synaptic loss and cognitive dysfunction, suggesting that overexpression is not required for the pathogenic effects of mutant human *APP*. However the phenotype they display is milder as a result of the lower levels of expression (Saito *et al.*, 2014).

Mice expressing mutant *PSEN1* and *PSEN2* have also been developed. Presenilin mutations alone do not result in amyloid plaque formation in mice; this may be due to differences in the amino acid sequence of murine *APP*, making it less susceptible to aggregation. However, mutant *PSEN1* does exacerbate pathology in mouse models expressing human *APP*, and a number of double transgenic models combining *APP* and *PSEN1* mutations have been created. These mice display more rapid disease progression, and unlike *APP*

single mutant mice, do experience neuronal loss (Casas *et al.*, 2004; Schmitz *et al.*, 2004; Oakley *et al.*, 2006) although they still do not develop NFTs.

As *APP* overexpression models have failed to recreate the tau pathology associated with AD, several models have been created expressing either wildtype human-*MAPT* (Andorfer *et al.*, 2003), or human *MAPT* containing mutations linked to frontotemporal dementia (Lewis *et al.*, 2001) in addition to *APP*. These mice do develop the plaque and tangle pathology that characterises human disease, although it is important to note that mutations in tau are not associated with AD, which may impact the mechanistic relevance of these models. *APP* overexpression models have also been crossed with tau knock-out mice, to assess the role of wildtype tau in the development of AD neuropathology. Reducing the levels of endogenous tau was shown to be protective against a number of phenotypes related to *APP* overexpression, as well as against non-*APP* related seizures and excitotoxicity, suggesting then even if NFT formation occurs downstream of A β , tau may still play a significant role in mediating neuronal dysfunction in AD (Roberson *et al.*, 2007).

The AD model used in this study was the Tg(PDGFB-APPSwInd)20Lms/J model (J20), which overexpresses human *APP* containing two mutations identified in pedigrees with EOAD: the Swedish mutation (KM670/671NL) and the Indiana mutation (V717F), under the neuron-specific PDGF β promoter (Mucke *et al.*, 2000). The Swedish mutation is associated with enhanced production of A β (Haass *et al.*, 1995) and the Indiana mutation with an increase in the A β 42:A β 40 ratio (De Jonghe *et al.*, 2001), leading to enhanced A β aggregation. This model recapitulates the amyloid pathology of AD, although not the tau pathology, and exhibits behavioural deficits and synaptic dysfunction.

It is important to note, however, that this phenotype results from overexpression at levels far beyond those associated with trisomy, and that the use of an exogenous promoter results in unnatural spatial and temporal patterns of APP expression, due to absence of the normal genetic regulation associated with the *APP* promoter. Consequently, the extent to which observed phenotypes represent the acceleration of disease-relevant processes, as opposed to artefacts of APP overexpression, or the disruption of normal developmental signalling, must be carefully considered (Born *et al.*, 2014). The validation of phenotypes in APP knock-in mice (Saito *et al.*, 2014) may help to resolve which changes are genuinely relevant to the pathogenesis of AD.

1.2.6 Synaptic dysfunction in Alzheimer's disease

Synaptic dysfunction is one of the earliest pathological events in AD, preceding the onset of A β and tau deposition (Lesne *et al.*, 2013; Jack *et al.*, 2013). Converging evidence from animal models suggests that oligomeric A β is the primary driver of synaptic dysfunction, although tau also appears to play a critical role. Both loss of synapses (Terry *et al.*, 1991), and the quantity of soluble A β (Wang *et al.*, 2016; Tomic *et al.*, 2009), reflect the severity of dementia more reliably than the degree of plaque and tangle pathology.

A multitude of mechanisms have been proposed through which A β oligomers contribute both directly and indirectly to synaptic dysfunction, including excitotoxicity, disruption to intracellular trafficking and mitochondrial impairment. In many of the studies looking at the effects of soluble A β , the nature of the A β oligomers used is poorly defined; multiple forms of A β are present in the brains of patients with AD, and it has been suggested that different forms of A β may contribute to different pathological events (Deshpande *et al.*, 2006). Oligomeric A β has also been reported to interact

with a number of receptors, including n-methyl-d-aspartate receptors (NMDARs) (Snyder *et al.*, 2005; Texidó *et al.*, 2011); the cellular prion protein (Laurén *et al.*, 2009; Kudo *et al.*, 2012); metabotropic glutamate receptors (mGluRs) (Renner *et al.*, 2010; Hamilton, Zamponi and Ferguson, 2015); α 7-nicotinic acetylcholine receptors (α 7nAChRs) (Wang *et al.*, 2000); the neurotrophin receptor p75NTR (Yaar *et al.*, 1997); and insulin receptors (Xie *et al.*, 2002; Zhao *et al.*, 2008).

Aberrant glutamatergic signalling appears to play a critical role in the synaptotoxic effects of A β . Reduced surface expression of α -amino-3-hydroxy-5-methyl-4-isoxazolepropionic acid receptors (AMPA), which mediate fast excitatory synaptic transmission, and NMDARs, which are critical for neuronal plasticity, have been reported in a variety of systems. Changes in levels of glutamate receptor subunits have been observed in hippocampal tissue from AD patients, including a decrease in the GluN1 and GluN2A subunits of NMDARs (Mishizen-Eberz *et al.*, 2004), and a decrease in the GluR2 subunit of AMPARs (Carter *et al.*, 2004). Such changes appear to be region and disease-stage specific, and the extent to which they represent changes in patterns of receptor expression, as opposed to in the total number of synapses or neurons remains unclear.

Reduction in the surface expression of glutamate receptors has also been reported in the brains of AD transgenic mice (Chang *et al.*, 2006). Furthermore, surface expression of the AMPAR GluA1 subunit, along with the scaffolding protein PSD-95, is reduced in cultured neurons from mutant *APP* transgenic mice (Almeida *et al.*, 2005) and wildtype rats exposed to exogenous A β (Gu, Liu and Yan, 2009). Soluble A β has been shown to selectively promote the endocytosis of synaptic NMDARs, reducing the NMDAR-mediated influx of Ca²⁺ into dendritic spines (Snyder *et al.*, 2005). This both impedes NMDAR-dependent neuroprotection, and contributes to impaired synaptic plasticity. AMPAR internalisation appears to be dependent

on reduced synaptic availability of CaMKII (Gu, Liu and Yan, 2009) and activation of the phosphatase calcineurin (Zhao *et al.*, 2010), while NMDAR internalisation requires $\alpha 7$ nAChRs activation of protein phosphatase 2B (PP2B), which dephosphorylates the tyrosine phosphatase STEP, a regulator of NMDA receptor trafficking (Snyder *et al.*, 2005).

Transport of glutamate itself is also dysregulated in AD. Soluble oligomers of A β have been suggested to decrease glutamate uptake in the mouse hippocampus, contributing to impaired synaptic function (Li *et al.*, 2009). Furthermore, glutamate transporter activity is reduced in the brains of AD patients, and expression of the glutamate transporters EAAT1 and EAAT2 is decreased, particularly in the region surrounding plaques (Masliah *et al.*, 1996; Jacob *et al.*, 2007).

In addition to impairments in glutamatergic signalling, dysfunctional insulin receptor signalling has been implicated in AD. Insulin serves multiple functions in the brain, including in the regulation of learning and memory (Zhao and Alkon, 2001) and in neuroprotection (De Felice *et al.*, 2009). Extracellular and intracellular A β both interfere with insulin signalling; A β binding extracellularly to synaptic sites induces insulin receptor internalisation, while intracellular A β blocks the interactions between phosphoinositide-dependent kinase (PDK) and Akt, which are required for neuroprotection.

Tau also appears to be necessary to mediate the synaptotoxic effects of A β . Tau is a microtubule associated protein, which is normally localised to the axon, where it is involved in stabilising microtubules. In AD, it becomes hyper-phosphorylated, and mislocalised to the somatodendritic compartment of the cell, where it accumulates and forms intracellular NFTs. Although tau pathology is thought to occur downstream of A β in AD, tau knockout mice are resistant to A β mediated cognitive impairments, and show

a reduced propensity for seizures (Roberson *et al.*, 2007). They are also protected against A β induced deficits in synaptic plasticity (Shipton *et al.*, 2011), suggesting tau plays an active role in disease progression.

In support of this, Ittner *et al.* (2010) have demonstrated that A β -mediated synaptotoxicity requires the tau-dependent targeting of the kinase Fyn to the postsynaptic terminal, where it phosphorylates the GluN2B subunit of the NMDA receptor, stabilising its interactions with PSD-95. Disruption of this interaction has been shown to be neuroprotective in a rat model of stroke (Aarts *et al.*, 2002), suggesting this complex may be required for excitotoxicity. Tau knockout mice show normal NMDAR-mediated synaptic currents, and although Ittner *et al.* suggest this may relate to reduced rather than absent Fyn, it is also consistent with a predominantly extra-synaptic localisation of GluN2B (Petrulia and Petrulia, 2012).

Oligomeric A β -mediated mitochondrial dysfunction also contributes to synaptotoxicity. Synapses are enriched in mitochondria, and synaptic mitochondria are critical both for meeting the high energetic demands of synaptic transmission and for Ca²⁺ homeostasis. A β accumulates inside mitochondria, and synaptic mitochondria appear to be particularly vulnerable (Du *et al.*, 2010), leading to increased oxidative stress, and impairment in their ability to buffer Ca²⁺ and their capacity to generate ATP. A β also appears to impair mitochondrial transport and promote mitochondrial fission via S-nitrosylation dynamin-related protein 1 (Drp1), leading to increased fragmentation of mitochondria (Cho *et al.*, 2009).

Although the relative contribution of each of these mechanisms to the progression of AD is not well understood, it is clear that soluble A β oligomers make a significant contribution to synaptotoxicity, and that synaptic dysfunction is a key mediator of cognitive decline in AD. Many of the pathways through which A β mediates synaptotoxicity are dysregulated by

trisomy of Hsa21 prior to the onset of dementia, which may have important consequences for disease progression in AD-DS.

1.2.7 Genetic modifiers of Alzheimer's disease in Down syndrome

APP duplication is sufficient to cause AD in the absence of any other genetic abnormalities. A rare case of partial trisomy of Hsa21, where an additional copy of *APP* was not present, was found to be negative for both dementia and AD pathology (Prasher *et al.*, 1998) suggesting *APP* duplication is both necessary and sufficient for early-onset AD in DS. However, although AD pathology is universal, not all individuals with DS develop clinical dementia, with some aging successfully into their 70s (Krinsky-McHale *et al.*, 2008). Furthermore, the age of dementia onset in DS is highly variable, suggesting that other factors on Hsa21 modify the risk associated with *APP* duplication.

Multiple genes on Hsa21 have been suggested as candidates for modifying the risk and presentation of dementia in DS (see

Table 1.3 Hsa21 candidate genes implicated in neuronal dysfunction in DS . Some of these are likely to exacerbate disease, while others may be protective. Several Hsa21 genes directly influence A β levels, for example the transcription factor *ETS2* interacts with the *APP* promoter, upregulating expression of A β (Wolvetang *et al.*, 2003), while SUMO-3, encoded by the *SUMO3* gene, may regulate the turnover of APP and β -secretase. Overexpression of SUMO-3 in transfected cells has also been shown to increase A β 40 and A β 42 secretion (Dorval *et al.*, 2007). The Hsa21 microRNA miR-155 may also contribute to increased A β generation, via downregulation of sorting nexin 27 (SNX27), as SNX27 binds to Presenilin 1, disrupting γ -cleavage (Wang *et al.*, 2014).

Other Hsa21 genes may contribute indirectly to the pathogenesis of AD, for example dysfunction of the endosomal-lysosomal system affects APP processing and clearance. Deletion of Cystatin B, encoded by the Hsa21 orthologue *Cstb*, prevented lysosomal pathology, reduced plaque load and levels of intracellular A β , and rescued deficits in learning and memory in a mouse model overexpressing mutant *APP*, suggesting *Cstb* overexpression may have a detrimental effect in AD (Yang *et al.*, 2011). Overexpression of *SYNJ1* has also been linked to the enlargement of early endosomes, contributing to endocytic dysfunction (Cossec *et al.*, 2012).

The immune system also plays an important role in AD, and A β deposition is associated with chronic inflammation (McGeer *et al.*, 2016). In transgenic mice, overexpression of *S100B*, an astrocytic calcium binding protein, in combination with mutant-*APP*, was associated with an increase in reactive astrocytes, microgliosis and pro-inflammatory cytokines, which exacerbated amyloid pathology (Mori *et al.*, 2010). Tau pathology may also be modified in DS; overexpression of the kinase DYRK1A has been shown to contribute to tau hyperphosphorylation (Ryoo *et al.*, 2007) and alter tau splicing (Shi *et al.*, 2008).

Furthermore, DS hippocampal function is impaired prior to dementia onset. As APP, A β , and many of their proposed targets, are regulated in an activity-dependent manner, this is likely to have important consequences for the way these networks respond to *APP* overexpression. AD-DS may therefore differ from sporadic AD not only because of differences in APP processing and trafficking, but as a result of a differential network response.

1.2.8 Epilepsy in AD-DS

Seizure susceptibility is enhanced in DS, and risk of seizures has been reported to show a tri-modal distribution, with an increased prevalence of

childhood seizure disorders, as well as an increase in seizure disorders beginning in the third decade of life (Pueschel, Louis and McKnight, 1991). A third peak in seizure susceptibility occurs after the age of 55; this peak largely represents late-onset myoclonic epilepsy in Down syndrome (LOMEDS) (De Simone, Daquin and Genton, 2006). LOMEDS is strongly associated with dementia; up to 84% of patients with AD-DS experience seizures, and they are linked to accelerated cognitive decline and poor clinical outcome (Menéndez, 2005). LOMEDS commonly presents as myoclonic jerks, particularly upon waking, and progresses to generalised tonic-clonic seizures (Möller *et al.*, 2002).

Although there are underlying alterations in neuronal excitability in DS which are likely to contribute to an increased risk of seizures throughout life, these discrete peaks in seizure risk indicate that other risk factors are developmental-stage specific. As the developing brain in general is more susceptible to seizures (Moshé and Albala, 1983), it is not surprising that the same should be the case in the DS population. Furthermore, a number of the metabolic and cardiovascular complications of DS manifest in infancy, and may contribute to the development of childhood epilepsy.

The association between seizures and dementia in DS indicates a role for A β in epileptogenesis. Sporadic AD is also associated with an increased risk of seizures; the cumulative incidence of seizures in patients with early-stage AD was found to be 8% over 7 years of follow up. Risk was reported to be particularly high in patients with early-onset AD; patients between the ages of 50 and 59 showed an 87-fold increase in risk compared with the general population (Amatniek *et al.*, 2006). These results suggest that the patients with the most aggressive amyloid pathology may be at the highest risk of seizures. In support of this connection, seizures have been reported in a number of familial AD pedigrees, including those with *APP*, *PSEN1* and *PSEN2* mutations, as well as pedigrees with *dup-APP* (Noebels, 2011). Furthermore,

seizures themselves exacerbate the progression of dementia, and epileptic activity may increase activity-dependant release of A β (Vossel *et al.*, 2017). However, these patients most commonly present with partial complex seizures, rather than myoclonic epilepsy, consistent with a modulatory role for other genes on Hsa21.

The high incidence of seizures in AD-DS, along with the associated poor outcome, suggests they represent a significant clinical challenge. However, very little research has been carried out to date regarding which Hsa21 genes influence the risk and presentation of seizures, or how seizures affect the progression of dementia. Understanding the mechanisms underlying seizure susceptibility in AD-DS therefore represents an important topic for future investigation.

1.3 Modelling AD-DS phenotypes in mice

1.3.1 Hippocampal phenotypes in AD and DS

The hippocampus is one of the earliest regions affected in AD, and plays an integral role in the cognitive dysfunction associated with DS. Despite extensive characterisation, the precise function of the hippocampus remains unknown, but it has been implicated in the consolidation of episodic memory, spatial navigation, and emotional processing. The dorsal and ventral subregions show different patterns of connectivity (Moser and Moser, 1998) which may reflect the dissociation between the between the emotional and spatial functions of the hippocampus.

The principal connectivity within the hippocampus is a tri-synaptic circuit. The hippocampus receives input from the entorhinal cortex via the medial perforant path (MPP) and lateral perforant path (LPP), which project primarily to the dentate granule cells (DGCs). The MPP terminates on the

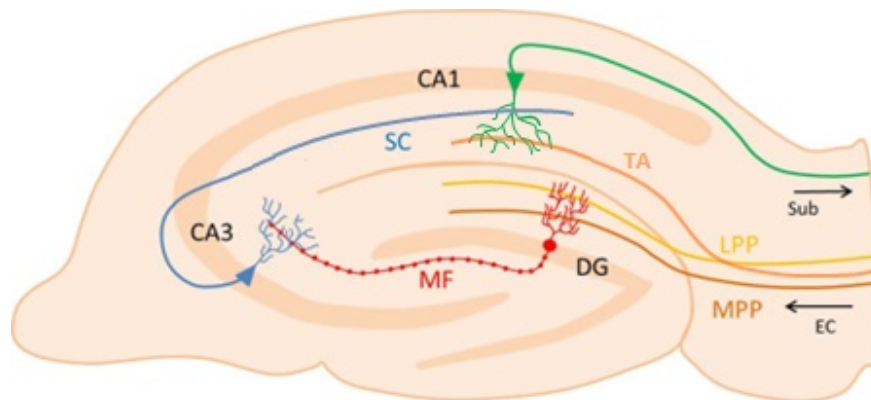


Figure 1.4. Tri-synaptic connectivity in a transverse section of the mouse hippocampus.

Projections from the entorhinal cortex (EC) synapse onto the dentate granule cells (DGCs) of the dentate gyrus (DG) via the medial (MPP) and lateral (LPP) perforant pathways, and onto the pyramidal cells of CA1 via the temporoammonic pathway (TA). DGCs project via the mossy fibres (MF) to the CA3 region, and CA3 pyramidal cells subsequently project to CA1 pyramidal cells via the Schaffer Collateral (SC). CA1 projects out of the hippocampus to the subiculum (Sub).

middle third of the molecular layer, while the LPP terminates on the outer third (McNaughton, 1980), targeting different regions of the DGC dendrites. The DGCs project via the mossy fibres to the pyramidal cells of the CA3 region. The CA3 pyramidal cells then project via the Schaffer collateral to CA1. The axons of the CA1 pyramidal cells project out of the hippocampal formation to the subiculum, and this projection constitutes the primary output of the hippocampus. However, the hippocampus also receives many other inputs, including GABAergic input via the septohippocampal pathway, and extensive neuromodulatory input from brainstem and forebrain nuclei.

Hippocampal function has been studied extensively in mouse models of both DS and AD, and deficits have been reported both in hippocampal synaptic plasticity and hippocampal-dependent behavioural tasks in a number of models. Examples of these are given in **Table 1.1 Examples of mouse models of DS** and **Table 1.2 Examples of mouse models of AD** respectively, although these lists are not exhaustive. However, to date, no model has specifically investigated the impact of A β overexpression on synaptic plasticity in the trisomy Hsa21 hippocampus. Although the majority of mouse models of DS carry a duplication of the murine *App* gene, murine APP does not have the same aggregation properties as human APP, and therefore the *App* overexpression in these models does not recapitulate the pathological processes associated with AD. It therefore remains unknown whether increased levels of A β differentially affects synaptic plasticity in the trisomy Hsa21 hippocampus.

1.3.2 Long-term potentiation

The cellular correlate of memory has been proposed to be synaptic plasticity. LTP is a persistent strengthening of synaptic transmission resulting from synaptic activity (Bliss and Lømo, 1973). Importantly, hippocampal circuits

show Hebbian plasticity, in which connectivity between neurons is strengthened if they are activated simultaneously. This form of plasticity is thought to be required for associative learning (Fanselow and Poulos, 2005). In addition to LTP, hippocampal circuits show long-term depression (LTD), suggesting that synaptic activity is able to induce bi-directional changes in synaptic strength (Dudek and Bear, 1993), depending on the pattern of activity and the prior state of the network.

Although LTP was first described in the hippocampus, it has since been observed in many other brain regions, including the cortex, amygdala and cerebellum (Iriki *et al.*, 1989; Heynen and Bear, 2001; Lev-Ram *et al.*, 2002; Rodrigues, Schafe and Ledoux, 2004). However, hippocampal LTP remains the most comprehensively characterised, due to both the critical role of the hippocampus in memory, and to its well-defined synaptic connectivity.

LTP and LTD rely on activation of many of the same signalling cascades that have been implicated in memory consolidation (discussed further in **Section 4.1**). Consequently, deficits in hippocampal LTP have become associated with memory impairment, and are frequently assessed in mouse models of neurological disease as a marker for cognitive dysfunction. A number of studies have suggested a link between hippocampal LTP and performance on hippocampal-dependent behavioural tasks. Much of this research has relied on pharmacological inhibition, or genetic ablation, of proteins involved in the induction or expression of LTP. For example, performance on the Morris water maze (MWM) — a spatial-reference memory task in which rodents are required to recall the location of a hidden escape platform in a pool of water using extra-maze spatial cues — was reported to be impaired by intraventricular infusion of an NMDA receptor antagonist (Morris, 1989). This was associated with a loss of hippocampal LTP, and it was suggested that NMDAR activity was a requirement for both hippocampal LTP and spatial-reference memory.

However, more recent studies have demonstrated a more complex relationship between spatial reference memory and hippocampal LTP, for example MWM performance is only impaired by NMDA receptor antagonism if the mouse has not been previously exposed to spatial learning tasks (Bannerman *et al.*, 1995), suggesting the related deficits may be more subtle than an inability to encode spatial memories. Furthermore, recent evidence from mice which have a specific knockout of hippocampal NMDARs suggests that NMDAR-dependent LTP in CA1 is not required for successful completion of the MWM (Bannerman *et al.*, 2014), indicating that extra-hippocampal NMDARs may mediate the previously observed deficits in spatial-reference memory.

Recently, optogenetic approaches have been used in investigating the link between LTP and memory. Nabavi *et al.* (2014) adapted a fear conditioning protocol so that rats were conditioned to associate optogenetic stimulation of auditory inputs amygdala with a foot shock. They then showed that applying an optical LTD protocol eliminated memory of the shock and that subsequent application of an LTP protocol restored it, demonstrating for the first time a direct association between LTP and associative memory.

1.3.3 Modelling hippocampal dysfunction in Down syndrome

Impaired performance on hippocampal-dependent behavioural tasks, and deficits in hippocampal synaptic plasticity, have been reported in nearly all mouse models of DS (summarized in **Table 1.1**). The Tc1 mouse model — which has been used for the experiments presented here, shows impaired performance on novel object recognition (NOR) tasks, but not on spontaneous alternation on in the T-maze (O'Doherty *et al.*, 2005). NOR requires animals to remember which objects they have previously been exposed to, while spontaneous alternation requires animals to remember

which arm of a 'T-shaped' maze they selected on a previous trial, and therefore tests spatial working memory. The difference in performance may relate to the specific cognitive demands of each task, or to the period of time the memory must be retained in order to successfully complete the task; the NOR protocol required memories to be retained for 10 minutes, while spontaneous alternation required retention for less than 1 minute. Notably, performance is impaired on the more complex 8-arm radial maze task, suggesting impairments in spatial working memory may depend on cognitive load. Tc1 mice also show reduced place cell selectivity and specificity in both CA3 and CA1, consistent with impairments to spatial working memory (Witton *et al.*, 2015).

Further phenotyping indicates that memory deficits in the Tc1 mice may be specific to short-term memory; spatial working memory is also impaired on the MWM, but long-term spatial reference memory on the MWM is preserved (Morice *et al.*, 2008). Furthermore, while NOR performance is impaired over 10 minute intervals, it is normal both immediately after exposure, and 24 hours later (Hall *et al.*, 2016). Short-term deficits in NOR occur for both visual and olfactory novelty, but short-term object-location memory is normal, suggesting the Tc1 mice have a specific deficit in object recognition, rather than a general deficit in detecting novelty (Hall *et al.*, 2016).

The dissociation between long-term and short-term memory in the Tc1 is mirrored by LTP deficits observed in the MPP; LTP *in vivo* is reduced 1 hour after induction, but normal 24 hours later (Morice *et al.*, 2008). A reduction in the hippocampal expression of the AMPAR subunit GluA1 was also observed by Morice *et al.* (2008), which may explain this phenotype, as it resembles the memory profile of GluR1 knockout mice (Reisel *et al.*, 2002). However, the mechanism by which GluR1 expression is altered by trisomy remains unknown. It may be linked to a reduction in the size and number of glutamatergic synapses (Witton *et al.*, 2015), although the expression of the

NMDA receptor obligatory subunit GluN1 was unchanged in the Tc1. Alternatively, it may reflect specific alterations in glutamate receptor trafficking or expression mediated by other Hsa21 genes.

In a study by Witton *et al.*, (2015), characterisation of hippocampal circuit function in the Tc1 mice also revealed impaired short-term plasticity in the mossy fibres, but not the Schaffer collateral, indicating that the DG-CA3 networks were the primary locus of hippocampal dysfunction. However, LTP was found to be normal in both the Schaffer collateral and mossy fibres, suggesting a specific LTP impairment in the MPP. This was supported by the observation of structural abnormalities in the DG and CA3 regions. Although input-output curves indicated that baseline synaptic transmission between the DG and CA3 of Tc1 mice was similar to that of wildtype animals, electron microscopy-generated three-dimensional reconstructions showed Tc1 mice to have a reduction in the density of synapses in the middle molecular layer of the DG, and a reduction in the number of postsynaptic thorny excrescences in the mossy fibres. Postsynaptic density size was also reduced in both the DG and CA3, and changes in thorny excrescence number correlated with reduced excitatory synaptic input from the mossy fibres to CA3. Two-photon excitation imaging in acute hippocampal slices showed similar ultrastructural synaptic abnormalities are also present in live cells. These results suggest that plasticity in both the DG and CA3 subregions is impaired, and that connectivity between the DG and CA3 is attenuated, with profound implications for information processing.

These findings are broadly consistent with those observed in other models of DS, although several important discrepancies exist. The Ts65Dn model, which is currently the most extensively characterised model of DS, has consistently shown deficits in a number of behavioural tasks considered to depend on the hippocampus. These include deficits in spatial working memory and spatial reference memory tasks on the MWM (Reeves *et al.*, 1995; Escorihuela *et al.*,

1998; Stasko and Costa, 2004), the radial maze (Demas *et al.*, 1996), spontaneous alternation in the T-maze (Faizi *et al.*, 2011), and contextual fear conditioning (Hyde, Frisone and Crnic, 2001; Faizi *et al.*, 2011). The phenotypes are generally reported to be more severe than those observed in the Tc1 model, although there are inconsistencies in the literature. Interestingly, in the Ts65Dn mice, short-term memory on the novel object recognition (NOR) task is preserved, while long-term memory is impaired (Smith, Kesner and Korenberg, 2014), the opposite of the phenotype observed in the Tc1 mouse, suggesting that these memory deficits may relate to specific combinations of genes. However, differences in genetic background may also be a factor, as Ts65Dn mice have been backcrossed to a C57BL/6 background, whereas Tc1 mice are maintained on a hybrid 129S8×C57BL/6 background.

These behavioural deficits are also associated with impaired hippocampal synaptic plasticity. LTP impairments have been reported in the DG, which can be rescued by antagonism of either GABA_A or GABA_B receptors (Kleschevnikov *et al.*, 2012; Kleschevnikov *et al.*, 2004). This suggests deficits in this model do not result from an inherent inability to undergo plasticity, but are due to excessive synaptic inhibition preventing the required signalling pathways from being activated. These findings have been replicated in the DG of the Ts1Cje mice (Belichenko *et al.*, 2007), the Ts1Rhr mice (Belichenko *et al.*, 2009) and the 'triple trisomic' mice (Belichenko *et al.*, 2015), suggesting that 'over-inhibition' may be an important mechanism for cognitive dysfunction in DS. Impaired LTP has also been reported in CA1 in the Ts65Dn mice (Siarey *et al.*, 1997), however deficits in CA1 appear to be variable, depending on the induction protocol and stimulus intensity (Costa and Grybko, 2005), which may reflect a differential impact on presynaptic and postsynaptic GABAergic signalling, (Stäubli, Scafidi and Chun, 1999).

Blocking GABAergic signalling has also been reported to rescue some of the behavioural phenotypes in the Ts65Dn; the GABA_A receptor antagonists picrotoxin (PTX) and pentylentetrazol (PTZ) have been shown to improve performance on NOR and spontaneous alternation respectively (Fernandez and Garner, 2007) and the GABA_A5 inverse agonist improves performance on the MWM and NOR (Braudeau *et al.*, 2011).

It has been suggested that GABA_A receptor mediated signalling in the Ts65Dn hippocampus may be excitatory rather than inhibitory, due to a less negative chloride reversal potential (E_{Cl}); Deidda *et al.*, (2015) observed E_{Cl} in wildtype mice to be -66.01 ± 1.46 , compared to -58.33 ± 1.33 in the Ts65Dn mice. The difference between the reversal potential of chloride and the membrane potential determines the size and direction of current through GABA_A receptors. Influx of chloride into the cell, which mediates GABA_Aergic inhibition, occurs when the chloride reversal potential is more negative than the membrane potential. A less negative reversal potential will therefore reduce the influx of chloride into the cell, or result in efflux of chloride from the cell, resulting in less effective GABA_Aergic inhibition or GABA_Aergic inhibition excitation, respectively. Such a change in the Ts65Dn mice could therefore have a profound impact on hippocampal network function.

Blocking the NKCC1 chloride transporter with bumetanide has also been reported to rescue LTP deficits and restore performance on the contextual fear-conditioning, object-location, and NOR tests in the Ts65Dn model (Deidda *et al.*, 2015). However, these findings do not appear to be consistent with previous data from the Ts65Dn mice, and their significance therefore remains unclear.

Although these data suggest a major role for excessive inhibitory signalling, it is apparent that other systems are also significantly affected by trisomy. β -adrenoreceptor agonists improve performance on NOR, contextual fear

conditioning, and T-maze spontaneous alternation in the Ts65Dn mouse (Faizi *et al.*, 2011; Dang *et al.*, 2014), indicating that abnormal noradrenergic input to the hippocampus may also contribute to behavioural deficits. Furthermore, early treatment with fluoxetine appears to be effective in rescuing performance in contextual fear conditioning by enhancing neurogenesis (Bianchi *et al.*, 2010), suggesting impairments in neurogenesis also contribute to cognitive deficits in DS.

This complexity is reflected in the results of genetic rescue experiments. Excessive inhibition can be rescued by restoring dosage of the transcription factor genes *Olig1* and *Olig2* to disomic levels (Chakrabarti *et al.*, 2010), while normalisation of *Dyrk1a* dosage rescued LTP deficits in CA1, contextual fear conditioning and performance in the MWM (García-Cerro *et al.*, 2014), suggesting that DS-associated cognitive phenotypes may result from the convergent activity of multiple genes.

Consistent with the idea that hippocampal dysfunction results from the combined action of multiple overexpressed genes, these deficits are present to varying degrees in models of segmental trisomy. The Ts1Cje mouse carries a smaller segment of Mmu16, containing Hsa21 homologues between *Sod1* and *Mx1*. These mice show impaired performance on the MWM (Sago *et al.*, 1998), although unlike the Ts65Dn these impairments are limited to the spatial version of the task. The Ms1Ts65 model, which is trisomic for the Mmu16 genes between *App* and *Sod1* that are missing from the Ts1Cje, also shows impairment in water maze performance, although less severely than those of Ts65Dn or Ts1Cje (Sago *et al.*, 2000). This indicates that when duplicated, genes in both these regions are independently sufficient to exert a detrimental impact on hippocampal function.

Although the majority of data on hippocampal dysfunction in DS models relates to duplication of genes on Mmu16, the impact of duplication of genes

on Mmu10 and Mmu17 has been investigated in Dp(10)1Yey, and Dp(17)1Yey mice respectively. Neither of these strains are impaired on the MWM or contextual fear conditioning. Dp(10)1Yey mice exhibit normal LTP in the CA1, and the Dp(17)1Yey actually showed enhanced LTP (Yu *et al.*, 2010). This enhancement was also identified in the Ts1Yah model, which is trisomic for 12 Mmu17 genes between *Abcg1-U2af1*, in addition to improved performance on the MWM, although spontaneous alternation and NOR were still impaired (Pereira *et al.*, 2009). Interestingly, the opposite phenotype is observed in the Ts1Cje mice, where MWM is impaired while NOR is intact (Fernandez and Garner, 2007). These data suggest that overexpression of one or more of the genes on Mmu17 may have a beneficial effect on memory, which is offset by the detrimental effect of duplication of other genes in cases of full trisomy.

The 'triple trisomic' mouse model of DS also shows impaired performance on the MWM and contextual fear conditioning test, as well as deficits in CA1 LTP, consistent with the phenotypes observed due to segmental trisomy of Mmu16. However, limited characterisation of hippocampal circuit function has been carried out to date, due to the practical difficulties in generating this strain.

These results illustrate both the complexity of the DS phenotype, and the importance of specificity in relating electrophysiological and behavioural measures of hippocampal function.

Table 1.1 Examples of mouse models of DS

Mouse model	Mutation	Learning and memory deficits	Synaptic plasticity deficits
Tc1*	Freely segregating copy of Hsa21	Impaired performance on a novel object recognition task after 10min delay but normal performance after 24h delay. Impaired spatial working memory but intact spatial reference memory in the water maze (Morice <i>et al.</i> , 2008)	Impairment in DG LTP <i>in vivo</i> after 1h but not after 24h (Morice <i>et al.</i> , 2008). Impaired short-term plasticity in the mossy fibres (Witton <i>et al.</i> , 2015)
Ts65Dn	Freely segregating orthologous region of Mmu16 fused to centromere of Mmu17	Impaired performance on novel place and object recognition, and contextual fear conditioning tasks (Kleschevnikov <i>et al.</i> 2012), impairments in T-maze spontaneous alternation and delayed matching-to-place in the water maze (Faizi <i>et al.</i> , 2011)	Reduced LTP in CA1 (Siarey <i>et al.</i> , 1997) and increased LTD in CA1 (Siarey <i>et al.</i> , 1999), loss of LTP in the DG (Kleschevnikov <i>et al.</i> , 2004) which can be rescued by blocking GABAergic inhibition
Dp16Yey	Mmu16 segmental duplication	Impaired spatial reference memory in the water maze and impaired contextual fear conditioning (Yu, Liu, <i>et al.</i> , 2010)	Reduced LTP in CA1 (Yu, Liu, <i>et al.</i> , 2010)
Dp17Yey	Mmu17 segmental duplication	No impairments identified to date	Enhanced LTP in CA1 (Yu, Li, <i>et al.</i> , 2010)

*Used in this work

Mouse model	Mutation	Learning and memory deficits	Synaptic plasticity deficits
Dp10Yey	Mmu10 segmental duplication	No impairments identified to date	No impairments identified to date
Ts1Tyb*	Mmu6 segmental duplication	No impairments published to date	No impairments published to date
Triple trisomic	Mmu16, 17 & 10 orthologous region duplication	Impaired spatial reference memory in the water maze, but intact performance on contextual fear conditioning tasks (Yu, Li, <i>et al.</i> , 2010)	Impaired LTP in CA1 (Yu <i>et al.</i> , 2010). Impaired LTP in the DG which can be rescued by blocking GABAergic inhibition (Belichenko <i>et al.</i> , 2015)
Dp1Rhr	DCSR duplication	Impaired performance on NOR after 24h delay and impaired T-maze spontaneous alternation (Belichenko <i>et al.</i> , 2009)	Impaired LTP in the DG which can be rescued by blocking GABAergic inhibition (Belichenko <i>et al.</i> , 2009)
Ts1Cje	Mmu16 segmental duplication	Impaired spatial reference memory and reversal learning on the water maze (Sago <i>et al.</i> , 1998), impaired spontaneous alternation in the T-maze (Belichenko <i>et al.</i> , 2007), no deficit in NOR (Fernandez and Garner, 2007)	Reduced LTP and increased LTD in CA1, but effect size smaller than in Ts65Dn (Siarey <i>et al.</i> , 2005), LTP deficit in the DG which can be rescued by blocking GABAergic inhibition (Belichenko <i>et al.</i> , 2007)

*Used in this work

Table 1.2 Examples of mouse models of AD

Mouse model	Mutation	Learning and memory deficits	Synaptic plasticity deficits
J20*	Overexpression <i>APP</i> _(Swe,Ind)	Deficits at 12 and 14 weeks in spatial reference memory on the radial arm maze weeks but no deficit in contextual fear conditioning (Wright <i>et al.</i> , 2013), impaired spatial working memory and spatial reference memory on the water maze (Palop <i>et al.</i> , 2003)	Impaired LTP in CA1 (Saganich <i>et al.</i> , 2006) and MPP (Palop <i>et al.</i> , 2007)
Tg2576	Overexpression <i>APP</i> _(Swe)	Impaired long-term memory on NOR but intact short-term memory (Hall <i>et al.</i> , 2016), deficits in contextual fear conditioning from 5 months of age (Jacobsen <i>et al.</i> , 2006), deficits T-maze spontaneous alternation at 15 months of age (Chapman <i>et al.</i> , 1999)	Impaired LTP in the DG at 5 months of age (Jacobsen <i>et al.</i> , 2006), impaired LTP in CA1 at 15 months of age (Chapman <i>et al.</i> , 1999), no impairment in MF LTP (Jung <i>et al.</i> , 2011)
3xTg	Overexpression <i>APP</i> _(Swe) , <i>MAPT</i> _(P301L) ; <i>PSEN1</i> _(M146V)	Impaired performance on the Barnes maze at 6.5 months (Stover <i>et al.</i> , 2015), progressive deficits in contextual fear conditioning and long-term memory on the MWM from 4 months of age, deficits in short-term memory from 6 months of age (Billings <i>et al.</i> , 2005).	Impaired LTP in CA1 at 6 months of age (Oddo <i>et al.</i> , 2003)
NL-F	Knock-in <i>APP</i> _(Swe, Iberian)	Impaired Y-maze spontaneous alternation at 18 months of age (Saito <i>et al.</i> , 2014)	Not known
5xFAD	Overexpression <i>APP</i> _(Swe, Flo¹, Lon) <i>PSEN1</i> _(M146L, L286V)	Deficits in contextual fear conditioning at 6 months of age (Kimura and Ohno, 2009), impaired Y-maze spontaneous alternation at 4-5 months of age (Oakley <i>et al.</i> , 2006)	Impaired LTP in CA1 at 6 months of age (Kimura and Ohno, 2009)

*Used in this work

Table 1.3 Hsa21 candidate genes implicated in neuronal dysfunction in DS

Gene	Function	References	Model
<i>APP</i>	Precursor protein cleaved to form A β , the primary component of amyloid plaques in AD. Sufficient to cause EOAD when mutated or triplicated. Physiological function is unclear, but implicated in a range of synaptic functions. A β appears to facilitate synaptic function at low doses, but is toxic at high doses.	Kamenetz <i>et al.</i> , 2003; Palop and Mucke, 2009; Selkoe, 2002; Slegers <i>et al.</i> , 2006	Tc1 Dp1Tyb
<i>KCNJ6</i>	Encodes G-protein coupled inwardly rectifying K ⁺ channel GIRK2. GABA _B R mediated GIRK2 currents may contribute to increased inhibitory K ⁺ current. Overexpression in mouse models indicates a role in cognition and neuronal plasticity. May also sensitise mice to epileptic spasms in response to baclofen.	Best <i>et al.</i> , 2012; Blichowski <i>et al.</i> , 2015; Chakrabarti <i>et al.</i> , 2010; Cooper <i>et al.</i> , 2012	Tc1 Dp1Tyb
<i>DYRK1A</i>	Protein kinase implicated in neuronal proliferation, differentiation and synaptic plasticity. Overexpression results in impairments in LTP and memory, and increased inhibitory neuron number. DYRK1A is also protective against PTZ induced seizures, and has been implicated in the hyperphosphorylation of tau in AD	García-Cerro <i>et al.</i> , 2014; Ryoo <i>et al.</i> , 2007; Souchet <i>et al.</i> , 2015; Grau <i>et al.</i> , 2014	Tc1 Dp1Tyb
<i>GRIK1</i>	GluK1 subunit of the kainate family of ionotropic glutamate receptors. Impact of overexpression is unknown, but implicated in regulation of excitatory and inhibitory neurotransmission, synaptic plasticity, and epileptogenesis.	Cossart <i>et al.</i> , 1998; Li <i>et al.</i> , 2010; Nisticò <i>et al.</i> , 2009; Rogawski <i>et al.</i> , 2003	Tc1 Dp1Tyb

Gene	Function	References	Model
<i>S100B</i>	Ca ²⁺ -binding protein expressed predominantly in astrocytes. Implicated in neuronal proliferation and migration in the developing brain, as well as apoptosis, inflammation and Ca ²⁺ homeostasis. <i>S100b</i> knockout mice show enhanced LTP, and <i>S100B</i> overexpression has been linked to memory impairments, exacerbated amyloidosis, gliosis, and a shift towards glial fate during development. Elevated <i>S100B</i> has been reported in a number of diseases, including Parkinson's disease, schizophrenia and epilepsy, and head trauma.	Bianchi <i>et al.</i> , 2011; Gerlai <i>et al.</i> , 1995; Lu <i>et al.</i> , 2011; Mori <i>et al.</i> , 2010; Nishiyama <i>et al.</i> , 2002; Sathe <i>et al.</i> , 2012	Tc1
<i>CSTB</i>	Thiol protease inhibitor. Mutations are linked to progressive myoclonic epilepsy.	Franceschetti <i>et al.</i> , 2007	Tc1
Mir-155	Negative regulator of SNX27, which plays a role in glutamate receptor trafficking. <i>Snx27</i> overexpression rescues synaptic deficits in a DS mouse model.	Wang <i>et al.</i> , 2013	Tc1 Dp1Tyb
<i>SIM2</i>	Transcription factor regulating neurogenesis. Overexpression leads to impairment on spatial memory tasks.	Chrast <i>et al.</i> , 2000; Ema <i>et al.</i> , 1999; Meng <i>et al.</i> , 2006; Rachidi <i>et al.</i> , 2005	Tc1
<i>DOPEY2</i>	Member of the dopey leucine zipper-like family. Shows homology with <i>c. elegans</i> gene <i>Pad1</i> , involved in embryonic patterning and cellular differentiation. Overexpressed by more than 50% in DS, with expression pattern corresponding to regions most affected by trisomy: hippocampus, cortex and cerebellum. Overexpression in mice leads to disrupted cortical lamination.	Lopes <i>et al.</i> , 2003; Rachidi <i>et al.</i> , 2009, 2005b	Dp1Tyb

Gene	Function	References	Model
<i>USP16</i>	De-ubiquitinating protein involved in chromatin modification and cell cycle progression. Overexpression reduces the capacity of neural progenitor cells and haematopoietic stem cells to self-renew.	Adorno <i>et al.</i> , 2013	Dp1Tyb
<i>SYNJ1</i>	Phosphoinositide phosphatase. Regulates clatherin mediated endocytosis, and overexpression induces enlargement of early endosomes	Cossec <i>et al.</i> , 2012; Herrera <i>et al.</i> , 2009; Voronov <i>et al.</i> , 2008	Dp1Tyb
<i>OLIG1/2</i>	Transcription factors implicated in neurogenesis. Normalisation of Olig1 and Olig2 in a mouse model of DS recues over-inhibition phenotype and misexpression of Olig2 in a mouse model contributes to disruption of neurogenesis and cortical lamination.	Chakrabarti <i>et al.</i> , 2010; Liu <i>et al.</i> , 2015	Dp1Tyb
<i>ITSN</i>	Scaffolding protein involved in endocytosis. Synaptic transmission and cell signalling. Expressed in proliferating and differentiating neurons and overexpressed in DS.	Hunter <i>et al.</i> , 2013; Pucharcós <i>et al.</i> , 1999	Dp1Tyb
<i>RCAN1</i>	Inhibitor of calcineurin-dependent signaling pathways. Overexpression in mice leads to deficits in hippocampal synaptic plasticity, reduced density of dendritic spines, reduced hippocampal volume and reduced adult neurogenesis.	Martin <i>et al.</i> , 2012	Dp1Tyb

1.3.4 Seizures in models of Alzheimer's disease and Down syndrome

The contribution of A β to network hyperexcitability has been investigated in a number of transgenic models. The J20 model has been the most extensively characterised in regards to hyperexcitability, and has been reported to experience spontaneous non-convulsive seizures. These are associated with ectopic expression of Neuropeptide Y (NPY), a neuronal marker of recurrent seizure activity. However, mossy fibre sprouting, which is generally observed together with aberrant NPY expression in temporal lobe epilepsy models was not present in the J20 mice (Palop *et al.*, 2007), suggesting the J20 animals share some, but not all of the network modifications which occur in temporal lobe epilepsy. A β may therefore induce specific network changes, which differ from those underlying other forms of epilepsy.

NPY alterations were confirmed in two further mutant human-*APP* overexpressing lines, but absent from a wildtype human-*APP* overexpressing line, indicating that wildtype *APP* is not sufficient to produce this phenotype (Palop *et al.*, 2007). Spontaneous seizures and ectopic NPY expression have also been reported in the *APP_{swe}/PSEN1 Δ E9* mouse, where they have been linked to abnormal A β -mediated hyperexcitability in neocortical layer 2/3 pyramidal cells (Minkeviciene *et al.*, 2009). Reduction in *APP* is also associated with increased susceptibility to seizures in response to a kainic acid challenge, suggesting that *APP* level may have a role in the physiological regulation of network excitability, independently of A β toxicity (Steinbach *et al.*, 1998). Interestingly, knockout of tau appears to be protective against seizures in both *APP* overexpression lines (Ittner *et al.*, 2010) and non-*APP* mediated genetic epilepsy models (Holth *et al.*, 2013), indicating tau may independently contribute to epileptogenesis.

However, the relationship between seizures and A β in the J20 mice has recently been called into question; genetic suppression experiments indicate that epileptiform activity may be related to overexpression of *APP* itself, rather than A β , and that such overexpression during development may be particularly detrimental (Born *et al.*, 2014). If this is the case, it may limit the mechanistic relevance of this model for seizures in sporadic AD. Despite this, as *APP* is duplicated in the DS population, it can still provide insight into the interactions of *APP* and other Hsa21 genes, although degree of overexpression combined with the presence of two disease mutations is likely to exacerbate and potentially modify the observed phenotypes.

Limited characterisation of seizure risk has been carried out in mouse models of DS. There are indications that the audiogenic seizure threshold may be reduced in both the Tg2575 model of AD and the Ts65Dn model of DS, through an A β and mGluR5 dependent mechanism (Westmark, Westmark and Malter, 2010). In addition, spontaneous epileptiform spike-wave discharges have been observed in Ts65Dn mice (Cortez *et al.*, 2009), which were exacerbated by the GABA_B receptor agonists baclofen and γ -butyrolactone, resulting in extensor spasms and an EEG pattern reminiscent of hypsarrythmia — characteristic of infantile spasms. Increased GABA_B mediated potassium current, due to duplication of the *GIRK2* potassium channel gene, was proposed as a mechanism. Conversely, duplication of the Hsa21 gene *CSTB*, which is linked to progressive myoclonic epilepsy, has been shown to have no impact on seizure threshold (Brault *et al.*, 2011), suggesting other Hsa21 genes must be involved. These results provide an indication that seizure susceptibility is enhanced in Ts65Dn mice, although this has yet to be replicated in other DS models.

1.3.5 *Tc1* × *J20* mouse cross

Previous work in the *Tc1* × *J20* cross has demonstrated that the interactions between *tgAPP* and trisomy 21 exacerbate A β deposition (**Figure 1.7**; Wiseman *et al.*, in preparation) and cause novel impairments in short-term memory (**Figure 1.7**; Wiseman *et al.*, in preparation) in the double transgenic animals. The mechanism for these memory impairments is not known, but they precede the onset of A β pathology, suggesting that they do not result from an increase in plaque load.

Furthermore, *tgAPP* is associated with increased mortality in the *J20* mice within the first 6 months of life, after which risk appears to stabilise (**Figure 1.7**; Wiseman *et al.*, in preparation). The cause of death in these animals is unknown, but a subset of *J20* mice are known to develop spontaneous seizures, and the peak in mortality reflects the developmental timeframe for epilepsy onset. The *Tc1*×*J20* mice show a similar initial increase in mortality, however the risk does not appear to stabilise with age, which would be consistent with a modification of the progression or severity of the epilepsy phenotype by trisomy 21. However, it could also suggest that interactions between trisomy 21 and *tgAPP* result in a novel mechanism, which contributes to an increased risk of mortality in aged *Tc1*×*J20* animals.

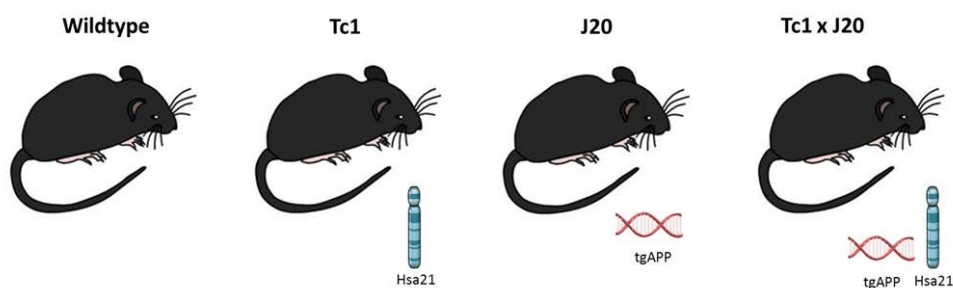


Figure 1.5 Illustration of the four genotypes produced by the *Tc1*×*J20* cross

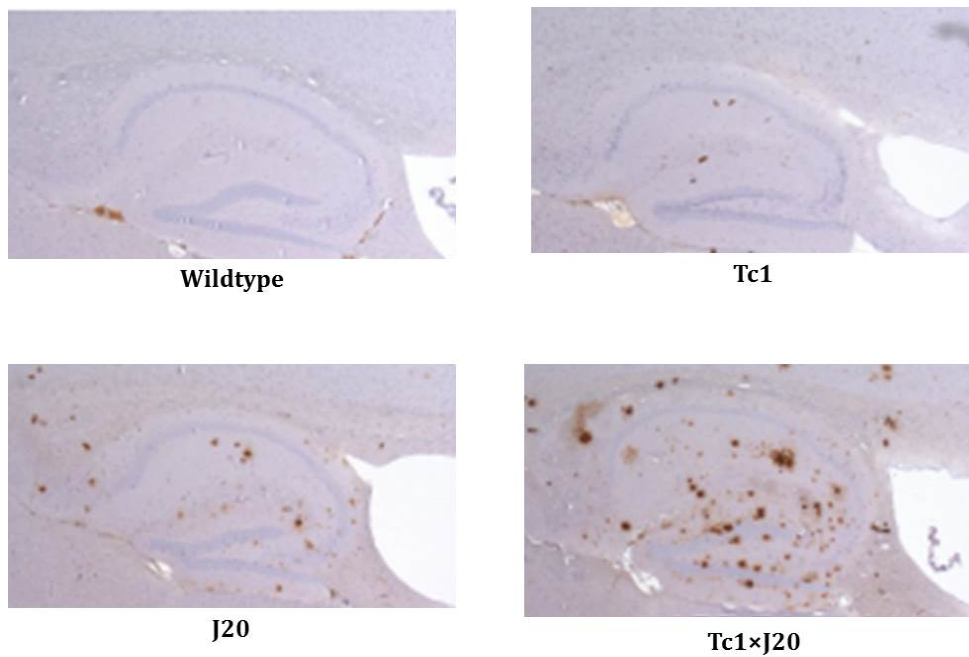


Figure 1.6 Aβ deposition in the Tc1xJ20 cross

Examples of Aβ deposition in the hippocampus and cortex of wildtype, Tc1, J20, Tc1xJ20 animals at 16 months of age (Frances Wiseman et al., unpublished data)

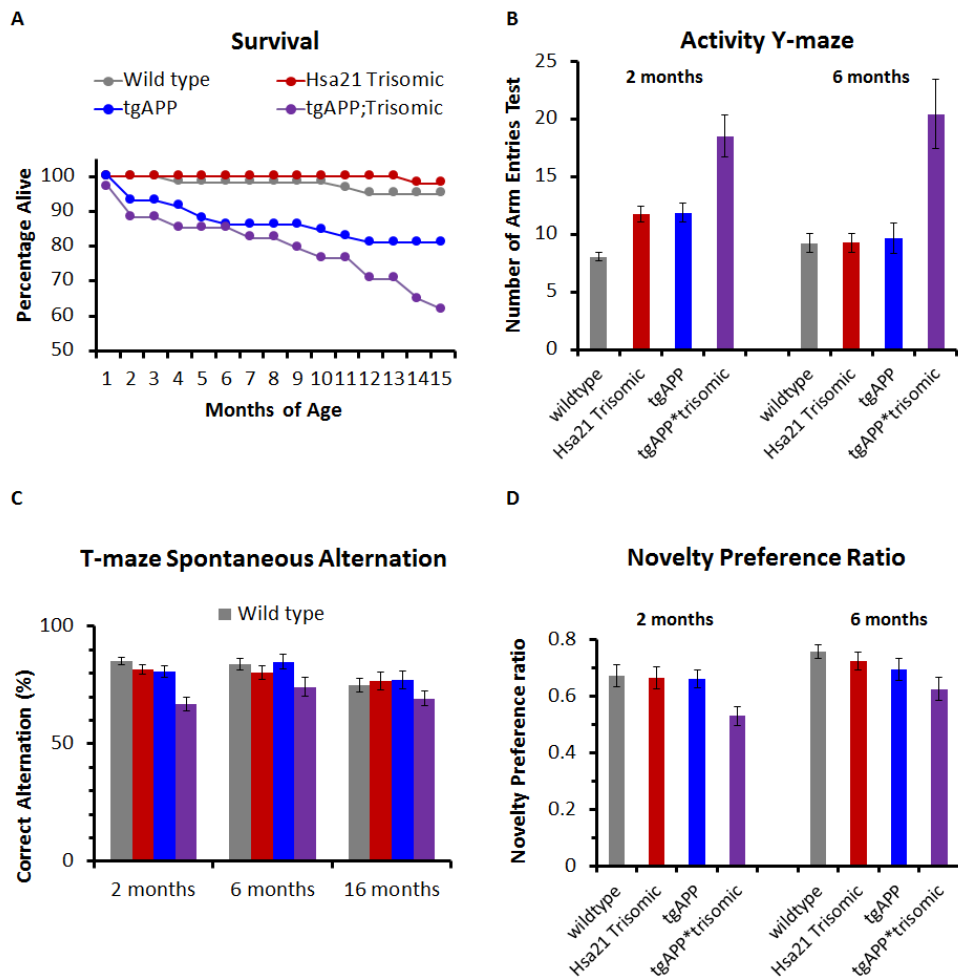


Figure 1.7 Behavioural phenotypes in the Tc1xJ20 cross

A) Trisomy of Hsa21 significantly decreases survival of tgAPP mice up to 15 months of age (Chi-squared = 3.88 $p = 0.048$). **B)** In the test phase of a Y-maze novelty preference task, the number of arm entries was increased by trisomy ($F(1,89) = 50.360$ $p < 0.001$) and by tgAPP ($F(1,89) = 47.001$ $p < 0.001$), with a significant interaction ($F(1,89) = 31.720$ $p < 0.001$). **C)** In a longitudinal spontaneous alternation task testing short-term memory (1 minute between first placement and test), interaction between trisomy and tgAPP resulted in a significant deficit (Trisomy*tgAPP $F(1,67) = 4.706$ $p = 0.034$). **D)** In a spatial novelty preference task testing short-term memory (1 minute inter-trial interval), the novelty preference ratio (time spent in the novel arm relative to time spent in the familiar arm) was impaired in mice carrying tgAPP in combination with trisomy (Trisomy*tgAPP transgene $F(1,89) = 5.736$ $p = 0.019$). All figures display group means, error bars SEM. (Frances Wiseman et al, unpublished data)

1.4 Thesis aims

1.4.1 Aims

As memory impairments are commonly associated with deficits in synaptic plasticity, this thesis aims to investigate whether, in addition to causing novel behavioural deficits, interactions between *tgAPP* (human APP with AD-associated point mutations) and trisomy 21 contribute to novel impairments in synaptic plasticity.

In addition, as both *tgAPP* and trisomy 21 have been linked to increased susceptibility to seizures, this thesis aims to determine whether increased mortality resulting from interactions between *tgAPP* and trisomy 21 relates to an increase in risk or severity of seizures, and whether seizures contribute to any observed deficits in synaptic plasticity.

1.4.2 Hypotheses

1. Interactions between *tgAPP* and trisomy 21 result in impaired synaptic plasticity at the medial perforant path to dentate granule cell synapse
2. Interactions between *tgAPP* and trisomy 21 result in an increased risk and/or severity of seizures

Chapter 2

Materials and Methods

2.1 Animal husbandry

All experiments were carried out in accordance with the Animals (Scientific Procedures) Act 1986 and Home Office Project License numbers 70/7684, 30/2758 and 30/3312.

Mice were housed in individually ventilated cages (Techniplast, Italy) with a 12 hour light dark-cycle (light phase: 7am – 7pm) and ad libitum access to food and water. Nesting materials and cardboard mouse tunnels or houses were provided for environmental enrichment. Mice were weaned at 21 days, and group housed with littermates of the same gender, with a maximum of 5 animals per cage. No animals were individually housed for a period in excess of 24 hours prior to experimental use, in order to minimize stress to the animal.

Mice were sacrificed between 5.5 and 7 months for a 6-month experimental time point and between 2.5 and 4 months for a 3-month experimental time point. Implantation of telemetry electrodes was carried out at between 4.5 and 5 months. Animals were ear notched for identification and genotyping, and genotype was confirmed by post-mortem tail biopsy. All experiments and analyses were conducted blind to genotype, and animals were identified using a numerical signifier. All experimental procedures were conducted in male mice to eliminate

variability resulting from the oestrus cycle, with the exception of NPY in the 16-month cohort which included both genders.

Tc(HSA21)1TybEmcf (Tc1) mice were generated by mating Tc1 females with F1 129S8×C57BL/6 males, as maternal transmission of the Hsa21 is more effective. The mice were bred on a hybrid 129S8×C57BL/6 background as transmission of the additional chromosome cannot be maintained on an inbred background. B6.Cg-Tg(PDGFB-APPSwInd)20Lms/2Mmjax (J20) were generated by mating J20 males to C57BL/6J females, as transgenic females exhibited deficits in maternal behaviour, and the Tc1 × J20 cross was generated by breeding Tc1 females with J20 males. C57BL/6J.129P2-Dp(16Lipi-Zbtb21)1TybEmcf (Dp1Tyb) mice were generated by mating male or female Dp1Tyb mice with C57BL/6J animals.

2.2 Hippocampal slice electrophysiology

2.2.1 Generation of isolated hippocampal slices

Electrophysiology was performed in transverse acute hippocampal slices. To generate slices, mice were transcardially perfused under terminal anaesthesia. Anaesthesia was induced with an intraperitoneal injection of 0.5ml 1mg/ml pentobarbital (Euthetal, Merial Animal Health, UK) and sufficient depth of anaesthesia was established by testing for loss of the pedal withdrawal reflex. Injections were administered following brief sedation in an isoflurane induction chamber (Cliniscav system, Clinipath Equipment Ltd, UK), using 4% 1mg/l isoflurane vapour (Isothesia, Henry Schein Animal Health, UK) to minimize stress to the animal.

Animals were perfused with NMDG-aCSF (**Table 2.1**) saturated with carbogen (5% carbon dioxide/95% oxygen, BOC, UK). The Na⁺

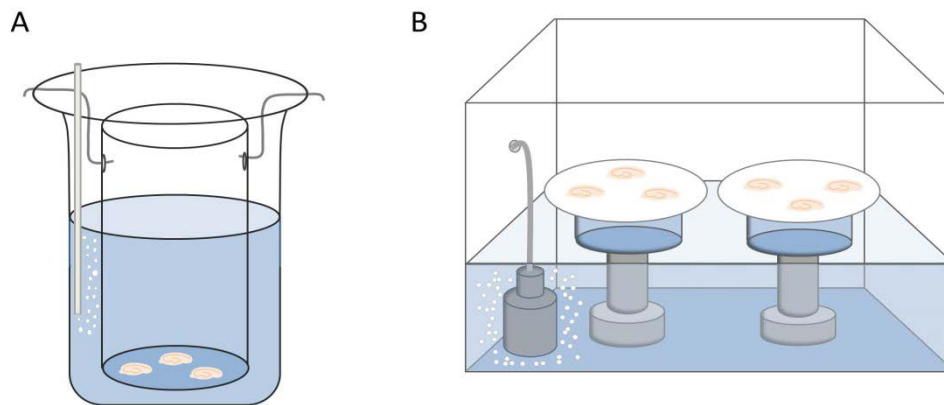


Figure 2.1 Storage of slices

A) Illustration of submerged chamber used for slice recovery **B)** Illustration of interface chamber used for slice storage

replacement N-methyl-D-glucamine (NMDG) was used as removing Na^+ from the extracellular solution blocks neuronal activity, therefore reducing excitotoxic damage to slices due to hypoxia during brain removal and slicing (Ting *et al.*, 2014).

Following perfusion, the brain was rapidly removed from the skull and placed into room temperature carbogenated NMDG-aCSF (**Table 2.1**) for dissection. Hippocampi were isolated from the brain and embedded in a block of 3% agar into which a small vertical groove was cut for each hippocampus. The agar was then secured into the slicing chamber using superglue and transverse hippocampal slices were generated using a Leica VT1200S vibrotome at a speed of 12mm/s, with a thickness of 350 μm .

Slices were left to recover in a submerged chamber containing carbogenated NMDG-aCSF. The recovery chamber was heated using a water bath set to 34°C, and the water bath was monitored with a thermometer to ensure a constant temperature was maintained. After 15 minutes, slices were removed from the recovery chamber and washed in storage-aCSF (**Table 2.1**) to remove residue of NMDG. They

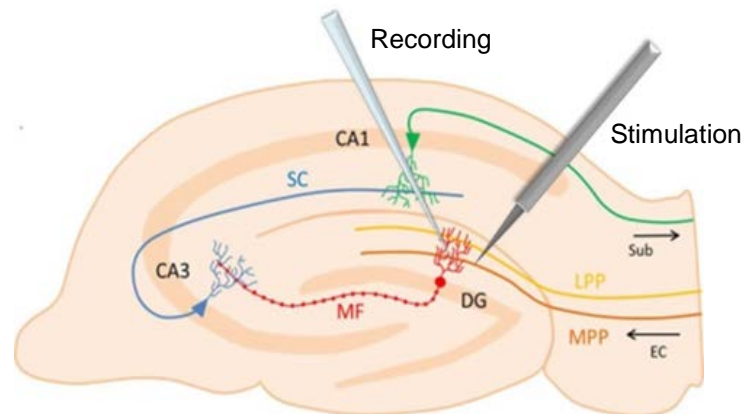


Figure 2.2 Location of recording and stimulation electrodes in the MPP

were then transferred to an interface chamber for storage (**Figure 2.1**). The interface chamber was stored at room temperature; this was normally between 22-25°C. In the chamber, slices were placed on a sheet of filter paper over an internal chamber containing storage-aCSF. The base of the external chamber was filled with carbogenated water to maintain a humid environment, in order to prevent the slices from dehydrating.

2.2.2 Solutions

All solutions were made using ultrapure water, purified at 15M Ω /cm using the PURELAB System (ELGA, UK) and all reagents were purchased from Sigma Aldrich (MO, USA) unless otherwise specified. Osmolality was maintained between 300-320mOsm, and pH between 7.3 and 7.4. Solutions were pH adjusted via the addition of 5M HCl. All solutions were made fresh and stored at 4°C for a maximum of 72 hours.

Table 2.1 Composition of aCSF

	NMDG-aSCF		Storage-aCSF		Recording-aCSF	
	g/L	mM	g/L	mM	g/L	mM
NaCl	-	-	6.95	119	6.95	119
KCl	0.19	2.5	0.186	2.5	0.186	2.5
MgSO ₄	-	-	0.32	1.3	0.32	1.3
NaH ₂ PO ₄	0.15	1.2	0.112	1.25	0.112	1.25
NaH ₂ CO ₃	2.52	30	2.21	25	2.21	25
Glucose	4.5	25	1.8	10	1.8	10
NMDG	17.96	93	-	-	-	-
HEPES	4.77	20	-	-	-	-
Sodium Ascorbate	0.99	5	-	-	-	-
Thiourea	0.15	2	-	-	-	-
Sodium Pyruvate	0.33	3	-	-	-	-
MgCl ₂	2.03	10	-	-	-	-
CaCl ₂ (1mM solution)	-	-	-	-	2.5ml	2.5

2.2.3 Recording and stimulation

All recordings were made at room temperature, in circulating carbogenated recording-aCSF (**Table 2.1**). Extracellular postsynaptic field potentials (fEPSPs) were recorded from the middle third of the molecular layer of the DG (Error! Reference source not found.) using a borosilicate glass microelectrode (Harvard apparatus, MA, USA). Recordings were made using a NeuroLog amplifier (Digitimer, UK) and a BNC-2090 digitizer (National Instruments, TX, USA). A HumBug (Quest Scientific, BC, Canada) was used to counteract the 50-60Hz noise resulting from mains hum. Responses were recorded using the program WinWCP v4.7.6 (Strathclyde Electrophysiology Software, UK) with a sampling interval of 0.122 ms. Stimulation was administered to the medial perforant path using a concentric microelectrode (ROYEM Scientific, UK) attached to a DS3 stimulator (Digitimer, UK). Recordings were low pass filtered at 500Hz.

All recordings were made using the stimulus intensity which elicited half of the maximal response. This was generally between 0.2 mV and 0.4mV, unless this resulted in a population spike which would have interfered with slope analysis. If this was the case, stimulation intensity was reduced to eliminate the population spike; however, this represented a minority of cases with no bias for genotype. Stimulus duration was set at 0.5ms and remained unchanged for all experiments. A paired stimulus with an interval of 50ms was used for baseline recordings before and after LTP induction, with a 20s interval between each recording sweep to ensure baseline stimulation was below the threshold for the induction of synaptic plasticity.

Input-output curves were obtained for a stimulation range of 0.1–0.8mV, at 0.1mV intervals. Paired pulse ratios were measured prior to the start of LTP or LTD protocols for inter-stimulus intervals of 25ms, 50ms, 100ms, 200ms and 400ms. LTP was induced by 4 trains of 50 pulses at 100Hz with a 30 second interval between each train (Bostrom *et al.*, 2013) and LTD was induced by a single train of 900 pulses, at 1Hz (Huang, Rowan and Anwyl, 1999). Initial responses were recorded 20s after the end of the LTP or LTD induction protocol

Chemical LTP was induced by exposure to recording-aCSF containing 50 μ M forskolin (Tocris, UK) for 15 minutes. Potentiation was recorded following wash-out with 10mls recording-aCSF. GABA_A receptor block was achieved with by the addition of picrotoxin (Tocris, UK) to the recording-aCSF at a concentration of 50 μ M for the duration of the recording.

2.2.4 Analysis of LTP data

Recording sweeps were averaged as blocks of 9 in WinWCP, with each resultant trace representing 3 minutes of responses. The gradient of the initial fEPSP slope was fitted in WinWCP with a linear function. The change in initial fEPSP slope following LTP or LTD is reported as a percentage of baseline. Baseline values are calculated using the average gradient of the initial fEPSP slope over the final 10 minutes of baseline prior to LTP or LTD induction. For input-output and paired pulse ratio measurements, 6 sweeps, with 20 second intervals between sweeps were averaged for each data point shown. Post-tetanic potentiation and short-term depression were analysed based on the first two data points following potentiation or depression, representing the first 40s of recording after the administration of the LTP or LTD protocol.

2.3 Electroencephalography

2.3.1 Implantation of subcutaneous EEG transmitters

Prior to surgery, animals were anaesthetised in an anaesthetic chamber (Cliniscav system, Clinipath Equipment Ltd, UK), using 4% 1mg/l isoflurane vapour (Isothesia, Henry Schein Animal Health, UK), then maintained on approximately 1.5% isoflurane 1mg/l isoflurane vapour administered via a nose cone throughout the procedure. Anaesthesia depth was closely monitored throughout the surgery adjusted throughout when necessary to ensure breathing rate remained stable and no pain reflexes were present. All animals received 0.3ml saline before and after surgery to prevent dehydration. Following surgery, 0.06ml 1.5mg/ml Metacam (Boehringer Ingelheim, Germany) and 0.04 ml 0.03mg/ml buprenorphine (Vibec, France) analgesia were given subcutaneously to control pain.

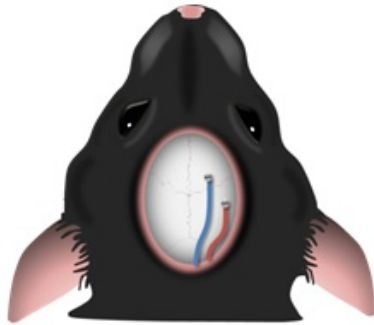
A**B**

Figure 2.3 EEG transmitter implantation

A) Illustration showing implantation of the EEG transmitter **B)** Photograph of a transmitter

Dp1tyb mice and their wildtype littermates were given 15 mg/kg Betamox (Norbrook, UK) antibiotic in addition to analgesia, as the duplication in the Dp1Tyb mice appeared to increase susceptibility to infection in initial experiments. Although immune function has not been investigated in this strain, an immunodeficiency phenotype would not be unexpected as immunological problems are common in DS patients (Ram and Chinen, 2011).

Prior to transmitter implantation, an electric razor was used to remove the fur on the back and head of the mouse surrounding the implantation site, and 10% iodine solution was applied to the shaved region with sterile cotton swabs to disinfect the skin. Viscotears gel (Alcon, TX, USA) was applied to the eyes to prevent them drying out during surgery, as they remain open while under isoflurane anaesthesia.

A stereotaxic frame (David Kopf Instruments, CA, USA) was used to keep head position stable during surgery and coordinates of the motor and parietal cortex were determined using the Allen mouse brain atlas. Small holes were drilled into the skull above the right parietal cortex

(stereotaxic coordinate -2.06, +2.50, with reference to bremga) and right motor cortex (stereotaxic coordinates +1.00, +1.5, with reference to bremga). A third hole was drilled in the left hemisphere, approximately at the central point between the two right hemisphere screws. This triangular configuration enhances the stability of the headpiece (**Figure 2.3**).

A small horizontal incision was then made in the skin of the back. The transmitter was inserted subcutaneously through the incision and wires were run from the transmitter around the side of the neck. Bare wires of approximately 1mm were inserted into the right parietal and motor cortices. These were then secured in place using stainless steel mounting screws for mice with a shaft diameter of 1.19 and a shaft length of 1.6mm (Plastics One, MN, USA). The headpiece was sealed with vetbond (3M, MN, USA) and dental cement. The skin over the transmitter was sutured using single stitching to minimise the chances of the incision reopening if individual stitches were lost. A heat mat was placed under the animals throughout surgery to prevent hypothermia, and animals were kept under a heat lamp or in an incubation chamber during recovery.

In accordance with the project license, animals with missing stitches or damaged headpieces were re-anaesthetised in order to carry out repairs, so long as there were no signs of distress or infection. However, if any further damage occurred after the initial repair, the experiment was terminated. Post-surgical outcomes are detailed in **Table 2.2**.

Table 2.2 Post-surgical outcomes

	Number of animals	Number of animals requiring repeat anaesthesia	Number of experiments terminated
Tc1xJ20 Cohort 1	10	2	1
Tc1xJ20 Cohort 2	9	1	0
Dp1Tyb Cohort 1	7	4	4
Dp1Tyb Cohort 2	4	0	0

2.3.2 EEG recording

EEG was recorded in freely moving animals continuously over a period of 3 – 6 weeks, dependent on transmitter type, using intracranial electrodes connected to subcutaneous transmitters. All equipment was obtained from Open Source Instruments (Massachusetts, USA). Single channel transmitters with bare-wire electrodes were used for all recordings. Transmitters had a volume of 1.4ml, with body dimensions of 14 mm × 14 mm × 8 mm and a 50-mm antenna loop.

For 3-week recordings, transmitter A3028B-AA was used. These transmitters have a 600h battery life, a voltage dynamic range of 20-mV, a frequency dynamic range of 0.3-160 Hz, and a sampling rate of 512 samples per second (SPS). For 6-week recordings, transmitter A3028C-AA was used. These transmitters also have a voltage dynamic range of 20-mV, but a longer battery life of 950h and a reduced frequency dynamic range of 0.3-80 Hz, along with a reduced sampling rate of 256 SPS.

Individually ventilated cages were placed inside a faraday cage or in a mesh covered cage rack to prevent interference in radio transmission between the subcutaneous transmitters and receiving antennae. To maximize signal transmission, multiple antennae were placed around

the cage, and were connected to an antennae combiner. The antennae combiner was connected to a data receiver, which decoded the received signals. An LWDAQ driver provided power and internet connectivity for the data receiver. Signals were then transmitted via the internet to a remote computer and recorded using the LWDAQ recording software. Data was saved in NDF file format.

2.3.3 Automated seizure detection

Automated seizure detection was performed by running the ECP16V1 processing script on all NDF files, using Neuroarchiver v101 (software available at <http://alignment.hep.brandeis.edu/Software/>). This script calculates numerical metrics with a value between 0 and 1 for 6 EEG properties: power, coastline, intermittency, coherence, asymmetry, and rhythm, over each second of EEG (source code available at: http://www.opensourceinstruments.com/Electronics/A3018/Seizure_Detection.html; **Annex A**).

The Power metric is calculated using the standard deviation from the mean of the signal, and reflects the absolute amplitude of the signal. The other metrics are normalised to signal amplitude and reflect the properties of the EEG signal rather than the strength. Coastline is the sum of the changes in signal value between each sample, normalised to the interval range, and reflects the degree of fluctuation in the signal. Intermittency reflects the spread of change in coastline throughout the EEG segment, and is a measure of the amount of change accounted for by the 20% of samples showing the greatest change, divided by the total coastline. Rhythm is a measure of the strength of the oscillatory component for the segment of EEG. Coherence measures the average absolute change in signal value between peaks and valleys in the signal which have a height of 10% of the signal range or greater. Asymmetry is

calculated using the ratio $(\text{maximum signal value} - \text{average signal value}) / (\text{minimum signal value} - \text{average signal value})$ and therefore differentiates between upward, downward, and symmetrical spikes. The resulting values are then passed through a sigmoidal function to obtain better separation of data points.

A library of 1-second EEG segments containing visually identified examples of seizure and interictal activity was created using the 'event classifier' feature in Neuroarchiver v101. Examples of baseline EEG and movement artefacts were also included in the library to aid classification. This event library was compared against the metric values for each second of recorded EEG from all animals. If all the metrics of an EEG segment were within a specified threshold of the values in the library, it was classified as an event. The threshold used was 0.04 for interictal spikes and 0.1 for seizures. The power threshold for events was set at 0.4. All output was checked manually to exclude false positives.

Although a seizure is defined by the behavioural correlate of abnormal brain activity rather than the activity itself, the telemetry set up used did not include video monitoring so the seizures referred to here have been identified electrographically. Seizures were defined as high frequency and high amplitude spiking activity lasting longer than 10s. This is generally considered the minimum length of abnormal activity required impact on behaviour in a clinical setting. Any spiking lasting less than 10 seconds was classified as 'interictal'. Although any fixed limit on seizure duration is by necessity arbitrary, all identified seizures significantly exceeded this limit, so the limit will not confound analysis.

2.3.4 Power analysis

EEG power was calculated using the Powerspectrum processor (**Annex B**) in Neuroarchiver v.101. This processing script performs a Fourier transform over 1 second segments of EEG, and returns the sum of squares for the frequency components within 8 specified bands: 1-4Hz (Delta), 4-8Hz (Theta), 8-12Hz (Alpha), 12-30Hz (Beta), 30-50Hz (Gamma), 50-70Hz, 70-120Hz and 120-160Hz. 160Hz represents the upper limit of the transmitter bandwidth. The output file of this script contains the power value for every second in each 1 hour NDF file. NDF files containing movement artefact were manually excluded from the analysis. To calculate average power for each genotype, all segments of EEG over the recording period for each animal of that genotype were averaged. In order to account for variation in electrode depth and position, all power bands were normalised to total power for the individual animal, calculated as the sum of the average power across all powerbands. To calculate circadian changes in EEG power, all seconds recorded over each a 1 hour period were averaged for all animals of each genotype, and normalised to total power. Analysis was performed using a custom python script (**Annex C**).

2.4 Histology

2.4.1 *Perfusion for paraffin embedding*

Following termination of EEG recording, mice were transcardially perfused (procedure as previously described in **section 2.2.1**) with 1× Phosphate Buffered Saline + heparin (80mg/L) until perfusate ran clear, followed by 10% Buffered Formalin (BFS). Brains were removed and bisected down the midline with a scalpel and then immersion fixed in 10ml BFS for 24h at 4C.

2.4.2 *Tissue processing*

Tissue processing was performed by Dr. Susanna Noy (Department of Neurodegenerative Disease, UCL Institute of Neurology). Neuropeptide Y (NPY) immunohistochemistry for the 16-month time point was performed on 4µm sections from previously sectioned brains from the Tc1 × J20 cross due to restrictions on the aging of current cohorts. NPY immunohistochemistry for the 6-month time point was performed on brains taken from the Tc1 × J20 EEG mouse cohorts, following the termination of EEG recording, in order to correlate electrographic phenotypes with histology. The left and right hemispheres were placed into plastic cassettes and processed overnight. Processing was performed under vacuum in a Leica ASP300S tissue processor. Tissue was dehydrated through a graded series of alcohols and cleared in xylene, then infiltrated with paraffin wax. The blocks were orientated sagittally and embedded in fresh wax using a Leica embedding centre (EG1150H) and cold plate. The blocks of tissue were trimmed laterally from the midline by approx. 0.9-1.4mm to produce a sagittal section of the hippocampal formation. A Leica RM2135 rotary microtome was

used to cut 4 μ m thick sections. Sections were dried overnight at 40°C before immunostaining for NPY.

2.4.3 IHC Staining of formalin fixed paraffin wax embedded sections for NPY

NPY staining protocol is shown in **Table 2.3: NPY staining procedure (Provided by Dr. Susanna Noy)**. Staining was carried out using the Ventana XT automated stainer (Roche Diagnostics). The sections were dewaxed, rehydrated and heat pre-treated for 60min in a Tris Boric Acid EDTA buffer pH9.0 (Standard CC1). They were then incubated in blocking solution for 8min (SuperBlock, ThermoFisher, MA, USA) prior to

Table 2.3: NPY staining procedure (Provided by Dr. Susanna Noy)

Step	Reagent	Conc / Dilution	Time	Temp
Fixation	NBF	10%	48hrs	RT
Wash	Reaction Buffer Ventana			
Pre-treatment	Standard CC1			
Wash	Reaction Buffer Ventana			
Enzyme Block				
Wash	Reaction Buffer Ventana			
Biotin Block				
Wash	Reaction Buffer Ventana			
Serum Block	Superblock	Neat	8 mins	
Primary Ab	Ab10980	1:5000	12hrs	
Wash	Reaction Buffer Ventana			
Secondary Ab/ Polymer Link	Biotinylated Swine anti-Rabbit	1:200	60 mins	
Wash	Reaction Buffer Ventana			
Tertiary Reagent	DABMap - Ventana			
Wash	Reaction Buffer Ventana			
Substrate	DAB - Ventana			
Wash	Reaction Buffer Ventana			
Counter-stain	Heamatoxylin - Ventana		4 mins	RT
Wash	Reaction Buffer Ventana			
Blueing Agent	Blueing - Ventana		4 mins	RT
Wash	Reaction Buffer Ventana			
Mountant	DPX	Neat		

titration of 100µl of primary antibody per slide. (Rabbit polyclonal IgG whole serum raised against full length porcine NPY Abcam Ab10980 1:5000). The sections were incubated for 12hrs in primary antibody, then for 30 minutes in biotinylated swine anti-rabbit secondary antibody (diluted 1:200). The immunostaining was visualised using the Ventana HRP DabMap kit. The sections were counterstained with haematoxylin, then washed in distilled water, dehydrated, cleared and mounted in DPX prior to being microscopically assessed.

2.4.4 Imaging and analysis of NPY immunohistochemistry

Digital images of the stained slides were acquired a Leica SCN400F Slide Scanner (Leica Microsystems) by Dr. Matthew Ellis (Department of Neuropathology, UCL Institute of Neurology) with 40x magnification. Images were stored on the Leica Slidepath image management system (Leica Microsystems). NPY staining was quantified as percentage area coverage using Definiens Tissue Studio software.

2.5 Genotyping

2.5.1 DNA extraction

DNA extraction and genotyping were performed by Matthew Rickman (Department of Neurodegenerative Disease, Institute of Neurology). DNA extraction was carried out using a protocol adapted from Truett *et al.*, (2000). A 1-2 mm tail (post-mortem) or ear (post-weaning) biopsy sample was placed in a 1.5 mL Eppendorf tube containing 75 µL of NaOH Extraction Solution (25 mM NaOH, 0.2 mM EDTA) (***Table 2.4 Solutions for DNA extraction***) then incubated in a hotblock at 98°C for 1 hour. 75 µL of Tris Neutralization Buffer (40 mM Tris-HCl, pH 5.5) was added, and the tube was briefly vortexed then centrifuged at maximum

speed in benchtop micro-centrifuge at room temperature for 5 minutes, to pellet cell debris. The pellet was then discarded and supernatant containing soluble DNA was taken as a template for genotyping PCR.

2.5.2 PCR for Tc1 and J20

Genotyping was carried out by polymerase chain reaction (PCR). PCR was conducted in parallel for both Hsa21 and tgAPP in all biopsy samples. PCR primers (Eurofins, Luxembourg) were reconstituted in ddH2O from desalted lyophilised pellets at a concentration of 100 µM and stored at -20°C. This was used to make 5 µM aliquots. The PCR protocol for the J20 strain was based on the Jackson laboratory protocol (available at: https://www2.jax.org/protocolsdb/f?p=116:5:0::NO:5:P5_MASTER_PROTocol_ID,P5_JRS_CODE:6839,006293) and the PCR protocol for the Tc1 was developed by O'Doherty *et al.*, (2005).

DNA was diluted 1:5 in ddH2O. 1 uL of diluted DNA from each sample was loaded into PCR tubes (Starlabs, Germany) and added to a mastermix containing 8uL MegaMix Blue (Microzone, UK) with 1 uL of either Tc1 or J20 primer mix (**Table 2.5** PCR reaction). Primers are

Table 2.4 Solutions for DNA extraction

NaOH Extraction Solution			Tris Neutralization Buffer		
Stock solution	Volume added	Final Conc.	Stock solution	Volume added	Final Conc.
2M NaOH	187.5 µL	25 mM	1M Tris-HCl pH 5.5	600 µL	40 mM
0.5M EDTA, pH 8.0	6 µL	0.2mM	PCR grade water	14.4 mL	-

listed in **Table 2.8 Tc1 PCR Primers** and **Table 2.9 J20 PCR Primers**. Samples were run on a thermal cycler with the cycle settings listed in **Table 2.6 Tc1 PCR Cycle** and **Table 2.7 J20 PCR Cycle**. Each set of samples was run with a tgAPP+ or Hsa21+ positive control, a wildtype negative control, and a no amplification control, containing no DNA.

Amplified PCR product was run on a 2% agarose gel. To make the gel, 2g agarose (Invitrogen, CA, USA) was dissolved in 100 ml 1× heated TBE buffer (National Diagnostics, GA, USA) and 0.05µg/ml of ethidium bromide (Sigma-Aldrich, MO, USA) was added to allow visualisation of DNA. Agarose gel was then poured into gel cast and left to set.

Gel electrophoresis was run at 120V for 1hr 30 mins in 1× TBE on a Horizon 11.14 Gel Casting System (Thistle Scientific, UK). HyperLadder™ 100bp (Bioline, UK) was used as a marker for molecular weight. Digital images of the gels were acquired by UV imaging using the Bio-Rad Gel Doc XR system and Quantity One software (version 4.5.1, Bio-Rad, CA, USA)

2.5.3 Genotyping for Dp1Tyb

Genotyping for Dp1Tyb mice was outsourced to Transnetyx (TN, USA) for automated genotyping via a proprietary real-time PCR based assay. Transnetyx designed custom qPCR probes (**Table 2.12**) mapping to the 5' and 3' breakpoints of the duplicated region of the chromosome to determine presence or absence of the duplication.

Table 2.5 PCR reaction

PCR Component	Volume (ul)
MegaMix blue	8
Tc1 primer mix	1
DNA	1
Total Volume	10

Table 2.6 Tc1 PCR Cycle

Stage	Temp	Time	
Mega-mix hot-start	95 °C	3 min	
Denature	94°C	45s	
Anneal	65°C	45s	Repeat x 30
Extend	72°C	60s	
Final Extend	72 C	10 min	

Table 2.7 J20 PCR Cycle

Stage	Temp	Time	
Mega-mix hot-start	95 °C	3 min	
Denature	95°C	30s	
Anneal	62°C	1 min	Repeat x 35
Extend	72°C	45s	
Final Extend	72 C	10 min	

Table 2.8 Tc1 PCR Primers

Primer	Sequence	Target
D21S55R	5'-ACAGAGCTACAGCCTCTGACACTATGAACT -3'	Tc1
D21S55	5'-GGTTTGAGGGAACACAAAGCTTAACTCCCA -3'	Tc1
MyoF	5'-TTACGTCCATCGTGGACAGCAT -3'	Control
MyoR	5'-TGGGCTGGGTGTTAGTCTTAT -3'	Control

Table 2.9 J20 PCR Primers

Primer	Sequence	Target
oIMR2044	5'-ggTgAgTTTgTAAgTgATgCC -3'	J20
oIMR2045	5'-TCTTCTTCTTCCACCTCAgC -3'	J20
oIMR0015	5'-CAAATgTTgCTTgTCTggTg -3'	Control
oIMR0016	5'-gTCAgTCgAgTgCAAgTTT -3'	Control

Table 2.10 Tc1 Primer Mix

Primer	Volume (ul)	Final Conc.
D21S55R	20	10 pmol
D21S55F	20	10 pmol
MyoF	10	5 pmol
Myo R	10	5 pmol
H2O	140	

Table 2.11 J20 Primer Mix

Primer	Volume (ul)	Final Conc.
D21S55R	20	10 pmol
D21S55F	20	10 pmol
MyoF	10	5 pmol
Myo R	10	5 pmol
H2O	140	

Table 2.12 qPCR primers and probes for Dp1Tyb

	Zfp295-1 KO (5' breakpoint)	Zfp295-3 KO (3' breakpoint)
Forward Primer	5'-CCTAAGTCCTTGTCCTCACA-3'	5'-CGGGCCTCTTCGCTATTACG-3'
Reverse Primer	5'-GCAGTTGTTTAACTTCT AGAGAATGAGTTC-3'	5'-CTCTCTCCCTGAGTGCATTCTC-3'
Reporter	5'-CAGTGCAGATCCGGCGCG-3'	5'-CTGCAAACCTCTAAAAGATCCGGC-3'

2.6 Statistics

Statistical analysis was carried out in IBM SPSS statistics 22 and OriginLab OriginPro 8.5, and graphs were generated using OriginLab OriginPro 8.5 and Microsoft Excel 14.0. Data was analysed by 2-way ANOVA for the factors Hsa21+ and tgAPP+ or by 2-tailed Student's t-test for comparison of wildtype and Dp1Tyb. Analysis of the proportion of slices showing LTP or LTD induction of greater than 115% was performed using Fisher's Exact Test. LTP with PTX was analysed by 3-way ANOVA with Hsa21+ and tgAPP+ and PTX+ as factors.

For input-output curves, repeat measures ANOVA was carried out to assess difference in maximal response, and 2-way ANOVA was carried out for area under the curve, to assess differences in rate of change. For paired pulse ratio, a 2-way ANOVA or 2-tailed Student's t-test was carried out for each of the 5 data points, and the Holm-Bonferroni method was used to correct for multiple comparisons. Paired pulse ratio during potentiation, and analysis of EEG power bands were also carried out using a 2-way ANOVA, followed by Holm-Bonferroni correction for multiple comparisons.

Seizure frequency and interictal spike count were analysed by 2-way ANOVA or 2-tailed Student's t-test, according to number of genotypes. Seizure duration data from the Tc1×J20 cross was analysed by 2-tailed Student's T-test, as seizures only occurred in 2 of the genotypes.

Power calculations were carried out for preliminary data to determine the appropriate sample size for future work. Power was calculated using an online tool, available at:

<http://powerandsamplesize.com/Calculators/>

Chapter 3

Synaptic function in AD-DS

3.1 Introduction

3.1.1 Synaptic transmission

Cognitive dysfunction is a ubiquitous feature of both AD and DS, indicating that in both disorders, the function of neuronal networks is impaired. The synapse constitutes a major locus for information processing within the neuronal network. Although synaptic dysfunction has been characterised in models of both DS and AD, A β -associated synaptic dysfunction has not previously been investigated in the context of trisomy 21.

Cortical neurons have an average of 7,000 synapses each, and there are approximately 1.5×10^{14} synapses in the human cortex (Pakkenberg *et al.*, 2003). Each neuron receives a combination of excitatory, inhibitory, and modulatory input, and the spatial and temporal pattern of this activity determines the probability that the neuron will fire an action potential. Consequently, if synaptic transmission is impaired, it is likely to have a substantial impact on the ability of neuronal networks to process information, and by extension on cognitive function.

3.1.2 The perforant path

The hippocampus plays a key role in the cognitive dysfunction associated with both AD and DS. The perforant path represents the major sensory input into the hippocampal formation. It arises from the entorhinal cortex, and is subdivided into a medial component (MPP) projecting from the medial entorhinal cortex (MEC) to the middle third of the DG molecular layer, and a lateral component (LPP), projecting from the lateral entorhinal cortex (LEC) and to the outer third of the DG molecular layer (van Groen, Miettinen and Kadish, 2003).

These pathways have distinct electrophysiological and pharmacological properties (McNaughton, 1980; Bramham, Errington and Bliss, 1988; Macek *et al.*, 1996). Lesion studies have also indicated a functional dissociation between the MPP and the LPP. The MPP receives spatial information from the grid cells of the MEC (Fyhn *et al.*, 2004), and consequently MPP lesions are associated with impairments in place learning (Ferbinteanu, Holsinger and McDonald, 1999), while lesions to the LPP are associated with a greater reduction in novelty preference (Myhrer, 1988).

The EC is one of most severely affected regions in AD patients. Tau pathology and neuronal loss occur in the EC early in the disease process (Hyman *et al.*, 1986; Gómez-Isla *et al.*, 1996), resulting in glutamate depletion in the perforant path (Hyman, Van Hoesen and Damasio, 1987), and dysfunction in the perforant path has therefore been implicated in many of the initial symptoms of AD (van Hoesen, Hyman and Damasio, 1991).

3.1.3 The basis of extracellular postsynaptic field potentials

Synaptic transmission in the MPP was assessed by recording extracellular postsynaptic field potentials (fEPSPs) in the molecular layer of the DG, in response to stimulation of axons in the MPP. Postsynaptic field potentials are generated by the movement of ions thorough extracellular space. The release of neurotransmitter from the presynaptic terminal results in the opening of ligand-gated and voltage-gated ion channels on the postsynaptic membrane. As movement through these channels is passive, the flow of ions is determined by the electrical and chemical gradient across the neuronal membrane and can be calculated using the Nernst equation:

$$v_{ion} = \frac{RT}{zF} \ln \frac{[ion]_o}{[ion]_i}$$

Nernst equation:

v_{ion} represents the reversal potential of the ion, R represents the universal gas constant, T represents the environmental temperature in kelvin, F represents the Faraday constant (the charge on 1 mole of electrons), z represents the number of moles of electrons transferred in the reaction, $[ion]_o$ represents the extracellular concentration of ions, and $[ion]_i$ represents the intracellular concentration of ions.

The influx of Ca^{2+} and Na^{+} through NMDA and AMPA receptors generates the majority of the field potential, but Cl^{-} permeable $GABA_A$ receptors are also involved. At resting potential, the movement of Cl^{-} ions make a minor contribution to the fEPSP, as the reversal potential of Cl^{-} is far closer to the resting membrane potential than the reversal potentials of Na^{+} or Ca^{2+} . However, as the membrane becomes depolarised during the fEPSP, the driving force for Cl^{-} ions increases and the contribution of the inhibitory current becomes more significant. Therefore, unless inhibitory neurotransmission is blocked, the fEPSP cannot be considered exclusively a reflection of excitatory activity.

The influx of positively charged ions through these channels generates a current sink at the synapse, which is balanced by a current source along the neuronal membrane. This creates a transient potential difference in the extracellular space, which can be detected using a recording electrode. The magnitude of the ionic influx during the fEPSP is reflected by the slope of the fEPSP recording. This is determined both by the strength of the synaptic response at individual synapses, as well as the total number of active synapses. Changes in the slope of the fEPSP can therefore be used to measure the baseline level of synaptic activity.

For evoked fEPSPs, the slope is determined in part by the strength of the stimulating current. Each response reflects the combined synaptic activity of a population of neurons in the stimulated pathway, as larger currents are able to recruit a greater number of axons, however the recruitment of axons is non-linear. For the experiments described here, a concentric bipolar stimulating electrode was used; this generates a field of current that decays exponentially with distance from the electrode, so larger currents will depolarise a greater number of axons across a greater length. Successful recruitment of axons is determined by a number of factors, including the diameter of the axon, the health of the axon, and the length of axon depolarised

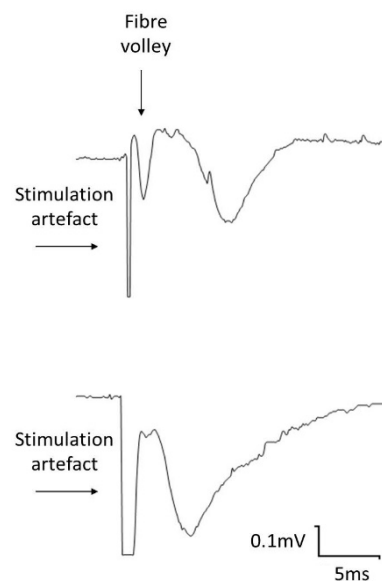


Figure 3.1 *Fibre volley*

A) *Example of fEPSP with preceded by a fibre volley* **B)** *Example of fEPSP where fibre volley is corrupted by stimulation*

by the current. Therefore, the magnitude of the fEPSP generated is not directly proportional to the stimulating current.

The number of axons recruited is reflected by the fibre volley. The fibre volley is a negative deflection in the recording which occurs prior to the fEPSP, and is generated by the movement of ions in the extracellular space during action potential firing in the presynaptic axons. Recruitment of a greater number of axons therefore produces a larger fibre volley. Normalising the fEPSP slope to the fibre volley reflects the strength of the synaptic response per fibre recruited, reducing the variability introduced by non-linear fibre recruitment. However, this was not possible to calculate in all cases, as in some slices the initial slope of the fibre volley was corrupted by the stimulation artefact (see *Error! Reference source not found.*).

3.1.4 Paired pulse ratio and release probability

The paired pulse ratio (PPR) is a measure of short-term synaptic plasticity; applying two successive current pulses to a synapse over a short interval results in either facilitation (PPF) or inhibition (PPI) of the second fEPSP response relative to the first. Several factors determine the degree of facilitation or depression, and these may vary extensively between synapses.

One of the major factors proposed to affect the PPR is presynaptic release probability (Regehr, 2012). High release probability results in the majority of vesicles being released in response to the first stimulus, leading to a depletion of docked vesicles available for release following the second stimulus, and therefore subsequent responses will show paired pulse inhibition (PPI). Conversely, if the initial release probability is low, repeated Ca^{2+} influx in response to the successive

stimuli will lead to an accumulation of intracellular Ca^{2+} at the presynaptic terminal. As vesicle release is Ca^{2+} -dependent, this will result in an increase in vesicular release probability after the second pulse, and therefore paired pulse facilitation (PPF). Saturation of Ca^{2+} buffers will further contribute to elevations in intracellular Ca^{2+} (Blatow *et al.*, 2003).

Activity-dependent modulation of Ca^{2+} influx may also be a factor. Ca^{2+} binding proteins modify the behaviour of Ca^{2+} channels, and depending on the synapse may result in either inactivation or enhancement of Ca^{2+} currents in response to Ca^{2+} , contributing to PPF or PPI respectively (Lee *et al.*, 2002; Xu and Wu, 2005; Catterall and Few, 2008). Retrograde signalling from the postsynaptic neuron and negative feedback through presynaptic auto-receptors (Contractor, Swanson and Heinemann, 2001; Maejima *et al.*, 2001) are also likely to be important, as are postsynaptic mechanisms such as receptor desensitisation (Belichenko *et al.*, 2009). Finally, glia have also been shown to play a role in modulating paired-pulse plasticity (de Pittà *et al.*, 2011). These processes act over different time scales, and will therefore differentially influence PPR at different response intervals.

The majority of studies of PPR have focused on the Calyx of Held synapse in the auditory system, as its large size makes it easily accessible to electrophysiological recordings. The extent to which these mechanisms can be generalised to other synapses is still unclear. There has been limited characterisation of the specific mechanisms of PPF and PPI in dentate granule cells. Stimulation of the MPP results in PPI (McNaughton, 1980), for which mGluRs appear to be important, with different classes of mGluR contributing at different time intervals. Although, at intervals of greater than 200ms, PPI appears to be mediated by other mechanisms, which have yet to be determined

(O'Leary, Cassidy and O'Connor, 1997). Brain derived neurotrophic factor (BDNF) has also been shown to regulate PPI in the medial perforant path. BDNF heterozygous knockout mice show enhanced PPI (Asztely *et al.*, 2000), which may be associated with an increase in synaptic inhibition in the DG (Olofsdotter, Lindvall and Asztély, 2000), and significantly, BDNF signalling has been reported to be disrupted in DS (Bimonte-Nelson *et al.*, 2003; Troca-Marín, Alves-Sampaio and Montesinos, 2011; Nosheny *et al.*, 2015).

3.1.5 Synaptic dysfunction in models of AD-DS

To investigate synaptic dysfunction in AD-DS, the Tc1 mouse model of DS, which carries a freely segregating copy of Hsa21, has been crossed to the J20 model of AD, which overexpresses *tgAPP*. Synaptic dysfunction was also investigated in the Dp1Tyb model of DS, which contains a segmental duplication of the Hsa21 syntenic region of Mmu16. Structural studies have reported a reduction in synapse number in the DG of both the Tc1 (Witton *et al.*, 2015) and J20 (Mucke *et al.*, 2000; Hong *et al.*, 2016) mice, suggesting baseline synaptic transmission may be impaired, although no change in the input-output curve of the fEPSP was observed in the J20 (Palop *et al.*, 2007). PPR was also not altered in the DG of the Tc1 mouse *in vivo* (O'Doherty *et al.*, 2005) although this has been reported to be reduced in the DG of hippocampal slices from the J20 mouse (Harris *et al.*, 2010). Neither baseline synaptic transmission, nor paired pulse plasticity, have previously been assessed in the Dp1Tyb model, or in double transgenic Tc1 × J20 animals.

3.2 Aims

1. To determine whether baseline synaptic function in the MPP is affected by trisomy 21, *tgAPP*, or interactions between them
2. To determine whether the PPR in the MPP is affected by trisomy 21, *tgAPP*, or interactions between them
3. To determine whether synaptic phenotypes are comparable across the Tc1 and Dp1Tyb models of DS

3.3 Results

3.3.1 Baseline synaptic transmission in the Tc1 × J20 cross

In order to assess baseline synaptic transmission, extracellular recordings were made in the MPP of acute hippocampal slices from 6-month-old mice. Input-output curves were generated using a range of stimulation intensities between 0.1mA and 0.8mA, at 0.1mA intervals (*Error! Reference source not found.A*). At maximal stimulation of 0.8mA, fEPSP slope the wildtype mice was $-0.26\text{mV/ms} \pm 0.05$ (SEM), n=16 slices, 11 animals; in the J20 was $-0.33\text{mV/ms} \pm 0.12$ (SEM), n=9 slices, 7 animals; in the Tc1 mice was $-0.46\text{mV/ms} \pm 0.11$ (SEM), n=18 slices, 17 animals; and in the Tc1×J20 mice was $-0.31\text{mV/ms} \pm 0.13$ (SEM), n=9 slices, 8 animals. There was no significant effect of trisomy 21 ($F(1,48)=0.033$, $P=0.856$) or *tgAPP* ($F(1,48)=0.982$, $p=0.340$), and no significant interaction between them ($F(1,48)=0.186$, $p=668$) by repeat-measures 2-way ANOVA.

As expected, stimulation intensity had a significant effect on fEPSP slope ($F(7,336)=24.545$, $p<0.001$), however there was no significant interaction between stimulation intensity and *tgAPP* ($F(7,336)=0.193$, $p=0.987$) or stimulation intensity and trisomy 21 ($F(7,336)=0.141$, $p=0.995$). This indicates that neither *tgAPP* nor trisomy 21 altered the maximal strength of synaptic response, and therefore that neither *tgAPP*, trisomy 21, nor interactions between the two contribute to a detectable reduction in baseline synaptic transmission at the 6-month time point, despite the exacerbation of amyloid pathology and behavioural deficits in the Tc1×J20 animals.

Normalising the fEPSP slope generated at each stimulation intensity to the maximal slope generated at 0.8mA for each genotype creates a

curve reflecting the rate at which the synaptic response reaches maximal strength for each slice (Error! Reference source not found.**B**). Within a slice, the strength of synaptic response at individual synapses remains constant with increasing stimulation intensity. The change in response magnitude is consequently determined by the proportion of total fibres which are recruited at each current step.

The area under the percentage maximum curves (AUC) was approximated using trapezoid sums. Again, no significant difference between genotypes was observed, suggesting the rate at which MPP fibres are recruited is not affected by genotype. Average AUC for the wildtype animals was 48.65 ± 4.11 (SEM); for the Tc1 animals was 54.68 ± 4.96 (SEM); for the J20 animals was 47.96 ± 3.31 (SEM); and for Tc1×J20 was 51.73 ± 3.98 . There was no significant effect of trisomy 21 ($F(3,44)=1.009$, $p=0.321$) or *tgAPP* ($F(3,44)=0.140$, $p=0.71$) and no significant interaction between trisomy 21 and *tgAPP* ($F(3,44)=0.054$, $p=0.817$) by two-way ANOVA.

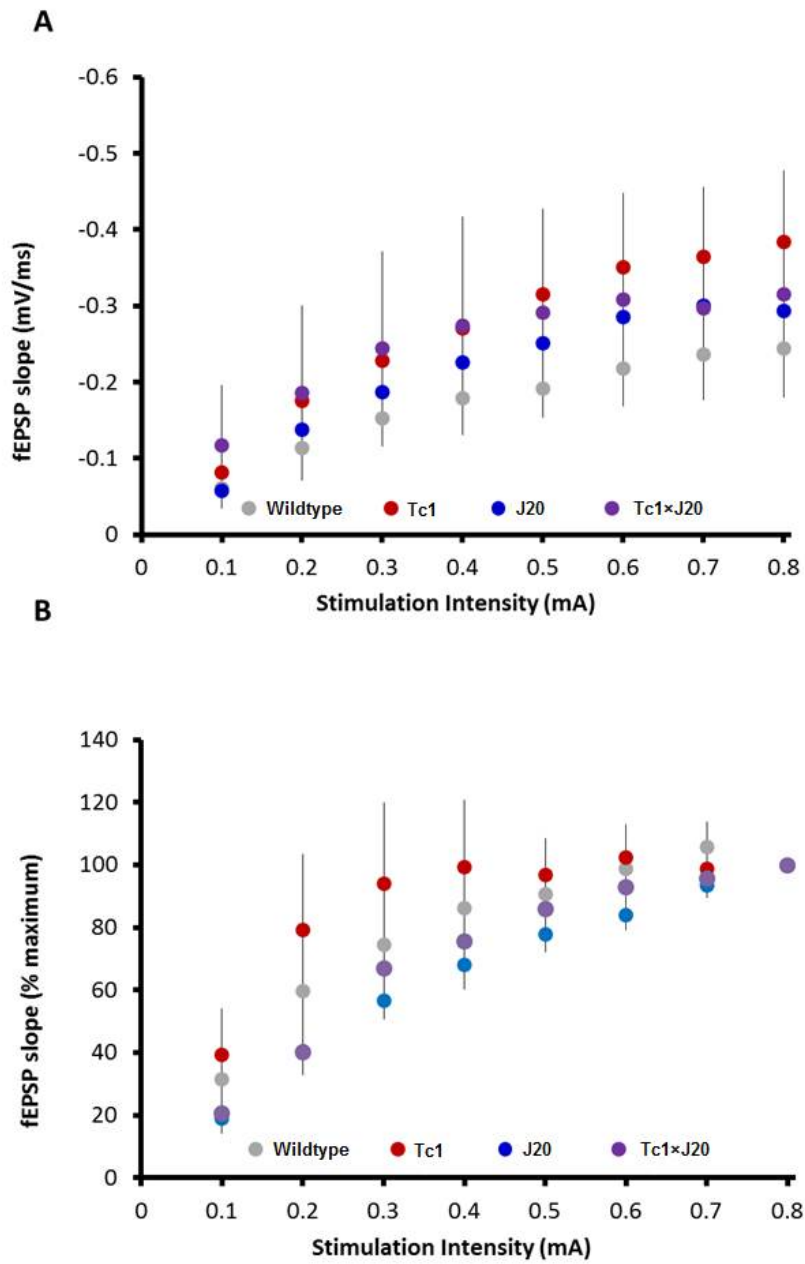


Figure 3.2 *Input-output curves in the Tc1xJ20 cross at 6 months of age*

A) *Input-output curve showing average fEPSP slope measured at stimulation intensities ranging between 0.1 mA and 0.8mA for wildtype (grey), Tc1 (red), J20 (blue) and Tc1xJ20 (purple). Error bars show standard error of the mean (SEM).* **B)** *Input-output curve showing fEPSP slope expressed as a percentage of the maximum for stimulation intensities ranging between 0.1mA and 0.8mA. Error bars show (SEM).*

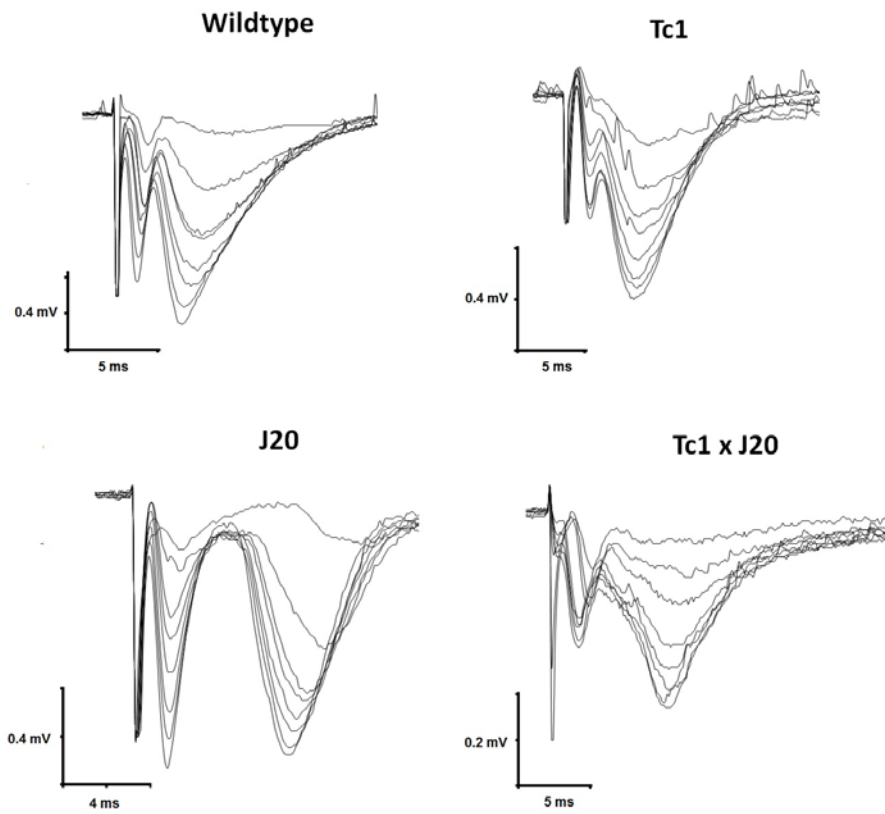


Figure 3.3 *Example responses during input-output curves in the Tc1xJ20 cross*

Superimposed example traces showing responses to stimulation pulses of 0.1, 0.2, 0.3, 0.4, 0.5, 0.6, 0.7 and, 0.8mA in wildtype, Tc1, J20 and Tc1xJ20 mice during input-output curves.

3.3.2 Paired pulse ratio in the Tc1 × J20 cross

To determine if PPR in the MPP was influenced by *tgAPP* or trisomy 21, paired stimuli were applied at intervals of 25ms, 50ms, 100ms, 200ms and 400ms (Error! Reference source not found.). PPR was calculated as the initial fEPSP slope of the second response (R2) divided by the initial fEPSP slope of the first response (R1). A ratio of greater than 1 indicates facilitation and a ratio of less than 1 indicates depression; MPP synapses generally undergo depression.

There was no significant difference in PPR between genotypes at any time point. At the 25ms stimulus interval, PPR in wildtype was: 0.69 ± 0.06 (SEM), n=18 slices from 12 animals; PPR in Tc1 was: 0.57 ± 0.06 (SEM), n=15 slices, 10 animals; PPR in J20 was: 0.80 ± 0.19 (SEM), n=7 slices, 5 animals; and PPR in Tc1×J20 was: 0.81 ± 0.17 (SEM), n= 6 slices, 4 animals. There was no significant effect of trisomy 21 ($F(3,43)=0.244$, $p=0.624$) or *tgAPP* ($F(3,43)=2.638$, $p=0.112$), and no interaction ($F(3,43)=0.476$, $p=0.494$).

At the 50ms stimulus interval, PPR in wildtype was: 0.81 ± 0.07 (SEM); PPR in Tc1 was: 0.75 ± 0.04 (SEM); PPR in J20 was: 0.85 ± 0.13 (SEM); PPR in Tc1×J20 was: 0.98 ± 0.09 (SEM). There was no significant effect of trisomy 21 ($F(3,43) = 0.114$, $p = 0.736$) or *tgAPP* ($F(3,43)=2.815$, $p=0.101$), and no interaction ($F(3,43)=1.266$, $p=0.267$).

At the 100ms stimulus interval, PPR in wildtype was: 0.83 ± 0.06 (SEM); PPR in Tc1 was: 0.80 ± 0.033 (SEM); PPR in J20 was: 0.88 ± 0.12 (SEM); PPR in Tc1×J20 was: 1.00 ± 0.098 (SEM). There was no significant effect of trisomy 21 and no interaction ($F(3,43)=0.476$, $p=0.494$). ($F(3,43)=1.953$, $p=0.299$). However *tgAPP* ($F(3,43)=4.366$, $p=0.043$) was associated with a trend towards a reduction in paired pulse depression, although this did not reach the threshold for significance

using Bonferroni-Holm adjusted α to correct for multiple comparisons ($\alpha=0.010$).

At the 200ms stimulus interval, PPR in wildtype was: 0.80 ± 0.06 (SEM); PPR in Tc1 was: 0.70 ± 0.04 (SEM); PPR in J20 was: 0.89 ± 0.04 (SEM); PPR in Tc1×J20 was: 0.98 ± 0.05 (SEM). There was no significant effect of trisomy 21 ($F(3,43)=0.636$, $p=0.430$) and no interaction ($F(3,43)=0.311$, $p=0.58$). However *tgAPP* ($F(3,43)=5.059$, $p=0.030$) was again associated with a trend towards a reduction in paired pulse depression, which did not reach the threshold for significance after correction for multiple comparisons ($\alpha=0.010$).

At the 400ms stimulus interval, PPR in wildtype was: 0.80 ± 0.06 (SEM); PPR in Tc1 was: 0.80 ± 0.039 (SEM); PPR in J20 was: 0.90 ± 0.06 (SEM); PPR in Tc1×J20 was: 0.98 ± 0.04 (SEM). There was no significant effect of trisomy 21 ($F(3,43)=0.352$, $p=0.556$) and no interaction ($F(3,43)=0.619$, $p=0.436$). However *tgAPP* ($F(3,43)=5.669$, $p=0.022$) was associated with a trend towards a reduction in paired pulse depression, although this did not reach the threshold for significance after correction for multiple comparisons ($\alpha=0.010$).

This suggests that presynaptic release probability is not altered by trisomy 21 at any of the tested time intervals, and there was no significant interaction between trisomy 21 and *tgAPP*.

tgAPP had no significant effect at the 25ms and 50ms intervals, however, there was a trend towards an effect at the 100ms, 200ms, and 400ms intervals, although this does not reach significance following the Holm-Bonferroni correction for multiple comparison.

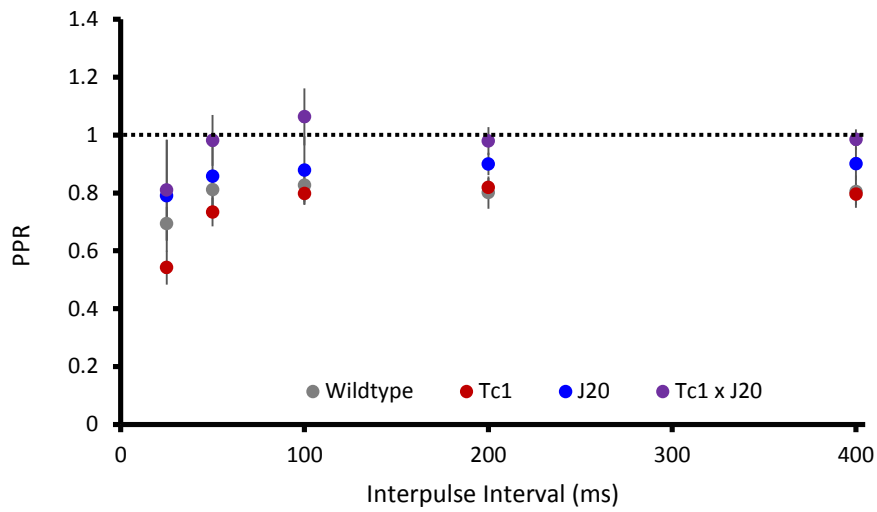


Figure 3.4 Paired pulse ratio in the Tc1×J20 cross

Ratio of the slope of the second fEPSP (R2) to the first fEPSP (R1) in response to paired stimuli at intervals of 25ms, 50ms, 100ms, 200ms, and 400ms in wildtype (grey), Tc1 (red), J20 (blue) and Tc1×J20 (purple) animals. Error bars show SEM

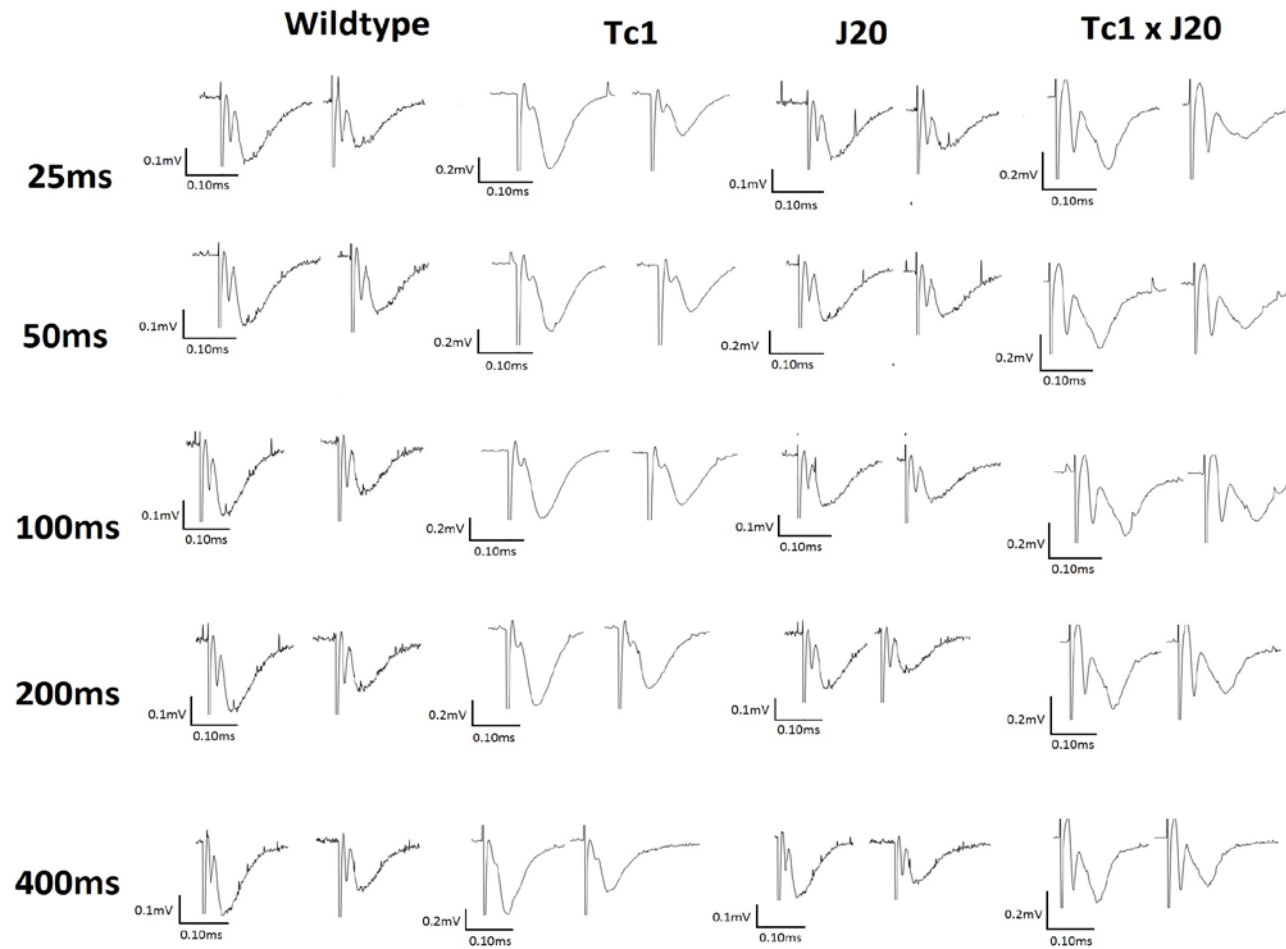


Figure 3.5 *Example traces showing paired pulse inhibition in the Tc1 x J20 cross*

Examples of fEPSPs responses to the first and second stimulation pulse, at inter-pulse intervals of 25ms, 50ms, 100ms, 200ms and 400ms in wildtype, Tc1, J20 and Tc1xJ20 animals. Responses represent the average of 6 traces (2 mins).

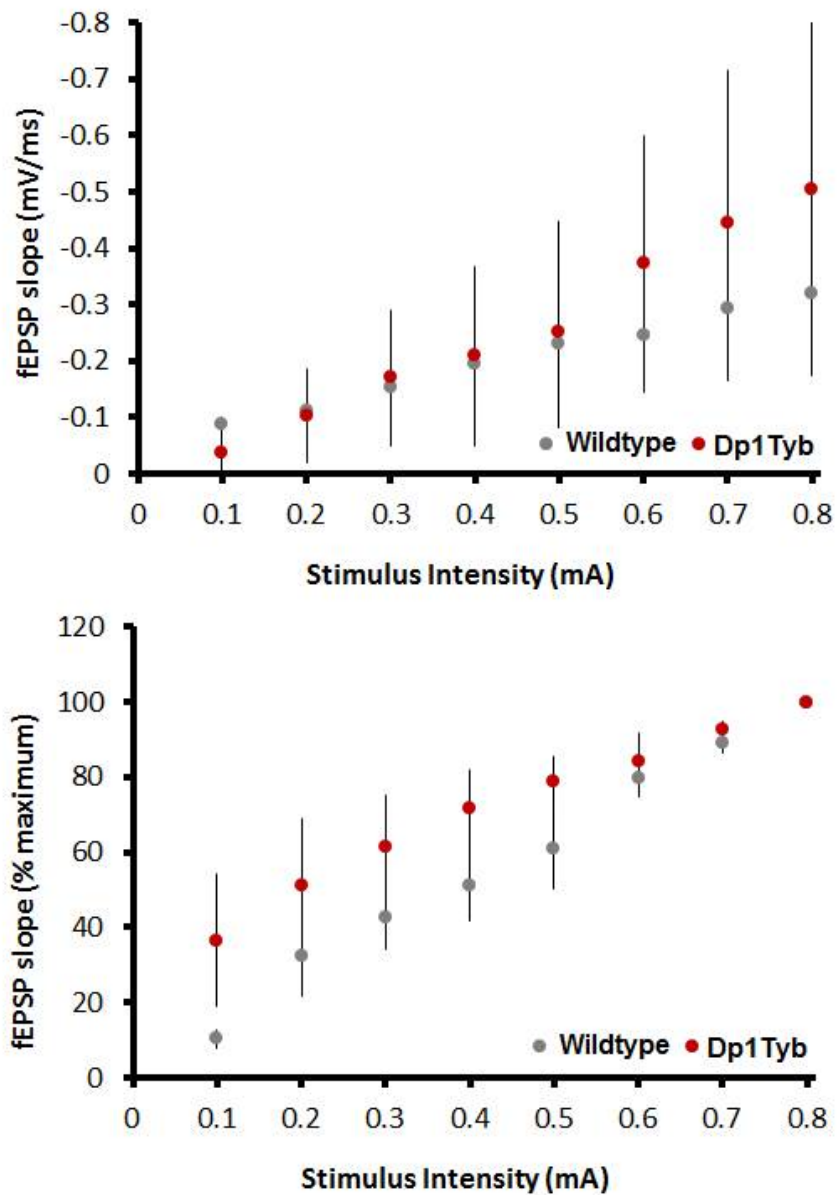
3.3.3 Preliminary data on baseline synaptic transmission in the Dp1Tyb model

The copy of Hsa21 carried by the Tc1 mouse carries a deletion which includes several candidate genes for the synaptic phenotypes associated with DS, including the transcription factors *OLIG1* and *OLIG2*, which have been implicated in disruption to ratio of excitation to inhibition in the DS brain, and *SYNJ1* which has been implicated in synaptic transmission and membrane trafficking. Any contribution of these deleted genes to the DS phenotype will therefore not be detected in the Tc1 mice.

To determine whether any of these missing genes contributed to an alteration in baseline synaptic transmission, input-output curves were recorded in acute hippocampal slices from the Dp1Tyb mouse model, which carries a duplication of the Hsa21 orthologous region of Mmu16 on a C57BL/6 inbred background. This model therefore overexpresses some of the genes which have been deleted from the copy of Hsa21 in the Tc1 mouse, and can be used to identify any additional contributions these genes may make to synaptic dysfunction in DS, although differences in genetic background must be taken into consideration.

There was no significant difference in the fEPSP slope at 0.8mA (*Error! Reference source not found.A*). Slope in the wildtype animals was $-0.495\text{mV/ms} \pm 0.15$ (SEM), $n=3$ slices, 3 animals and slope in the Dp1Tyb animals was $-0.32\text{mV/ms} \pm 0.16$ (SEM), $n=4$ slices, 4 animals; Student's t-test $p=0.467$. There was also no significant difference in area under the percentage maximum curve (*Error! Reference source not found.B*): AUC in the wildtypes was 25.36 ± 7.58 (SEM) and AUC in the Dp1Tyb mice was 36.3 ± 4.93 ; Students t-test: $p= 0.259$. This suggests

that the additional genes in the Dp1Tyb mice do not alter baseline synaptic transmission.



Input-output curves in the Dp1Tyb model

A) Input-output curve showing average fEPSP slope measured at stimulation intensities between 0.1mV and 0.8mV for wildtype (grey) and Dp1Tyb mice (red). Error bars show SEM. **B)** Input-output curve showing fEPSP slope expressed as a percentage of the maximum response for stimulation intensities of 0.1mV -0.8mV. Error bars show SEM.

3.3.4 Paired pulse ratio in the Dp1Tyb model

PPR was also recorded in the Dp1Tyb model to determine whether any of the genes missing from the copy of Hsa21 in the Tc1 mice influenced presynaptic release probability. The Dp1Tyb mice showed a consistent trend towards a decrease in PPR (*Error! Reference source not found.*).

At the 25ms interval, PPR in wildtype mice was 0.826 ± 0.080 (SEM), n=4 slices, 3 animals; and PPR in Dp1Tyb mice was 0.569 ± 0.172 (SEM), n=5 slices, 4 animals; Student's t-test $p = 0.254$.

At the 50ms interval, PPR in wildtype mice was 0.882 ± 0.059 (SEM); and PPR in Dp1Tyb mice was 0.696 ± 0.136 (SEM); Student's t-test $p=0.289$.

At the 100ms interval PPR in wildtype mice was 0.910 ± 0.057 (SEM); and PPR in Dp1Tyb mice was 0.729 ± 0.066 (SEM); Student's t-test $p=0.085$.

At the 200ms interval, PPR in wildtype mice was 0.894 ± 0.023 (SEM); and PPR in Dp1Tyb mice was 0.756 ± 0.096 (SEM); Student's t-test $p=0.248$.

At the 400ms interval, PPR in wildtype mice was 0.969 ± 0.023 (SEM) and PPR in Dp1Tyb mice was 0.717 ± 0.080 (SEM); Student's t-test $p=0.030$.

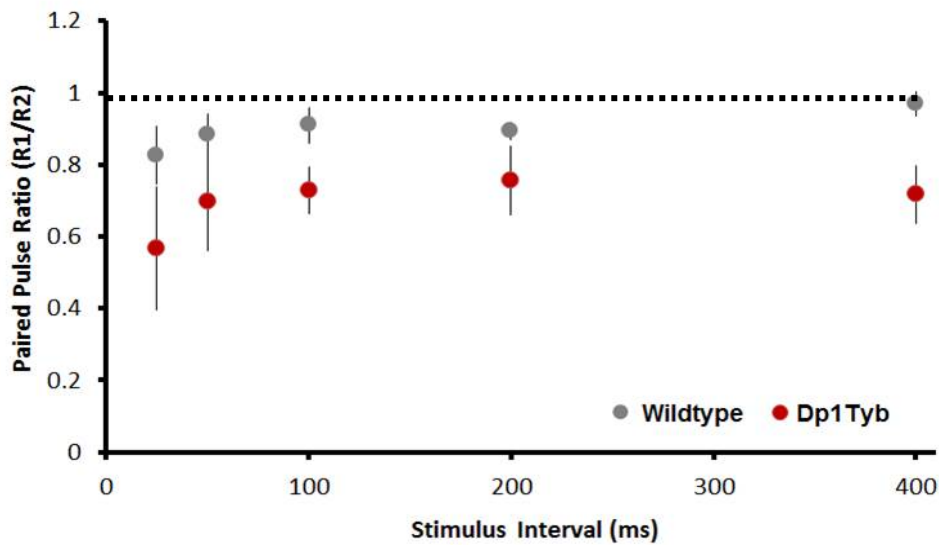


Figure 3.6 Paired pulse ratio in the Dp1Tyb model

Ratio of the slope of the second fEPSP (R2) to the first fEPSP (R1) in response to paired stimuli at intervals of 25ms, 50ms, 100ms, 200ms, and 400ms in wildtype (grey) and Dp1Tyb (red) animals.

Although none of the values reached the significance when corrected for multiple comparisons (Holms-Bonferroni adjusted α threshold for the first comparison = 0.01) the PPR at 400ms reached significance for the uncorrected α threshold of 0.05. These data suggest a possible reduction in PPR in the Dp1Tyb mice, especially at the 400ms interval. However, as the number of mice available for this pilot experiment was low, the experiment did not have sufficient power to detect a significant effect following correction for multiple comparisons.

Power calculations using a β value of 0.20 and the Holm-Bonferroni adjusted α value of 0.010 suggest a sample size of 11 animals would be required to detect a difference at 0.25ms, using a σ value of 0.172; corresponding to the highest standard deviation of the two groups. At 400ms however, a sample size of 4 would be required; $\beta=0.20$, $\alpha=0.010$, $\sigma=0.080$.

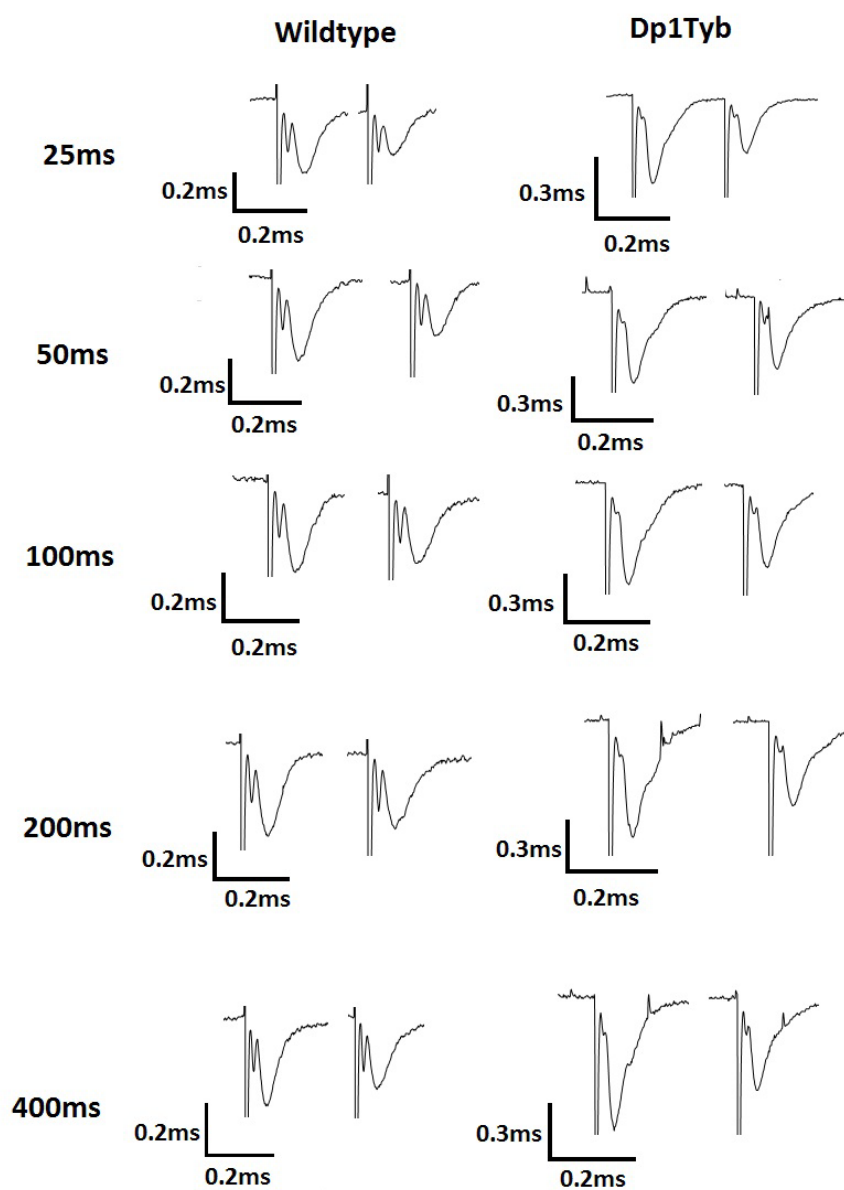


Figure 3.7 Example traces showing paired pulse inhibition in the Dp1Tyb Model

Examples of fEPSPs generated in response to the first and second stimulation pulse, at inter-pulse intervals of 25ms, 50ms, 100ms, 200ms and 400ms in wildtype and Dp1Tyb animals. Responses represent the average of 6 traces (2 mins).

3.4 Discussion

These data suggest that baseline synaptic transmission is not altered by either trisomy 21 or the overexpression of *tgAPP*, and that no novel phenotypes result from interactions between the two. Changes in baseline synaptic transmission are caused by either a change in the number of functional synapses, or a change in the magnitude of synaptic response. However, without normalising to the fibre volley, it is not possible to differentiate between these mechanisms. Although these data suggest that baseline synaptic transmission is not impaired, loss of synapses has been reported in the DG of the J20 animals (Mucke *et al.*, 2000; Hong *et al.*, 2016), and a reduction in synaptic density and the size of postsynaptic densities has been reported in the DG of Tc1 mice (Witton *et al.*, 2015).

Such changes would be expected to lead to a reduction in baseline synaptic transmission; the lack of effect observed in these experiments may therefore simply reflect limitations in the sensitivity of the recording technique. If substantial variability results from external factors such as the health of the slices, fluctuations in recording temperature, or variation in depth and position of electrodes, the impact of these changes may simply be too subtle to be detected above variability from other sources.

For the Tc1 mice, mosaicism creates a further source of variability. The proportion of neurons that contain the additional chromosome is likely to vary between animals, and the proportion contributing to the fEPSP will also vary between experiments. It remains unknown whether the neuronal dysfunction in the Tc1 model is cell autonomous, and present only in trisomic neurons, or whether there is generalised disruption to

network development, and dysfunction occurs throughout the entire neuronal population. It is likely that both occur under different circumstances, and therefore the extent to which mosaicism modifies the presentation of specific phenotypes is unclear. Nevertheless, it is likely that many phenotypes may be milder, or more variable due to mosaicism.

Alternatively, homeostatic compensation may occur to maintain the baseline level of synaptic transmission despite loss of synapses. However, structural characterisation of the DG in the Tc1 mice provides no evidence for compensatory changes. Both the number of synapses and the size of the postsynaptic density were reduced; as synaptic strength correlates with size (Meyer, Bonhoeffer and Scheuss, 2014), it is unlikely that a reduction of synapse number is compensated for by an increase in synaptic strength. Furthermore, no change in granule cell excitability was observed, and the lack of change in PPR reported here suggests that presynaptic release probability is also unaffected. Therefore, the occurrence of significant homeostatic changes in the Tc1 mice appears unlikely.

The lack of change in baseline synaptic transmission in the DG of the J20 mice is consistent with the results of Palop *et al.* (2007), suggesting that the loss of synapses in these animals may not result in a detectable impairment in the strength of synaptic transmission. Palop *et al.*, (2007) also report increased network excitability in the DG, resulting in spontaneous epileptiform discharges, along with compensatory changes in inhibitory networks resembling those observed in models of temporal lobe epilepsy. These mice therefore appear to have a complex pattern of changes in inhibitory and excitatory circuitry, resulting from the combined effect of multiple mechanisms of tgAPP-mediated toxicity,

and corresponding homeostatic compensation. The net result of this may be a normal baseline level of synaptic transmission, despite overall network function being profoundly abnormal.

PPR is not affected by trisomy 21, suggesting none of the genes on Hsa21 influence release probability or modulate inhibitory feedback. This is consistent with observations in the DG of the Ts65Dn model, where PPR in the MPP is also reported to be unchanged (Kleschevnikov *et al.*, 2004). O'Doherty *et al.* (2005) also observed no change in PPR *in vivo* in the DG of the Tc1 mice, although they reported PPF rather than PPI, suggesting they may have been recording from a different population of neurons, as they do not specify which part of the perforant pathway they are recording from.

PPR in CA1 has been studied more frequently, and has also been reported to be unchanged in a number of DS models, including the Ts65Dn (Siarey *et al.*, 1999; Costa and Grybko, 2005), the Ts1Cje (Siarey *et al.*, 2005), the Dp(16)1Yey (Zhang *et al.*, 2014), and the 'triple trisomic' model (Zhang *et al.*, 2014). However, decreased PPF was reported in the mossy fibres of the Tc1 mice, suggesting deficits related to trisomy may be pathway specific (Witton *et al.*, 2015).

Although the Dp1Tyb study is underpowered, it suggests that PPI may be enhanced by segmental duplication of Mmu16, particularly at longer inter-stimulus intervals. The mechanisms underlying PPI at a 400ms interval in the DG are not known; it does not appear to be dependent on mGluR receptors (O'Leary, Cassidy and O'Connor, 1997), although the long timescale suggests that it is likely to be mediated by another type of metabotropic receptor signalling. There is some evidence that BDNF signalling is disrupted in mouse models of DS (Bimonte-Nelson *et al.*, 2003; Troca-Marín, Alves-Sampaio and Montesinos, 2011; Nosheny *et*

al., 2015). If this is the case in the Tc1 hippocampus, it may contribute to the observed reduction in PPI. Another candidate is GABA_B receptors, as downstream signalling via GABA_B receptors is modified in the Ts65Dn model, however altered GABA_B receptor signalling was not associated with change in PPI in the Ts65Dn (Kleschevnikov *et al.*, 2004). This does not necessarily preclude a role for GABA_B receptors, as differences in phenotype may relate to the difference in the gene content between the two models, or to differences in genetic background or experimental parameters.

PPI in the MPP was also not significantly altered by *tgAPP* at any time point, however a trend towards a reduction was observed at the 100ms, 200ms, and 400ms intervals, suggesting that *tgAPP* may have a subtle effect on PPI at longer intervals, consistent with changes in metabotropic receptor signalling. The impact of A β on PPR in the DG is not clear. Wang *et al.* (2002) report a reduction in PPI at a 20ms inter-stimulus interval, following the application of A β derived diffusible ligands (ADDLs), but no difference in subsequent intervals from 50-300ms. Palop *et al.* (2007) also report a change in PPR in the DG of the J20 mice, however they report PPF rather than PPI in the wildtype animals, suggesting they may be recording from a different population of synapses. Together, these data indicate that A β may affect presynaptic release probability in the DG only under specific conditions or at specific synapses; further investigation to elucidate the impact of A β on PPR in the DG is therefore required.

3.5 Conclusion

Input-output curves in the Tc1 × J20 cross were not altered by overexpression of *tgAPP*, trisomy of Hsa21, or interactions between them, suggesting there were no deficits in baseline synaptic transmission in any of the genotypes resulting from the cross. Loss of synapses or reduction in synaptic strength is therefore unlikely to contribute to the observed cognitive deficits in the Tc1 mice, or to the exacerbation observed in the Tc1×J20 double transgenic mice. Similarly, the Dp1Tyb pilot study suggested that Mmu16 segmental duplication also had no effect on baseline synaptic transmission, indicating that none of the genes duplicated in the Dp1Tyb mice contribute to additional deficits in baseline synaptic transmission.

Trisomy of Hsa21 also did not impact paired pulse ratio at any time point, suggesting that presynaptic release is not altered in the Tc1 model of DS. Although no significant effect of *tgAPP* was observed, the data is consistent with subtle effects on paired pulse ratio at inter-pulse intervals of between 100 and 400ms. However, there was no significant interaction between trisomy 21 and *tgAPP* at any time point, suggesting such changes are unlikely to contribute to the observed cognitive deficits in the Tc1 animals, or to the exacerbation observed in the Tc1×J20 animals.

The data from the Dp1Tyb pilot study also suggests that paired pulse ratio may be altered at inter-pulse intervals of between 100 and 400ms, as a result of the duplication of one or more genes on Mmu16. Alterations of presynaptic release probability in this model therefore requires further investigation.

Chapter 4

Synaptic plasticity in AD-DS

4.1 Introduction

4.1.1 Synaptic plasticity

The strength of transmission at individual synapses can be modified by synaptic activity. The ability to undergo changes in synaptic strength is required for neuronal networks to encode new information. Long-term potentiation (LTP) and long-term depression (LTD) are two of the major forms of long-term synaptic plasticity. LTP results in a persistent increase in the strength of synaptic transmission, and is considered to be the cellular correlate of memory, while LTD results in a decrease in the strength of synaptic transmission, and is required to refine the storage of memories and ensure that a dynamic range in synaptic strength exists. Deficits in LTP and LTD in animal models are therefore regarded as substrates for cognitive dysfunction.

4.1.2 Mechanisms underlying long-term potentiation

The regulation of LTP is complex; the mechanisms of induction and expression vary according to model organism, brain region, cell-type and developmental stage, as well as being influenced by environmental factors, experimental conditions and the pattern and intensity of the induction stimulus (Malenka and Bear, 2004). Although specific

signalling pathways appear to be required for LTP at particular types of synapse, many other pathways seem to exert a modulatory effect, and these modulatory factors can vary extensively.

At most synapses, LTP induction is a predominantly postsynaptic phenomenon, and requires an elevation of intracellular Ca^{2+} in the postsynaptic terminal. However, presynaptic mechanisms for LTP induction also exist; for example in the mossy fibres of the hippocampus, LTP occurs independently of a postsynaptic rise in Ca^{2+} . In the MPP, LTP is primarily dependent on the activation of postsynaptic NMDA receptors (Colino and Malenka, 1993). These receptors act as coincidence detectors for concurrent activation of presynaptic and postsynaptic neurons. At resting potential, NMDA receptors are blocked by Mg^{2+} ions, making them impermeable to Ca^{2+} . Depolarisation of the postsynaptic membrane forces Mg^{2+} out of the channel; Ca^{2+} influx therefore occurs only if glutamate binds while the neuron is already depolarised. This requirement for simultaneous presynaptic and postsynaptic neuronal activity mediates the associative element of LTP (Bliss and Collingridge, 1993).

Influx of Ca^{2+} leads to the activation of Ca^{2+} -dependent signalling pathways, which facilitate an increase in synaptic strength. Although all forms of LTP appear to require Ca^{2+} , multiple downstream targets have been identified, and these seem to be involved to different degrees at different synapses. Protein kinase C (PKC) activation of the MAPK pathway appears to be critical in the MPP, while calcium/calmodulin-dependent protein kinase II (CaMKII), which is critical for LTP in the LPP and Schaffer collateral pathway, appears to play a lesser role (Zhang *et al.*, 2005; Cooke *et al.*, 2006).

The increase in the postsynaptic response depends on the phosphorylation and insertion of AMPAR into the postsynaptic

membrane. AMPAR phosphorylation is regulated by CaMKII and PKA, and depending on the phosphorylation site, alters the conductance or open probability of the channel, leading to an increase in postsynaptic current (Lee *et al.*, 2000). Regulation of AMPAR trafficking is also mediated by Ca²⁺-dependent activation of CaMKII, and requires AMPAR phosphorylation by PKA (Esteban *et al.*, 2003). AMPAR insertion is subunit specific; AMPARs containing the GluA1 subunit are inserted specifically in response to plasticity, while GluA3 containing subunits are constitutively trafficked (Shi *et al.*, 2001).

The late phase of LTP requires gene transcription and results in structural modification of the synapse, mediated by the transcription factor CREB (Pang and Lu, 2004). These processes occur too slowly to be required for LTP within the first hour after induction, and therefore would have little influence on the data presented here. However, they are critical for the persistence of LTP *in vivo*. Differences in the impact of trisomy on early and late mechanisms of LTP are likely to underlie the observation that *in vivo* LTP in the DG of the Tc1 mice is impaired after 1h, but normal 24h later (Morice *et al.*, 2008).

4.1.3 Post-tetanic potentiation

In addition to LTP, high frequency stimulation induces a form of short-term plasticity called post-tetanic potentiation (PTP). PTP causes an increase in the size of the fEPSP lasting several minutes, and is predominantly presynaptic in origin, resulting from an increase in neurotransmitter release. The mechanisms underlying PTP have been studied most extensively in the Calyx of Held, a large synapse in the auditory system. At this synapse, an increase in Ca²⁺ influx (Habets and Borst, 2007), an increase in the Ca²⁺ sensitivity of vesicle fusion to the presynaptic membrane mediated by PKC (Korogod, Lou and

Schneggenburger, 2007), and an increase in the release probability and readily releasable pool size (Lee *et al.*, 2008) have all been implicated. However, the extent to which these mechanisms underlie PTP in the hippocampus remains unclear. PKC has been strongly implicated as a mediator of PTP at a number of synapses, including those within the hippocampus (Brager *et al.*, 2003; Alle *et al.*, 2001). However recent evidence from PKC knockout mice suggests that contrary to previous claims, PKC is not required for PTP in the Schaeffer collateral, and that pharmacological agents used in previous studies may interact with other targets (Wang *et al.*, 2016).

The mechanisms of PTP in the DG are not well defined, but are likely to be similar to those in other hippocampal pathways. A change in the magnitude of PTP would therefore suggest alterations in the mechanisms regulating presynaptic release probability. To determine PTP for the data presented here, the average slope of the first data point following the application of the LTP induction protocol, representing the average of first 3 minutes post-LTP, was measured for each genotype.

4.1.4 Mechanisms underlying long-term depression

The mechanisms contributing to the induction of long-term depression are also highly variable. Two major forms of hippocampal long-term depression exist; one which is dependent on the activation of NMDA receptors, and one which requires activation of metabotropic glutamate receptors (mGluRs) (Collingridge *et al.*, 2010).

Like NMDAR-dependent LTP, NMDAR-dependent LTD is mediated by Ca^{2+} influx into the cell. Although the precise mechanisms differentiating the induction of Ca^{2+} -mediated LTP from Ca^{2+} -mediated

LTD are unknown, it appears transient exposure to high levels of Ca^{2+} predisposes to LTP induction, while prolonged exposure to intermediate levels of Ca^{2+} predisposes to LTD induction (Lüscher and Malenka, 2012). One of the major pathways proposed to contribute to NMDA-dependent LTD induction requires Ca^{2+} binding to calmodulin, to activate calcineurin. Calcineurin dephosphorylates inhibitor-1, activating protein phosphatase 1 (PP1). PP1 then mediates the dephosphorylation of postsynaptic proteins including the AMPAR subunit GluA1 and PSD-95, leading to AMPAR internalisation (Lisman, 1989; Lüscher and Malenka, 2012).

Multiple mGluR receptor subtypes have been implicated in LTD, depending on the synapse, developmental stage, and induction protocol, and the mechanisms of LTD expression may vary depending on the receptor subtype involved. In the rat DG, low frequency stimulation (LFS) *in vivo* induces a form of LTD mediated by mGluR1, which is independent of NMDA receptors, L-type voltage-gated calcium channels and protein synthesis (Pöschel and Manahan-Vaughan, 2007). Furthermore, antagonism of mGluR3 has been reported to block LFS-dependent LTD in the DG (Pöschel *et al.*, 2005) and pharmacological activation of mGluR5 appears to induce a form of LTD for which voltage-gated calcium channels are required (Naie, Tsanov and Manahan-Vaughan, 2007). However, the respective roles these mechanisms play in physiological modulation of synaptic strength and the extent to which they are conserved across species is not known.

4.1.5 Induction of long-term potentiation and long-term depression in hippocampal slices

LTP was first induced experimentally in the hippocampus using high frequency trains of electrical stimulation (Bliss and Lømo, 1973) while

LTD was first induced by a prolonged train of low frequency stimulation (Dudek and Bear, 1992). Although such patterns of stimulation are effective at inducing plasticity, they do not resemble physiological patterns of neuronal activity. Bursts of stimulation resembling naturally occurring hippocampal theta or delta frequency have been suggested to be more effective at inducing LTP in CA1, which may relate to differential suppression of synaptic inhibition (Grover *et al.*, 2009).

The protocols used here were a high frequency train of 50 stimuli at 100Hz, repeated 4 times with a 30s interval between trains, for the induction of LTP, and a low frequency train of 900 stimuli at 1Hz for the induction of LTD. Initial experiments were conducted without any pharmacological blockers of inhibitory signalling, as the balance between excitatory and inhibitory signalling is disrupted in DS. Blockade of both fast inhibitory signalling via GABA_ARs, and of slow inhibitory signalling via GABA_BRs have been shown to rescue LTP deficits in the Ts56dn model of DS, and thus blocking inhibition has the potential to mask a phenotype (Kleschevnikov *et al.*, 2004).

Due to the mosaic nature of the Tc1 transgenic mice, all LTP experiments have investigated changes in the extracellular field potential, as this represents the activity of a population of neurons, and therefore eliminates the requirement of identifying which neurons contain the additional chromosome.

4.2 Aims

1. To determine whether synaptic plasticity in the MPP is altered by trisomy 21, *tgAPP*, or by interactions between them.
2. To determine whether differences in synaptic plasticity due to duplication of Hsa21 genes also occur in Dp1Tyb mice

4.3 Results

4.3.1 Long-term potentiation in the Tc1 × J20 cross

To assess the impact of trisomy 21 and *tgAPP* on synaptic plasticity, LTP was induced in the MPP of mice from the Tc1 × J20 cross at 6 months of age (**Figure 4.1A**). At 1 hour post LTP induction, average fEPSP slope was $134.21\% \pm 8.86$ (SEM) of baseline in the wildtype mice, n=9 slices, 9 animals; $108.13\% \pm 4.39$ (SEM) of baseline in the Tc1 mice, n=10 slices, 10 animals; $129.86\% \pm 11.25$ (SEM) of baseline in the J20 animals, n=6 slices, 6 animals; and $100.69\% \pm 1.61$ (SEM) of baseline in Tc1×J20 animals, n=4 slices, 4 animals.

Trisomy resulted in a significant loss of potentiation by 2-way ANOVA ($F(3,27)=1.830$, $p=0.004$). This suggests that overexpression of one or more of the genes on the copy of Hsa21 carried by the Tc1 mice contributes to an impairment in synaptic plasticity. Interestingly, *tgAPP* had no effect on potentiation ($F(3,27)=0.362$, $p=0.552$) despite deficits in the J20 animals being reported previously in the literature (Palop *et al.*, 2007), and there was no interaction between *tgAPP* and trisomy ($F(3,27)=0.009$, $p=0.926$).

The percentage of slices showing LTP was calculated for each genotype. The threshold for LTP was potentiation greater than 115% of baseline response (see **Table 4.1**). Effect of genotype was significant by 4×2 Fisher's Exact Test ($p=0.012$). Pairwise comparisons showed there was a significant difference between wildtype and Tc1 mice ($p=0.023$) and between wildtype and Tc1×J20 mice by 2×2 Fisher's Exact Test ($p=0.015$), however there was no difference between wildtype and J20 ($p=0.489$). α was adjusted for multiple comparisons using the Holm-

Bonferroni method ($\alpha = 0.017$, for the first hypothesis, $\alpha = 0.025$ for the second hypothesis).

There was no significant difference in post-tetanic potentiation as a result of trisomy 21 ($F(3,27)=0.173$, $p=0.680$) or *tgAPP* ($F(3,27)=0.707$, $p=0.40$), and no interaction between trisomy 21 and *tgAPP* ($F(3,27)=1.116$, $p=0.300$) (**Figure 4.1C**). Average post-tetanic potentiation in wildtype mice was $149.50\% \pm 12.97$ (SEM); in Tc1 mice was $158.70\% \pm 26.825$ (SEM); in J20 mice was $149.5\% \pm 37.63$ (SEM); and in Tc1×J20 mice was $96.05\% \pm 26.95$ (SEM).

There was also no difference rate of fEPSP decline during tetanic stimulation. Superimposed averages of the tetanus for each genotype show that following the first stimulus, no measurable fEPSP was observed in response to any of the further stimuli for any genotype. This is consistent with there being no alteration in presynaptic plasticity in the Tc1 × J20 cross (**Figure 4.4**). ANOVA showed no significant effect of Has21 ($F(3,13)=1.297$, $p=0.237$) or *tgAPP* ($F(3,13)=3.608$ $p=0.273$) and no interaction ($F(3,13)=0.203$, $p=0.659$). Threshold for significance was adjusted using Holm-Bonferroni correction for multiple comparisons: $\alpha=0.017$.

Average PPR during PTP was 0.87 ± 0.11 in the wildtype animals; 0.67 ± 0.08 in the Tc1 animals; 0.63 ± 0.10 in the J20 animals, and 0.72 ± 0.12 in the Tc1×J20 animals. 2-way ANOVA showed no significant effect of trisomy 21 ($F(3,13)=0.017$, $p=0.898$) or *tgAPP* ($F(3,13)=0.162$ $p=0.693$) and no interaction ($F(3,13)=2.273$, $p=0.153$).

Average PPR during LTP was 0.75 ± 0.02 in the wildtype animals; 0.84 ± 0.13 in the Tc1 animals; 0.84 ± 0.11 in the J20 animals, and 0.92 ± 0.17 in the Tc1×J20 animals. Two-way ANOVA showed no significant effect

of trisomy 21 ($F(3,13)=0.04$, $p=0.844$) or *tgAPP* ($F(3,13)=1.567$, $p=0.230$) and no interaction ($F(3,13)=2.267$, $p=0.61$).

Table 4.1 Proportion of slices showing LTP in the *Tc1*×*J20* cross

	Wildtype	Tc1	J20	Tc1 x J20
LTP	8	3	4	0
No LTP	2	8	2	4
% LTP Induction	80%	27%	67%	0%

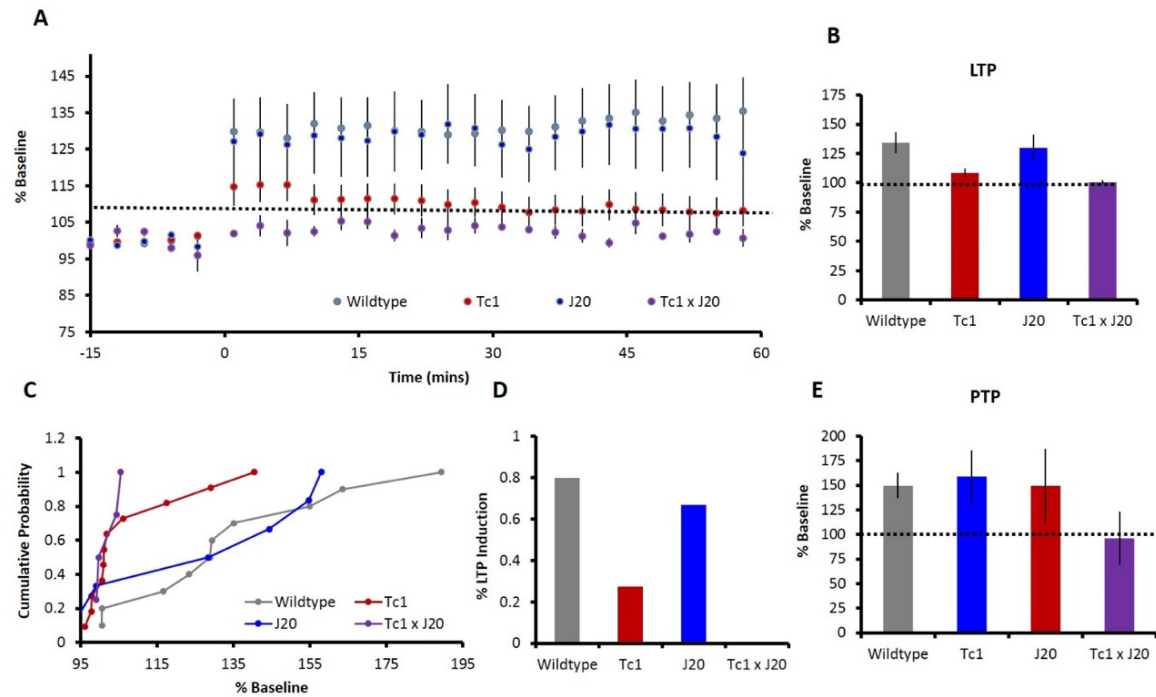


Figure 4.1 LTP in the Tc1 x J20 cross

A) Averaged fEPSP response expressed as percentage of baseline for wildtype (grey), Tc1 (red), J20 (blue) and Tc1xJ20 (purple) mice. Each data point represents an average of 9 responses recorded over 3 minutes. LTP was induced a time 0. Error bars show SEM. **B)** Average fEPSP slope for wildtype, Tc1, J20 and Tc1xJ20 mice 46-60mins after LTP induction. Error bars show SEM. **C)** Cumulative probability curves for LTP induction in Tc1, J20 and Tc1xJ20 mice. **D)** Percentage of animals showing potentiation greater than 115% baseline for each genotype. **E)** Average fEPSP slope during post-tetanic potentiation for each genotype. Error bars show SEM.

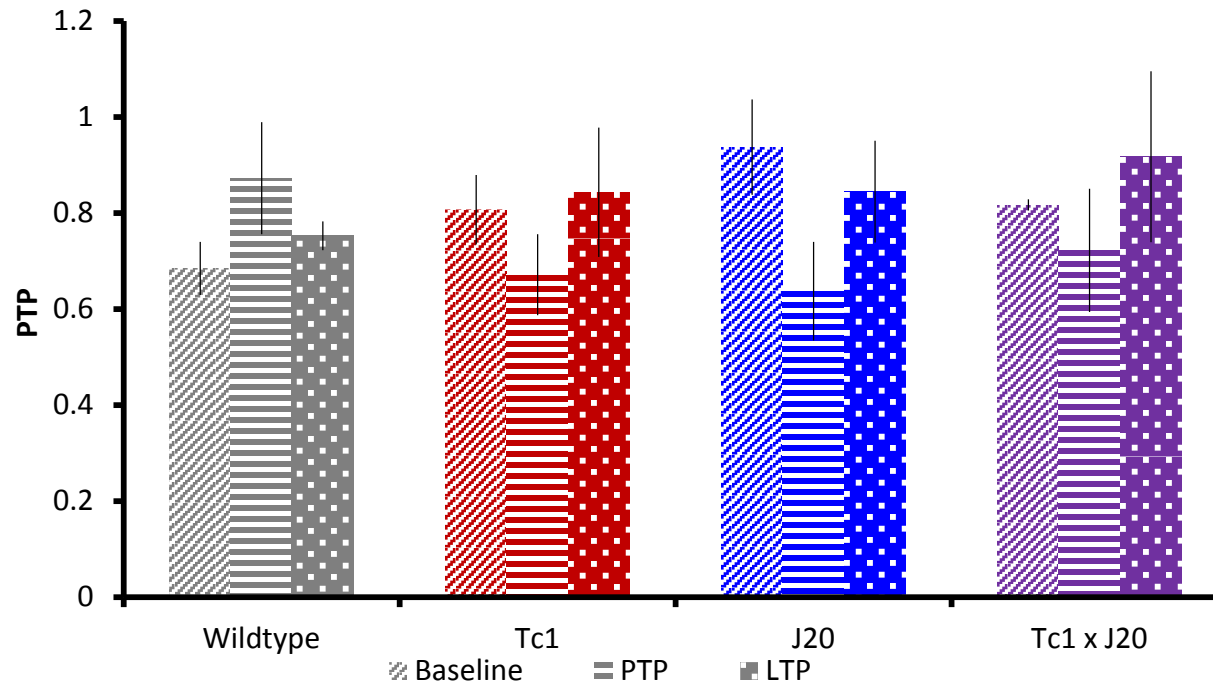


Figure 4.2 Paired pulse ratio during baseline, LTP and PTP in the Tc1xJ20 cross.

Average paired pulse ratio for wildtype, Tc1, J20, and Tc1xJ20 mice. Averages represent PPR during the 15 minutes of baseline, post-tetanic potentiation, and the final 15 minutes of LTP

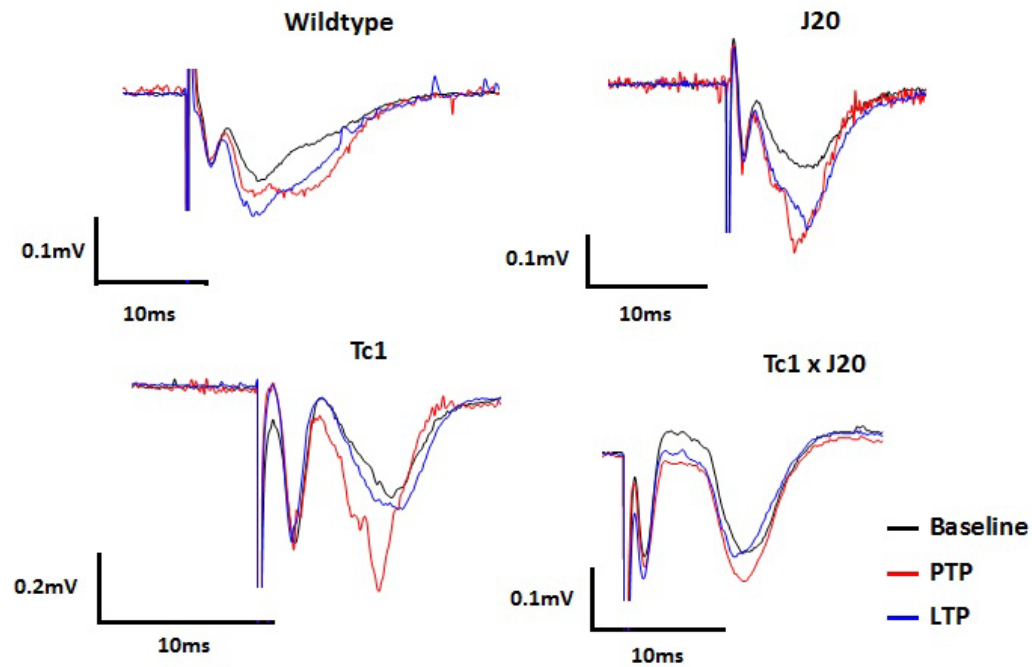


Figure 4.3 Example fEPSPs during LTP in the Tc1 × J20 cross

Examples of fEPSPs recorded during baseline, post-tetanic potentiation, and LTP for individual wildtype, Tc1, J20 and Tc1×J20 mice. Baseline and LTP responses represent the average of 9 traces (3min) taken from the first and last 15 minutes of the recording and PTP. Post-tetanic potentiation represents an average of the first 2 traces recorded following the LTP induction protocol (40s).

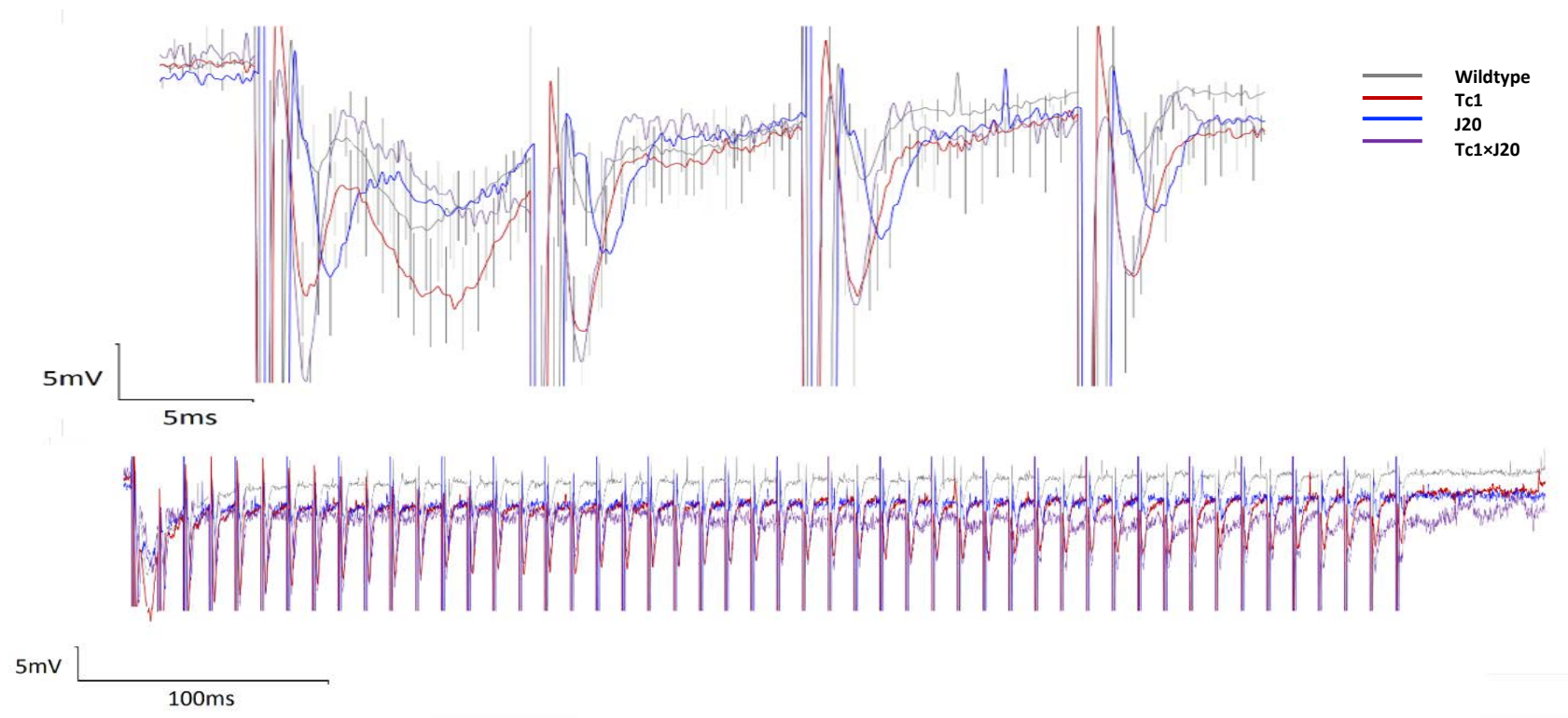


Figure 4.4 Superimposed average responses during tetanic stimulation

Superimposed traces representing average response in wildtype (grey), Tc1 (red), J20 (blue) and Tc1xJ20 (purple) for the first 4 pulses of the 50 pulse train (top) and for the entire train (bottom). Error bars (SEM) are shown on the first 4 pulses, and are depicted alternately for every 4th data point for each genotype to prevent the signal being obscured.

4.3.2 Preliminary data on Long-term depression in the Tc1 × J20 cross

In addition to deficits in LTP, enhanced LTD has been reported in the hippocampus of both AD and DS mouse models. To determine whether this was the case in the Tc1 × J20 cross, LTD was induced in the MPP of acute hippocampal slices, which had not undergone any previous plasticity inducing protocol (**Figure 4.6A**). Some degree of depression was observed in slices from all genotypes. LTD was observed in all J20 slices, however for wildtype, Tc1 and Tc1×J20 animals, depression occurred in some but not all of the slices. Wildtype mice showed an average response of $95.50\% \pm 7.79$ (SEM), n=6 slices, 6 animals, 1 hour after application of a low frequency stimulus train. In the Tc1 animals, average depression after 1 hour was $91.63\% \pm 13.0$, n=5 slices, 5 animals. In the J20 animals, average response was $60.19\% \pm 2.82$ (SEM), n=4 slices, 4 animals, and in the Tc1×J20 animals, average response was $88.21\% \pm 13.39$, n=2 slices, 2 animals. Neither trisomy 21 ($F(3,13)=1.223$, $p=0.289$) nor *tgAPP* ($F(3,13)=3.143$, $p=.100$) had a significant effect on LTD by two-way ANOVA, and there was no interaction ($F=(3,13)=2.133$, $p=0.168$).

The percentage of slices showing LTD was calculated for each genotype with a threshold for LTD of 90% of baseline (see **Table 4.2**). Effect of genotype was not significant by 4×2 Fisher's Exact Test ($p=0.121$).

Table 4.2 Proportion of slices showing LTD in the Tc1×J20 cross

	Wildtype	Tc1	J20	Tc1 x J20
LTD	3	2	4	1
No LTD	3	3	0	1
% LTD induction	50%	40%	100%	50%

Genotype also had no significant impact on the amount of short-term depression (STD) immediately following the LTD inducing protocol (**Figure 4.6C**). Average fEPSP slope in the wildtype mice for the first 3 minutes following LTD induction was $91.59\% \pm 0.25$ (SEM); in the Tc1 mice was $79.98\% \pm 20.068$ (SEM); in the J20 mice was $34.65\% \pm 16.92$ (SEM); and in the Tc1×J20 mice was $87.79\% \pm 10.13$ (SEM). Two-way ANOVA showed no significant effect of Hsa21 ($F(3,13)=0.01$, $p=0.93$) or J20 ($F(3,13)=2.15$, $p=0.65$) and no interaction ($F(3,13)=1.574$, $p=0.23$), suggesting that STD is not enhanced by Hsa21 or *tgAPP* in this model.

Average PPR was also measured during baseline, STD and LTD. Average PPR during baseline was 0.82 ± 0.06 in the wildtype animals; 0.90 ± 0.10 in the Tc1 animals; 1.01 ± 0.06 in the J20 animals, and 1.15 ± 0.14 in the Tc1×J20 animals. Two-way ANOVA showed no significant effect of trisomy 21 ($F(3,13)=1.451$, $p=0.250$) or *tgAPP* ($F(3,13)=5.831$, $p=0.031$) and no interaction ($F(3,13)=0.104$, $p=0.6752$), although there was a trend towards an effect of *tgAPP*. Threshold for significance was adjusted using Holm-Bonferroni correction for multiple comparisons: $\alpha = 0.017$.

Average PPR during STD was 0.76 ± 0.04 in the wildtype animals; 1.57 ± 0.55 in the Tc1 animals; 1.30 ± 0.13 in the J20 animals, and 0.91 ± 0.21 in the Tc1×J20 animals. Two-way ANOVA showed no significant effect of trisomy 21 ($F(3,13)=0.319$, $p=0.582$) or *tgAPP* ($F(3,13)=0.027$, $p=0.872$) and no interaction ($F(3,13)=2.594$, $p=0.131$).

Average PPR during LTD was 0.85 ± 0.07 in the wildtype animals; 0.83 ± 0.06 in the Tc1 animals; 0.92 ± 0.15 in the J20 animals, and 0.86 ± 0.19 in the Tc1×J20 animals. Two-way ANOVA showed no significant

effect of trisomy 21 ($F(3,13)=0.135$, $p=0.719$) or *tgAPP* ($F(3,13)=0.222$, $p=0.645$) and no interaction ($F(3,13)=0.041$, $p=0.844$).

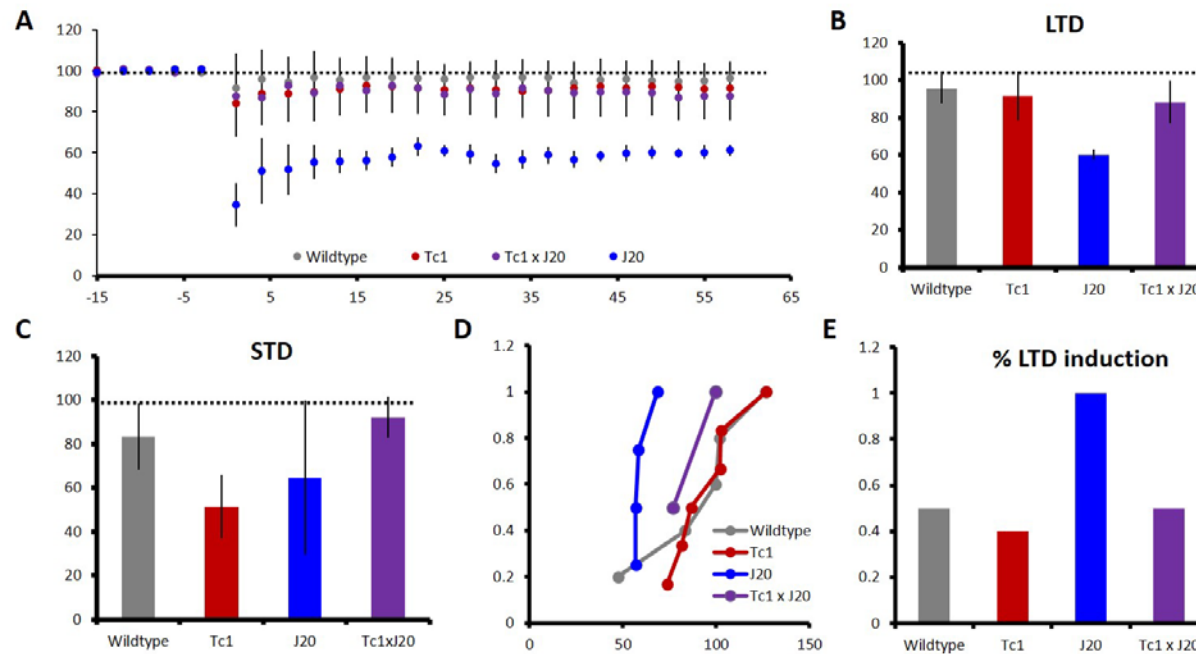


Figure 4.5 LTD in the Tc1 x J20 cross

A) Averaged fEPSP response expressed as percentage of baseline for wildtype (grey), Tc1 (red), J20 (blue) and Tc1xJ20 (purple) mice. Each data point represents an average of 9 responses recorded over 3 minutes. LTD was induced a time 0. Error bars show SEM. **B)** Average fEPSP slope for wildtype, Tc1, J20 and Tc1xJ20 mice 46-60mins after LTD induction. Error bars show SEM. **C)** Average fEPSP slope during short term depression for each genotype. Error bars show SEM. **D)** Cumulative probability curves for LTD induction in Tc1, J20 and Tc1xJ20 mice. **E)** Percentage of animals showing depression less than 90% baseline for each genotype.

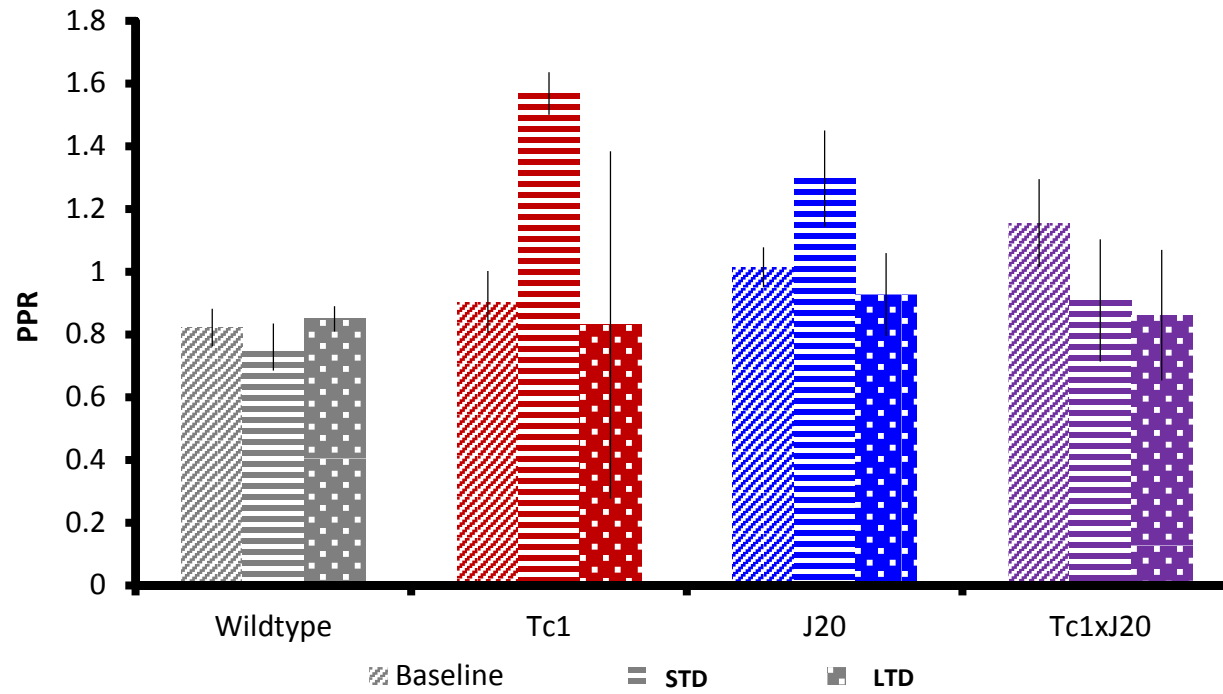


Figure 4.6 Paired pulse ratio during baseline, LTD and STD in the Tc1xJ20 cross.

Average paired pulse ratio for wildtype, Tc1, J20, and Tc1xJ20 mice. Values represent average PPR during the 15 minutes of baseline, PPR during short term depression, and average PPR during the final 15 minutes of LTD.

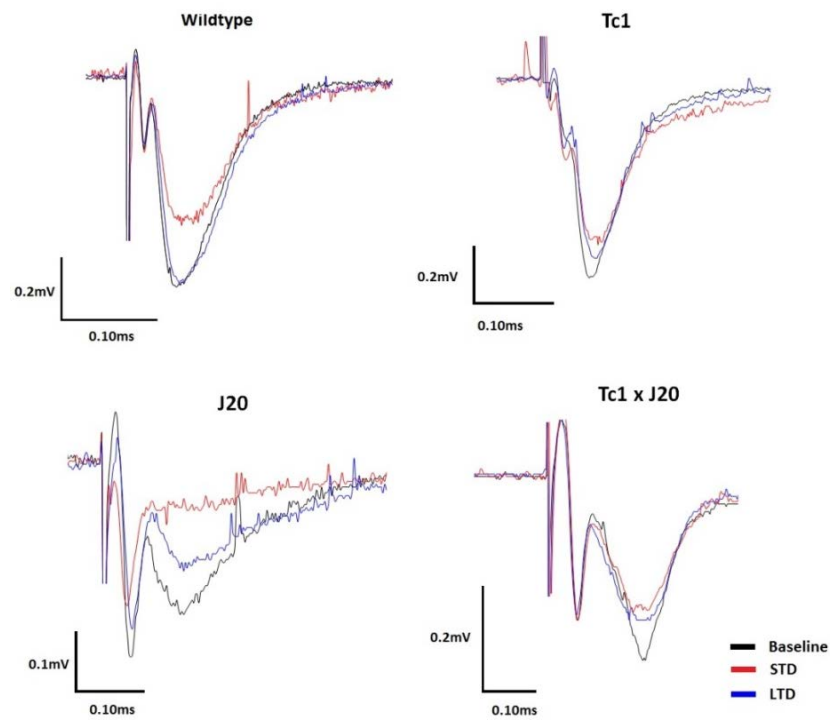


Figure 4.7 Example fEPSPs during LTD in the Tc1 × J20 cross

Examples of fEPSPs recorded during baseline, short-term depression, and LTD for individual wildtype, Tc1, J20 and Tc1×J20 mice. Baseline and LTD responses represent the average of 9 traces (3min) taken from the first and last 15 minutes of the recording and PTP. Short-term depression represents an average of the first 2 traces recorded following the LTD induction protocol (40s).

4.3.3 Preliminary data on LTP in the Dp1Tyb model at 6 months of age

LTP was also induced in the MPP of the Dp1Tyb mice and their wildtype littermates at 6 months of age (**Figure 4.8A**). Synaptic plasticity in the DG is known to be impaired in the Ts65Dn model and the 'triple trisomic' model of DS, however it has not been investigated in a mouse model trisomic only for the Hsa21 syntenic region of Mmu16. As was the case for the Tc1 × J20 cross, inhibitory signalling was not blocked to avoid masking any potential phenotypes.

1 hour post LTP induction, fEPSP slope in the wildtype mice was $143.38\% \pm 27.88$ (SEM) of baseline, n=4 slices, 3 animals, and fEPSP slope in the Dp1Tyb mice was $105.27\% \pm 4.89$ (SEM) baseline, n=6 slices, 5 animals. Although the difference did not reach statistical significance (Student's t-test: p=0.13), none of the Dp1Tyb mice showed potentiation, consistent with the effect observed in the Tc1 mice.

The percentage of slices showing LTP was calculated for wildtype and Dp1Tybs mice with threshold for LTP of 115% (see **Table 4.3**) however effect of genotype did significant by 2×2 Fisher's Exact Test (p=0.119).

Table 4.3 Proportion of slices showing LTP in the Dp1Tyb Model

	Wildtype	Dp1Tyb
LTP	3	1
No LTP	1	5
% LTP Induction	75%	17%

A retrospective power calculation suggests that due to the high standard deviation which results from the variability in the wildtype animals ($\sigma=27.88$), a sample size of 63 animals would be necessary to detect a difference in LTP between Dp1Tyb and wildtype animals, using an α value of 0.05 and a β value of 0.20. This suggests that future work

may require optimisation of the protocol to reduce the variability of LTP expression in the wildtype animals.

There was also no significant difference in PTP (**Figure 4.9C**). Averaged fEPSP for the first 3 minutes after tetanic stimulation was $179.46\% \pm 30.87$ (SEM) of baseline in the wildtype animals and $147.37\% \pm 5.04$ (SEM) of baseline in the Dp1Tyb animals (Student's t-test $p=0.500$).

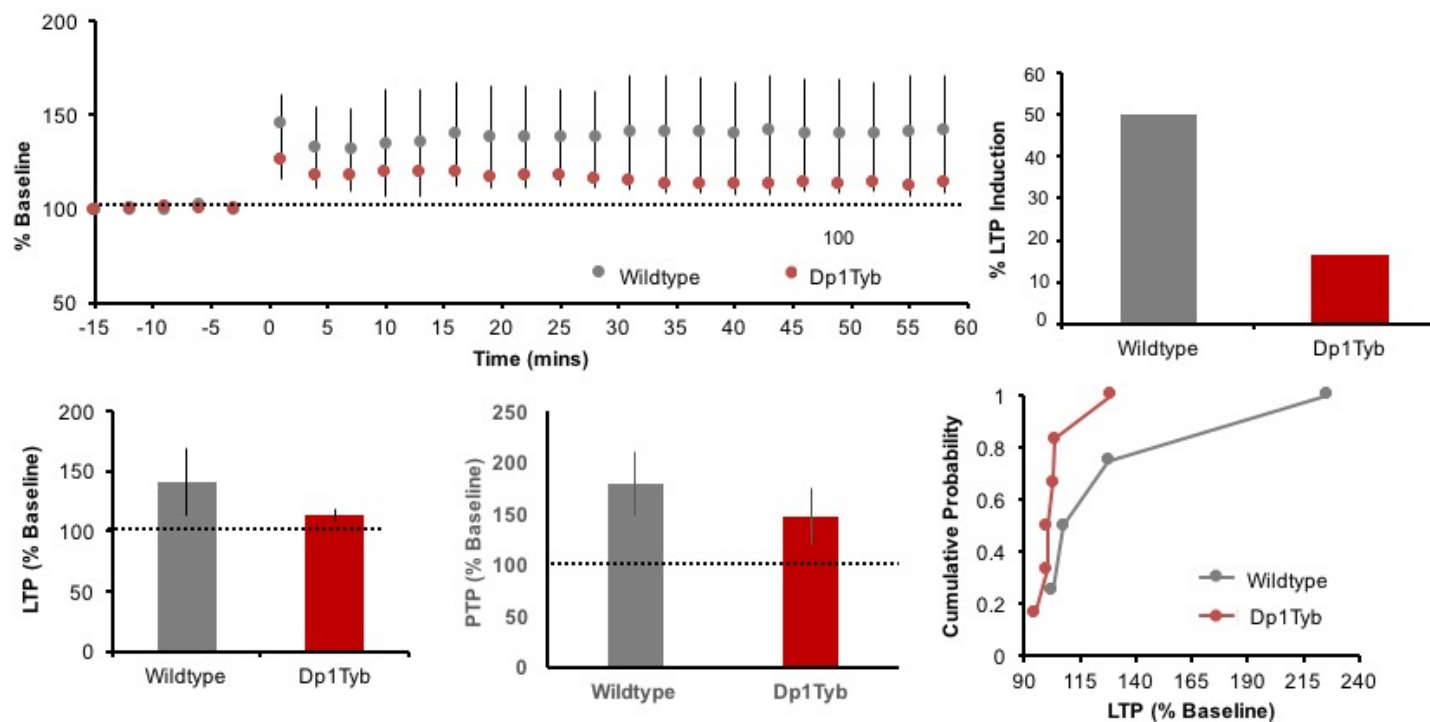


Figure 4.8 LTP in the MPP of the Dp1Tyb mice at 6 months of age

A) Averaged fEPSP response expressed as percentage of baseline for wildtype (grey) and Dp1Tyb (red) animals. Each data point represents an average of 9 responses recorded over 3 minutes. LTP was induced a time 0. Error bars show SEM. **B)** Average fEPSP slope for Dp1Tyb and wildtype animals 46-60mins after LTP induction, expressed as percentage of baseline. Error bars show SEM. **C)** Average fEPSP during PTP, expressed as a percentage of baseline. Error bars show SEM. **D)** Cumulative probability curves, showing the range of fEPSP potentiation, and the probability of potentiation occurring within the range for each genotype.

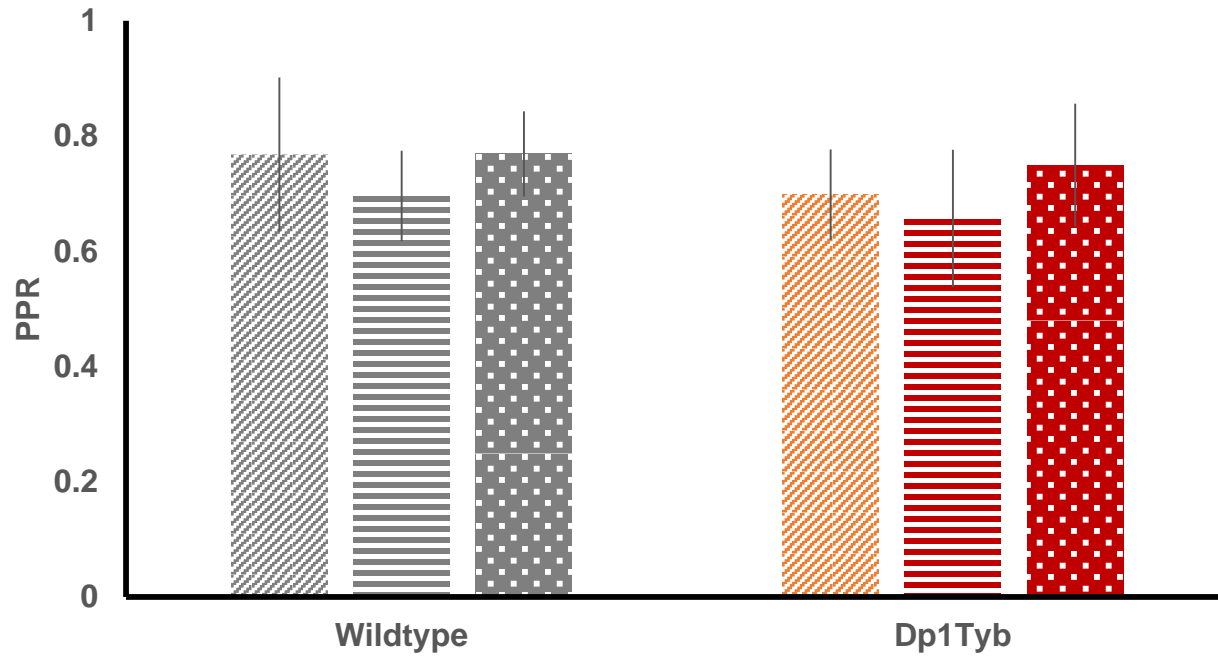


Figure 4.9 Paired pulse ratio during baseline, PTP and LTD in Dp1Tyb Model.

Average paired pulse ratio for wildtype and Dp1Tyb mice. Values represent average PPR during the 15 minutes of baseline, PPR during post-tetanic potentiation, and average PPR during the final 15 minutes of LTD.

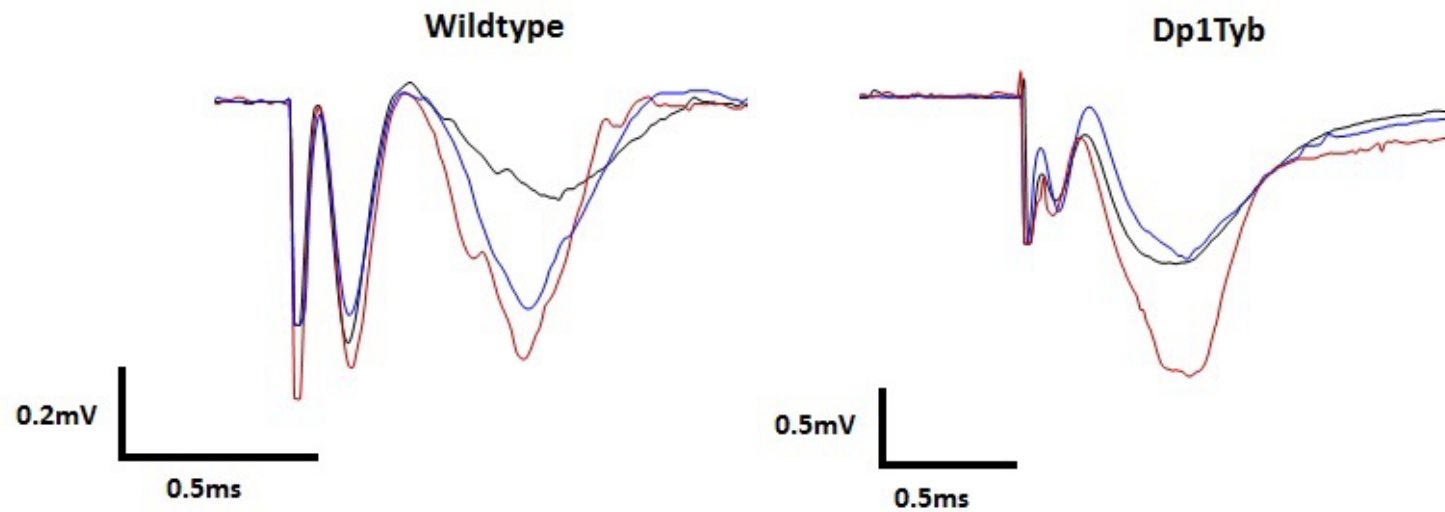


Figure 4.10 Example fEPSPs during LTP in the Dp1Tyb model

Examples of fEPSPs recorded during baseline (grey), PTP (red) and LTP (blue) for individual wildtype and Dp1Tyb mice. Baseline and LTP responses represent the average of 3 traces (1min) taken from the first and last 15 minutes of the recording and PTP represents an average of the first 2 traces recorded following the LTP induction protocol (40s).

4.4 Discussion

The data presented here suggest that trisomy of Hsa21 is associated with a deficit in LTP in the MPP. This is consistent with previously published *in vivo* data from the Tc1 model (O'Doherty *et al.*, 2005), which reports a deficit in perforant path LTP 1 hour after induction, as well as with observations from other mouse models of DS. Interestingly, LTP in the DG of Tc1 mice after 24 hours is unimpaired *in vivo* (Morice *et al.*, 2008) suggesting the mechanism of LTP impairment in this model may relate specifically to early LTP, the expression of which is protein-synthesis independent.

The presence of *tgAPP* did not exacerbate LTP deficits in the Tc1 animals, despite being associated with an exacerbation of behavioural deficits and amyloid pathology. It is possible that this is the result of a floor effect in the extent of the potentiation deficit, rather than a genuine lack of interaction between *tgAPP* and trisomy. In the Ts65Dn model, there is a profound loss of potentiation in the DG (Kleschevnikov *et al.*, 2004), while deficits in CA1 are more subtle (Costa and Grybko, 2005). Consistent with this, Tc1 mice showed a profound loss of potentiation in the DG, which for the majority of slices would have precluded any further impairment by other mechanisms.

Although a deficit in LTP has previously been reported in the MPP of the J20 mice used to generate this cross (Palop *et al.*, 2007), no deficit was observed under the experimental conditions used here, suggesting that *tgAPP* alone is not sufficient to produce a deficit in LTP in this context. The failure to replicate this deficit may be attributed to differences in recording conditions, induction protocol or genetic background. Palop *et al.* (2007) used a theta burst protocol to induce LTP, while the data presented here was obtained using HFS. Notably,

different LTP induction protocols are known to induce different signalling cascades, which may be of differing significance in the context of *tgAPP*. Palop *et al.* (2007) also reported extensive remodelling of excitatory and inhibitory circuitry in J20 mice; the LTP deficits they report may therefore reflect differences in the effectiveness of particular patterns of activity in eliciting LTP, rather than a general inability of the J20 mice to express plasticity in the DG.

Furthermore, Palop *et al.* (2007) reported PPF in the DG of the J20 animals, while in the data presented here, the Tc1 × J20 cross showed PPI across all genotypes (*see Chapter 3*). This suggests that they may have been recording from a different population of synapses, possibly in the LPP, rather than the MPP. If this were the case, it would imply that *tgAPP*-associated alternations to synaptic plasticity in the DG are pathway specific.

In addition, the mice used for these experiments are maintained on a hybrid background in order to prevent loss of Hsa21 transmission, and differences in synaptic plasticity between strains may be pronounced (Nguyen *et al.*, 2000). Furthermore, non-inbred mice exhibit hybrid vigour, for example the offspring of 129 and B16 mice outperform both inbred strains on the MWM (Wolfer and Lipp, 2000). As MWM behavioural deficits commonly correspond to deficits in LTP, it is possible that LTP is also more robust in hybrid animals.

Alternatively, the animals used for the experiments presented here were transcardially perfused with a neuroprotective solution containing NMDG (*see Section 2.2.1* for further details), which has been reported to reduce neuronal stress during the production of hippocampal slices. Excitotoxicity and oxidative stress have been identified as key contributors to AD pathology; it is therefore possible that the J20 slices are more susceptible to damage during the slicing

process than wildtype slices, which may enhance deficits in plasticity. The protective slicing protocol used here may therefore have been more effective in ameliorating this damage than the protocol used by Palop *et al.* (2007), resulting in a preservation of synaptic plasticity.

Enhanced LTD has been reported in the CA1 region of the Ts65Dn (Siarey *et al.*, 1999; Scott-McKean and Costa, 2011) and Ts1Cje (Siarey *et al.*, 2005) models of DS. However, it has not been previously characterised in the DG of any DS model. The data presented here shows no significant difference in LTD in the DG between the wildtype and Tc1 animals. This suggests that enhanced LTD in DS may be pathway specific, although it is also possible that it relates to differences in the combination of duplicated genes present within these models, and that one or more of the genes that are not overexpressed in the Tc1 mice mediate an increased propensity to depression.

The degree of mosaicism in the Tc1 model may also be relevant. This would be consistent with the large degree of variability in response to the LTD induction protocol observed in these animals, with some Tc1 slices showing substantial depression and others showing none. If this were the case, LTD in non-mosaic models would be expected to show a more consistent enhancement of depression. Further characterisation of hippocampal LTD across DS mouse models is therefore required to understand how trisomy affects LTD in different hippocampal pathways.

The J20 mice showed a trend towards an enhancement of LTD. Enhanced LTD in the J20 mice would be consistent with previous reports that soluble A β enhances synaptic depression (Shankar *et al.*, 2008; Li *et al.*, 2009). Interestingly, there was no evidence of an enhancement in the Tc1 \times J20 animals, although the number of Tc1 \times J20 animals available was n=2. Levels of soluble A β are not elevated in the

Tc1×J20 animals, compared to those expressing tgAPP alone (Wiseman *et al.*, in preparation). This suggests that if LTD were differentially affected in the Tc1×J20 animals, it would be mediated through an alteration in the response of trisomic neurons to A β , rather than an alteration in A β level. Further investigation is therefore required to determine whether this is the case, and if so, how it relates to the presence of Hsa21 or to interactions between Hsa21 and tgAPP.

Consistent with the results observed in the Tc1 model, and in other Mmu16 segmental trisomy models, none of the Dp1Tyb animals showed potentiation in response to the LTP induction protocol. However, LTP in Dp1Tyb animals was not significantly different in comparison to the wildtype group, as only a subset of the wildtype animals underwent potentiation, resulting in a high level of variability in the data. Therefore, although these data do not preclude an LTP deficit in the Dp1Tyb model, the degree of variability in the wildtype mice suggests that a very large number of animals would be required to determine whether this is a real effect. Although variability in LTP was observed in the control group for all experiments, and is therefore not unexpected, the genetic background of the Dp1Tyb animals differs from that of the Tc1 × J20 cross, which may influence the efficiency of LTP induction. Modification of the LTP induction protocol, or the experimental set up, to enhance LTP induction in the wildtype control group may therefore be necessary for a deficit in the Dp1Tyb mice to be reliably detected.

Regulation of both LTP and LTD are complex, and a number of interventions have been proposed to rescue LTP deficits in both DS and AD transgenic mice, suggesting that in both models, dysfunction may occur simultaneously in multiple pathways, which interact to contribute to a deficit. The deficits in LTP, LTD and PTP reported here

must therefore be considered carefully in the context of the model and experimental protocol used, before inferences can be made regarding the relevance of these deficits to human pathology.

4.5 Conclusion

These data demonstrate that trisomy 21 results in a deficit in LTP in the medial perforant path of the Tc1×J20 cross at 6 months of age. Contrary to previously published work, *tgAPP* was not associated with a deficit in LTP and there was no interaction between *tgAPP* and trisomy 21, suggesting that the exacerbation in cognitive deficits observed in the Tc1×J20 animals did not result from an exacerbation of impairments in synaptic plasticity in the medial perforant path. Preliminary data also showed no significant effect of trisomy 21, *tgAPP*, or interactions between them, on LTD or STD in the Tc1 x J20.

No effect of *tgAPP* or trisomy 21, and no interactions between them, was observed on PTP, suggesting that this form of short term plasticity was unimpaired. Furthermore, no significant changes in PPR were observed during LTP or LTD. These data therefore suggest that neither *tgAPP* nor trisomy 21 modify presynaptic plasticity in Tc1×J20 cross at 6 months of age.

Preliminary data from the Dp1Tyb model showed no significant effect of segmental duplication of Mmu16 on LTP or PTP, and no changes in PPR during LTP. However, power calculations based on the data obtained suggest a very high level of variability in the wildtype animals. Optimization of the LTP induction protocol to account for differences in genetic background may therefore be necessary to produce more consistent potentiation in these animals.

Chapter 5

Mechanisms of impaired synaptic plasticity in AD-DS

5.1 Introduction

5.1.1 Impaired synaptic plasticity in DS and AD-DS

The genetic complexity of DS suggests that multiple mechanisms may contribute to cognitive impairment. In mouse models of DS, the influence of these mechanisms on synaptic plasticity is likely to be of differing importance, depending on the combination of duplicated genes, and on the genetic background of the model. However, other factors such as the presence of human DNA, or of an additional unpaired chromosome may also be relevant.

5.1.2 The role of inhibition in long-term potentiation

Excessive inhibition in the hippocampus has been proposed as key mechanism underlying cognitive dysfunction in DS. Inhibition is primarily mediated by the neurotransmitter GABA. There are two types of GABA receptor: GABA_A receptors (GABA_ARs) are Cl⁻ permeable ion

channels, and mediate fast inhibitory neurotransmission in the adult brain, by contributing to neuronal hyperpolarisation and decreasing membrane resistance, making the neuron more difficult to depolarise; GABA_B receptors (GABA_BRs) are metabotropic receptors, and couple to K⁺ channels via G-proteins. Activation of GABA_B receptors has the same net effect of increasing neuronal hyperpolarisation, but they act over a slower timescale, and therefore exert a different effect on the computational properties of the network.

The level of synaptic inhibition influences the conditions required for the induction of LTP. Antagonism of GABA_AR has been shown to facilitate the induction of LTP, by reducing the amount of stimulation required. However GABA_AR antagonists did not appear to increase the maximum expression of LTP, nor did they affect predominantly presynaptic forms of short-term plasticity, suggesting a specific postsynaptic effect on LTP induction (Gustafsson and Wigström., 1985). This effect is likely to be mediated by a decrease in inhibition of the postsynaptic neuron, allowing depolarisation to occur with reduced levels of synaptic input, and facilitating the activation of postsynaptic NMDA receptors (Grover and Yan, 1999). Consistent with a role for inhibition in determining the threshold for LTP induction, LTP in the perforant path *in vivo* can be blocked if tetanic stimulation is preceded by stimulation of the contralateral commissural afferents, which activates the inhibitory interneurons targeting the DGCs, suggesting increased postsynaptic inhibition is sufficient to block the induction of LTP (Douglas, Goddard and Riives, 1982).

Inhibition via GABA_BRs is also important in regulating synaptic plasticity, and appears to contribute to determining the threshold between LTP and LTD by modifying the levels of feedback inhibition, whereby active excitatory neurons stimulate inhibitory interneurons,

which subsequently feedback to inhibit the excitatory cells. Differential activation of presynaptic and postsynaptic GABA_B receptors appear to exert opposing effects on the initiation of LTP. Presynaptic GABA_B receptors mediate the auto-inhibition of GABAergic interneurons, therefore, blockade of these receptors enhances GABAergic neurotransmission, suppressing LTP. Conversely, postsynaptic GABA_B receptors mediate hyperpolarisation of the postsynaptic neuron. Consequently, blocking these receptors facilitates the depolarisation that is required for activation of NMDA receptors.

The resulting effect of GABA_B receptor block on LTP appears to depend on both the concentration and selectivity of the antagonist, and on the induction protocol (Stäubli, Scafidi and Chun, 1999). LTP resulting from high frequency tetanic stimulation (HFS-LTP) is facilitated in the presence of GABA_BR antagonism at all concentrations, while LTP induced by theta burst stimulation (TBS-LTP) was facilitated at a low concentrations, but depressed at high concentrations, suggesting that auto-inhibition of GABAergic transmission occurs over the same timescale as theta bursts. This effect was also reflected in the impact of GABA_BR antagonism on memory *in vivo*, suggesting that this mechanism more closely reflects the physiological regulation of LTP.

5.1.3 Inhibition in DS

Blocking GABAergic neurotransmission has been shown to rescue deficits in synaptic plasticity and behaviour in mouse models of DS. The majority of evidence for a role of 'over-inhibition' in DS has been obtained from the Ts65Dn mouse model. Kleschevnikov *et al.* (2004) reported that the GABA_AR antagonist picrotoxin (PTX) rescued deficits in LTP in the DG, and their data suggests that an increase in feedback

inhibition leads to reduced postsynaptic depolarisation, and therefore to reduced NMDA receptor activation, which they attribute to an increase in release probability at GABAergic synapses. PTX has also been reported to rescue deficits in LTP in the DG of the 'triple trisomic' model of DS, suggesting inhibition is also increased in this model, although the mechanisms for this have not been characterised (Belichenko *et al.*, 2015).

Deficits in LTP in the Schaffer collateral of the Ts65Dn mice have also been reported to be rescued by PTX (Costa and Grybko, 2005). However, there has been some discrepancy over the severity of LTP deficits in the CA1 region of the Ts65Dn model. Deficits in HFS-LTP were identified, along with enhanced LTD by Siarey *et al.*, (1999; 1997) yet Costa and Grybko, (2005) found HFS-LTP to be normal, and observed deficits only in TBS-LTP. Notably, the extent of LTP induced by HFS and TBS protocols were similar in the Ts65Dn animals, while the degree of LTP in the wildtypes was greater in response to TBS-LTP.

TBS and HFS have been shown to differentially affect the potentiation of inhibitory postsynaptic potentials (IPSPs). IPSPs in CA1 pyramidal cells were consistently potentiated following TBS, while HFS had variable results, with individual inputs showing a mixture of depression, potentiation and no response, leading to no net change in network activity (Perez *et al.*, 1999). This diversity was suggested to result from a combination of two opposing mechanisms; an NMDA dependent potentiation of IPSPs and a Ca²⁺ mediated depression of IPSPs. The authors also suggested that TBS may be more effective at inducing plasticity at inhibitory synapses. If this is the case, the deficit in TBS induced LTP in the Ts65Dn animals may reflect enhanced plasticity of inhibitory inputs rather than reduced plasticity of excitatory inputs. The reason for the discrepancy in results between Costa and Grybko, and

Siarey *et al.*, remains unclear; Costa and Grybko demonstrate that it does not relate to differences in stimulation protocol or genetic background, however they suggest that differences in the stimulation intensity for HFS may affect the expression of plasticity at GABAergic synapses.

Kleschevnikov *et al.* (2004) also observed an increase in postsynaptic GABA_B signalling in the Ts65Dn mouse, resulting from an increase in expression of Kir3.2 inwardly rectifying K⁺ channels, which are coupled to GABA_B receptors, and are encoded by the *Kcnj6* gene, the orthologue of which is on Hsa21. The levels of GABA_AR and GABA_BR subunits in the hippocampus were not changed, and immunoreactivity for GAD-65 — required for the synthesis of GABA — was also unaffected, consistent with functional rather than structural changes in GABAergic signalling.

However, this is contrary to the observations of Chakrabarti *et al.*, (2010) who reported an increase in the number of interneurons in the CA1 region of the Ts56dn mouse, which could be rescued by normalising the gene dose of the transcription factors *Olig1* and *Olig2*. This was accompanied by an increase in the frequency of spontaneous inhibitory postsynaptic currents (sIPSPs), which are triggered by spontaneous action potential firing in interneurons, but not in miniature inhibitory postsynaptic currents (mIPSPs), which correspond to the unprovoked fusion of single vesicles to the presynaptic membrane. Chakrabarti *et al.* (2010) reported this to be consistent with an increase in interneuron number, but not in inhibitory synapses per neuron. However, Kleschevnikov *et al.* (2004) did report an increase in the frequency of mIPSPs in the DG, corresponding to the increase in release probability at GABAergic synapses that they proposed. These data therefore suggest that inhibitory neurotransmission may be disrupted by multiple mechanisms in a region specific way

In addition to the putative roles of *Kcnj6* and the *Olig1* and *Olig2* transcription factors in regulating interneuron number, duplication of *Grik1*, encoding the GluK1 kainate receptor subunit may also contribute to enhanced inhibition. Cossart *et al.* (1998) suggest that two kainate receptor mediated systems exist in the hippocampus; one mediated by GluK2-containing receptors, which excites pyramidal neurons, contributing to kainic acid induced epileptogenesis, and a GluK1-mediated system which excites inhibitory interneurons, contributing to an increase in tonic inhibition. An increase in GluK1 expression may therefore promote activation of the second system, leading to increased inhibition.

However, it should be noted that the evidence for increased inhibition in the brains of DS patients is negligible. A limited number of studies have looked at levels of GABA in DS neurons, and none of them have found it to be increased. GABA has been reported to be decreased in foetal frontal cortex tissue (Whittle *et al.*, 2007) and the ratio of GABA to the metabolic marker creatine was found to be reduced in proton magnetic resonance spectroscopy studies of the brains of children with DS (Śmigielska-Kuzia *et al.*, 2010). Furthermore, post-mortem studies of DS brains reported no change in GABA (Seidl *et al.*, 2001). While this does not preclude the occurrence of functional changes in inhibitory circuitry leading to increased network inhibition, it suggests that evidence from mouse models regarding excessive inhibition should be treated with caution until corresponding deficits are demonstrated to exist in the DS patient population.

5.1.4 Chemical LTP

In addition to the use of electrical stimulation protocols, LTP in the MPP can be induced pharmacologically, using drugs that directly activate the downstream effectors in the signalling cascades mediating LTP expression. If chemical LTP is intact despite deficits in stimulation induced LTP, it suggests that the mechanisms underlying LTP expression are preserved, and that the deficit therefore results from a failure in the activity-dependent induction of LTP.

To determine whether the LTP deficits in the trisomic animals were caused by a deficit in LTP induction, or a deficit in the downstream signalling pathways mediating LTP expression, chemical LTP was induced in acute hippocampal slices using the adenylyl cyclase activator forskolin. Forskolin activation of adenylyl cyclase results in an increase in the production of 3',5'-cyclic adenosine monophosphate (cAMP), which activates protein kinase A (PKA). PKA has been implicated in the expression of late-LTP, and has been shown to act in part via the transcription factor cyclic AMP response element-binding protein (CREB). PKA-dependent LTP has been most extensively characterised in CA1 (Frey, Huang and Kandel, 1993; Abel *et al.*, 1997), but has also been reported in the medial perforant path (Nguyen and Kandel, 1996).

However, it has also been suggested that forskolin-mediated LTP in CA1 does not result from a direct activation of cAMP-dependent signalling processes, but that the activation of NMDA receptors is still required, albeit at a far lower frequency than would be required for stimulation-induced LTP (Otmakhov *et al.*, 2004). This suggests that cooperation between PKA and Ca²⁺ is required for the induction of chemical LTP in CA1. It is not known whether this is also the case in the DG. Otmakhov *et al.*, (2004) reported forskolin-mediated LTP required the application

of a low frequency test stimulus, and could be induced only if applied together with low Mg^{2+} or a $GABA_A$ antagonist to increase excitability. However, in the MPP recordings presented here, LTP was reliably induced via the addition of forskolin alone and no stimulation was given during forskolin application, suggesting there may be mechanistic differences between the two regions.

5.2 Aims

1. To determine whether excessive $GABA_A$ signalling mediates impairments to synaptic plasticity in the MPP of Tc1 and Tc1×J20 mice
2. To determine whether forskolin-induced LTP is preserved in the medial perforant path in Tc1 and Tc1×J20 mice

5.3 Results

5.3.1 *Blocking GABA_ARs does not rescue LTP at 6 months of age in the Tc1 × J20 cross*

To assess whether blockade of GABA_ARs rescued deficits in synaptic plasticity in the DG, as has been reported in the Ts65Dn model and the 'triple trisomic' model of DS, LTP experiments in the Tc1 × J20 cross were repeated in the presence of PTX, an antagonist of GABA_A receptors (**Figure 5.1**). Average potentiation was increased in the wildtype mice: 160.07% ± 32.48 (SEM), n=10 slices, 6 animals; and J20 mice: 179.8% ± 51.645 (SEM), n=5 slices, 5 animals, relative to the LTP recordings made in the absence of PTX, suggesting the induction protocol used does not induce maximal LTP without PTX. However, once again, no potentiation was observed in the Tc1 animals: 106.45% ± 5.48 (SEM), n=6 slices, 6 animals, or Tc1×J20 animals: 104.99% ± 5.56 (SEM), n=6 slices, 5 animals, respectively. Although the maximal potentiation in the wildtype and J20 animals was substantially greater, as in previous experiments, potentiation did not occur in every slice, contributing to a large degree of variability in the data.

A multivariate ANOVA for the effect of PTX, tgAPP and trisomy 21 on LTP again showed a significant effect of Hsa21, but no significant effect of tgAPP or PTX, and no significant interactions: for trisomy 21 $F(7,51)=9.060$, $p=0.004$; for tgAPP $F(7,51)=0.007$, $p=0.111$; for PTX $F(7,51)=1.458$, $p=0.233$; trisomy 21 × tgAPP $F(7,51)=0.173$, $p=0.213$; for Hsa21 × PTX $F(1,51)=1.587$ $F(7,51)=1.407$, $p=0.213$; for tgAPP × PTX $F(1,51)=0.177$ $F(7,51)=1.407$, $p=0.676$; for trisomy 21 × tgAPP × PTX $F(1,51)=0.132$, $p=0.718$.

The percentage of slices showing LTP was calculated for each genotype with a threshold for LTP of 115% of baseline response (see **Table 6.1**), however the effect of genotype was not significant by 4×2 Fisher’s Exact Test (p=0. 165).

Table 5.1 Proportion of slices at 6 months of age showing LTP in the presence of PTX in the Tc1×J20 cross

	Wildtype	Tc1	J20	Tc1 x J20
LTP	6	2	3	1
No LTP	4	4	2	5
% LTP	60%	33%	60%	17%
Induction				

Average LTP in the Tc1 and Tc1×J20 mice was almost identical both with and without PTX; 106.45% ± 5.48 (SEM) compared to 108.55% ± 4.40 (SEM) for Tc1 and 104.99% ± 5.56 (SEM) compared to 101.17% ± 1.61 (SEM) for Tc1×J20. These data therefore suggest that PTX was not able to rescue LTP deficits associated with trisomy in the Tc1 × J20 cross.

Average PPR was also measured during baseline, LTP and PTP. Average PPR during baseline was 0.99± 0.11 in the wildtype animals; 1.04 ± 0.08 in the Tc1 animals; 0.95 ± 0.20 in the J20 animals, and 0.84 ± 0.09 in the Tc1×J20 animals. Two-way ANOVA showed no significant effect of Hsa21 (F(3,23)=0.004, p=0.950) or tgAPP (F(3,23)=0.945 p=0.341) and no interaction (F(3,23)=0.020, p=0.887). Threshold for significance was adjusted using Holm-Bonferroni correction for multiple comparisons (α = 0.017).

Average PPR during PTP was 0.82 ± 0.08 in the wildtype animals; 0.68 ± 0.05 in the Tc1 animals; 0.81± 0.15 in the J20 animals, and 0.70 ± 0.11 in the Tc1×J20 animals. Two-way ANOVA showed no significant effect

of trisomy 21 ($F(3,23)=0.540$, $p=0.470$) or *tgAPP* ($F(3,23)=0.523$, $p=0.477$) and no interaction ($F(3,23)=0.541$, $p=0.470$).

Average PPR during LTP was 0.96 ± 0.08 in the wildtype animals; 0.88 ± 0.08 in the Tc1 animals; 0.90 ± 0.23 in the J20 animals, and 0.75 ± 0.12 in the Tc1×J20 animals. Two-way ANOVA showed no significant effect of trisomy 21 ($F(3,23)=0.778$, $p=0.387$) or *tgAPP* ($F(3,23)=0.843$, $p=0.368$) and no interaction ($F(3,23)=0.102$, $p=0.753$).

All genotypes showed extensive variability in post-tetanic potentiation (PTP). Average fEPSP slope after LTP induction in the wildtype mice was $219.804\% \pm 40.34$ (SEM); in the Tc1 mice was $123.48\% \pm 27.11$ (SEM); in the J20 mice was $217.96\% \pm 72.47$ (SEM) and in the Tc1×J20 mice was $141.87\% \pm 47.13$ (SEM). There was no significant effect of Hsa21, *tgAPP* or PTX on PTP (**Figure 5.1E**) by 3-way ANOVA: Hsa21 $F(7,51)=3.136$, $p=0.083$; *tgAPP* $F(7,51)=0.256$, $p=0.615$; PTX $F(7,51)=0.398$, $p=0.531$; Hsa21 × *tgAPP* $F(7,51)=0.001$, $p=0.975$; Tc1 × PTX $F(7,51)=0.803$, $p=0.375$; *tgAPP* × PTX $F(7,51)=0.279$, $p=0.600$; Hsa21 × *tgAPP* × PTX $F(7,51)=1.004$, $p=0.321$.

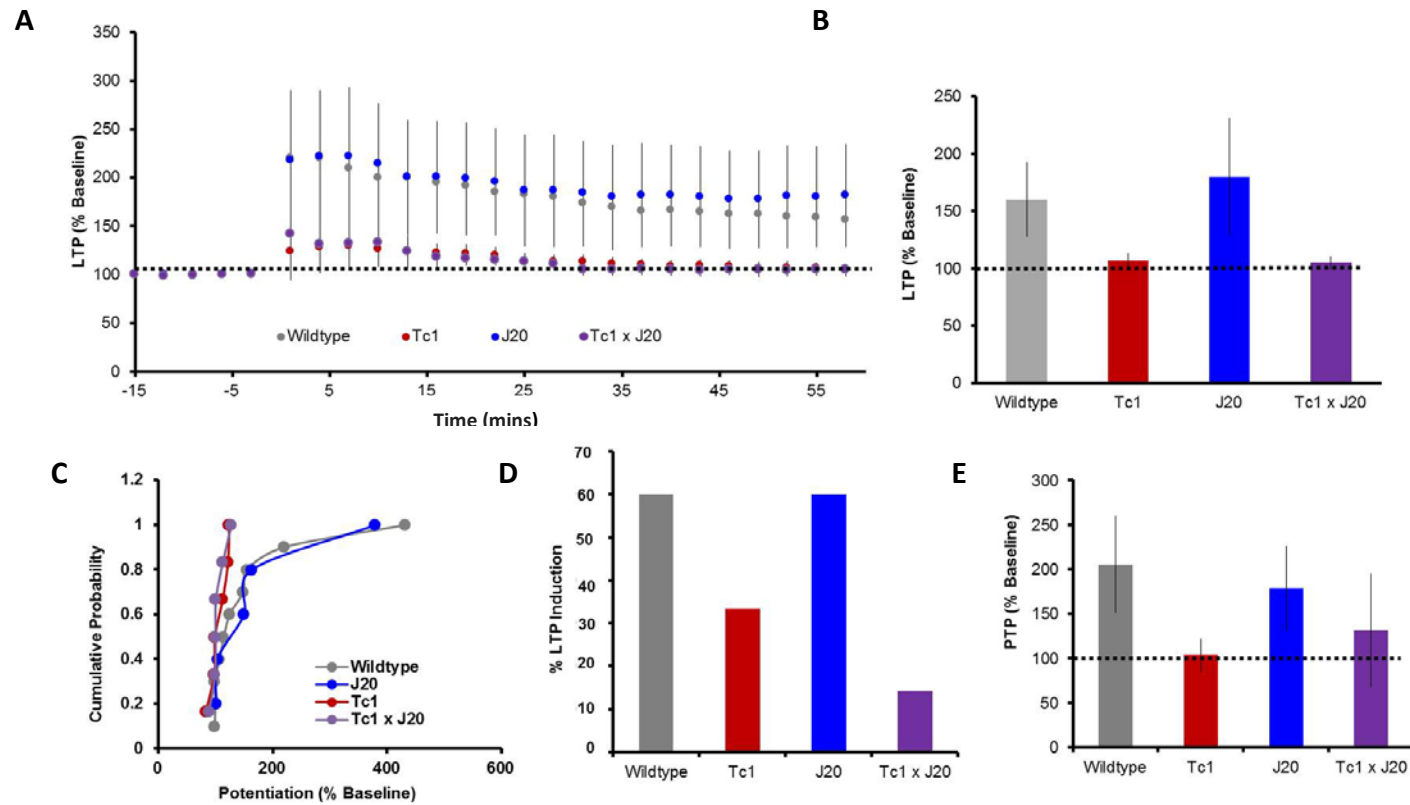


Figure 5.1 LTP following $GABA_A$ block in the MPP of the Tc1 x J20 cross at 6 months of age

A) Average fEPSP response expressed as percentage baseline for wildtype (grey), Tc1 (red), J20 (blue), Tc1xJ20 (purple) animals. Each data point represents an average of 9 responses recorded over 3 minutes. LTP was induced a time 0. Error bars show SEM. **B)** Average fEPSP slope for each genotype 46-60mins after LTP induction, expressed as percentage of baseline. Error bars show SEM.

C) Cumulative probability curves, showing the range of potentiation, and the probability of potentiation occurring within the range for each genotype. Error bars show SEM. **D)** Percentage of animals showing potentiation greater than 115% baseline for each genotype. **E)** Average fEPSP slope for the first 3 minutes after tetanisation, representing PTP, expressed as a percentage of baseline

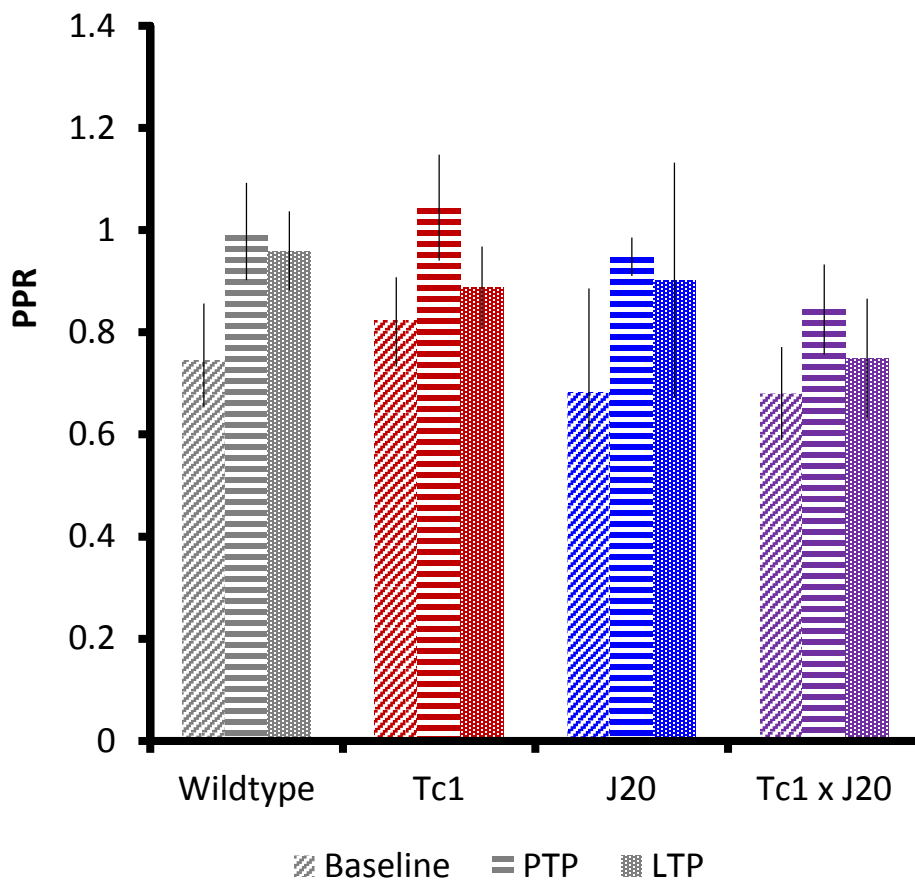


Figure 5.2 Paired Pulse Ratio during LTP at 6 months of age with $GABA_A$ R block

Average paired pulse ratio for wildtype, Tc1, J20, and Tc1 x J20 mice during LTP in the presence of PTX. Values represent average PPR during 15 minutes of baseline, PPR during PTP, and average PPR during the final 15 minutes of LTP

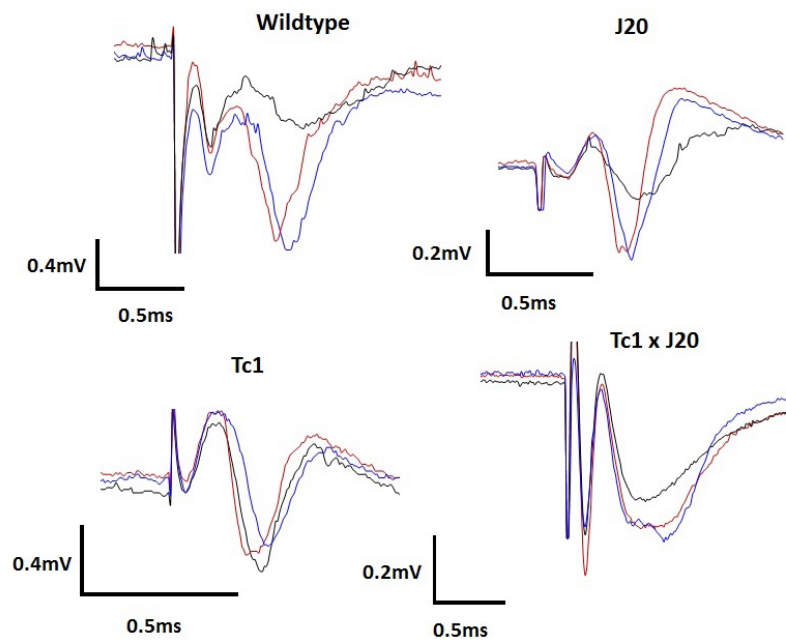


Figure 5.3 Examples of fEPSPs during LTP in the presence of PTX in the Tc1 x J20 cross

Examples of fEPSPs recorded during baseline (grey), post-tetanic potentiation (red), and LTP (blue) in the presence of PTX for individual wildtype, Tc1, J20 and Tc1 x J20 mice. Baseline and LTP responses represent the average of 3 traces (1min) taken from the first and last 15 minutes of the recording and PTP represents an average of the first 2 traces recorded following the LTP induction protocol (40s).

5.3.2 Blocking GABA_ARs has no effect on baseline synaptic transmission at 6 months of age

Input-output curves were also measured in the presence of PTX. There was no effect of genotype at 6 months of age (**Figure 5.4**), suggesting baseline synaptic transmission with GABA_A receptors blocked was not altered by *tgAPP*, trisomy or interactions between them.

At 6 months of age, average fEPSP slope at a stimulation intensity of 0.8mV was 0.37mV/ms \pm 0.13 (SEM), n=8 slices, 5 animals, in the wildtype mice; 0.30mV/ms \pm 0.18 (SEM), n=4 slices, 4 animals, in the Tc1 mice; 0.23mV/ms \pm 0.072 (SEM), n=3 slices, 3 animals, in the J20 mice; and 0.32 \pm 0.11 (SEM), n=6 slices, 5 animals, in the Tc1 \times J20 mice. There was no significant effect of trisomy 21 (F(1,17)=0.290, p=0.597) or *tgAPP* (F(1,17)=0.081, p=0.779) by 2-way repeat measures ANOVA, and no interaction (F(1,17)=0.228, p=0.639).

Stimulation intensity had a significant effect on fEPSP slope (F(7,119)=16.177, p<0.001) but there was no significant interaction between stimulation intensity (F(7,119)=0.545, p=0.789) and trisomy 21 or stimulation intensity and *tgAPP* (F(7,119)=0.209, p=0.983).

Genotype also had no effect on area under the percentage maximum curve (AUC) at 6 months of age (**Figure 5.5B**). AUC for wildtype mice was 44.80 \pm 3.545; AU for Tc1 mice was 44.19 \pm 7.60 (SEM); AUC for J20 mice was 50.71 \pm 8.91 (SEM); and AUC for Tc1 \times J20 mice was 55.43 \pm 2.96 (SEM). There was no significant effect of trisomy 21 (F(3,17)=0.152, p=0.701), *tgAPP* (F(3,17)=2.651, p=0.1220), and no interaction (F(3,17)=0.256, p=0.619).

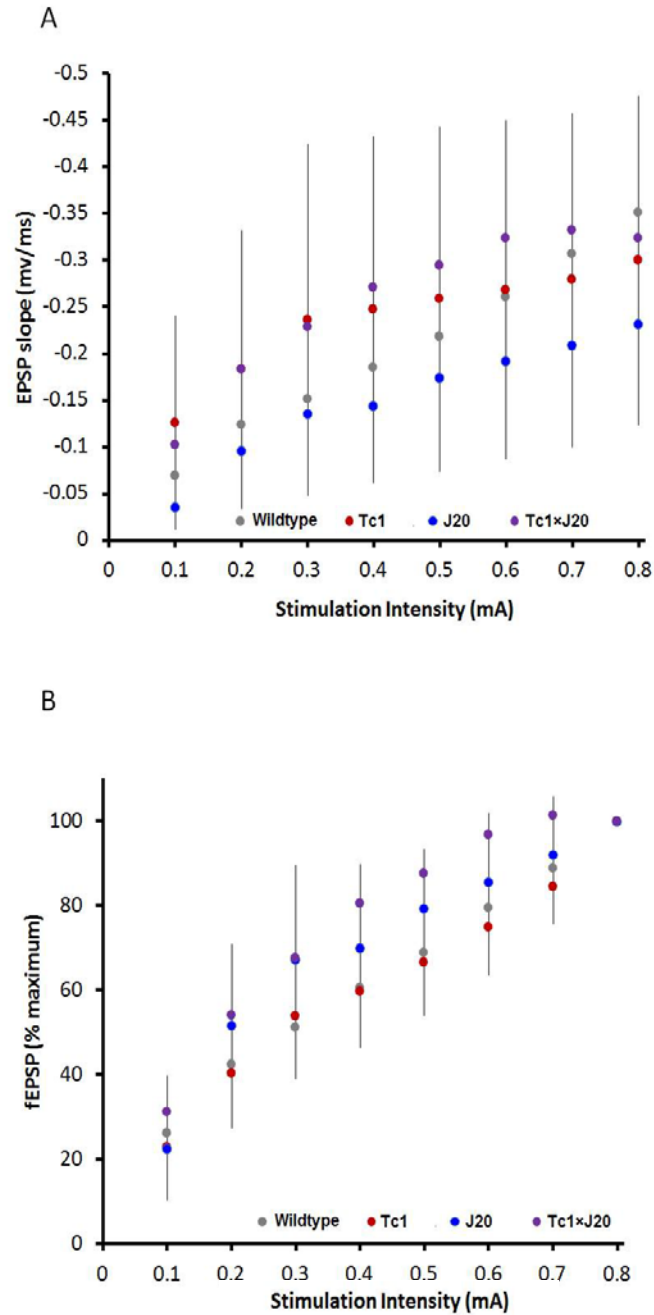


Figure 5.4 *Input-output curves following GABA_AR block in the MPP of the Tc1 × J20 cross at 6 months of age*

A) *Input-output curve in the presence of PTX for 6-month-old mice, showing average fEPSP slope measured at stimulation intensities between 0.1 and 0.8mV for wildtype (grey), Tc1 (red), J20 (blue) and Tc1×J20 (purple). Error bars show SEM. B)* *Input-output curve in the presence of PTX for 6-month-old mice, showing fEPSP slope expressed as a percentage of the maximum response for stimulation intensities between 0.1 -0.8mV. Error bars show SEM.*

5.3.3 Preliminary data on the effect of PTX on LTP at 3 months of age in the Tc1 × J20 cross

LTP in the Tc1 × J20 cross was also tested in a 3-month-old cohort of mice, to assess whether any of the interactions were age-dependent. Consistent with previous experiments, LTP was reduced in the Tc1 and Tc1×J20 animals (**Figure 5.5A**). Potentiation in the wildtype animals was 122.61% ± 9.65 (SEM), n=4 slices, 4 animals; in the Tc1 animals was 101.82% ± 7.58 (SEM), n=4 slices, 3 animals; in the J20 animals was 122.36% ± 10.56, n=5 slices, 4 animals (SEM); in the Tc1×J20 animals was 103.23% ±5.95 (SEM), n=8 slices, 6 animals. Hsa21 had a significant effect on LTP by 2-way ANOVA F(3,15)= 9.958, p=0.007); with no effect of tgAPP F(3,16)=0.063, p=0.806) and no interaction Hsa21 x J20 F(3,17)=0.056, p=0.816).

The percentage of slices showing LTP was calculated for each genotype with a threshold for LTP of 115% of baseline response (see **Table 5.2**), however the effect of genotype was not significant by 4×2 Fisher’s Exact Test (p=0.587), suggesting the number of animals available for this study may be too low for an effect on percentage induction to be detected.

Table 5.2 Proportion of slices at 3 months of age showing LTP in the presence of PTX in the Tc1×J20 cross

	Wildtype	Tc1	J20	Tc1 x J20
LTP	2	1	3	2
No LTP	2	3	2	6
% LTP Induction	50%	25%	60%	25%

There also was no difference in PTP at the 3-month time point (**Figure 5.5C**). Average fEPSP slope during PTP in wildtypes was 165.16% ± 26.43 (SEM); in Tc1 116.62% ± 2.93 (SEM); in J20 was 121.34%±10.73

(SEM); and in Tc1×J20 was $136.21\% \pm 11.10$ (SEM). Two-way ANOVA showed no significant effect of trisomy 21 ($F(3,15) = 0.085$, $p = 0.775$), no significant effect of tg*APP* ($F(3,15) = 1.824$, $p = 0.170$), and no interaction ($F(3,15) = 1.124$, $p = 0.306$).

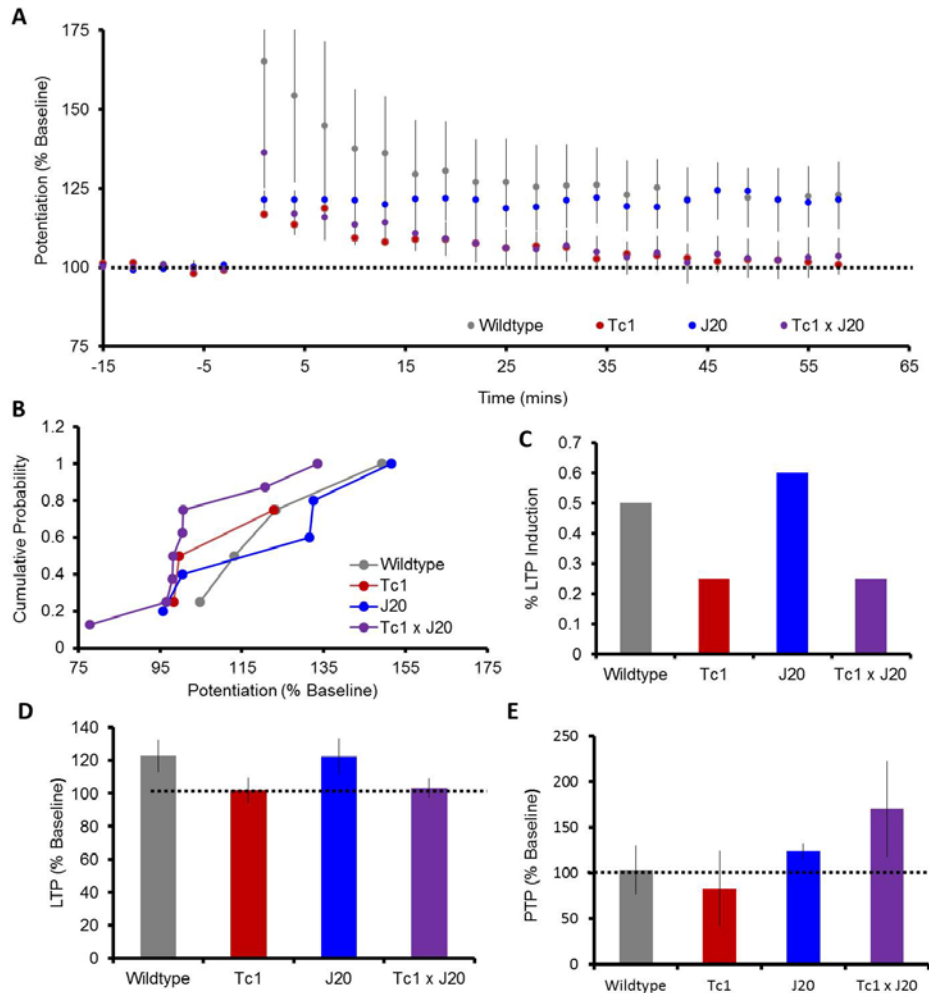


Figure 5.5 LTP following $GABA_A$ block in the MPP of the Tc1 \times J20 cross at 3 months of age

A) Average fEPSP response expressed as percentage baseline for wildtype (grey), Tc1 (red), J20 (blue), Tc1 \times J20 (purple). Each data point represents an average of 9 responses recorded over 3 minutes. LTP was induced a time 0. Error bars show SEM. **B)** Cumulative probability curves, showing the range of potentiation, and the probability of potentiation occurring within the range for each genotype. Error bars show SEM. **Average C)** Percentage of animals showing potentiation greater than 115% baseline for each genotype. **D)** fEPSP slope for each genotype 46-60mins after LTP induction, expressed as percentage of baseline. Error bars show SEM. **E)** Average fEPSP slope for the first 3 minutes after tetanisation, representing PTP, expressed as a percentage of baseline

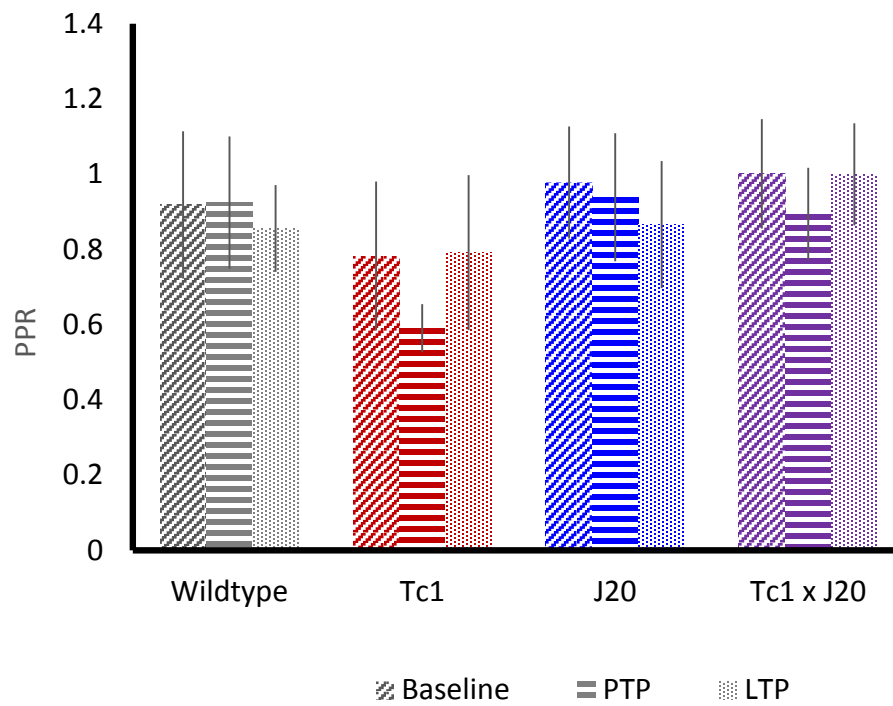


Figure 5.6 Paired Pulse Ratio during LTP at 3-months of age with $GABA_A$ R block

Average paired pulse ratio for wildtype, Tc1, J20, and Tc×J20 mice at 3 months of age during LTP in the presence of PTX. Values represent average PPR during 15 minutes of baseline, PPR during PTP, and average PPR during the final 15 minutes of LTP

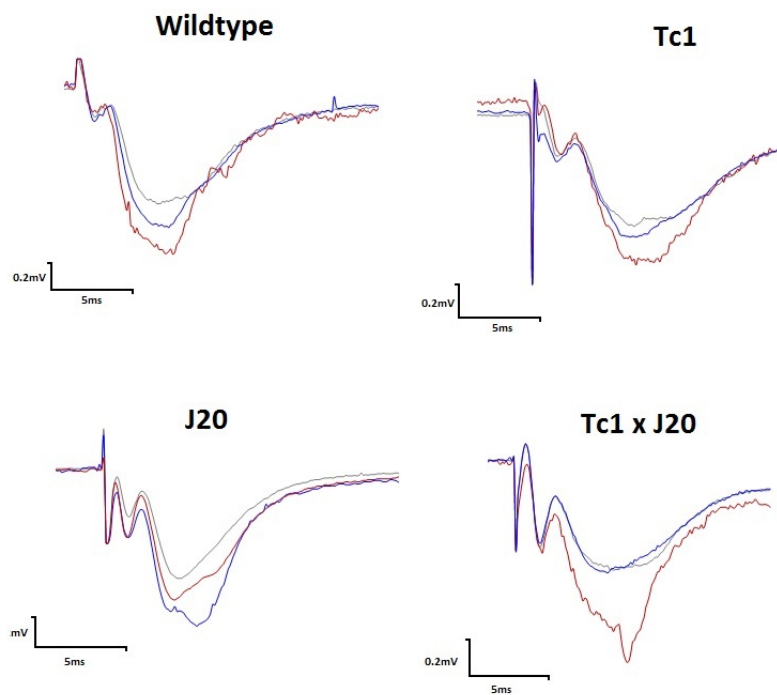


Figure 5.7 *Examples of fEPSPs during LTP in the presence of PTX in the Tc1 x J20 cross at 3 months of age*

Examples of fEPSPs recorded during baseline (grey), post-tetanic potentiation (red), and LTP (blue) in the presence of PTX for individual wildtype, Tc1, J20 and Tc1 x J20 mice. Baseline and LTP responses represent the average of 3 traces (1min) taken from the first and last 15 minutes of the recording and PTP represents an average of the first 2 traces recorded following the LTP induction protocol (40s).

5.3.4 Preliminary data on the effect of blocking GABA_ARs on baseline synaptic transmission at 3 months of age

Input-output curves were also measured in the presence of PTX at 3 months of age. Average fEPSP slope at a stimulation intensity of 0.8mV was $-0.27\text{mV/ms} \pm 0.10$ (SEM), $n=3$ slices, 3 animals, in the wildtype mice; $-0.29\text{mV/ms} \pm 0.18$ (SEM), $n=4$ slices, 3 animals, in the Tc1 mice; $0.29\text{mV/ms} \pm 0.11$ (SEM), $n=2$ slices, 2 animals, in the J20 mice; and 0.30 ± 0.12 (SEM), $n=6$ slices, 5 animals, in the Tc1×J20 mice. There was no significant effect of trisomy 21 ($F(1,11)=372$, $p=0.554$) or tgAPP ($F(1,11)=0.031$, $p=0.864$) by 2-way repeat measures ANOVA, and no interaction ($F(1,11)=0.014$, $p=0.909$).

Stimulation intensity had a significant effect on fEPSP slope ($F(1,11)=8.718$, $p=0.013$) but there was no significant interaction between stimulation intensity and trisomy 21 ($F(1,11)=0.357$, $p=0.562$) or stimulation intensity and tgAPP ($F(1,11)=0.030$, $p=0.866$).

Genotype also had no effect on area under the percentage maximum curve (AUC) at 6 months of age. AUC for wildtype mice was 60.32 ± 10.19 ; AU for Tc1 mice was 46.76 ± 5.02 (SEM); AUC for J20 mice was 56.31 ± 2.04 (SEM); and AUC for Tc1×J20 mice was 55.67 ± 8.42 (SEM). There was no significant effect of trisomy 21 ($F(3,11)=0.074$, $p=0.790$), tgAPP ($F(3,11)=622$, $p=0.790$), and no interaction ($F(3,11)=0.515$, $p=0.488$).

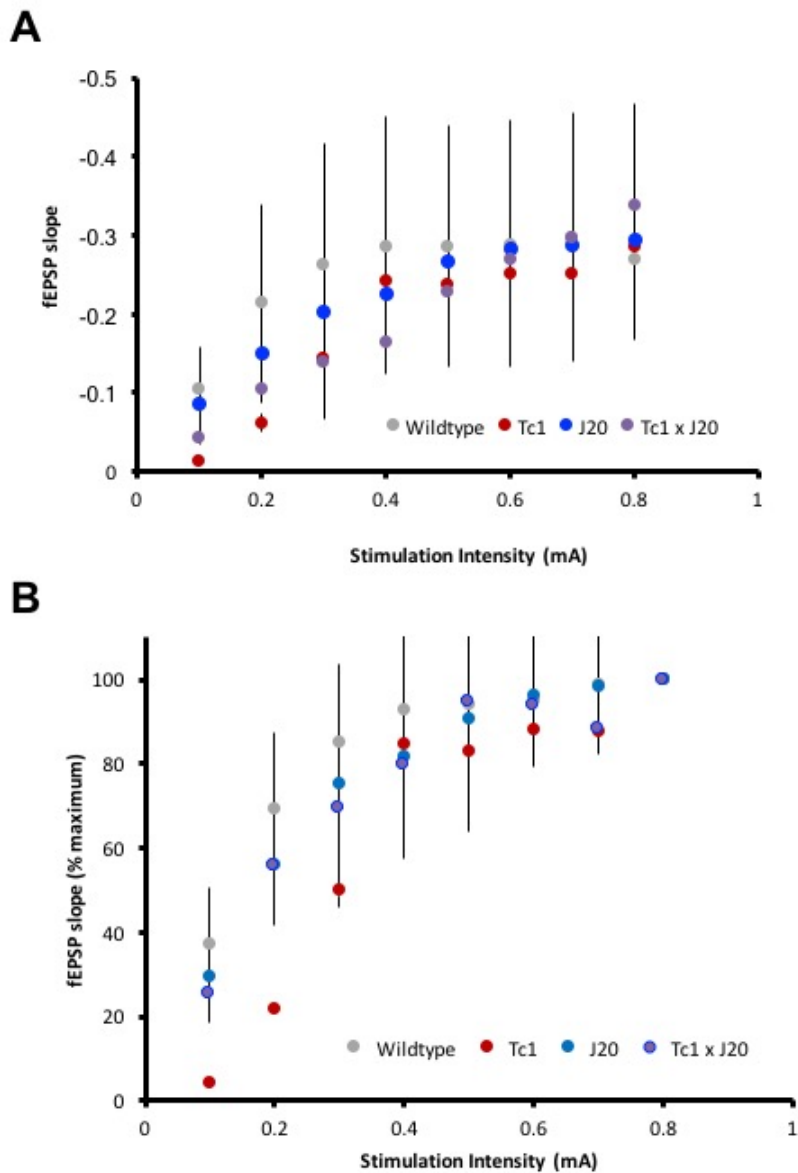


Figure 5.8 Input-output curves following $GABA_A R$ block in the MPP of the Tc1 \times J20 cross at 6 months of age

A) Input-output curve in the presence of PTX for 3-month-old mice, showing average fEPSP slope measured at stimulation intensities between 0.1 and 0.8mV for wildtype (grey), Tc1 (red), J20 (blue) and Tc1 \times J20 (purple). Error bars show SEM. **B)** Input-output curve in the presence of PTX for 3-month-old mice, showing fEPSP slope expressed as a percentage of the maximum response for stimulation intensities between 0.1 -0.8mV. Error bars show SEM.

5.3.5 Chemical LTP in the Tc1 × J20 cross

Chemical LTP was assessed in the Tc1 × J20 cross using the adenylyl cyclase activator forskolin. In contrast to the deficits observed in LTP induced by electrical stimulation in the trisomic animals, forskolin induced potentiation in all genotypes (*Error! Reference source not found.A*). Average potentiation in the wildtype mice was 204.04% ± 52.65 (SEM), n=7 slices, 7 animals; average potentiation in the Tc1 mice was 148.10% ± 8.65 (SEM), n=3 slices, 3 animals; average potentiation in the J20 mice was 140.016% ± 10.67 (SEM), n=2 slices, 2 animals; average potentiation in the Tc1×J20 mice was 156.69% ± 20.62 (SEM), n=3 slices, 3 animals. Multivariate ANOVA indicated that chemical LTP was not affected by trisomy 21 ($F(1,12)=0.135$, $p=0.720$) nor by *tgAPP* ($F(1,12)=0.098$, $p=0.760$) and there was no interaction $F(1,12)=0.713$ $p=0.415$.

Although average potentiation was higher in the wildtype animals, this was predominantly due to a single animal showing exceptionally high potentiation of 506.43% of baseline (**Figure 5.12**). The cause of this exaggerated response is unclear, however after excluding this animal, average potentiation in the wildtype group was 150.97% ± 17.40 (SEM), n=6 slices, 6 animals, almost identical to the degree of potentiation observed in the transgenic animals, suggesting there was no overall trend towards enhanced potentiation in the wildtype mice.

The percentage of slices showing LTP was calculated for each genotype with a threshold for LTP of 115% of baseline response (see **Table 5.3**), however the effect of genotype was not significant by 4×2 Fisher's Exact Test ($p=1.00$), suggesting genotype had no effect on chemical LTP.

Table 5.3 Proportion of slices showing chemical LTP in the Tc1×J20 cross

	Wildtype	Tc1	J20	Tc1 x J20
LTP	5	4	2	3
No LTP	1	0	0	0
% LTP induction	83%	100%	100%	100%

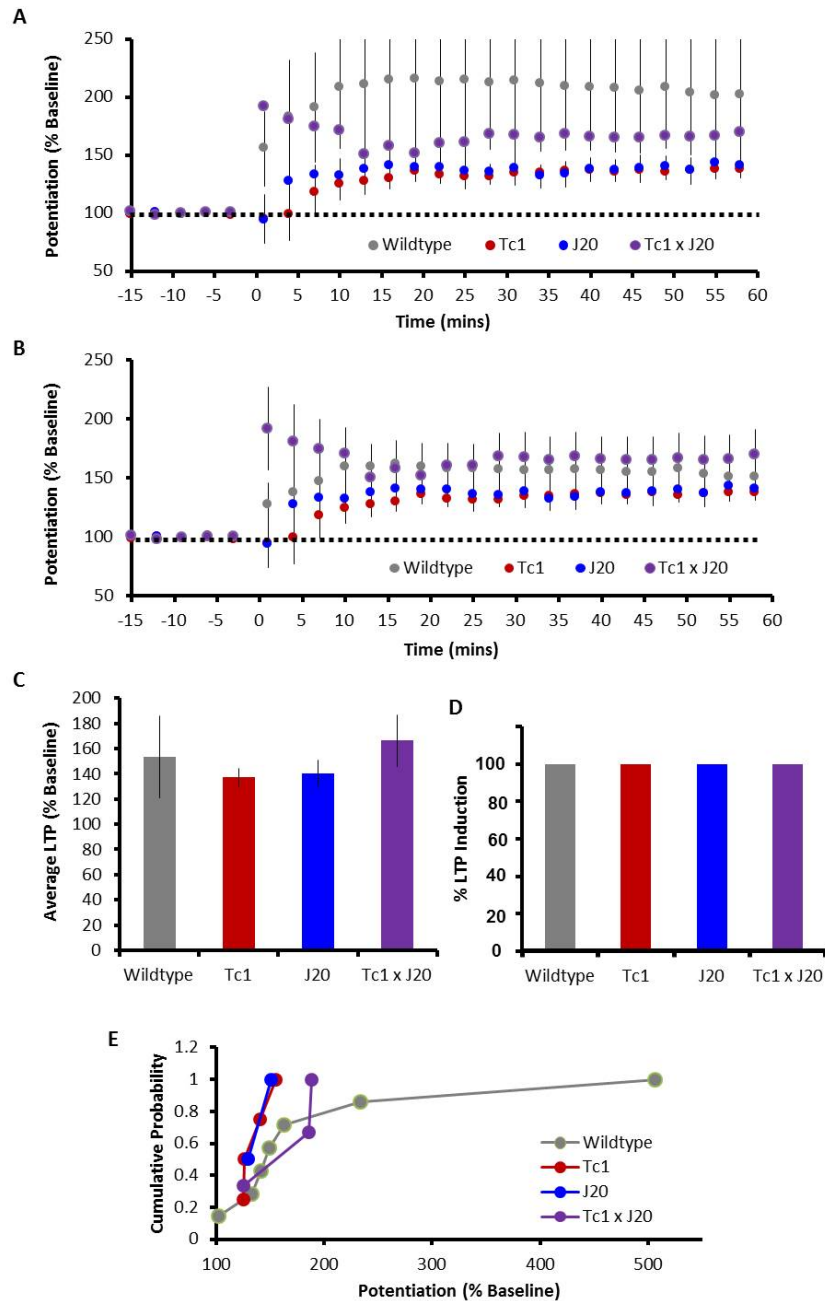


Figure 5.9 Chemical LTP in the MPP of the Tc1xJ20 cross at 6 months of age

A) Average fEPSP response during LTP expressed as percentage of baseline for wildtype (grey), Tc1 (red), J20 (blue), Tc1xJ20 (purple). Each data point represents an average of 9 responses recorded over 3 minutes. Error bars show SEM. **B)** Average fEPSP response during LTP following exclusion of outliers **C)** Average fEPSP slope for each genotype 46-60mins after forskolin washout, expressed as percentage of baseline. Error bars show SEM. **D)** Percentage of slices for each genotype showing potentiation of greater than 115% **E)** Cumulative probability curves, showing the range of potentiation, and the probability of potentiation occurring within the range for each genotype. Curves are similar between genotypes, with the exceptions of one wildtype outlier, which showed a strongly exaggerated response

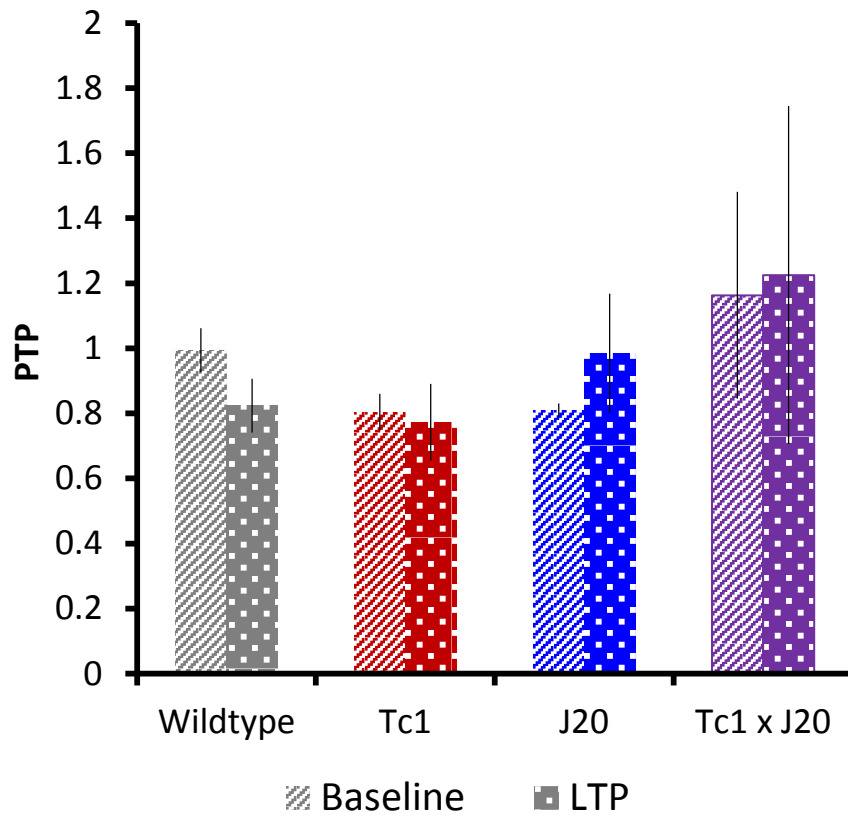


Figure 5.10 Paired Pulse Ratio during Chemical LTP

Average paired pulse ratio for wildtype, Tc1, J20, and Tc1xJ20 mice before and after the application of forskolin to induce LTP. Averages represent PPR during the 15 minutes of baseline, and the final 15 minutes of LTP.

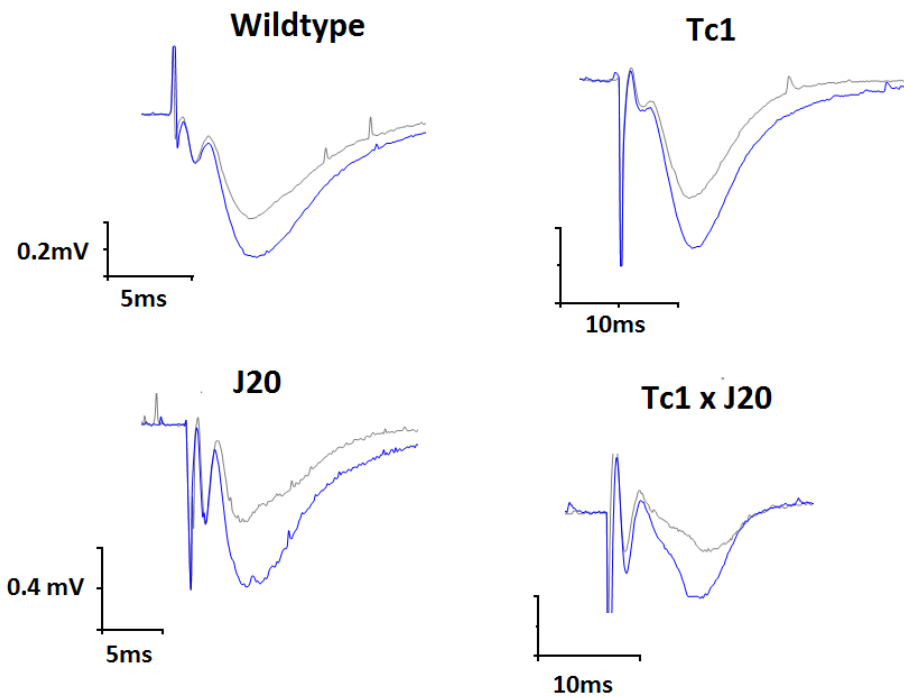


Figure 5.11 *Examples of fEPSPs during Chemical LTP in the Tc1xJ20 cross*

Examples of fEPSPs recorded during baseline (grey) and chemical LTP (blue) for individual wildtype, Tc1, J20 and Tc1xJ20 mice. Baseline and LTP responses represent the average of 3 traces (1min) taken from the first and last 15 minutes of the recording.

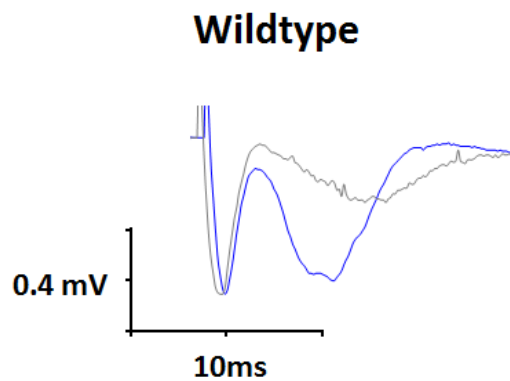


Figure 5.12 *Example outlying fEPSP from a wildtype animal*

Examples of fEPSPs recorded during baseline (grey) and chemical LTP (blue) for an individual wildtype animal which showed potentiation of 506.43% of baseline.

5.4 Discussion

These data suggest that LTP is impaired in the MPP of the Tc1 mice through a GABA_AR independent mechanism, and that the observed deficits are stable throughout adult life, and not modified by the progression of amyloid pathology in the Tc1×J20 animals. The observation that PTX was not sufficient to rescue the deficit in LTP in Tc1 and Tc1×J20 animals contrasts with what has been observed in other models of DS, however, it is not necessarily an unexpected result. Several of the genes which have been implicated in the ‘over-inhibition’ phenotype are absent from the Tc1 animals. For example, duplication of *Olig1* and *Olig2* (Chakrabarti *et al.*, 2010) has been linked to a disruption of the excitation-inhibition balance in DS, and the human orthologues of these genes, *OLIG1* and *OLIG2*, have both been deleted from the Tc1 model due to chromosomal rearrangements. In addition, the *SYNJ1* gene, which has been implicated in the regulation of GABAergic neurotransmission, is also deleted in the Tc1 model (Luthi *et al.*, 2001). However, GABA_BRs were not blocked in these experiments; it therefore remains possible that interactions between GABA_BRs and *GRIK1*, which is also located on Hsa21, play a role in the LTP deficits in these animals.

The extent to which these genes contribute to increased synaptic inhibition in DS mouse models remains unclear. Furthermore, many of the phenotypes underlying the observed changes in inhibition have only been characterised in detail in the Ts65Dn model. The Ts65Dn model overexpresses a number of Mmu17 genes not relevant to DS, which are likely to modify the phenotype. Therefore, it cannot be assumed that all the phenotypes present in Ts65Dn mice are of direct relevance to human disease, or will be consistent across other models. Nevertheless, the fact that alterations in inhibition have been observed

in several other models carrying duplications only of DS relevant genes suggests that Hsa21 genes mediate at least some of the observed changes in inhibition.

Mosaicism in the Tc1 mice may also modify phenotypes that depend on changes in overall network function. In the Tc1 mice, 60% of neurons in the dentate gyrus, CA1 and CA3 of the hippocampus have been estimated to be trisomic (personal communication Frances Wiseman UCL); if release probability is only altered in trisomic interneurons, this may not have sufficient impact on network function to affect the induction threshold for LTP. Alternatively, homeostatic plasticity in non-trisomic neurons may be sufficient to compensate for trisomy-induced alterations in network function, acting as a buffer to maintain overall network stability.

The persistence of deficits in the absence of the genes mediating 'over-inhibition' indicates that disruption to the balance of excitatory and inhibitory signalling is not the only factor contributing the impairment of synaptic plasticity in DS. Consistent with this, LTP can be rescued in other trisomy models through a range of interventions that do not target GABAergic signalling, suggesting that other mechanisms contribute to synaptic plasticity deficits DS. These pathways are likely to interact extensively, and targeting any of them may be sufficient to rescue a deficit by altering their relative balance. The absence of changes in inhibition in the Tc1 mice may therefore unmask other changes in synaptic function.

The lack of difference between the phenotypes present at 3 months of age and 6 months of age suggest that changes in synaptic plasticity are developmental rather than progressive in the Tc1 animals. This is consistent with the behavioural data from the Tc1 × J20 cross, which suggests that impairments in memory remain stable between the ages

of 2 and 6 months of age (**Figure 1.7**). The amyloid pathology in the J20 mice is progressive, with plaques appearing between 4-5 months of age. A β deposition will therefore be present in the 6-month-old cohort but not the 3-month-old cohort. However, as no phenotype is apparent in the J20 mice at either time point, and trisomy appears to result in a floor effect in synaptic potentiation in Tc1 \times J20 mice at both 3 and 6 months of age, these data do not provide sufficient scope to assess the effect of plaque onset on synaptic plasticity.

LTP in the MPP requires activation of NMDARs, and results in the phosphorylation and insertion of AMPARs containing the GluA1 subunit. This process appears to be mediated through the Ca²⁺-dependent activation of PKC, although CaMKII has also been implicated. Identifying which stage of this processes is impaired by trisomy will provide an insight into which genes contribute to the loss of synaptic plasticity in the Tc1 mice.

Although LTP induced by tetanic stimulation is impaired by trisomy, chemical LTP is normal in both the Tc1 and Tc1 \times J20 mice. This suggests that trisomy causes a deficit in the induction of LTP in the MPP, but that the mechanisms underlying the expression of LTP in the MPP are intact, and trisomic mice are therefore still capable of undergoing synaptic potentiation. Furthermore, it demonstrates that tgAPP does not interact with trisomy to cause novel deficits in LTP expression in the Tc1 \times J20 mice, although it remains possible that the interaction contributes to further deficits in LTP induction.

Surface expression of the GluA1 AMPA subunit has been shown previously to be reduced in the Tc1 mice by western blot, although surface expression of the NMDAR obligatory subunit GluN1 was unchanged (Morice *et al.*, 2008). However, as this has not been investigated in the Tc1 \times J20 mice, the impact of tgAPP on these

phenotypes is unknown. This indicates that the overall level of NMDAR expression is not affected by trisomy, suggesting that LTP deficits in the Tc1 mice do not result from a decrease in available NMDARs, but rather from a failure of NMDAR activation, or a failure in the activation of downstream signalling pathways following NMDAR activation. However, it remains possible that there are subtle, or cell-type specific, alterations in NMDARs which were not detected. In addition, the distribution and relative proportions of the GluN2A and GluN2B subunits have not been investigated, and the ratio of these subunits has been suggested to regulate the balance between synaptic potentiation and synaptic depression (Xu *et al.*, 2009).

It is not clear whether the reduction in GluA1 surface expression is due to impaired plasticity leading to a reduction in GluR1 insertion, a specific failure of synaptic insertion of GluA1 contributing to impaired plasticity, or to a more general reduction in synapses, as proposed by Witton *et al.* (2015). However, the observation that forskolin-mediated LTP is unimpaired makes a specific deficit in insertion unlikely.

This indicates that although excessive inhibition may contribute to cognitive impairment in DS, trisomy of Hsa21 also results in profound deficits in LTP induction in the MPP via an alternative mechanism, suggesting that therapy targeted towards reducing excessive inhibition may not be sufficient to restore cognitive function in DS patients.

5.5 Conclusion

The data presented here suggest that trisomy of the genes expressed on Hsa21 in the Tc1 mouse results in a specific deficit in LTP induction in the MPP. In contrast to other models of DS, this deficit did not appear to be mediated by increased synaptic inhibition, as it could not be rescued by blocking GABA_A receptors. The deficit was stable between the ages of 3 and 6 months, suggesting a developmental rather than progressive aetiology.

Following direct activation of adenylyl cyclase with forskolin, trisomic animals showed equivalent potentiation to wildtype animals, suggesting that the trisomic synapses have the capacity to express normal potentiation, but fail to do in response to the LTP induction protocols tested here. These data point to a novel deficit in LTP induction in trisomic animals, which may contribute to cognitive dysfunction in DS. Furthermore, no significant alterations in PTP were observed, and PPR during LTP was not significantly different between genotypes in the presence of PTX, or following treatment with forskolin, suggesting the phenotype is not mediated by presynaptic changes.

No interactions between *tgAPP* and trisomy 21 were observed under any of the experimental conditions tested, suggesting that the deficits observed here do not underlie the exacerbation in cognitive impairment observed in the double transgenic animals.

Chapter 6

Synaptic plasticity and seizures in AD-DS

6.1 Introduction

6.1.1 Seizures in mouse models of AD and DS

AD-DS is characterised by an increase in the risk of seizures in comparison to sporadic AD. Increased levels of A β have been implicated in epileptogenesis in AD-DS, as well as in Dup-*APP*, and other familial forms of AD (Noebels, 2011). However, individuals with DS also show an increased risk of seizures throughout life, with peaks in epilepsy onset both during childhood and in early adulthood, prior to the onset of dementia. This suggests that genes on Hsa21 other than *APP* may modify seizure risk in AD-DS.

Spontaneous seizures have previously been reported to occur in the J20 mouse (Palop *et al.*, 2007) along with an aberrant expression Neuropeptide Y (NPY) in the mossy fibres, which is characteristic of temporal lobe epilepsy. However, the risk of seizures has not previously been characterised in the Tc1 or Dp1Tyb models of DS, and very little investigation of seizure risk has been carried out to date in other DS models, although there is some indication of increased susceptibility to seizures in the Ts65Dn model (See **Section 1.3.4**).

The electroencephalogram (EEG) was recorded in the Tc1 \times J20 cross and the Dp1Tyb mice in order to assess whether trisomy of Hsa21

modified the frequency or severity of seizures in the J20 animals, and whether the Tc1 or Dp1Tyb mice experienced spontaneous seizures, or other epileptiform abnormalities.

6.1.2 The basis of EEG

EEG provides a readout of the electrical activity in the brain. The EEG signal represents the change in potential difference over time between two recording electrodes placed over different regions of the cortex, and is generated by the extracellular movement of ions that occurs during neuronal activity. In a physiological state, the EEG signal predominately reflects the ionic currents generated as result of excitatory and inhibitory synaptic activity during the synchronous activation of populations of neurons (Buzsáki, Anastassiou and Koch, 2012).

As described in **Section 3.1.3**, synaptic transmission requires an influx of ions across the postsynaptic membrane, creating a local current sink at the dendrites, which is matched by a current source at the soma. As cortical pyramidal neurons are organised in a regular, polarised way, synchronous synaptic activity in populations of cortical pyramidal neurons generate dipoles in the cortex, which are of sufficient strength to be detected by EEG recording electrodes.

The dominant frequency of EEG oscillations reflects the level of arousal. In a healthy adult, low frequency delta (1-4Hz) waves predominate during deep sleep, and theta (4-8Hz) activity is associated with the early stages of sleep and drowsiness. During wakefulness, higher frequency alpha (8-12Hz) activity is the dominant rhythm, and beta activity (12-30Hz) is observed during active concentration. The function of gamma oscillations (30 – 100Hz) remain controversial, but

have been linked the integration of different neuronal networks in the context of sensory processing, memory formation and attention. (Jia and Kohn, 2011)

These EEG patterns are disrupted in disease states, reflecting dysfunction of neuronal networks; for example, both Alzheimer's disease (Moretti, 2004) and Down syndrome (Politoff *et al.*, 1996) are associated with a generalised slowing of cortical rhythms, and a downward shift in alpha peak

Depending on the recording conditions and brain state, other forms of neuronal activity also contribute to the EEG signal, including neuronal spiking and hyperpolarising currents. EEG has high temporal resolution, allowing it to detect changes in neuronal activity in the order of milliseconds, but comparatively poor spatial resolution, dependent on the number and positioning of the recording electrodes. Although mathematical approaches to EEG source localisation have been developed, EEG is often combined with neuroimaging techniques such as fMRI to ensure accurate spatial localisation neuronal activity (Huster *et al.*, 2012).

The mouse EEG presented here was recorded using just two electrodes due to the practical constraints of implanting intracranial electrodes which can be maintained in freely moving animals over a period of weeks; for example, steric hindrance in positioning of the screws over the skull, and limitations on the transmitter size which can be tolerated subcutaneously by a small animal. One electrode was positioned over the right parietal cortex and one over the right motor cortex, thus the EEG readout represents the difference between the two regions. This bipolar recording is sufficient to detect seizures and interictal abnormalities, but does not allow for detailed localisation of the seizure foci.

6.1.3 EEG and seizures

An epileptic seizure is defined by The International League Against Epilepsy as: “*a transient occurrence of signs and/or symptoms due to abnormal excessive or synchronous neuronal activity in the brain*” (Fisher *et al.*, 2005). This excessive synchronous activity produces a characteristic evolving pattern of activity on the EEG, generally of high amplitude spiking, or spikes and waves, depending upon on the type and origin of the seizure, and is generated by simultaneous synaptic activation across large regions of the cortex.

Seizures are associated with cortical hyperexcitability, which can lead to bursts of abnormal epileptiform activity on the EEG in between seizures. This interictal activity is a frequently used biomarker in the clinical diagnosis of epilepsy (Chang, 2013), and is reported in approximately a third of individuals presenting with new onset seizures (Wirrell, 2010). However, bursts of epileptiform activity have also been reported in individuals without seizure disorders, and in particular in association with other neurological disorders. The clinical significance of this in terms of cognition and future seizure risk remains unclear (So, 2010), although interictal discharges have been proposed to contribute to memory impairment by inducing pathological coupling between hippocampal and cortical networks, which disrupts ongoing physiological activity (Gelinas *et al.*, 2016). Furthermore, these discharges remain rare in the general population, consistent with the suggestion that they signify a form of pathological activity.

6.1.4 Seizures and synaptic plasticity

Epilepsy is frequently associated with memory impairment, both in a clinical context (Rayner, Jackson and Wilson, 2016) and in animal

models. Acute seizures have been reported to disrupt activity-dependent hippocampal synaptic plasticity under multiple experimental conditions, and common mechanisms have been proposed to contribute to both the synaptic potentiation underlying memory formation, and to epileptogenesis (Scharfman, 2002).

Deficits in LTP have been reported in a number of epilepsy models. Repeated induction of electroconvulsive seizures in rats results in impaired LTP in the DG (Reid and Stewart, 1997) and in CA1 (Anwyl, Walshe and Rowan, 1987), and LTP deficits in the DG correlated with impaired performance on the water maze. Loss of LTP in the DG was also associated with an increase in baseline synaptic transmission, suggesting repeated seizure activity may result in a 'saturation' of transmission, precluding any further potentiation (Reid and Stewart, 1997). However, no increase in the baseline field potential was reported in CA1, suggesting mechanisms of seizure-induced LTP impairment may be multifactorial, or region specific.

LTP deficits in the DG only occurred after multiple electroconvulsive seizures, indicating loss of plasticity was driven by a chronic process. Reid and Stewart (1997) suggested that the mechanism for the loss of plasticity was NMDA receptor dependent, consistent with a saturation of synaptic strength, as ketamine but not halothane anaesthesia had a protective effect. However, although ketamine acts primarily through antagonism of NMDA receptors, it should be noted that both halothane and ketamine interact with multiple targets (Kirson, Yaari and Perouansky, 1998; Wood *et al.*, 2003; Sleight *et al.*, 2014).

LTP has also been reported to be impaired in CA1, and in the lateral amygdala, of rats with kindling-induced seizures (Schubert *et al.*, 2005). Consistent with the reports of Reid and Stewart (1997), the extent of the deficit was dependent on the number of seizures previously

experienced by the animal. Kindling not only resulted in a reduction in the magnitude of LTP, but also altered the balance of stimulation thresholds for LTP and LTD, such that stimulation protocols which induced LTD in control animals resulted in LTP in kindled animals. This suggests that seizures do not simply inhibit activity-dependent plasticity, but may produce metaplastic changes in the conditions under which plasticity occurs.

Inducing status epilepticus with kainic acid in both the developing, and the mature rat brain also induces subsequent impairments in LTP. Seizures induced within the first two weeks of life resulted in a loss of LTP in CA1 six months later, suggesting seizures during development are capable exerting a long-term effect on hippocampal synaptic plasticity (Lynch *et al.*, 2000). In adult rats, the degree of the deficit in LTP correlated with the impact on memory function (Suárez *et al.*, 2012), suggesting seizure-induced cognitive impairments share a common mechanism with LTP deficits. As was observed following the induction of electroconvulsive seizures, LTP impairment in CA1 was not associated with an increase in baseline synaptic transmission, although interestingly, rats which did not develop status epilepticus following kainic acid treatment showed both enhanced LTP and enhanced baseline synaptic transition, suggesting a role for plasticity in seizure resistance (Suárez *et al.*, 2012). LTP was also impaired in the CA1 region of a genetic epilepsy mouse model, which lacks the scaffolding protein Bassoon (Sgobio *et al.*, 2010). LTP and seizures in this model were both rescued by treatment with the antiepileptic drug valproate, although morphological abnormalities and memory impairments were not, suggesting a direct association between the LTP deficit and seizures.

These results are consistent with observations from epilepsy patients. In resected hippocampal tissue from patients with temporal lobe epilepsy, both electrical and chemical LTP were found to be impaired in the DG of patients for whom the hippocampus was the primary seizure focus, but not in tissues from patients with a primary seizure focus elsewhere in the temporal lobe (Beck *et al.*, 2000). Furthermore, increased expression of the kinase CaMKII and decreased expression of the phosphatase calcineurin have been reported in resected tissue from the epileptic focus of temporal lobe epilepsy patients with hippocampal sclerosis (Lie *et al.*, 1998). Although expression levels are not necessarily indicative of function, this alteration in the balance of CaMKII and calcineurin would be consistent with a shift in receptor phosphorylation patterns promoting LTP over LTD (See **Section 4.1**).

As well as chronic changes in plasticity associated with ongoing seizures, acute changes in response to isolated seizure activity have also been reported. In support of the suggestion that seizures induce synaptic plasticity, both LTP and LTD-like changes have been reported in hippocampal slices treated with high K⁺ to induce acute transient seizures, although the direction of change varied between slices. Like classical LTP and LTD, the plasticity induced by epileptiform activity was NMDAR-dependent, suggesting a common mechanism underlies both forms of plasticity. However, it is unclear what determines whether the slices underwent potentiation or depression, as it did not appear to relate to the type of epileptiform activity in the slice (Contzen and Witte, 1994).

Furthermore, seizures induced following the application of an LTP protocol have been shown to result in depotentiation of the response back to baseline, suggesting an acute reversal of plasticity. *In vivo*, the electrical induction of seizures reversed LTP in the CA1 region of the rat

brain, however potentiation could be reinstated by repetition of the induction protocol, suggesting seizures transiently disrupt LTP expression (Hesse and Teyler, 1976). Similar results have been observed *in vitro*; the induction of epileptic activity in acute hippocampal slices via pharmacological block of GABA_A receptors has been reported to reverse potentiation in CA1 via an mGluR-dependent mechanism (Hu *et al.*, 2005). The induction of LTP also appears to be transiently blocked immediately following seizures, due to post-ictal depression (Barr *et al.*, 1997).

Seizures therefore appear to disrupt hippocampal synaptic plasticity via a number of mechanisms, ranging from transient effects on the induction or expression of LTP in response to acute seizure activity, to persistent alterations in network function induced by chronic epilepsy. Furthermore, this disruption to synaptic plasticity appears to have a direct impact memory. Alterations in seizure susceptibility in DS may therefore contribute to the exacerbation in behavioural impairments observed in the Tc1×J20 animals.

6.1.5 Neuropeptide Y expression in epilepsy

NPY is an inhibitory neuropeptide normally expressed in somatostatin positive interneurons in the hilus of the hippocampus. Following seizures, NPY is aberrantly co-expressed with glutamate in the hippocampal mossy fibres, where it acts via Y2 receptors to inhibit presynaptic glutamate release. This ectopic expression appears to be a homeostatic response to restrain the hyperexcitability resulting from the recurrent mossy fibre sprouting onto dentate granule cells that occurs in the epileptic hippocampus (Vezzani and Sperk, 2004). The combination of mossy fibre sprouting and NPY expression is therefore characteristic of temporal lobe epilepsy, and has been reported in a

number of experimental epilepsy models, as well as in post-mortem patient tissue. NPY immunoreactivity was therefore assessed in hippocampal slices from the Tc1 × J20 cross cohort following EEG, and in a second cohort of mice aged to 16 months.

6.1.6 Sudden death in epilepsy

The J20 mice are at increased risk of sudden death, and this risk is exacerbated by trisomy (**Figure 1.7 Behavioural phenotypes in the Tc1×J20 crossA**). Although the reason for the increase in mortality in these animals remains unknown, spontaneous seizures are a potential cause; affected animals are otherwise healthy, and risk is highest within the first six months of life but appears to stabilise with age, suggesting the mechanism is independent of the progressive amyloid pathology that occurs in these animals.

Sudden unexpected death in epilepsy (SUDEP) is a well-documented phenomenon. Epilepsy patients have a 20-fold greater risk of sudden death compared to the general population; risk appears to be associated with frequency of seizures, and may be substantially higher in specific subsets of patients (Massey *et al.*, 2014). The mechanisms for SUDEP are not well understood, but appear to relate to respiratory depression or cardiac dysfunction, resulting from the effects of seizures on the autonomic system, midbrain and brainstem (Massey *et al.*, 2014). However, as there are currently no definitive post-mortem signifiers of sudden death in epilepsy, and as no sudden deaths occurred in J20 or Tc1×J20 mice during the periods of EEG monitoring, it is not possible to establish the cause of sudden death with certainty.

6.2 Results

6.2.1 Frequency of seizures in the *Tc1* × *J20* cross

Over a 3 week recording period, 4 seizures were picked up in 2 of 5 *J20* mice (40%), and 5 seizures were picked up in 1 of 4 *J20*×*Tc1* (25%), using the Neuroarchiver Event Classifier. No seizures were picked up in the wildtype (n=5) or trisomic mice (n=4). These data indicate that seizure risk is not substantially increased by the presence of *Hsa21* although the frequency of seizures was too low for statistical analysis to be performed. Comparison of average seizure duration showed seizures were significantly longer in the *Tc1*×*J20* animal, lasting on average 45 ± 5.45 s, while in the *J20* animals, duration was 26 ± 5.62 s ($p=0.04$). This may indicate that while trisomy 21 does not increase the risk of developing epilepsy, it does exacerbate the phenotype in the subset of epileptic animals. However, as only one of the 4 *Tc1*×*J20* animals developed spontaneous seizures, it is not possible to determine the significance of this effect.

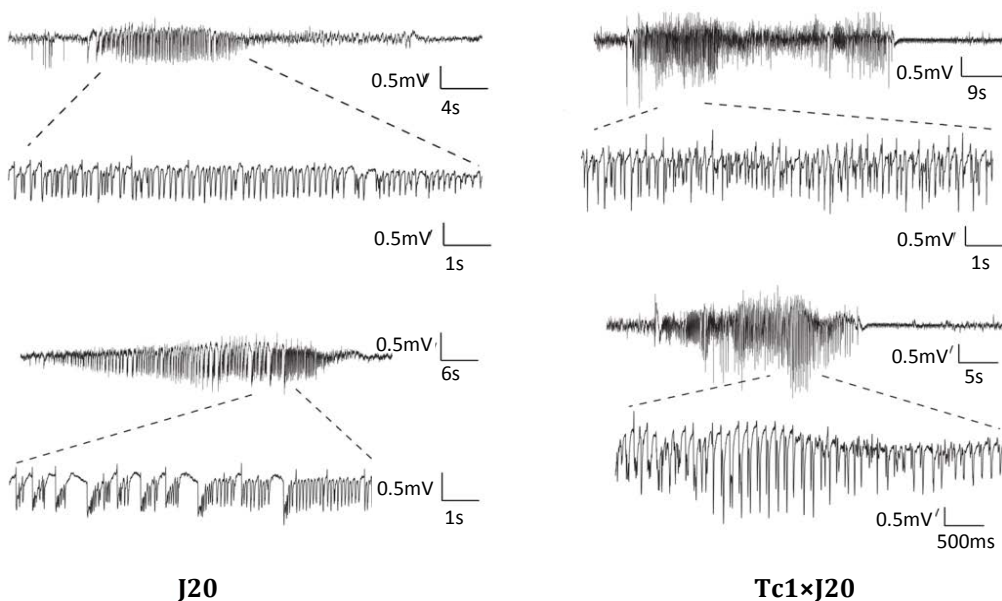


Figure 6.1 Examples of seizures from a *J20* mice and a *Tc1*×*J20* mouse

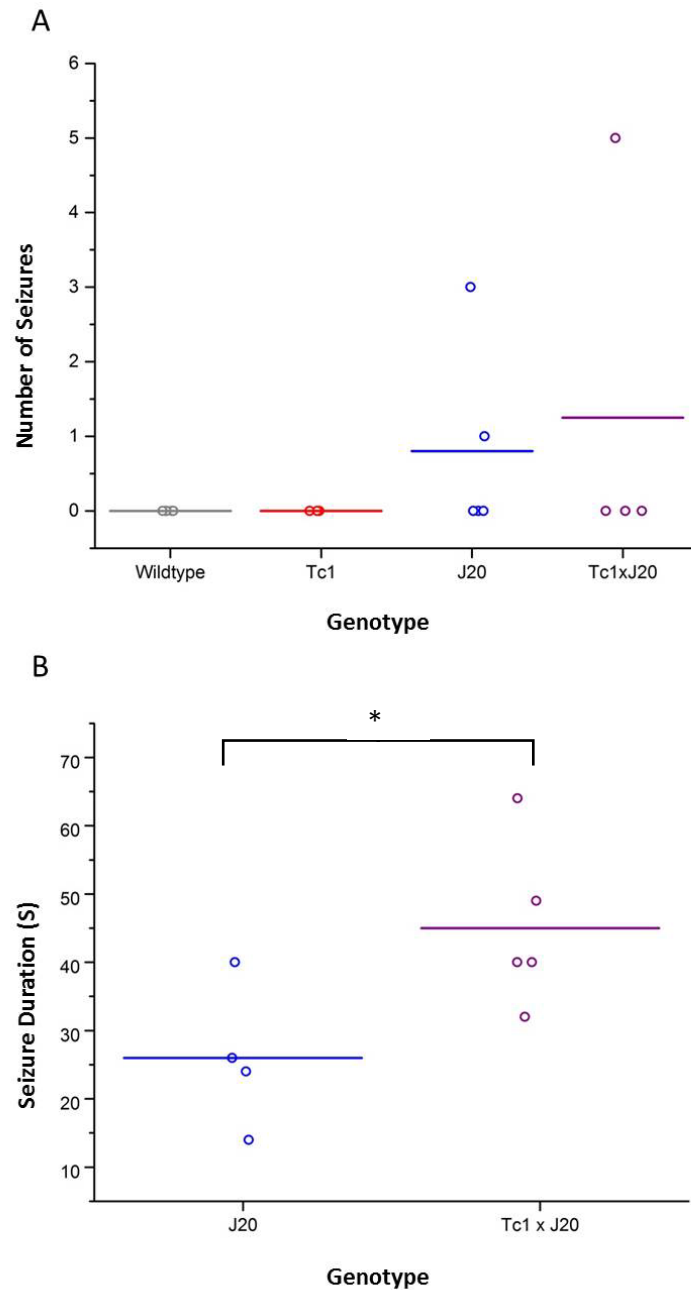


Figure 6.2 Seizures in the Tc1 × J20 cross

A) Number of seizures recorded in each animal per genotype. No seizures were recorded in any of the wildtype ($n=5$) or Tc1 ($n=4$) animals. Of the 5 J20 animals, 3 had no seizures during the 3 recording period, 1 had 1 seizure, and 1 had 3 seizures. Of the 4 Tc1×J20 animals, 3 had no seizures, however the remaining animal had 5 seizures. **B)** Average duration of each seizure recorded in the J20 and Tc1 × J20 animals. The Tc1×J20 animal had an average seizure duration of 45 ± 5.45 seconds, while the 2 J20 animals had an average seizure duration of $26 \pm 5.62s$ (Student's t -test $p = 0.04$).

6.2.2 Interictal spikes in the Tc1 × J20 cross

As electrographic seizures were rare, interictal activity was quantified as a surrogate marker for cortical hyperexcitability. Quantification was semi-automated using a Neuroarchiver event library. Event lists were then checked manually to exclude movement artefacts and other non-events identified in the EEG.

Consistent with the seizure data, frequent spiking was observed in a subset of J20 and Tc1×J20 animals; an average of 154.2 ± 76.73 spikes were picked up in the J20 mice and 1119.25 ± 986.94 in the Tc1×J20 mice over the 3 week recording period. An average of 1.8 ± 3.36 interictal spikes were picked up in the wildtype mice, and an average of 1.0 ± 0.41 were picked up in Tc1 mice, suggesting trisomy does not result in abnormal cortical hyperexcitability at this age.

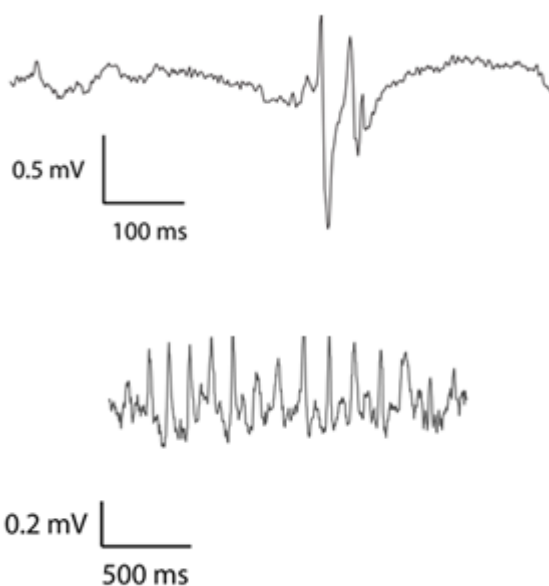


Figure 6.3 *Examples of interictal activity taken from a Tc1×J20 mouse*

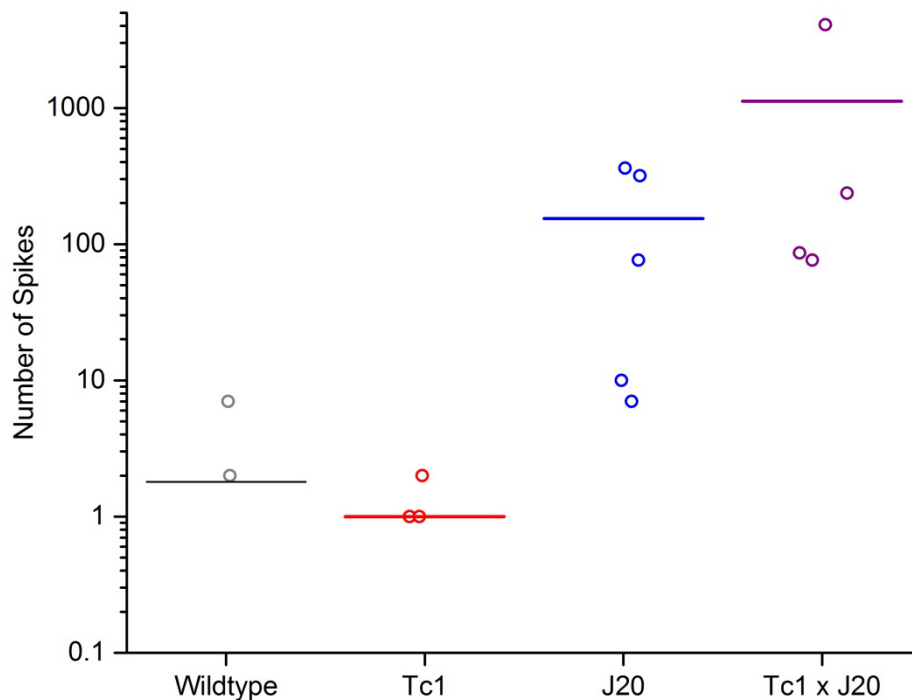


Figure 6.4 Quantification of interictal spikes in the Tc1 × J20 cross

Genotype had no significant effect on interictal spike frequency by univariate ANOVA: $F(3,14)=1.420$, $p=0.279$, however spiking was increased in a subset of J20 and Tc1 × J20 animals.

Genotype had no significant effect by univariate ANOVA ($F(3,14)= 1.420$, $p=0.279$). Although the frequency of interictal spiking was clearly increased in a subset of J20 and Tc1×J20 animals, there was a large amount of variability in the frequency of spiking between animals, consistent with only a subset of these animals displaying an epileptic phenotype. As expected, a higher frequency of interictal spiking was observed in the animals that experienced seizures, however, several J20 and Tc1×J20 animals showed frequent spiking on the EEG even though no seizures were recorded in these animals. It remains possible that these animals experienced seizures too infrequently to be detected over a 3-week recording period.

Due to the high variability, the data set was too small to determine whether an interaction occurred between *tgAPP* and trisomy 21. Although the mean spike count was substantially higher in the Tc1×J20 animals, it was strongly skewed by a very high spike count in the one animal, which had 5 seizures during the recording period.

6.2.3 Interictal spikes in the Dp1Tyb model

EEG was recorded over a period of 6 weeks from 3 wildtype animals and 4 Dp1Tyb animals. No seizures were recorded in either genotype, suggesting the Mmu16 segmental duplication is not sufficient to cause spontaneous seizures. Quantification of interictal spiking identified 1 Dp1Tyb animal with a substantial number of spikes; 292 over the recording period. A second Dp1Tyb animal had only 7 spikes, and no spikes were identified in the remaining 2 animals. Of the 3 wildtype animals, 2 of the 3 showed a low number of spikes; 11 and 23, and the third showed no spikes. As a substantial increase in spiking only occurred in one animal, there was no significant difference between genotypes by Student's t-test ($p=0.493$). It is not possible to determine whether the increased spiking in this animal was due to a variably penetrant effect of genotype, as observed in the J20 mice, or to other factors such as post-surgical trauma. However, it does suggest that any impact Mmu16 segmental trisomy does have on cortical excitability is likely to be small.

6.2.4 NPY staining at 6 months of age

NPY staining was performed on post-mortem brains from the EEG cohort, following termination of the EEG recording at 6 months of age. Although 2 J20 and 1 Tc1×J20 animal experienced seizures, no NPY

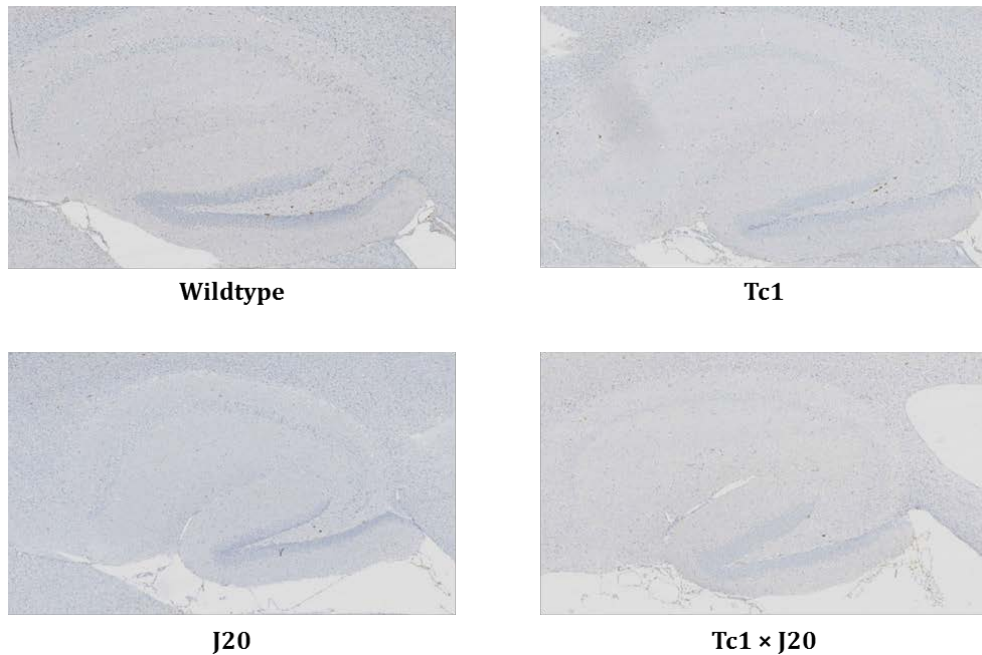


Figure 6.5 NPY immunoreactivity in the Tc1 × J20 cross at 6 months of age
Examples of hippocampal sections taken from wildtype, Tc1, J20 and Tc1×J20 animals. No aberrant expression of NPY was detected in any genotype (tissue preparation and staining carried out by Dr Sue Noy).

staining was present in the mossy fibres of any of the J20 or Tc1×J20 animals in the cohort, suggesting epileptic activity was not severe enough to result in aberrant expression of NPY.

6.2.5 NPY staining at 16 months of age

NPY staining was also carried out on hippocampal slices from mice aged to 16 months. Aberrant expression of NPY was present in subset of Tc1×J20 at this age. NPY staining in the DG was quantified by percentage area coverage for the hilus; the Stratum Moleculare; the Stratum Radiatum and the Stratum Lucidum. Staining intensity was significantly increased in the Stratum Lucidum ($F(1,33)=4.670$ $p=0.038$) and Stratum Moleculare ($F(1,33)=5.706$ $p=0.023$) of the trisomic mice and in the Stratum Lucidum of the tgAPP mice ($(F(1,33)=4.38, P=0.044)$ by two-way ANOVA.

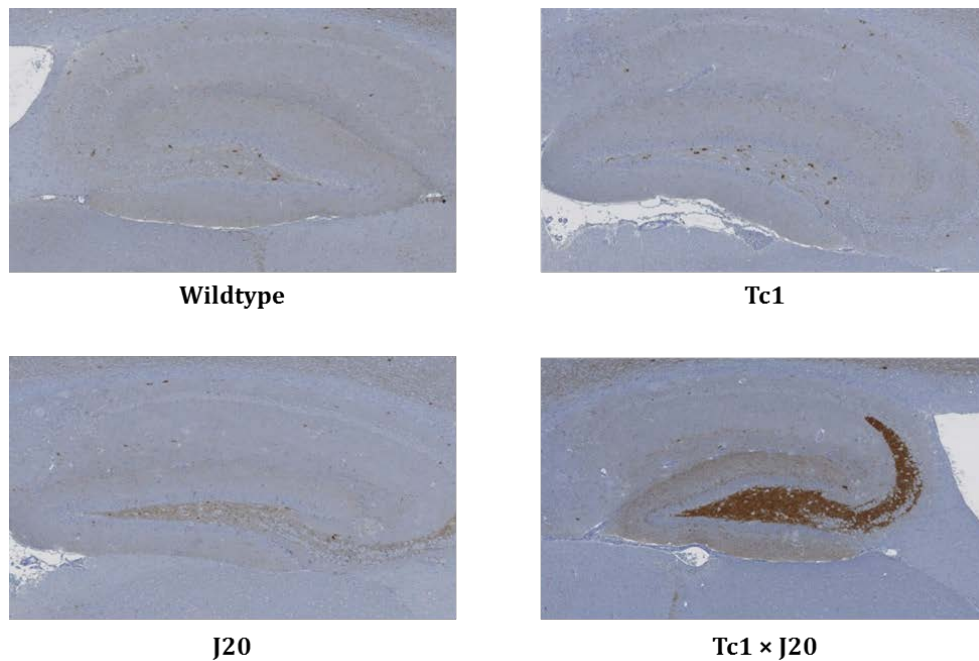


Figure 6.6 NPY immunoreactivity in the Tc1 × J20 cross at 16 months of age
Examples of hippocampal sections taken from wildtype, Tc1, J20 and Tc1×J20 animals. NPY was aberrantly expressed in a subset of J20 and Tc1×J20 animals (tissue preparation and staining carried out by Dr Sue Noy)

The Stratum Lucidum contains the mossy fibre tract; increased Stratum Lucidum staining therefore represents aberrant expression of NPY in the mossy fibres. This expression pattern is characteristic of models of temporal lobe epilepsy, and is associated with ongoing seizures. Collateralisation of the mossy fibre axons in the inner layer of the Stratum Moleculare also occurs as a result of epilepsy and NPY is similarly aberrantly expressed in these ‘sprouted mossy fibres’ (Scharfman & Gray, 2006). However, NPY expressing hilar interneurons also project to this region, and Palop *et al* (2007), suggest that NPY staining in the Stratum Moleculare of the J20 mice may originate from these interneurons, as they are also positive for the interneuron marker somatostatin, but do not show the Timm staining, which detects zinc present in mossy fibres.

An increase in NPY immunoreactivity in the Stratum Radiatum and Stratum Lucidum would therefore be consistent with an exacerbation of

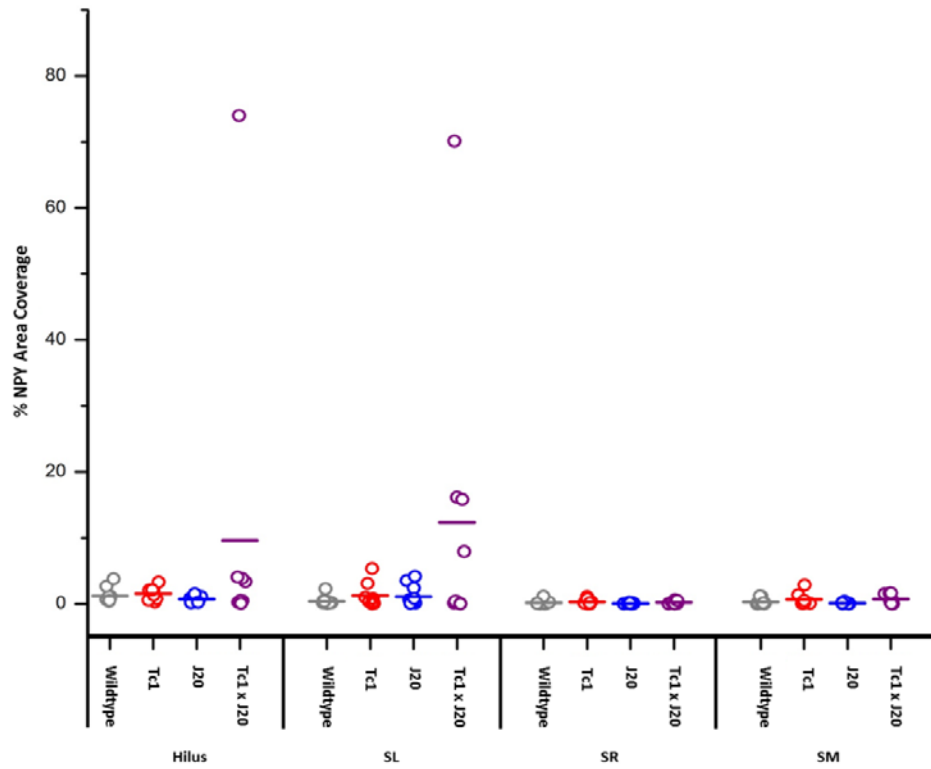


Figure 6.7 *Quantification of NPY staining in the Tc1 × J20 cross at 16 months of age*

Quantification of NPY staining by percentage area coverage for the Hilus

the seizure phenotype in the Tc1×J20 mice at 16 months of age, as indicated by the survival data from the Tc1×J20 animals (**Figure 1.7**).

6.3 Power spectrum

A Fourier transform was used to calculate EEG power across 8 predefined bands: 1-4Hz, corresponding to delta; 4-8 Hz, corresponding to theta; 8-14 Hz, corresponding to alpha, 14-30 Hz, corresponding to beta; 30-50Hz, corresponding to low gamma; 50-70 Hz corresponding to high gamma; 70-120 Hz and 120-160 Hz. Power in each band was normalised to total power to account for variation in electrode depth between animals.

The average EEG power for each genotype was calculated for total recording time, to give an indication of alterations to global network activity, and for each hour of recording time, to give an indication of alterations to circadian rhythms.

All genotypes showed circadian fluctuations in EEG power, with delta and theta peaks during the light period (7am – 7pm), and alpha and gamma peaks during the dark period (7pm – 7am) as would be expected in a nocturnal animal. Although alterations in circadian rhythm have been reported previously in the Tc1 animals (Heise et al., 2015) cycles did not differ between genotypes, suggesting that a more detailed analysis is required to pick up these differences.

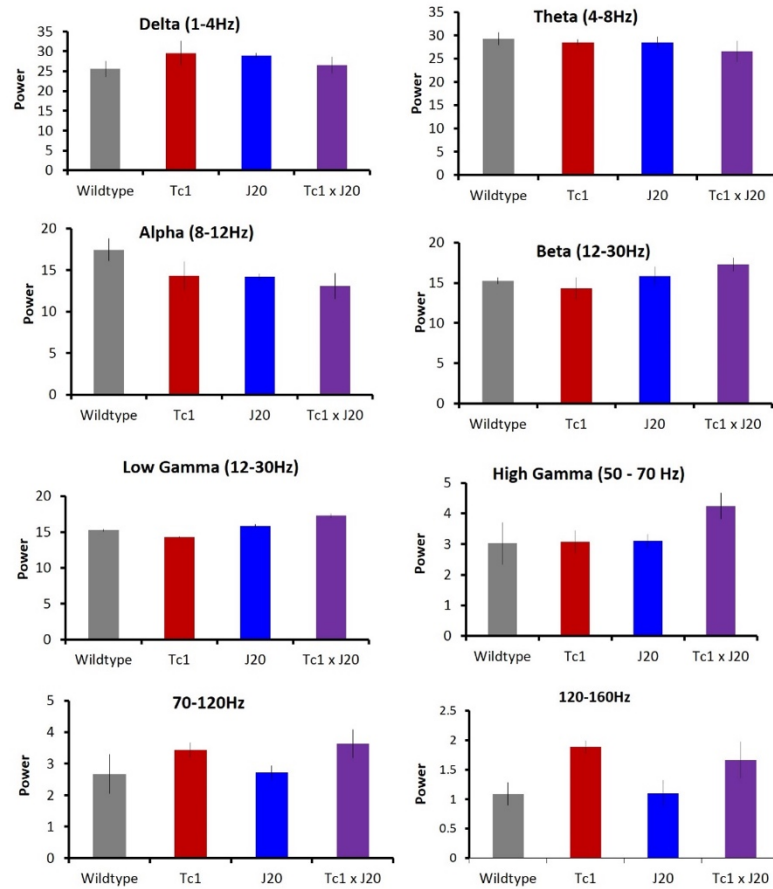


Figure 6.7 Normalised power spectrum across all EEG bands in the Tc1 x J20 cross

Average power in each band across the whole recording period for wildtype (grey), Tc1 (red), J20 (blue) and Tc1 x J20 (purple) mice.

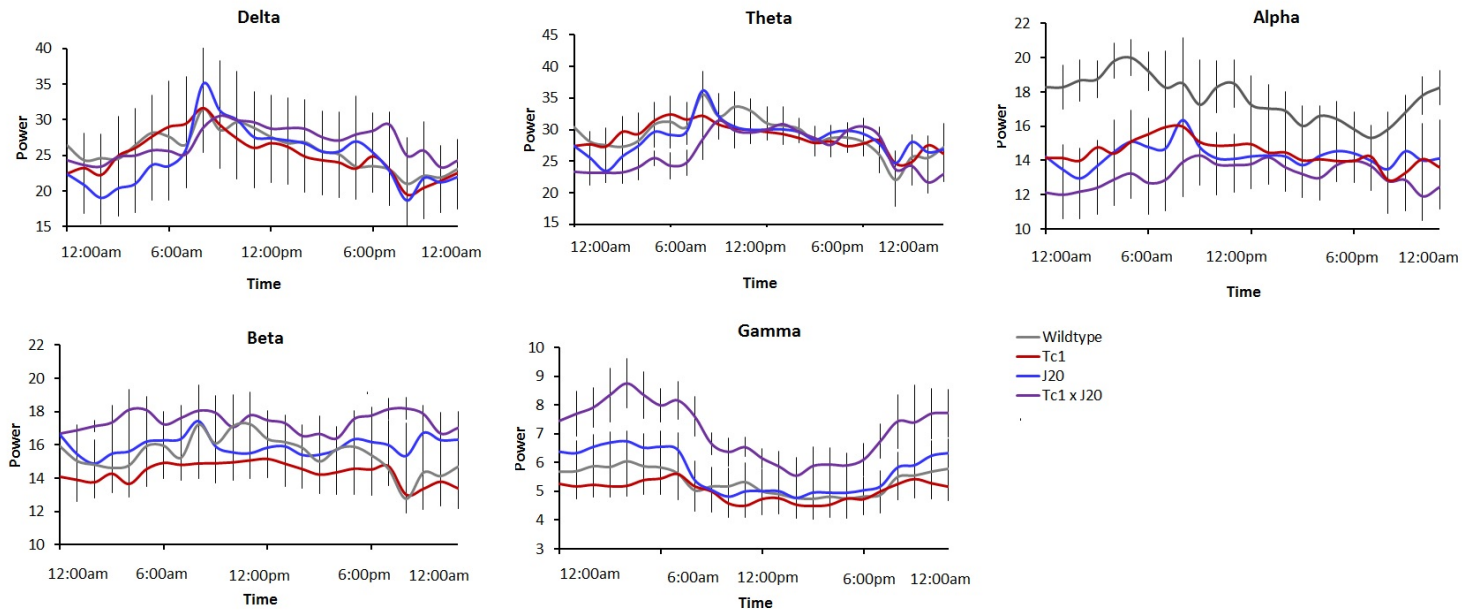


Figure 6.9 Power spectra over a 24h light-dark cycle

Average delta, theta, alpha, beta and gamma power for each hour-long period, plotted from 12am to 12pm in all genotypes. Light period was 7am to 7pm. The first data point corresponds to 12am-1am and the final data point corresponds to 11pm-12am.

No significant changes were observed in total delta power (trisomy: $F(1,13)=0.189$ $p = 0.671$; *tgAPP* $F(1,13)=2.044$ $p= 0.176$; interaction: $F(1,13)=0.358$ $p=0.554$) theta power (trisomy: $F(1,13)=0.110$ $p=0.746$; *tgAPP* $F(1,13)=4.500$ $p=0.0537$; interaction: $p= F(1,13)=0.045$ $p=0.835$), alpha (trisomy: $F(1,13)=0.605$ $p= 0.451$; *tgAPP* $F(1,13)=1.498$ $p=0.242$; interaction: $F(1,13)=0.015$ $p=0.902$), or beta power (trisomy: $F(1,13)=<0.001$ $p=0.990$; *tgAPP* $F(1,13)=0.320$ $p=0.581$; interaction: $F(1,13)=0.175$ $p=0.682$), although there was a trend towards reduced theta in the *tgAPP* animals. This contrasts with previous reports of EEG slowing in AD and DS patients, indicating either that the analysis did not have sufficient sensitivity to detect such changes, or that they may occur later in disease progression, or fail to translate into mouse models.

Power in the low gamma range showed a trend towards an increase in the *tgAPP* animals ($F(1,13)=4.974$ $p=0.044$) and trisomic animals ($F(1,13)=4.529$ $p=0.053$) with no interaction ($F(1,13)=0.582$ $p=0.459$). Power in the high gamma range showed trend towards an increase in the trisomic animals ($F(1,13)=5.911$ $p=0.030$) although not in the *tgAPP* animals ($F(1,13)=2.736$ $p=0.122$), with no interaction ($F(1,13)=0.717$ $p=0.412$). However, these did not reach significance when corrected for multiple comparisons (Bonferroni adjusted α level: 0.00625)

Trisomic animals also showed trend towards increased power in the 70-120Hz band ($F(1,13)=8.589$ $p=0.011$) and 120-160Hz band ($F(1,13)=10.188$ $p=0.007$) although again these did not reach significance when corrected for multiple comparisons. No changes were observed in 70-120 Hz ($F(1,13)=0.053$ $p=0.820$) or 120 - 160Hz ($F(1,13)=0.264$ $p=0.616$) in *tgAPP* mice and no interaction was observed between *tgAPP* and trisomy ($F(1,13)=0.111$ $p=0.767$; $F(1,13)=0.089$ $p=0.363$).

Despite not reaching significance, the consistency of the increase in high frequency power across Tc1 and Tc1×J20 animals in both the 70-120Hz and 120-160Hz power bands indicate that it is likely to represent a real effect. If this is the case, it may represent an increased number of high frequency bursts in these animals, although whether these events are physiological or pathological, and what their functional significance may be, remains unclear.

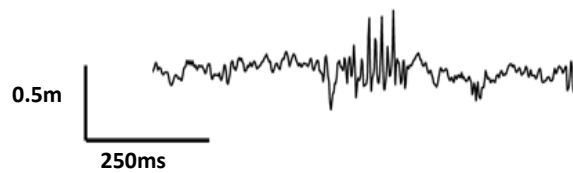


Figure 6.10 *Example of a short high frequency burst in a Tc1×J20 animal*

6.4 Discussion

Individuals with DS have an increased risk of seizures throughout life; the highest incidence occurs in the aged DS population, and is associated with the onset of dementia. The risk of seizures is also elevated in the AD population, particularly in association with EOAD, suggesting A β has a critical role in epileptogenesis. However, late onset myoclonic epilepsy in Down syndrome (LOMEDS) appears to be a clinically distinct entity, indicating a key role for other Hsa21 genes, or for trisomy itself.

Consistent with previously published data, J20 animals exhibited spontaneous seizures as well as frequent interictal epileptiform spiking, suggestive of generalised cortical hyperexcitability. Seizures and interictal spiking were also observed in the Tc1 \times J20 animals, however, no modification of the J20 phenotype was apparent as a result of trisomy. It is possible that the Tc1 \times J20 animals experience more severe seizures, but further data are required to determine if this is the case.

A small number of spikes were observed in wildtype and trisomic animals although markedly less than in either the J20 or Tc1 \times J20 animals. As EEG was recorded via the implantation of electrodes into the upper layers of the cortex, the process of implantation may have resulted in localized tissue damage, which has the potential to impact on neuronal activity in the recording region. It should therefore be recognised that the wildtype recordings may not truly reflect baseline activity in a healthy animal. However, as this trauma will be common across all genotypes and the effect appears to be small, this does not represent a major confound to the analysis.

No spontaneous seizures were observed in either the Tc1 or the Dp1Tyb mice. The Tc1 mice also showed no increase in interictal spiking, and only one Dp1Tyb animal showed an increase in interictal activity relative to wildtype controls, making it difficult to determine whether this was genuinely related to genotype. The impact of the differences in genetic background on seizure susceptibility between the strains also remains unknown.

The majority of phenotypes in DS patients, including seizures, are variably penetrant. Although the degree of environmental and genetic variability in the patient population is clearly far greater than it is for inbred mouse strains housed under controlled conditions, other Dp1Tyb phenotypes, such as congenital heart defects (Lana-Elola *et al.*, 2016) have also been reported to occur only in a subset of animals. This suggests phenotypic variability may also be an intrinsic aspect of aneuploidy; it therefore remains possible that Mmu16 segmental trisomy increases cortical hyperexcitability, but only in a small proportion of animals.

As interictal activity only occurred in a single mouse, there is no way to eliminate the possibility that the observed phenotype was due to other causes, such as surgical trauma. Although all animals underwent the same surgery, minor variations in surgical procedure and in anatomy may have resulted in variable degrees of post-surgical trauma between animals. Variation in body temperature, blood loss, and drug exposure may also have occurred during the procedure, affecting the outcome of recovery. Therefore, although limited conclusions can be drawn from these data, it does suggest that neither trisomy of Hsa21, nor the segmental duplication on Mmu16, is sufficient to substantially alter cortical excitability.

Due to the number of genes on Hsa21, it is inevitable that while some will promote seizures, others will exert a protective effect. This may result in no net effect on seizure risk, yet still cause major structural and functional alterations of the neuronal network, with implications for the initiation and propagation of seizures in the trisomic brain. It may also contribute to the variability in seizure risk and presentation in DS individuals, as the relative contribution of these genes will be modified both by the genetic background and environment, and by stochastic processes during development and within individual cells. Duplication of *APP* independently of trisomy is rare, and there is therefore limited information regarding the incidence of seizures in this population, although it is likely to be high. The extent to which the risk of seizures in the context of *APP* duplication is modified by trisomy in a clinical setting is therefore not known.

EEG was recorded between 4.5 and 6 months of age, the period during which amyloid deposition begins in the brains of the J20 animals. Although amyloid deposition is enhanced by trisomy at 6 months of age in the Tc1×J20 animals (**Figure 1.6**) the survival rates for the J20 and Tc1×J20 animals do not begin to diverge until 10 months (**Figure 1.7A**). Together, these data suggest that the increased mortality in the Tc1×J20 animals does not result from an enhanced susceptibility to seizures throughout life, but represents a differential response to late stage amyloid pathology. Whether this response is a sensitization to seizures, or an entirely separate mechanism, remains an area for further investigation. As the greatest risk of sudden death for the J20 mice is in the first few months of life, the most severely affected animals are likely to be excluded by a 4.5 month time point. However, as there is no difference in mortality between the J20 and Tc1×J20 mice prior to this point, early mortality is unlikely to mask any interactions.

There has been some controversy over the cause of seizures in the J20 animal. Palop *et al.*, (2007) claim that the network hyperexcitability and associated changes observed in tgAPP overexpressing animals result from the synaptic actions of A β , rather than APP overexpression artefact or a non-specific transgene insertion effect, as they occur only in animals overexpressing human APP containing disease-linked mutations, and not animals overexpressing wildtype human APP.

However, this has been challenged by Born *et al.* (2014), who suggest that the hyperexcitability phenotype observed in tgAPP overexpressing mice is not directly due to A β , as it could not be rescued with γ -secretase inhibitors, which block the production of A β from APP. In addition, they observed no epileptic activity in double knock-in APP/PS1 mice, which have increased levels of A β but not of full-length APP, suggesting that rather than A β , increased levels of full-length APP or an alternative cleavage product may be responsible for seizures in tgAPP overexpressing transgenic mouse models.

Furthermore, they showed using an AD model expressing mutant humanised APP under a tetracycline-controllable promoter, that postponing expression of the transgene for a period of 6 weeks during early development delayed the onset of seizures by more than 6 months. This suggests a substantial developmental component to the hyperexcitability phenotype; although animals with adult onset expression did eventually develop seizures of the same level of severity.

If seizures in the J20 mice are not due to the actions of A β , this would be consistent with the initial increase in mortality resulting from spontaneous seizures, and unrelated to the later progressive A β accumulation. It may also explain why although Hsa21 enhances A β deposition and memory deficits, it has no impact on seizures; if Hsa21 genes specifically modify A β deposition, it is unlikely to impact on the

actions of full length APP. The exact contributions made by full length APP, A β , and other APP cleavage products to the observed cortical hyperexcitability at different developmental stages have yet to be determined. However, regardless of the mechanistic relevance of the seizures which occur in the J20 mice to epileptogenic processes that occur in sporadic AD, it remains a useful model to investigate the modulatory impact of trisomy 21 on phenotypes linked to *APP* overexpression.

The issue of why *tgAPP* caused severe epilepsy in some J20 mice, while others showed no electrographic abnormalities at all, requires further investigation. Interestingly, Palop *et al.* (2007) reported interictal spikes to be present in all animals they recorded from at a frequency of 5–50 spikes per minute; a much higher rate than was observed in this study. As suggested for the LTP results, this discrepancy may relate to a protective effect of the hybrid background on which the Tc1 \times J20 cross is maintained, as pronounced differences in susceptibility to seizures and seizure induced neuronal damage have been reported to occur between mouse strains. For example, 129S mice show an increased tolerance to kainic acid and decreased mortality following kainic acid injection compared to C57BL/6 mice, while hybrid 129S \times C57BL/6 strains show a mix of parental phenotypes (McKhann *et al.*, 2003). It is therefore plausible that the 129S \times C57BL/6 mixed background of the J20 animals from the Tc1 \times J20 cross have a milder phenotype than the J20 animals on a C57BL/6 used by Palop *et al.*, (2007).

A protective effect of genetic background may also explain the discrepancy in NPY staining at 6 months of age. Palop *et al.* (2007) reported pronounced NPY immunoreactivity in the mossy fibres of the J20 mice between 3 and 7 months of age, as well as in two other lines overexpressing *tgAPP*: hAPPARC48 and hAPP-J9/FYN. By contrast, no

NPY immunoreactivity was observed in any of the J20 or Tc1×J20 animals used in the EEG study, even though electrographic seizures were recorded in three of the animals.

NPY was ectopically expressed in the mossy fibres of a subset of the J20 and Tc1×J20 mice at 16 months of age. This is likely to be representative of a subset of these animals experiencing seizures, and suggests that aging may increase the frequency or severity of seizures. However, the incidence of aberrant NPY expression remains lower than the incidence of seizures reported in the EEG cohort. This may reflect an elevated risk of sudden death among epileptic animals, with a smaller proportion of epileptic animals surviving to the 16 month time point, or it may suggest that even at age 16 months, not all epileptic animals show aberrant expression of NPY.

Although the low incidence of aberrant NPY expression precludes definitive conclusions, the increase in NPY in the Tc1×J20 mice relative to the J20 mice is consistent with an exacerbation of seizures by Hsa21 at age 16 months. This is further supported by the increased mortality in the Tc1×J20 mice at this time point, but this should be verified with electrographic data.

Generalised slowing of the EEG rhythm is associated with diffuse brain dysfunction, and has been reported in both AD and DS patients (Moretti, 2004; Politoff *et al.*, 1996). However, analysis of the EEG power spectrum revealed no significant differences in delta, theta or alpha power resulting from either *tgAPP* or Hsa21. Although this may indicate that such changes fail to translate into mouse models, abnormalities in EEG spectra have been reported in a range of AD models, suggesting that a more sensitive analysis may be required to detect them.

Circadian cycles in the EEG did not differ between genotypes for any of the any power bands, although circadian changes in EEG power were apparent in all genotypes. This contrasts with previous reports of circadian anomalies and sleep fragmentation in the Tc1 mouse (Heise et al., 2015), which paralleled those observed in DS patients. However, averaging across predefined powerbands or time periods and normalising to total power may obscure more subtle differences in EEG spectra within individual animals. Hsa21 was associated with a trend towards an increase in high frequency power, which could represent an increased number of high frequency bursts. These bursts, however are not specific to transgenic animals, and their functional significance remains unclear.

6.5 Conclusion

EEG data from the Tc1 × J20 cross suggests that Tc1 mice do not experience spontaneous seizures, and that trisomy 21 does not exacerbate seizures in the Tc1 × J20 animals. Although it is possible that seizure are too infrequent, or have too low an incidence to be detected in this study, these results suggest that the cognitive deficits and LTP impairments reported in this model do not result from epileptic activity.

Immunohistochemistry for NPY in the EEG cohort showed no aberrant expression of NPY in any genotype, consistent with there being no exacerbation in seizure severity. However, NPY was ectopically expressed in the mossy fibres of a subset of the J20 and Tc1×J20 mice at 16 months of age, suggesting that an exacerbation of seizures may occur in aged animals. This would be consistent with the divergence in survival trajectories of the J20 and Tc1×J20 mice observed at 10 months of age.

Analysis of EEG power showed no evidence of EEG slowing, and no alteration to circadian rhythms. There was a trend towards an increase in high frequency power as a result of Hsa21, suggesting that trisomy 21 may be associated with an increase in high frequency bursts. However, the function of these bursts, and the extent to which they represent physiological or pathological activity remains unclear.

Dp1Tyb mice also did not experience any spontaneous seizures over the 6-week recording period, suggesting segmental duplication of Mmu16 is also not associated with an increased risk of seizures.

Chapter 7

Discussion

7.1 Overview

Individuals with DS have a dramatically increased risk of developing dementia, due to the presence of the *APP* gene on Hsa21. Duplication of *APP* alone is sufficient to cause early-onset *Alzheimer's* disease, however, other genes on Hsa21 are likely to modify the phenotype. The Tc1 mouse model of DS carries a freely segregating copy of Hsa21, but is not functionally trisomic for *APP*. Crossing the Tc1 model of DS with the J20 mouse, which overexpresses *tgAPP* therefore represents a unique opportunity to model the impact of a trisomic background on *tgAPP* overexpression.

The work presented here builds upon previously obtained data from the Tc1×J20 mouse cross, which shows that interactions between trisomy 21 and *tgAPP* exacerbate amyloid pathology, increase mortality, and cause novel cognitive deficits in this model. This thesis aimed firstly, to investigate whether the novel memory impairments observed as a result of interactions between trisomy 21 and *tgAPP* are associated with novel impairments in synaptic plasticity. Secondly, it aimed to determine whether interactions between trisomy 21 and *tgAPP* result in an increased risk or severity of seizures, which many contribute to the observed increase in mortality or cognitive impairments.

7.2 Synaptic plasticity in AD-DS

It was hypothesised that the exacerbation of cognitive deficits in the Tc1×J20 animals would correspond to enhanced deficits in synaptic plasticity in these animals. As expected, trisomy resulted in a deficit in LTP in the MPP of hippocampal slices, consistent with the *in vivo* results of Morice *et al.*, (2008). However, surprisingly J20 animals did not show a deficit in LTP, and no interaction between trisomy 21 and *tgAPP* was identified in the Tc1×J20 double transgenic animals. It is possible the lack of interaction results from a floor effect; the majority of trisomic animals showed a total loss of potentiation, precluding any further LTP deficit, even if further synaptic dysregulation occurred as a result of *tgAPP*. Such an effect is a clear limitation of the experimental design for the initial LTP study, but if novel mechanisms do contribute to deficits in plasticity in the Tc1×J20 cross, it would be expected that LTP in the Tc1 and Tc1×J20 animals would be differentially affected by altering the experimental conditions. However, no dissociation between the magnitude of LTP in the Tc1 and Tc1×J20 mice was observed under any of the experimental conditions tested.

GABA_AR antagonism did not rescue LTP in either genotype, but both Tc1 and Tc1×J20 mice showed normal LTP in response to forskolin. Furthermore, neither the deficit in the Tc1 nor in the Tc1×J20 appeared to be age-dependent, and neither genotype showed a deficit in LTD. Although it remains possible that Tc1 and Tc1×J20 mice may respond differently to LTP induction under conditions which have not been tested, the data obtained here do not support the hypothesis that interactions between *tgAPP* and trisomy 21 exacerbate LTP deficits in the MPP.

This would suggest that the exacerbation of behavioural deficits observed in the Tc1×J20 cross may result from novel network dysfunction occurring outside of the DG in the Tc1×J20 animals, rather than an exacerbation of deficits in the DG. Although the hippocampus has been implicated in both NOR and spontaneous alternation, the neurobiological basis of both tasks remains controversial, and other brain regions are almost certainly required. For example, Hall *et al.* (2016) suggest the deficits in NOR over short intervals in the Tc1 may be mediated by the perirhinal cortex rather than the hippocampus. The behavioural deficits in the Tc1×J20 cross may therefore represent novel dysfunction in interactions between brain regions, rather than an exacerbation of dysfunction in the DG.

The absence of a deficit in the J20 animals was surprising, as Palop *et al.*, (2007) have previously reported a deficit in LTP in the MPP in this model, and overexpression of *tgAPP* is commonly associated with deficits in synaptic plasticity. The copy number of the transgene array was checked in all experimental animals; the differences in phenotype were therefore not due to copy number variation. There are several notable differences in the experimental protocols used for the LTP experiments presented here, and those of Palop *et al.*, which may have contributed to the discrepancy. However, the fact that the EEG phenotype observed in this strain was also considerably milder than the one reported by Palop *et al.* suggests that the hybrid genetic background of the animals that had to be used for these experiments may be protective against some of the effect of *tgAPP*. Genetic background has been shown to exert a strong influence on both synaptic plasticity and seizure threshold, and such an effect would be generally consistent with previous reports of improved memory in hybrid mouse lines, and increased resistance to kainic acid induced seizures in S129 mice (McKhann *et al.*, 2003). However, this remains

speculative, as a direct comparison of *tgAPP*-mediated phenotypes on these genetic backgrounds has not been carried out.

Increased synaptic inhibition has been proposed as a key mechanism contributing to the cognitive deficits in DS; however, contrary to observations in other models of DS, LTP deficits in the Tc1 model could not be rescued by blocking GABA_ARs with PTX. Blocking inhibition facilitates depolarisation of the postsynaptic terminal, promoting the activation of NMDA receptors, which are required for the induction of LTP. PTX increased the maximal LTP in both the wildtype and J20 animals, suggesting this lack of rescue was not due to a general failure of PTX to facilitate LTP induction under the experimental conditions used.

The rearrangements and deletions in the Tc1 mouse result in a unique combination of genes in this model; mouse segmental trisomy models of DS contain Hsa21 genes which are located together on the Hsa21 syntenic regions of Mmu16, 17 or 10, however, the Tc1 model expresses genes distributed across all of Hsa21. It is therefore not surprising that the Tc1 mouse shows phenotypic differences in comparison to other DS models. The fact that the 'over-inhibition' phenotype is not present in the Tc1 model suggests that the genes which mediate this phenotype are among those which are absent from the copy of Hsa21 in the Tc1 mouse.

This is consistent with several candidate genes reported in the literature, which are known to have been deleted from the Tc1 mouse, including *Olig1/OLIG1* and *Olig2/OLIG2* and *Synj1/SYNJ1*. The data presented here therefore lends further support to the suggestion that increased synaptic inhibition in DS requires one or several of these genes. If this were the case, it would be expected that the Dp1Tyb mice would show a deficit in LTP which could be rescued by PTX, as these

candidate genes are duplicated in this model; this is a testable hypothesis and should be addressed in future work. Discrepancies in the literature also suggest that multiple mechanisms may alter synaptic inhibition in DS, and that these may differ between CA1 and DG. However, the fact that the Tc1 mice do not display a deficit in LTP in CA1 suggests inhibitory signalling is not dysregulated in CA1 either (Witton *et al.*, 2015).

The data presented here suggest that impaired synaptic plasticity in DS is therefore likely to be multifactorial, and while 'over-inhibition' may contribute to cognitive impairment, profound deficits in synaptic plasticity in the DG continue to exist in the absence of enhanced GABA_AR signalling. The clinical implications of this are not yet clear, but it may indicate that targeting GABAergic signalling alone will not be sufficient to produce a substantial improvement in cognition in DS, and that combination therapies may be more effective.

It should also be noted that much of the data supporting the 'over-inhibition' hypothesis comes from the Ts65Dn model, which carries duplications of around 40 additional Mmu17 genes not relevant to DS. Although blocking inhibition has also been shown to rescue LTP deficits in several other models that do not contain duplications of non-Hsa21 orthologous genes, no further characterisation of the phenotype has been carried out in these models. Mechanistic insights into over-inhibition have therefore been based solely on the phenotype in the Ts65Dn. Furthermore, to date there is no conclusive evidence that GABAergic signalling is disrupted in the hippocampus of DS patients. Phase II clinical trials of the α 5 GABA_AR inverse agonist basmisanil found no significant impact on cognition and function for adults and adolescents, and consequently, paediatric trials of basmisanil were halted due to lack of efficacy (Roche, Statement on CLEMATIS trial June

28, 2016). The clinical relevance of the increased inhibition observed in DS mouse models therefore remains unclear.

Chemical LTP induced by the adenylyl cyclase activator forskolin was intact in the MPP of both the Tc1 and the Tc1×J20 animals, suggesting that the deficit in LTP in the Tc1 mouse is specific to LTP induction, and that if adenylyl cyclase is directly activated, normal expression of plasticity occurs. Furthermore, this suggests that if any novel interactions do occur in the Tc1×J20 cross, they must be specific to the induction phase, as LTP expression in these mice is unimpaired.

Impaired induction but intact expression of LTP is consistent with the pattern of memory deficits observed in the Tc1 mouse by Hall *et al.* (2016), and Morice *et al.* (2008). Tc1 animals showed impairments in short-term memory but not long-term memory, and deficits in *in vivo* LTP in the MPP were reported 1 hour after induction, but not 24 hours later. Trisomy may therefore cause a specific deficit in the mechanisms underlying LTP induction, which correspond to impaired performance on memory tasks requiring retention of information over short intervals, such as the 10 minute test phase used by Hall *et al.* (2016).

The observed LTP deficit in the Tc1×J20 cross appears to be specific to the MPP, as LTP induction in the mossy fibres and Schaeffer collateral are unimpaired (Witton *et al.*, 2015), although cortical LTP has not yet been assessed in the Tc1 mouse. However, the hippocampal-dependence of the tasks tested by Hall *et al.* has not been conclusively established, and the extent to which the DG is involved remains unclear; Hall *et al.* suggest cortical dysfunction may be more significant for successful completion of these tests. Consequently, caution is required in making connections between deficits in synaptic plasticity and behaviour.

The mechanism by which trisomy impairs LTP induction in the MPP of the Tc1 mice therefore requires further investigation. If synaptic inhibition is not increased, NMDAR surface expression is not altered, (Morice *et al.*, 2008) and there are no deficits in PKA-mediated signalling, several possible mechanisms remain. Either an alternative mechanism may be contributing to ineffective activity-dependent activation of NMDA receptors, or NMDA receptor activation may be failing to effectively engage downstream signalling cascades. One interesting possibility is that the deficit is mediated by glia. Glia have received limited attention in the DS field, particularly in relation to synaptic plasticity, however glia are known to play a critical role in hippocampal LTP (Henneberger *et al.*, 2010). Furthermore, while glial transmitters are important for LTP induction, they are unlikely to be required for LTP expression following direct activation of adenylyl cyclase, as this process is dependent on signalling cascades within the neuron. This would therefore be consistent with the data obtained from the Tc1×J20 cross.

One of the genes triplicated in the Tc1 model, which is not located on Mmu16, and therefore absent from the Ts65Dn model is *S100b*, an astrocytic Ca²⁺ binding protein. Duplication of *S100b* is associated with memory deficits (Gerlai *et al.*, 1995; Roder, Roder and Gerlai, 1996; Winocur, Roder and Lobaugh, 2001), and knockout of *S100b* results in an enhancement of LTP (Nishiyama *et al.*, 2002). S100B has also been implicated in astrocytic dysfunction in iPSCs, and siRNA knockdown of S100B rescued astrocytic dysfunction in DS stem cells, leading to reduced astrocytic ROS production and a decrease in neuronal apoptosis (Chen *et al.*, 2014). Overexpression of *S100B* is therefore a possible candidate for LTP deficits in the Tc1 mouse.

In addition, not all forms of LTP expression rely on PKA, and the importance of PKA-mediated signalling for LTP expression in the mouse MPP, relative to other signalling pathways, is not known, and furthermore, may vary due to genetic background, age and experimental parameters. It is therefore possible that while activation of PKA can induce normal LTP expression, this is not the pathway induced via activity-dependent plasticity, and deficits in other pathways may contribute to impaired LTP expression under physiological conditions. To assess this, further experiments would be required to test whether PKA-induced LTP occludes activity-dependent LTP in the MPP of the Tc1×J20 cross.

There was no change in baseline synaptic transmission for any genotype in the Tc1×J20 cross, despite loss of synapses being reported in the DG of both the Tc1 and the J20 mice. The most likely explanation for this is simply that the assessment of baseline synaptic transmission in these experiments lacked sufficient sensitivity to detect these differences, due to variability introduced by other factors, such the health of the slices, fluctuations in room temperature between experiments, or variation in depth and position of electrodes. This would be consistent with the large variability in synaptic transmission observed within genotypes. There were also no changes in PPR or PTP in any of the genotypes in the Tc1×J20 cross, consistent with previous observations in both the Tc1 and J20 models, suggesting short-term plasticity was not impaired by either trisomy or *tgAPP*, and no novel interactions were observed between *tgAPP* and *Hsa21*.

Synaptic properties were also assessed in the Dp1Typ model, which is segmentally trisomic for Mmu16. Although this model also showed no change in baseline synaptic transmission, short-term plasticity did appear to be altered. PTP was significantly reduced in the MPP, and

there was a trend towards a reduction in PPI at longer time intervals. Further experimental data is required to confirm this trend, as only a small number of animals were available for this study, however, if the trend were real, it would suggest that Hsa21 orthologous genes on Mmu16 that are not present in the Tc1 model contribute to impairments in short-term synaptic plasticity. Although it is also possible that other factors such as mosaicism, or differences between human and mouse genes underlie the difference between models.

The mechanisms mediating PPI and PTP in the DG are poorly characterised, making candidate genes difficult to identify. It is possible that these deficits in short-term plasticity are mediated by disrupted inhibitory neurotransmission, and share common mechanisms with 'over-inhibition' phenotype, as this phenotype also appears to be linked to Mmu16 orthologous genes missing from the Tc1 model, and inhibitory auto-receptors have been implicated in synaptic plasticity. However, as the effects of blocking inhibition have not yet been determined in the Dp1Tyb model, this remains speculative.

Other potential mechanisms include disrupted BDNF signalling; a reduction in BDNF signalling has been linked to reduced PPI in the MPP (Asztely *et al.*, 2000), suggesting BDNF signalling modulates short-term synaptic plasticity in this pathway. In support of this, increased BDNF immunoreactivity has been observed in the DG and CA1 (Troca-Marín, Alves-Sampaio and Montesinos, 2011) of the Ts1Cje mouse model of DS, which carries genes from the Mmu16 orthologous region, and BDNF induced synaptic potentiation has also been reported to be impaired in the CA1 region of this model (Andrade-Talavera *et al.*, 2015). This impairment may be due to elevated endogenous BDNF in CA1 occluding any further modulatory effect of exogenously applied BDNF (Troca-Marín, Alves-Sampaio and Montesinos, 2011; Andrade-Talavera *et al.*,

2015), however, the functional implications of disrupted BDNF signalling in the DG have not yet been investigated.

7.3 Seizures in AD-DS

Limited characterisation of seizure susceptibility has been carried out in DS models to date, although there is some evidence to support an increase in seizure susceptibility in the Ts65Dn model (Cortez *et al.*, 2009; Westmark *et al.*, 2010). However, the Ts65Dn and other models of segmental trisomy cannot be regarded as models of AD-DS, as although they express an additional copy of *App*, overexpression of murine-APP does not result in the A β aggregation, and so these models do not reflect the pathogenic process occurring in AD. The data presented here therefore represents the first assessment of seizure susceptibility in a model of AD-DS.

It was hypothesised that an exacerbation in the frequency or severity of seizures in the Tc1 \times J20 mice may contribute to the reduction in survival and enhanced cognitive impairments observed in this model. However, contrary to expectations, no exacerbation of the J20 spontaneous seizure phenotype was observed in the Tc1 \times J20 mice; 4 seizures were observed in 2 of 5 J20 mice, and 5 seizures were observed in 1 of 4 J20 \times Tc1 mice. No seizures or spontaneous epileptiform activity were observed in the Tc1 or wildtype mice, suggesting trisomy does not have a major impact on cortical hyperexcitability.

Interpretation of these data was therefore limited by the fact that the incidence and frequency of both electrographic seizures and interictal

spikes in the J20 animals was substantially lower than was anticipated, based on previously published data (Palop *et al.*, 2007), and therefore too low for statistical analysis. This may relate to a protective effect of the hybrid background of the Tc1×J20 cross; if this were the case, it would suggest that genetic background exerts a stronger modulatory effect on *tgAPP*-mediated cortical hyperexcitability than trisomy, implying that any impact of trisomy of the Hsa21 genes in the Tc1 mouse is of limited clinical relevance.

Despite this, the incidence of seizures in AD-DS has been reported to be very high (Menéndez, 2005; De Simone *et al.*, 2010), and to have a clinically distinct presentation in comparison to the seizures that occur in other forms of familial and sporadic AD (Möller *et al.*, 2002; De Simone, Daquin and Genton, 2006; Wiseman *et al.*, 2015). It is possible that this relates to duplication of genes which are absent from the Tc1 model. Alternatively, the modulatory effects of trisomy on *tgAPP*-related seizures may be age-dependent, which would be consistent with the late-onset epilepsy associated with dementia in DS patients.

In support of this, the survival trajectories of the J20 and Tc1×J20 animals do not diverge until 10 months of age; several months after the EEG studies were performed. Furthermore, aberrant expression of NPY appears to be exacerbated in the Tc1×J20 mice at 16 months of age, although no aberrant expression is observed at 6 months of age in any genotype, suggesting seizures may be more severe or more frequent in older mice. Unfortunately, EEG data could not be obtained at this time point, as the increased mortality in the Tc1×J20 resulted in restrictions on aging the mice in accordance with the Home Office project license. Thus the electrographic phenotype in mice at this age remains unknown.

It is also possible other developmental-stage specific mechanisms may modify seizure risk at other time points in the Tc1 and Dp1Tyb mice. The second largest peak in seizure onset in DS occurs during infancy; these childhood seizure disorders often do not persist into adulthood, although they may still have a lasting impact on development. However, as the focus of the work presented here was on AD-DS, EEG was not assessed in the Tc1 or Dp1Tyb mice during early development. This therefore remains an interesting area for further investigation.

Although both AD and DS have been associated with generalised EEG slowing, the EEG pilot study revealed no significant effect of genotype on average delta, theta or alpha power. A more in-depth analysis of EEG to identify shifts in specific peaks within these bands may be necessary to detect a phenotype in these animals. This could be particularly relevant for the J20 mice, as the current data was obtained in 4.5–6-month-old animals and therefore reflects an early stage of the disease process, when phenotypes may be subtle and more difficult to detect.

However, the power analysis did suggest that trisomy may increase power in the 70-120Hz and 120-160Hz power bands. Further investigation is required to verify this effect, and to understand the biological basis of the high frequency bursts observed in the trisomic animals and how these relate to alterations in EEG high frequency power.

Several limitations of the pilot study could be addressed in future studies; studies should be designed to look specifically at high frequency activity, thus avoiding the need to correct for multiple comparisons across frequency bands. Furthermore, the EEG transmitters used for this study are unable to detect frequencies of greater than 160Hz, as higher sampling rates reduce battery lifespan, and therefore make the transmitters unsuitable for use in long-term

recording. As the current data suggests that the effect is most pronounced in the highest frequency band, further experiments with transmitters operating over a greater frequency range would need to be carried out to fully observe the effect. The poor spatial resolution of EEG means it is only possible to observe activity over a large region of the cortex. EEG recordings could therefore be combined with single cell or local field recordings to further characterise activity during high frequency bursts.

Greater sensitivity to disrupted circadian rhythm could also be obtained by combining analysis of circadian changes with electromyography or video recording, in order to correlate EEG with activity levels.

7.4 Modelling AD-DS

Inevitably, no animal model of DS is able to recapitulate fully the impact of human trisomy. Similarly, mouse models of AD are unlikely to completely replicate the processes underlying human disease. Different mouse models should therefore be regarded as modelling different aspects of the disease process in DS and AD, rather than the diseases in their entirety.

The DS phenotype is likely to result from complex interactions between the overexpression of multiple genes, which are subject to varying degrees of feedback and feedforward regulation, as well as changes in transcription factors, microRNAs, and other epigenetic regulators affecting gene expression on other chromosomes. These effects will be modified by homeostatic compensatory changes, and potentially by non-specific effects of aneuploidy on cellular stress or transcriptional regulation. In addition, not all genes and regulatory elements are conserved between mice and humans, and where genes are conserved, small sequence differences may result in significant differences in

protein interactions. It is therefore important to consider the relative impact of these mechanisms in specific models of DS, in order to understand the clinical relevance of the data obtained.

AD is a progressive disorder for which the greatest risk factor is age; mouse models are therefore required to accelerate pathological processes occurring over decades, so that they occur over a period of months, in order to produce an experimentally tractable phenotype. This generally relies on a combination of aggressive *APP* overexpression via exogenous promoters, and the introduction of disease-linked mutations into *APP* or other AD associated genes. Such an acceleration risks both generating overexpression artefacts, and conversely, failing to replicate chronic processes. Furthermore, human neurodevelopmental processes are far more complex than those observed in the mouse, and many of the functions disrupted by DS and AD relate to human-specific cognitive process such as language. Consequently, the use of multiple approaches to investigating DS and AD pathology is critical to gaining an accurate understanding of the mechanisms contributing to human disease.

The data presented here has been obtained predominantly using the Tc1 model of DS and the J20 model of AD. The Tc1 mouse is the only model of DS that contains a freely segregating copy of Hsa21. The Tc1 therefore replicates not only the impact of gene duplication, but also the impact of aneuploidy (an abnormal number of chromosomes). This model also contains approximately 75% of Hsa21 genes across all three mouse syntenic regions, making it one of the most genetically complete models of DS currently available. However, it cannot be assumed that regulatory processes are conserved between mice and humans, or that mouse proteins will interact with human proteins and regulatory

elements in the same was that human proteins do, and the effects of mosaicism in this model are not yet clear.

Furthermore, the Tc1 model lacks a number of Hsa21 genes, which have been implicated in synaptic dysfunction in other models of DS. In order to better understand the role of these genes, some experiments were repeated in a second model of DS, the Dp1Tyb model, although time constraints, and animal availability, meant it was not possible to repeat all the experiments, nor assess the impact of the Dp1Tyb segmental trisomy on *APP* overexpression. However, comparison of phenotypes across different models offers a valuable insight into the contributions of different genetic mechanisms to the disease processes, particularly in complex diseases such as AD and DS, and well as helping to distinguish disease-relevant phenotypes from model-associated artefacts.

The degree of variability in the data from the Tc1 cross has made interpretation of the results difficult. This may result, to some extent, from the fact that the Tc1 mice are mosaic for trisomy, and the proportion and distribution of neurons containing the additional chromosome is likely to be variable between individual mice, meaning the proportion of trisomic cells represented may not be consistent between experiments. Unfortunately identifying the proportion of trisomic cells in individual animals was outside the technical scope of this project, and this therefore represents a limitation of the model. However, the variability may also be intrinsic to DS; the clinical presentation of DS is highly heterogeneous, many DS features are present in only a subset of patients, and while cognitive deficits are considered to be universal in DS, the severity of the deficit differs extensively between individuals. Although differences in genetic background undoubtedly account for some of this variability, DS is fundamentally a disorder of dysregulated gene expression, which

means the DS phenotype may be highly influenced by the stochastic variations in gene expression which underlie 'developmental noise' (Raser and O'Shea, 2005).

Due to the high phenotypic variability, the numbers for many of the experiments were not large enough to detect a significant effect. Although for some experiments, the number of animals needed to detect significance was in retrospect unfeasibly high, this was also due to limitations on the availability of animals during the course of this study. Chromosomal abnormalities are known to have a negative impact on fertility, and consequently failure to breed, failure to transmit the additional chromosome, small litters, and litters that failed to survive occurred frequently and unpredictably in the Tc1×J20 strain. This resulted on occasion in substantial delays in obtaining the necessary experimental cohorts. The problem was compounded by the increased incidence of spontaneous mortality, which resulted in the loss of 20-30% of J20 and double transgenic animals by the 6 month time point, and in addition, by restrictions on import between research institutes, meaning unproductive females could not easily be replaced. Therefore, further data is required in order to verify many of the trends observed here.

7.5 Conclusion

The data presented in this thesis confirms previous observations that trisomy results in a deficit in LTP in the MPP. No interactions between Hsa21 and *tgAPP* were observed, suggesting the exacerbated behavioural deficits in the Tc1×J20 animals may relate to novel impairments in interactions between brain regions, rather than a specific exacerbation of deficits in the DG. However, it remains possible

that subtle interactions in synaptic plasticity in the DG occur which could not be detected under the experimental conditions used here.

Contrary to observations in other models of DS, LTP deficits in the MPP were not rescued by blocking GABA_A receptors, suggesting the LTP deficit was not due to increased synaptic inhibition, providing support for previous reports that the genes which contribute to this phenotype may be absent from the Tc1 model of DS. This suggests that other mechanisms make a substantial contribution to synaptic dysfunction in DS, and identifying these mechanisms may provide novel therapeutic targets for improving cognition in DS.

No effect of trisomy on seizure risk was observed at 6 months of age, however histology and mortality data suggest that a potential interaction may occur in aged animals; this would be consistent with a late onset phenotype in the DS population. As epilepsy in DS remains a clinically significant and underdiagnosed problem, further investigation of these mechanisms is necessary.

Bibliography

Aarts, M., Liu, Y., Liu, L., Besshoh, S., Arundine, M., Gurd, J. W., Wang, Y.-T., Salter, M. W. and Tymianski, M. (2002) 'Treatment of ischemic brain damage by perturbing NMDA receptor- PSD-95 protein interactions.', *Science* 298(5594), pp. 846–50. doi: 10.1126/science.1072873.

Abel, T., Nguyen, P. V, Barad, M., Deuel, T. A. , Kandel, E. R. and Bourtchouladze, R. (1997) 'Genetic Demonstration of a Role for PKA in the Late Phase of LTP and in Hippocampus-Based Long-Term Memory', *Cell*, 88(5), pp. 615–626. doi: 10.1016/S0092-8674(00)81904-2.

Adams, D. and Oliver, C. (2010) 'The relationship between acquired impairments of executive function and behaviour change in adults with Down syndrome', *Journal of Intellectual Disability Research*. Blackwell Publishing Ltd, 54(5), pp. 393–405. doi: 10.1111/j.1365-2788.2010.01271.x.

Adorno, M., Sikandar, S., Mitra, S. S., Kuo, A., Di Robilant, B. N., Haro-Acosta, V., Ouadah, Y., Quarta, M., Rodriguez, J., Qian, D., Reddy, V. M., Cheshier, S., Garner, C. C. and Clarke, M. F. (2013) 'Usp16 contributes to somatic stem-cell defects in Down's syndrome', *Nature*. Nature Publishing Group, 501(7467), pp. 380–384. doi: 10.1038/nature12530.

Aït Yahya-Graison, E., Aubert, J., Dauphinot, L., Rivals, I., Prieur, M., Golfier, G., Rossier, J., Personnaz, L., Creau, N., Bléhaut, H., Robin, S., Delabar, J. M. and Potier, M.-C. (2007) 'Classification of human chromosome 21 gene-expression variations in Down syndrome: impact on disease phenotypes.', *American journal of human genetics*, 81(3), pp. 475–91. doi: 10.1086/520000.

Almeida, C. G., Tampellini, D., Takahashi, R. H., Greengard, P., Lin, M. T., Snyder, E. M. and Gouras, G. K. (2005) 'Beta-amyloid accumulation in APP mutant neurons reduces PSD-95 and GluR1 in synapses', *Neurobiology of Disease*, 20(2), pp. 187–198. doi: 10.1016/j.nbd.2005.02.008.

Altafaj, X., Martín, E. D., Ortiz-Abalia, J., Valderrama, A., Lao-Peregrín, C., Dierssen, M. and Fillat, C. (2013) 'Normalization of Dyrk1A expression by AAV2/1-shDyrk1A attenuates hippocampal-dependent defects in the Ts65Dn mouse model of Down syndrome', *Neurobiology of Disease*, 52, pp. 117–127. doi: 10.1016/j.nbd.2012.11.017.

Amatniek, J. C., Hauser, W. A., DelCastillo-Castaneda, C., Jacobs, D. M., Marder, K., Bell, K., Albert, M., Brandt, J. and Stern, Y. (2006) 'Incidence and predictors of seizures in patients with Alzheimer's disease.', *Epilepsia*, 47(5), pp. 867–72. doi: 10.1111/j.1528-1167.2006.00554.x.

Andorfer, C., Kress, Y., Espinoza, M., De Silva, R., Tucker, K. L., Barde, Y. A., Duff, K. and Davies, P. (2003) 'Hyperphosphorylation and aggregation of tau in mice expressing

normal human tau isoforms', *Journal of Neurochemistry*. 86(3), pp. 582–590. doi: 10.1046/j.1471-4159.2003.01879.x.

Andrade-Talavera, Y., Benito, I., Casañas, J. J., Rodríguez-Moreno, A. and Montesinos, M. L. (2015) 'Rapamycin restores BDNF-LTP and the persistence of long-term memory in a model of Down's syndrome', *Neurobiology of Disease*, 82, pp. 516–525. doi: 10.1016/j.nbd.2015.09.005.

Antonarakis, S. E. (1991) 'Parental origin of the extra chromosome in trisomy 21 as indicated by analysis of DNA polymorphisms. Down Syndrome Collaborative Group.', *The New England journal of medicine*. 324(13), pp. 872–6. doi: 10.1056/NEJM199103283241302.

Antonarakis, S. E., Petersen, M. B., McInnis, M. G., Adelsberger, P. A., Schinzel, A. A., Binkert, F., Pangalos, C., Raoul, O., Slaugenhaupt, S. A. and Hafez, M. (1992) 'The meiotic stage of nondisjunction in trisomy 21: determination by using DNA polymorphisms.', *American journal of human genetics*. Elsevier, 50(3), pp. 544–50.

Anwyl, R., Walshe, J. and Rowan, M. (1987) 'Electroconvulsive treatment reduces long-term potentiation in rat hippocampus', *Brain Research*, 435(1–2), pp. 377–379. doi: 10.1016/0006-8993(87)91629-5.

Asztely, F., Kokaia, M., Olofsdotter, K., Örtengren, U. and Lindvall, O. (2000) 'Afferent-specific modulation of short-term synaptic plasticity by neurotrophins in dentate gyrus', *European Journal of Neuroscience*. 12(2), pp. 662–669. doi: 10.1046/j.1460-9568.2000.00956.x.

Ball, S. L., Holland, A. J., Treppner, P., Watson, P. C. and Huppert, F. A. (2008) 'Executive dysfunction and its association with personality and behaviour changes in the development of Alzheimer's disease in adults with Down syndrome and mild to moderate learning disabilities.', *The British journal of clinical psychology*, pp. 1–29. doi: 10.1348/014466507X230967.

Bannerman, D. M., Good, M. A., Butcher, S. P., Ramsay, M. and Morris, R. G. M. (1995) 'Distinct components of spatial learning revealed by prior training and NMDA receptor blockade', *Nature*, 378(6553), pp. 182–186. doi: 10.1038/378182a0.

Bannerman, D. M., Sprengel, R., Sanderson, D. J., McHugh, S. B., Rawlins, J. N. P., Monyer, H. and Seeburg, P. H. (2014) 'Hippocampal synaptic plasticity, spatial memory and anxiety', *Nature Reviews Neuroscience*, 15(3), pp. 181–192. doi: 10.1038/nrn3677.

Barr, D. S., Hoyt, K. L., Moore, S. D. and Wilson, W. A. (1997) 'Post-ictal depression transiently inhibits induction of LTP in area CA1 of the rat hippocampal slice', *Epilepsy Research*, 27(2), pp. 111–118. doi: 10.1016/S0920-1211(97)01027-9.

- Beck, H., Goussakov, I. V., Lie, A., Helmstaedter, C. and Elger, C. E. (2000) 'Synaptic plasticity in the human dentate gyrus.', *Journal of Neuroscience*, 20(18), pp. 7080–7086. doi: 20/18/7080
- Becker, L. E., Armstrong, D. L. and Chan, F. (1986) 'Dendritic atrophy in children with Down's syndrome.', *Annals of neurology*, 20(4), pp. 520–6. doi: 10.1002/ana.410200413.
- Belichenko, N. P., Belichenko, P. V., Kleschevnikov, A. M., Salehi, A., Reeves, R. H. and Mobley, W. C. (2009) 'The "Down syndrome critical region" is sufficient in the mouse model to confer behavioral, neurophysiological, and synaptic phenotypes characteristic of Down syndrome.', *The Journal of Neuroscience*, 29(18), pp. 5938–48. doi: 10.1523/JNEUROSCI.1547-09.2009.
- Belichenko, P. V., Kleschevnikov, A. M., Salehi, A., Epstein, C. J. and Mobley, W. C. (2007) 'Synaptic and cognitive abnormalities in mouse models of Down syndrome: Exploring genotype-phenotype relationships', *Journal of Comparative Neurology*, 504(4), pp. 329–345. doi: 10.1002/cne.21433.
- Belichenko, P. V., Kleschevnikov, A. M., Becker, A., Wagner, G. E., Lysenko, L. V., Yu, Y. E. and Mobley, W. C. (2015) 'Down Syndrome Cognitive Phenotypes Modeled in Mice Trisomic for All HSA 21 Homologues.', *PloS One*, 10(7), p. e0134861. doi: 10.1371/journal.pone.0134861.
- Benilova, I., Karran, E. and De Strooper, B. (2012) 'The toxic A β oligomer and Alzheimer's disease: an emperor in need of clothes.', *Nature neuroscience*, 15(3), pp. 349–57. doi: 10.1038/nn.3028.
- Best, T. K., Cramer, N. P., Chakrabarti, L., Haydar, T. F. and Galdzicki, Z. (2012) 'Dysfunctional hippocampal inhibition in the Ts65Dn mouse model of Down syndrome', *Experimental Neurology*, 233(2), pp. 749–757. doi: 10.1016/j.expneurol.2011.11.033.
- Bianchi, P., Ciani, E., Guidi, S., Trazzi, S., Felice, D., Grossi, G., Fernandez, M., Giuliani, A., Calzà, L. and Bartesaghi, R. (2010) 'Early pharmacotherapy restores neurogenesis and cognitive performance in the Ts65Dn mouse model for Down syndrome.', *The Journal of Neuroscience*, 30(26), pp. 8769–79. doi: 10.1523/JNEUROSCI.0534-10.2010.
- Bianchi, R., Kastrisianaki, E., Giambanco, I. and Donato, R. (2011) 'S100B protein stimulates microglia migration via RAGE-dependent up-regulation of chemokine expression and release.', *The Journal of Biological Chemistry*, 286(9), pp. 7214–26. doi: 10.1074/jbc.M110.169342.
- Billings, L. M., Oddo, S., Green, K. N., McGaugh, J. L. and LaFerla, F. M. (2005) 'Intraneuronal A β causes the onset of early Alzheimer's disease-related cognitive deficits in transgenic mice', *Neuron*, 45(5), pp. 675–688. doi: 10.1016/j.neuron.2005.01.040.

Bimonte-Nelson, H. A., Hunter, C. L., Nelson, M. E. and Granholm, A.-C. E. (2003) 'Frontal cortex BDNF levels correlate with working memory in an animal model of Down syndrome', *Behavioural Brain Research*, 139(1-2), pp. 47-57. doi: 10.1016/S0166-4328(02)00082-7.

Bittles, A. H. and Glasson, E. J. (2004) 'Clinical, social, and ethical implications of changing life expectancy in Down syndrome.', *Developmental Medicine and Child Neurology*, 46(4), pp. 282-286. doi: 10.1017/S0012162204000441.

Blatow, M., Caputi, A., Burnashev, N., Monyer, H., Rozov, A., Acsady, L., Kamondi, A., Sik, A., Freund, T., Buzsaki, G., Alcantara, S., Lecea, L. de, Rio, J. A. Del, Ferrer, I., Soriano, E., Atluri, P. P., Regehr, W. G., Caillard, O., Moreno, H., Schwaller, B., Llano, I., Celio, M. R., Marty, A., Catania, M. V., Tolle, T. R., Monyer, H., Celio, M. R., Fisher, S. A., Fischer, T. M., Carew, T. J., Freund, T. F., Buzsaki, G., Gupta, A., Wang, Y., Markram, H., Henze, D. A., Urban, N. N., Barrionuevo, G., Jiang, M., Swann, J. W., Jones, H. C., Keep, R. F., Jones, H. C., Keep, R. F., Kamiya, H., Shinozaki, H., Yamamoto, C., Kamiya, H., Ozawa, S., Manabe, T., Katz, B., Miledi, R., Klapstein, G. J., Vietla, S., Lieberman, D. N., Gray, P. A., Airaksinen, M. S., Thoenen, H., Meyer, M., Mody, I., Lee, S. H., Schwaller, B., Neher, E., Maccaferri, G., McBain, C. J., Maccaferri, G., Toth, K., McBain, C. J., Markram, H., Lubke, J., Frotscher, M., Roth, A., Sakmann, B., Nagerl, U. V., Novo, D., Mody, I., Vergara, J. L., Naraghi, M., Neher, E., Neher, E., Rahamimoff, R., Reyes, A., Lujan, R., Rozov, A., Burnashev, N., Somogyi, P., Sakmann, B., Rozov, A., Burnashev, N., Sakmann, B., Neher, E., Salin, P. A., Scanziani, M., Malenka, R. C., Nicoll, R. A., Sansig, G., Bushell, T. J., Clarke, V. R., Rozov, A., Burnashev, N., Portet, C., Gasparini, F., Schmutz, M., Klebs, K., Shigemoto, R., al., et, Schmitz, D., Mellor, J., Frerking, M., Nicoll, R. A., Stuart, G. J., Dodt, H. U., Sakmann, B., Thomson, A. M., Thomson, A. M., Deuchars, J., Thomson, A. M., Deuchars, J., West, D. C., Toth, K., Soares, G., Lawrence, J. J., Philips-Tansey, E., McBain, C. J., Winslow, J. L., Duffy, S. N., Charlton, M. P., Zucker, R. S., Zucker, R. S. and Zucker, R. S. (2003) 'Ca²⁺ Buffer Saturation Underlies Paired Pulse Facilitation in Calbindin-D28k-Containing Terminals', *Neuron*, 38(1), pp. 79-88. doi: 10.1016/S0896-6273(03)00196-X.

Blichowski, M., Shephard, A., Armstrong, J., Shen, L., Cortez, M. A., Eubanks, J. H. and Snead, O. C. (2015) 'The GIRK2 subunit is involved in IS-like seizures induced by GABAB receptor agonists', *Epilepsia*, 56(7), pp. 1081-1087. doi: 10.1111/EPI.13034.

Bliss, T. V. P. and Collingridge, G. L. (1993) 'A synaptic model of memory: long-term potentiation in the hippocampus.', *Nature*, 361(6407), pp. 31-39. doi: 10.1038/361031a0.

Bliss, T. V. P., Lømo, T. (1973) 'Long-lasting potentiation of synaptic transmission in the dentate area of the anaesthetized rabbit following stimulation of the perforant path', *Journal of Physiology*, 232(2), pp. 331-356. doi: 4727084.

Born, H. A., Kim, J.-Y., Savjani, R. R., Das, P., Dabaghian, Y. A., Guo, Q., Yoo, J. W., Schuler, D. R., Cirrito, J. R., Zheng, H., Golde, T. E., Noebels, J. L. and Jankowsky, J. L. (2014) 'Genetic suppression of transgenic APP rescues Hypersynchronous network activity in a mouse model of Alzheimer's disease.', *The Journal of Neuroscience*, 34(11), pp. 3826-3840. doi: 10.1523/JNEUROSCI.5171-13.2014.

- Bostrom, C. A., Majaess, N.-M., Morch, K., White, E., Eadie, B. D. and Christie, B. R. (2013) 'Rescue of NMDAR-dependent synaptic plasticity in Fmr1 knock-out mice.', *Cerebral cortex*, 25(1), pp. 271–9. doi: 10.1093/cercor/bht237.
- Braak, H. and Braak, E. (1996) 'Evolution of the neuropathology of Alzheimer's disease.', *Acta neurologica Scandinavica. Supplementum*, 165, pp. 3–12. doi: 10.1111/j.1600-0404.1996.tb05866.x.
- Bramham, C. R., Errington, M. L. and Bliss, T. V (1988) 'Naloxone blocks the induction of long-term potentiation in the lateral but not in the medial perforant pathway in the anesthetized rat.', *Brain research*, 449, pp. 352–6. doi: 10.1016/0006-8993(88)91052-9.
- Braudeau, J., Delatour, B., Duchon, A., Pereira, P. L., Dauphinot, L., de Chaumont, F., Olivo-Marin, J.-C. J.-C., Dodd, R. H., Hérault, Y., Potier, M.-C. M.-C., Herault, Y. and Potier, M.-C. M.-C. (2011) 'Specific targeting of the GABA-A receptor $\alpha 5$ subtype by a selective inverse agonist restores cognitive deficits in Down syndrome mice.', *Journal of Psychopharmacology*, 25(8), pp. 1030–42. doi: 10.1177/0269881111405366.
- Brault, V., Martin, B., Costet, N., Bizot, J.-C. and Hérault, Y. (2011) 'Characterization of PTZ-induced seizure susceptibility in a down syndrome mouse model that overexpresses CSTB.', *PloS One*, 6(11), p. e27845. doi: 10.1371/journal.pone.0027845.
- Busciglio, J. and Yankner, B. (1995) 'Apoptosis and increased generation of reactive oxygen species in Down's syndrome neurons in vitro', *Nature*, 378(6559), pp. 776–779. doi: 10.1038/378776a0.
- Buzsáki, G., Anastassiou, C. A. and Koch, C. (2012) 'The origin of extracellular fields and currents - EEG, ECoG, LFP and spikes.', *Nature Reviews Neuroscience*, 13(6), pp. 407–420. doi: 10.1038/nrn3241.
- Cabrejo, L., Guyant-Maréchal, L., Laquerrière, A., Vercelletto, M., De La Fournière, F., Thomas-Antérion, C., Verny, C., Letournel, F., Pasquier, F., Vital, A., Checler, F., Frebourg, T., Campion, D. and Hannequin, D. (2006) 'Phenotype associated with APP duplication in five families', *Brain*, 129(11), pp. 2966–2976. doi: 10.1093/brain/awl237.
- Cai, Y., An, S. S. A. and Kim, S. (2015) 'Mutations in presenilin 2 and its implications in Alzheimer's disease and other dementia-associated disorders.', *Clinical interventions in aging*, 10, pp. 1163–72. doi: 10.2147/CIA.S85808.
- Carter, T. L., Rissman, R. A., Mishizen-Eberz, A. J., Wolfe, B. B., Hamilton, R. L., Gandy, S. and Armstrong, D. M. (2004) 'Differential preservation of AMPA receptor subunits in the hippocampi of Alzheimer's disease patients according to Braak stage', *Experimental Neurology*, 187(2), pp. 299–309. doi: 10.1016/j.expneurol.2003.12.010.

- Casanova, M. F., Walker, L. C., Whitehouse, P. J. and Price, D. L. (1985) 'Abnormalities of the nucleus basalis in Down's syndrome.', *Annals of Neurology*, 18(3), pp. 310–3. doi: 10.1002/ana.410180306.
- Casas, C., Sergeant, N., Itier, J.-M., Blanchard, V., Wirths, O., van der Kolk, N., Vingtdoux, V., van de Steeg, E., Ret, G., Canton, T., Drobecq, H., Clark, A., Bonici, B., Delacourte, A., Benavides, J., Schmitz, C., Tremp, G., Bayer, T. A., Benoit, P. and Pradier, L. (2004) 'Massive CA1/2 neuronal loss with intraneuronal and N-terminal truncated Abeta42 accumulation in a novel Alzheimer transgenic model.', *The American Journal of Pathology*, 165(4), pp. 1289–300.
- Catterall, W. A. and Few, A. P. (2008) 'Calcium Channel Regulation and Presynaptic Plasticity', *Neuron*, pp. 882–901. doi: 10.1016/j.neuron.2008.09.005.
- Chakrabarti, L., Best, T. K., Cramer, N. P., Carney, R. S. E., Isaac, J. T. R., Galdzicki, Z. and Haydar, T. F. (2010) 'Olig1 and Olig2 triplication causes developmental brain defects in Down syndrome.', *Nature Neuroscience*, 13(8), pp. 927–934. doi: 10.1038/nn.2600.
- Chang, B. S. (2013) 'Cortical hyperexcitability: A new biomarker in generalized epilepsy syndromes', *Epilepsy Currents*, 13(6), pp. 287–288. doi: 10.5698/1535-7597-13.6.287.
- Chang, E. H., Savage, M. J., Flood, D. G., Thomas, J. M., Levy, R. B., Mahadomrongkul, V., Shirao, T., Aoki, C. and Huerta, P. T. (2006) 'AMPA receptor downscaling at the onset of Alzheimer's disease pathology in double knockin mice.', *Proceedings of the National Academy of Sciences of the United States of America*, 103(9), pp. 3410–5. doi: 10.1073/pnas.0507313103.
- Chapman, P. F., White, G. L., Jones, M. W., Cooper-Blacketer, D., Marshall, V. J., Irizarry, M., Younkin, L., Good, M. A., Bliss, T. V., Hyman, B. T., Younkin, S. G. and Hsiao, K. K. (1999) 'Impaired synaptic plasticity and learning in aged amyloid precursor protein transgenic mice.', *Nature Neuroscience*, 2(3), pp. 271–6. doi: 10.1038/6374.
- Chen, C., Jiang, P., Xue, H., Peterson, S. E., Tran, H. T., McCann, A. E., Parast, M. M., Li, S., Pleasure, D. E., Laurent, L. C., Loring, J. F., Liu, Y. and Deng, W. (2014) 'Role of astroglia in Down's syndrome revealed by patient-derived human-induced pluripotent stem cells.', *Nature Communications*, 5, p. 4430. doi: 10.1038/ncomms5430.
- Cho, D.-H. H., Nakamura, T., Fang, J., Cieplak, P., Godzik, A., Gu, Z. and Lipton, S. A. (2009) 'S-nitrosylation of Drp1 mediates beta-amyloid-related mitochondrial fission and neuronal injury.', *Science*, 324(5923), pp. 102–105. doi: 10.1126/science.1171091.
- Chrast, R., Scott, H. S., Madani, R., Huber, L., Wolfer, D. P., Prinz, M., Aguzzi, A., Lipp, H. P. and Antonarakis, S. E. (2000) 'Mice trisomic for a bacterial artificial chromosome with the single-minded 2 gene (Sim2) show phenotypes similar to some of those present in the partial trisomy 16 mouse models of Down syndrome.', *Human Molecular Genetics*, 9(12), pp. 1853–64. doi: 10.1093/HMG/9.12.1853.

Colino, A. and Malenka, R. C. (1993) 'Mechanisms underlying induction of long-term potentiation in rat medial and lateral perforant paths in vitro.', *Journal of Neurophysiology*, 69(4), pp. 1150–1159.

Collingridge, G. L., Peineau, S., Howland, J. G. and Wang, Y. T. (2010) 'Long-term depression in the CNS.', *Nature Reviews Neuroscience*, 11(7), pp. 459–473. doi: 10.1038/nrn2867.

Contestabile, A., Fila, T., Ceccarelli, C., Bonasoni, P., Bonapace, L., Santini, D., Bartesaghi, R. and Ciani, E. (2007) 'Cell cycle alteration and decreased cell proliferation in the hippocampal dentate gyrus and in the neocortical germinal matrix of fetuses with down syndrome and in Ts65Dn mice', *Hippocampus*, 17(8), pp. 665–678. doi: 10.1002/hipo.20308.

Contractor, A., Swanson, G. and Heinemann, S. F. (2001) 'Kainate Receptors Are Involved in Short- and Long-Term Plasticity at Mossy Fiber Synapses in the Hippocampus', *Neuron*, 29(1), pp. 209–216. doi: 10.1016/S0896-6273(01)00191-X.

Contzen, R. and Witte, O. W. (1994) 'Epileptic activity can induce both long-lasting potentiation and long-lasting depression', *Brain Research*, 653(1–2), pp. 340–344. doi: 10.1016/0006-8993(94)90410-3.

Cooke, S. F., Wu, J., Plattner, F., Errington, M., Rowan, M., Peters, M., Hirano, A., Bradshaw, K. D., Anwyl, R., Bliss, T. V. P. and Giese, K. P. (2006) 'Autophosphorylation of alphaCaMKII is not a general requirement for NMDA receptor-dependent LTP in the adult mouse.', *The Journal of Physiology*, 574(Pt 3), pp. 805–18. doi: 10.1113/jphysiol.2006.111559.

Cooper, A., Grigoryan, G., Guy-David, L., Tsoory, M. M., Chen, A. and Reuveny, E. (2012) 'Trisomy of the G protein-coupled K⁺ channel gene, *Kcnj6*, affects reward mechanisms, cognitive functions, and synaptic plasticity in mice.', *Proceedings of the National Academy of Sciences of the United States of America*, 109(7), pp. 2642–7. doi: 10.1073/pnas.1109099109.

Cortez, M. a, Shen, L., Wu, Y., Aleem, I. S., Trepanier, C. H., Sadeghnia, H. R., Ashraf, A., Kanawaty, A., Liu, C.-C., Stewart, L. and Snead, O. C. (2009) 'Infantile spasms and Down syndrome: a new animal model.', *Pediatric research*, 65(5), pp. 499–503. doi: 10.1203/PDR.0b013e31819d9076.

Cossart, R., Esclapez, M., Hirsch, J. C., Bernard, C. and Ben-Ari, Y. (1998) 'GluR5 kainate receptor activation in interneurons increases tonic inhibition of pyramidal cells', *Nature Neuroscience*, 1(6), pp. 470–478. doi: 10.1038/2185.

Cossec, J. C., Lavaur, J., Berman, D. E., Rivals, I., Hoischen, A., Stora, S., Ripoll, C., Mircher, C., Grattau, Y., Olivomarin, J. C., De chaumont, F., Lecourtois, M., Antonarakis, S. E., Veltman, J. A., Delabar, J. M., Duyckaerts, C., Di paolo, G. and Potier, M. C. (2012) 'Trisomy for synaptotagmin1 in down syndrome is functionally linked to the

enlargement of early endosomes', *Human Molecular Genetics*. Oxford University Press, 21(14), pp. 3156–3172. doi: 10.1093/hmg/dds142.

Costa, A. C. S. and Grybko, M. J. (2005) 'Deficits in hippocampal CA1 LTP induced by TBS but not HFS in the Ts65Dn mouse: A model of Down syndrome', *Neuroscience Letters*, 382(3), pp. 317–322. doi: 10.1016/j.neulet.2005.03.031.

Cramer, N. P., Best, T. K., Stoffel, M., Siarey, R. J. and Galdzicki, Z. (2010) 'GABAB-GIRK2-Mediated Signaling in Down Syndrome', *Advances in Pharmacology*, 58, pp. 397–426. doi: 10.1016/S1054-3589(10)58015-3.

Dang, V., Medina, B., Das, D., Moghadam, S., Martin, K. J., Lin, B., Naik, P., Patel, D., Nosheny, R., Wesson Ashford, J. and Salehi, A. (2014) 'Formoterol, a long-acting β 2 adrenergic agonist, improves cognitive function and promotes dendritic complexity in a mouse model of Down syndrome.', *Biological Psychiatry*, 75(3), pp. 179–88. doi: 10.1016/j.biopsych.2013.05.024.

Davisson, M. T., Schmidt, C., Reeves, R. H., Irving, N. G., Akeson, E. C., Harris, B. S. and Bronson, R. T. (1993) 'Segmental trisomy as a mouse model for Down syndrome.', *Progress in clinical and biological research*, 384, pp. 117–33. Available at: <http://www.ncbi.nlm.nih.gov/pubmed/8115398> (Accessed: 13 September 2016).

Deidda, G., Parrini, M., Naskar, S., Bozarth, I. F., Contestabile, A. and Cancedda, L. (2015) 'Reversing excitatory GABAAR signaling restores synaptic plasticity and memory in a mouse model of Down syndrome.', *Nature medicine*, 21(4), pp. 318–26. doi: 10.1038/nm.3827.

Dekker, A. D., De Deyn, P. P. and Rots, M. G. (2014) 'Epigenetics: The neglected key to minimize learning and memory deficits in Down syndrome', *Neuroscience and Biobehavioral Reviews*, 45, pp. 72–84. doi: 10.1016/j.neubiorev.2014.05.004.

Deshpande, A., Mina, E., Glabe, C. and Busciglio, J. (2006) 'Different Conformations of Amyloid β Induce Neurotoxicity by Distinct Mechanisms in Human Cortical Neurons', *The Journal of Neuroscience*, 26(22), pp. 6011–6018. doi: 10.1523/JNEUROSCI.1189-06.2006.

Dierssen, M. (2012) 'Down syndrome: the brain in trisomic mode.', *Nature reviews. Neuroscience*. Nature Publishing Group, 13(12), pp. 844–58. doi: 10.1038/nrn3314.

Dierssen, M., Herault, Y. and Estivill, X. (2009) 'Aneuploidy: From a Physiological Mechanism of Variance to Down Syndrome', *Physiological Reviews*, 89(3), pp. 887–920. doi: 10.1152/physrev.00032.2007.

Do, L. H., Mobley, W. C. and Singhal, N. (2015) 'Questioned validity of Gene Expression Dysregulated Domains in Down's Syndrome', *F1000Research*, 269, pp. 2–9. doi: 10.12688/f1000research.6735.1.

Dorval, V., Mazzella, M. J., Mathews, P. M., Hay, R. T. and Fraser, P. E. (2007) 'Modulation of A β generation by small ubiquitin-like modifiers does not require

- conjugation to target proteins.', *The Biochemical Journal*, 404(2), pp. 309–16. doi: 10.1042/BJ20061451.
- Douglas, R. M., Goddard, G. V. and Riives, M. (1982) 'Inhibitory modulation of long-term potentiation: Evidence for a postsynaptic locus of control', *Brain Research*, 240(2), pp. 259–272. doi: 10.1016/0006-8993(82)90221-9.
- Down, J. L. (1866) 'Observations on an ethnic classification of idiots.', *Mental Retardation*, 33(1), pp. 54–56. doi: 10.1192/bjp.13.61.121.
- Du, H., Guo, L., Yan, S. S. S., Sosunov, A. A., McKhann, G. M. and Yan, S. S. S. (2010) 'Early deficits in synaptic mitochondria in an Alzheimer's disease mouse model.', *Proceedings of the National Academy of Sciences of the United States of America*, 107(43), pp. 18670–18675. doi: 10.1073/pnas.1006586107.
- Duchon, A., Raveau, M., Chevalier, C., Nalesso, V., Sharp, A. J. and Hérault, Y. (2011) 'Identification of the translocation breakpoints in the Ts65Dn and Ts1Cje mouse lines: Relevance for modeling down syndrome', *Mammalian Genome*, 22(11–12), pp. 674–684. doi: 10.1007/s00335-011-9356-0.
- Dudek, S. M. and Bear, M. F. (1992) 'Homosynaptic long-term depression in area CA1 of hippocampus and effects of N-methyl-D-aspartate receptor blockade.', *Proceedings of the National Academy of Sciences of the United States of America*, 89(10), pp. 4363–7. doi: 10.1073/pnas.89.10.4363.
- Dudek, S. M. and Bear, M. F. (1993) 'Bidirectional long-term modification of synaptic effectiveness in the adult and immature hippocampus.', *The Journal of Neuroscience*, 13(7), pp. 2910–8.
- Edgin, J. O., Pennington, B. F. and Mervis, C. B. (2010) 'Neuropsychological components of intellectual disability: The contributions of immediate, working, and associative memory', *Journal of Intellectual Disability Research*, 54(5), pp. 406–417. doi: 10.1111/j.1365-2788.2010.01278.x.
- Ema, M., Ikegami, S., Hosoya, T., Mimura, J., Ohtani, H., Nakao, K., Inokuchi, K., Katsuki, M. and Fujii-Kuriyama, Y. (1999) 'Mild impairment of learning and memory in mice overexpressing the mSim2 gene located on chromosome 16: an animal model of Down's syndrome.', *Human Molecular Genetics*, 8(8), pp. 1409–15. doi: 10.1093/HMG/8.8.1409.
- Escorihuela, R. M., Vallina, I. F., Martínez-Cué, C., Baamonde, C., Dierssen, M., Tobeña, A., Flórez, J. and Fernández-Teruel, A. (1998) 'Impaired short- and long-term memory in Ts65Dn mice, a model for Down syndrome.', *Neuroscience Letters*, 247(2–3), pp. 171–174. doi: 10.1016/S0304-3940(98)00317-6.
- Esteban, J. a, Shi, S.-H., Wilson, C., Nuriya, M., Huganir, R. L. and Malinow, R. (2003) 'PKA phosphorylation of AMPA receptor subunits controls synaptic trafficking underlying plasticity.', *Nature Neuroscience*, 6(2), pp. 136–143. doi: 10.1038/nn997.

Faizi, M., Bader, P. L., Tun, C., Encarnacion, A., Kleschevnikov, A., Belichenko, P., Saw, N., Priestley, M., Tsien, R. W., Mobley, W. C. and Shamloo, M. (2011) 'Comprehensive behavioral phenotyping of Ts65Dn mouse model of Down Syndrome: Activation of β 1-adrenergic receptor by xamoterol as a potential cognitive enhancer', *Neurobiology of Disease*, 43(2), pp. 397–413. doi: 10.1016/j.nbd.2011.04.011.

Fanselow, M. S. and Poulos, A. M. (2005) 'The neuroscience of mammalian associative learning.', *Annual Review of Psychology*, 56(1), pp. 207–34. doi: 10.1146/annurev.psych.56.091103.070213.

Farrer, L. A., Cupples, L. A., Haines, J. L., Hyman, B., Kukull, W. A., Mayeux, R., Myers, R. H., Pericak-Vance, M. A., Risch, N. and van Duijn, C. M. (1997) 'Effects of age, sex, and ethnicity on the association between apolipoprotein E genotype and Alzheimer disease. A meta-analysis. APOE and Alzheimer Disease Meta Analysis Consortium.', *JAMA*, 278(16), pp. 1349–56. doi: 10.1001/jama.1997.03550160069041.

De Felice, F. G., Vieira, M. N. N., Bomfim, T. R., Decker, H., Velasco, P. T., Lambert, M. P., Viola, K. L., Zhao, W.-Q., Ferreira, S. T. and Klein, W. L. (2009) 'Protection of synapses against Alzheimer's-linked toxins: Insulin signaling prevents the pathogenic binding of A β oligomers', *Proceedings of the National Academy of Sciences*, 106(6), pp. 1971–1976. doi: 10.1073/pnas.0809158106.

Ferbinteanu, J., Holsinger, R. M. D. and McDonald, R. J. (1999) 'Lesions of the medial or lateral perforant path have different effects on hippocampal contributions to place learning and on fear conditioning to context', *Behavioural Brain Research*, 101(1), pp. 65–84. doi: 10.1016/S0166-4328(98)00144-2.

Fernandez, F. and Garner, C. C. (2007) 'Object recognition memory is conserved in Ts1Cje, a mouse model of Down syndrome', *Neuroscience Letters*, 421(2), pp. 137–141. doi: 10.1016/j.neulet.2007.04.075.

Filley, C. M., Kelly, J. and Heaton, R. K. (1986) 'Neuropsychologic features of early- and late-onset Alzheimer's disease', *Archives of Neurology*, 43(0003–9942), pp. 574–576

Fisher, R. S., van Emde Boas, W., Blume, W., Elger, C., Genton, P., Lee, P. and Engel, J. (2005) 'Epileptic seizures and epilepsy: definitions proposed by the International League Against Epilepsy (ILAE) and the International Bureau for Epilepsy (IBE).', *Epilepsia*, 46(4), pp. 470–2. doi: 10.1111/j.0013-9580.2005.66104.x.

Fitzjohn, S. M., Morton, R. A., Kuenzi, F., Rosahl, T. W., Shearman, M., Lewis, H., Smith, D., Reynolds, D. S., Davies, C. H., Collingridge, G. L. and Seabrook, G. R. (2001) 'Age-related impairment of synaptic transmission but normal long-term potentiation in transgenic mice that overexpress the human APP695SWE mutant form of amyloid precursor protein.', *The Journal of Neuroscience*, 21(13), pp. 4691–8.

Fotaki, V., Dierssen, M., Alcántara, S., Martínez, S., Martí, E., Casas, C., Visa, J., Soriano, E., Estivill, X. and Arbonés, M. L. (2002) 'Dyrk1A haploinsufficiency affects viability

and causes developmental delay and abnormal brain morphology in mice.’, *Molecular and Cellular Biology*, 22(18), pp. 6636–47. doi: 10.1128/MCB.22.18.6636.

Franceschetti, S., Sancini, G., Buzzi, A., Zucchini, S., Paradiso, B., Magnaghi, G., Frassoni, C., Chikhladze, M., Avanzini, G. and Simonato, M. (2007) ‘A pathogenetic hypothesis of Unverricht–Lundborg disease onset and progression’, *Neurobiology of Disease*, 25(3), pp. 675–685. doi: 10.1016/j.nbd.2006.11.006.

Fratiglioni, L., De Ronchi, D. and Agüero-Torres, H. (1999) ‘Worldwide prevalence and incidence of dementia’, *Drugs and Aging*, pp. 365–375. doi: 10.2165/00002512-199915050-00004.

Frey, U., Huang, Y. and Kandel, E. (1993) ‘Effects of cAMP simulate a late stage of LTP in hippocampal CA1 neurons’, *Science*, 260(5114), pp. 1661–1664. doi: 10.1126/science.8389057.

Fyhn, M., Molden, S., Witter, M. P., Moser, E. I. and Moser, M.-B. (2004) ‘Spatial representation in the entorhinal cortex.’, *Science*, 305(5688), pp. 1258–64. doi: 10.1126/science.1099901.

García-Cerro, S., Martínez, P., Vidal, V., Corrales, A., Flórez, J., Vidal, R., Rueda, N., Arbonés, M. L. and Martínez-Cué, C. (2014) ‘Overexpression of Dyrk1A is implicated in several cognitive, electrophysiological and neuromorphological alterations found in a mouse model of down syndrome’, *PLoS One*, 9(9). doi: 10.1371/journal.pone.0106572.

Gardiner, K. (2004) ‘Gene-dosage effects in Down syndrome and trisomic mouse models.’, *Genome Biology*, 5(10), p. 244. doi: 10.1186/gb-2004-5-10-244.

Gardiner, K., Fortna, A., Bechtel, L., Davisson, M. T. and Bernardi, G. (2003) ‘Mouse models of Down syndrome: how useful can they be? Comparison of the gene content of human chromosome 21 with orthologous mouse genomic regions’, *Gene*, 318, pp. 137–47. doi: 10.1016/S0378-1119(03)00769-8.

Gelinas, J. N., Khodagholy, D., Thesen, T., Devinsky, O. and Buzsáki, G. (2016) ‘Interictal epileptiform discharges induce hippocampal–cortical coupling in temporal lobe epilepsy’, *Nature Medicine*, 22(6), pp. 641–648. doi: 10.1038/nm.4084.

Gerlai, R., Wojtowicz, J. M., Marks, A. and Roder, J. (1995) ‘Overexpression of a calcium-binding protein, S100 beta, in astrocytes alters synaptic plasticity and impairs spatial learning in transgenic mice.’, *Learning & Memory*, 2(1), pp. 26–39. doi: 10.1101/LM.2.1.26.

Goedert, M. (2005) ‘Tau gene mutations and their effects’, *Movement Disorders*, (SUPPL. 12), pp. S45–S52. doi: 10.1002/mds.20539.

Gómez-Isla, T., Price, J. L., McKeel, D. W., Morris, J. C., Growdon, J. H. and Hyman, B. T. (1996) ‘Profound loss of layer II entorhinal cortex neurons occurs in very mild Alzheimer’s disease.’, *The Journal of Neuroscience*, 16(14), pp. 4491–500.

Grau, C., Arató, K., Fernández-Fernández, J. M., Valderrama, A., Sindreu, C., Fillat, C., Ferrer, I., de la Luna, S. and Altafaj, X. (2014) 'DYRK1A-mediated phosphorylation of GluN2A at Ser(1048) regulates the surface expression and channel activity of GluN1/GluN2A receptors.', *Frontiers in Cellular Neuroscience*, 8, p. 331. doi: 10.3389/fncel.2014.00331.

Gribble, S. M., Wiseman, F. K., Clayton, S., Prigmore, E., Langley, E., Yang, F., Maguire, S., Fu, B., Rajan, D., Sheppard, O., Scott, C., Hauser, H., Stephens, P. J. P., Stebbings, L. A., Ng, B. L. B. L., Fitzgerald, T., Quail, M. A. M., Banerjee, R., Rothkamm, K., Tybulewicz, V. V. L. J., Fisher, E. M. C. E. E. M. C., Carter, N. N. P., Sherman, S., Allen, E., Bean, L., Freeman, S., Wiseman, F. F. K., Alford, K., Tybulewicz, V. V. L. J., Fisher, E. M. C. E. E. M. C., O'Doherty, A., Ruf, S., Mulligan, C., Hildreth, V., Errington, M., Rasheed, S., Nelson-Rees, W., Toth, E., Arnstein, P., Gardner, M., Morice, E., Andreae, L., Cooke, S., Vanes, L., Fisher, E. M. C. E. E. M. C., Galante, M., Jani, H., Vanes, L., Daniel, H., Fisher, E. M. C. E. E. M. C., Alford, K., Slender, A., Vanes, L., Li, Z., Fisher, E. M. C. E. E. M. C., Dunlevy, L., Bennett, M., Slender, A., Lana-Elola, E., Tybulewicz, V. V. L. J., Reynolds, L., Watson, A., Baker, M., Jones, T., D'Amico, G., Wilson, M., Barbosa-Morais, N., Schmidt, D., Conboy, C., Vanes, L., Wang, Y., Gao, L., Tse, S., Andreadis, A., Claros, M., Vincens, P., Loblrich, M., Rydberg, B., Cooper, P., Rothkamm, K., Kuhne, M., Jeggo, P., Loblrich, M., Povirk, L., Lee, J., Carvalho, C., Lupski, J., Zhang, F., Carvalho, C., Lupski, J., Prandini, P., Deutsch, S., Lyle, R., Gagnebin, M., Vivier, C. D., Yahya-Graison, E. A., Aubert, J., Dauphinot, L., Rivals, I., Prieur, M., Reeves, R., Yao, J., Crowley, M., Buck, S., Zhang, X., Elagib, K., Racke, F., Mogass, M., Khetawat, R., Delehanty, L., Goate, A., Chartier-Harlin, M., Mullan, M., Brown, J., Crawford, F., Chang, K., Min, K., Tybulewicz, V. V. L. J., Fisher, E. M. C. E. E. M. C., Duchon, A., Besson, V., Pereira, P., Magnol, L., Herault, Y., Besson, V., Brault, V., Duchon, A., Togbe, D., Bizot, J., Reinholdt, L., Ding, Y., Gilbert, G., Czechanski, A., Solzak, J., Duchon, A., Raveau, M., Chevalier, C., Nalesso, V., Sharp, A., Li, Z., Yu, T., Morishima, M., Pao, A., LaDuca, J., Yu, T., Li, Z., Jia, Z., Clapcote, S., Liu, C., Fiegler, H., Redon, R., Carter, N. N. P., Rabbitts, P., Impey, H., Heppell-Parton, A., Langford, C., Tease, C., Ng, B. L. B. L., Carter, N. N. P., Ng, B. L. B. L., Yang, F., Carter, N. N. P., Kozarewa, I., Ning, Z., Quail, M. A. M., Sanders, M., Berriman, M., Quail, M. A. M., Kozarewa, I., Smith, F., Scally, A., Stephens, P. J. P., Campbell, P., Stephens, P. J. P., Pleasance, E., O'Meara, S., Li, H., Gardiner, K., Rogers, M., Langbein, L., Praetzel-Wunder, S., Winter, H., Schweizer, J., Weitzner, J., Shibuya, K., Nagamine, K., Okui, M., Ohsawa, Y. and Asakawa, S. (2013) 'Massively parallel sequencing reveals the complex structure of an irradiated human chromosome on a mouse background in the Tc1 model of Down syndrome.', *PloS One*, 8(4), p. e60482. doi: 10.1371/journal.pone.0060482.

van Groen, T., Miettinen, P. and Kadish, I. (2003) 'The entorhinal cortex of the mouse: Organization of the projection to the hippocampal formation', *Hippocampus*, pp. 133–149. doi: 10.1002/hipo.10037.

Grover, L. M., Kim, E., Cooke, J. D. and Holmes, W. R. (2009) 'LTP in hippocampal area CA1 is induced by burst stimulation over a broad frequency range centered around delta.', *Learning & Memory*, 16(1), pp. 69–81. doi: 10.1101/lm.1179109.

Grover, L. M. and Yan, C. (1999) 'Blockade of GABAA receptors facilitates induction of NMDA receptor-independent long-term potentiation', *Journal of Neurophysiology*, 81(6), pp. 2814–2822

Gu, Z., Liu, W. and Yan, Z. (2009) ' β -amyloid impairs AMPA receptor trafficking and function by reducing Ca²⁺/calmodulin-dependent protein kinase II synaptic distribution', *Journal of Biological Chemistry*, 284(16), pp. 10639–10649. doi: 10.1074/jbc.M806508200.

Guerreiro, R., Brás, J., Wojtas, A., Rademakers, R., Hardy, J. and Graff-Radford, N. (2014) 'A nonsense mutation in PRNP associated with clinical Alzheimer's disease', *Neurobiology of Aging*, 35(11), p. 2656.e13-e16. doi: 10.1016/j.neurobiolaging.2014.05.013.

Guidi, S., Bonasoni, P., Ceccarelli, C., Santini, D., Gualtieri, F., Ciani, E. and Bartesaghi, R. (2008) 'Neurogenesis impairment and increased cell death reduce total neuron number in the hippocampal region of fetuses with Down syndrome', *Brain Pathology*, 18(2), pp. 180–197. doi: 10.1111/j.1750-3639.2007.00113.x.

Gustafsson B and Wigström H. (1985) 'Facilitation of hippocampal long-lasting potentiation by GABA antagonists', *Acta Physiologica Scandinavica*, 125(1), pp. 159–172. doi: 10.1111/j.1748-1716.1985.tb07703.x.

Haas, M. A., Bell, D., Slender, A., Lana-Elola, E., Watson-Scales, S., Fisher, E. M. C., Tybulewicz, V. L. J. and Guillemot, F. (2013) 'Alterations to dendritic spine morphology, but not dendrite patterning, of cortical projection neurons in Tc1 and Ts1Rhr mouse models of Down syndrome.', *PloS One*, 8(10), p. e78561. doi: 10.1371/journal.pone.0078561.

Haass, C., Hung, A. Y., Selkoe, D. J. and Teplow, D. B. (1994) 'Mutations associated with a locus for familial Alzheimer's disease result in alternative processing of amyloid beta-protein precursor', *Journal of Biological Chemistry*, 269(26), pp. 17741–17748

Haass, C., Kaether, C., Thinakaran, G. and Sisodia, S. (2012) 'Trafficking and proteolytic processing of APP', *Cold Spring Harbor Perspectives in Medicine*, 2(5), p. a006270. doi: 10.1101/cshperspect.a006270.

Haass, C., Lemere, C. A., Capell, A., Citron, M., Seubert, P., Schenk, D., Lannfelt, L. and Selkoe, D. J. (1995) 'The Swedish mutation causes early-onset Alzheimer's disease by beta-secretase cleavage within the secretory pathway.', *Nature Medicine*, 1(12), pp. 1291–6.

Habets, R. L. P. and Borst, J. G. G. (2007) 'Dynamics of the readily releasable pool during post-tetanic potentiation in the rat calyx of Held synapse.', *The Journal of Physiology*, 581(Pt 2), pp. 467–78. doi: 10.1113/jphysiol.2006.127365.

Hall, A. M., Roberson, E. D., (2012) 'Mouse Models of Alzheimer's Disease', *Brain Research Bulletin*, 88(1) pp. 3–12. doi: 10.1016/j.brainresbull.2011.11.017.Mouse.

- Hall, J. H., Wiseman, F. K., Fisher, E. M. C., Tybulewicz, V. L. J., Harwood, J. L. and Good, M. A. (2016) 'Tc1 mouse model of trisomy-21 dissociates properties of short- and long-term recognition memory Europe PMC Funders Group', *Neurobiology of Learning and Memory*, 130, pp. 118–128. doi: 10.1016/j.nlm.2016.02.002.
- Hamilton, A., Zamponi, G. W. and Ferguson, S. S. G. (2015) 'Glutamate receptors function as scaffolds for the regulation of β -amyloid and cellular prion protein signaling complexes.', *Molecular brain*, 8(1), p. 18. doi: 10.1186/s13041-015-0107-0.
- Hardy, J. A. and Higgins, G. A. (1992) 'Alzheimer's disease: the amyloid cascade hypothesis.', *Science*, 256(5054), pp. 184–5. doi: 10.1126/science.1566067.
- Hardy, J. and Selkoe, D. J. (2002) 'The amyloid hypothesis of Alzheimer's disease: progress and problems on the road to therapeutics.', *Science*, 297(5580), pp. 353–356. doi: 10.1126/science.1072994.
- Harris, J., Devidze, N., Verret, L. and Ho, K. (2010) 'Transsynaptic progression of amyloid- β -induced neuronal dysfunction within the entorhinal-hippocampal network', *Neuron*, 68(3), pp. 428–441. doi: 10.1016/j.neuron.2010.10.020.
- Heise, I., Fisher, S.P., Banks, G.T., Wells, S., Peirson, S.N., Foster, R.G., Nolan, P.M., 2015. Sleep-like behavior and 24-h rhythm disruption in the Tc1 mouse model of Down syndrome. *Genes Brain and Behaviour*. 14 (2), pp. 209–16. doi: 10.1111/gbb.12198
- Henneberger, C., Papouin, T., Oliek, S. H. R. and Rusakov, D. A. (2010) 'Long-term potentiation depends on release of D-serine from astrocytes.', *Nature*, 463(Jan), pp. 232–236. doi: 10.1038/nature08673.
- Herrera, F., Chen, Q., Fischer, W. H., Maher, P. and Schubert, D. R. (2009) 'Synaptotagmin-1 plays a key role in astrogliogenesis: possible relevance for Down's syndrome.', *Cell Death and Differentiation*, 16(6), pp. 910–20. doi: 10.1038/cdd.2009.24.
- Hesse, G. W. and Teyler, T. J. (1976) 'Reversible loss of hippocampal long term potentiation following electroconvulsive seizures.', *Nature*, 264(5586), pp. 562–4. doi: 10.1038/264562a0.
- Heynen, A. J. and Bear, M. F. (2001) 'Long-term potentiation of thalamocortical transmission in the adult visual cortex in vivo.', *The Journal of Neuroscience*, 21(24), pp. 9801–13. doi: 10.1523/JNEUROSCI.2124-01.2001
- Hibaoui, Y., Grad, I., Letourneau, A., Sailani, M. R., Dahoun, S., Santoni, F. a, Gimelli, S., Guipponi, M., Pelte, M. F., Béna, F., Antonarakis, S. E. and Feki, A. (2014) 'Modelling and rescuing neurodevelopmental defect of Down syndrome using induced pluripotent stem cells from monozygotic twins discordant for trisomy 21.', *EMBO molecular medicine*, 6(2), pp. 259–77. doi: 10.1002/emmm.201302848.
- van Hoesen, G. W., Hyman, B. T. and Damasio, A. R. (1991) 'Entorhinal cortex pathology in Alzheimer's disease', *Hippocampus*, 1(1), pp. 1–8. doi: 10.1002/hipo.450010102.

Holland, A. J., Hon, J., Huppert, F. A. and Stevens, F. (2000) 'Incidence and course of dementia in people with Down's syndrome: Findings from a population-based study', *Journal of Intellectual Disability Research*, 44(2), pp. 138–146. doi: 10.1046/j.1365-2788.2000.00263.x.

Holth, J. K., Bomben, V. C., Reed, J. G., Inoue, T., Younkin, L., Younkin, S. G., Pautler, R. G., Botas, J. and Noebels, J. L. (2013) 'Tau loss attenuates neuronal network hyperexcitability in mouse and *Drosophila* genetic models of epilepsy.', *The Journal of Neuroscience*, 33(4), pp. 1651–9. doi: 10.1523/JNEUROSCI.3191-12.2013.

Hong, S., Beja-Glasser, V. F., Nfonoyim, B. M., Frouin, A., Li, S., Ramakrishnan, S., Merry, K. M., Shi, Q., Rosenthal, A., Barres, B. A., Lemere, C. A., Selkoe, D. J. and Stevens, B. (2016) 'Complement and microglia mediate early synapse loss in Alzheimer mouse models.', *Science*, 352(6286), pp. 712–6. doi: 10.1126/science.aad8373.

Hooli, B. V., Mohapatra, G., Mattheisen, M., Parrado, A. R., Roehr, J. T., Shen, Y., Gusella, J. F., Moir, R., Saunders, A. J., Lange, C., Tanzi, R. E. and Bertram, L. (2012) 'Role of common and rare APP DNA sequence variants in Alzheimer disease', *Neurology*, 78(16), pp. 1250–1257. doi: 10.1212/WNL.0b013e3182515972.

Hu, B., Karnup, S., Zhou, L. and Stelzer, A. (2005) 'Reversal of hippocampal LTP by spontaneous seizure-like activity: role of group I mGluR and cell depolarization.', *Journal of Neurophysiology*, 93(1), pp. 316–36. doi: 10.1152/jn.00172.2004.

Huang, L-Q., Rowan, M.J., Anwyl, R., (1999) 'Role of protein kinases A and C in the induction of mGluR-dependent long-term depression in the medial perforant path of the rat dentate gyrus in vitro', *Neuroscience Letters*, 274(2), pp. 71-74. doi:10.1016/S0304-3940(99)00561-3.

Hunter, M. P., Russo, A. and O'Bryan, J. P. (2013) 'Emerging roles for intersectin (ITSN) in regulating signaling and disease pathways.', *International journal of molecular sciences*, 14(4), pp. 7829–52. doi: 10.3390/ijms14047829.

Huster, R. J., Debener, S., Eichele, T. and Herrmann, C. S. (2012) 'Methods for simultaneous EEG-fMRI: an introductory review.', *The Journal of Neuroscience*, 32(18), pp. 6053–60. doi: 10.1523/JNEUROSCI.0447-12.2012.

Hyde, L. A., Frisone, D. F. and Crnic, L. S. (2001) 'Ts65Dn mice, a model for Down syndrome, have deficits in context discrimination learning suggesting impaired hippocampal function', *Behavioural Brain Research*, 118(1), pp. 53–60. doi: 10.1016/S0166-4328(00)00313-2.

Hyman, B. T., Van Hoesen, G. W. and Damasio, A. R. (1987) 'Alzheimer's disease: glutamate depletion in the hippocampal perforant pathway zone', *Annals of neurology*, 22(1), pp. 37–40. doi: 10.1002/ana.410220110.

- Hyman, B. T., Van Hoesen, G. W., Kromer, L. J. and Damasio, A. R. (1986) 'Perforant pathway changes and the memory impairment of Alzheimer's disease.', *Annals of Neurology*, 20(4), pp. 472–81. doi: 10.1002/ana.410200406.
- Iriki, A., Pavlides, C., Keller, A. and Asanuma, H. (1989) 'Long-Term Potentiation in the Motor Cortex', *Science*, 245(4924), pp. 1385–7. doi: 10.1126/science.2551038.
- Ittner, L. M., Ke, Y. D., Delerue, F., Bi, M., Gladbach, A., van Eersel, J., Wölfing, H., Chieng, B. C., Christie, M. J., Napier, I. A., Eckert, A., Staufienbiel, M., Hardeman, E. and Götz, J. (2010) 'Dendritic function of tau mediates amyloid- β toxicity in Alzheimer's disease mouse models', *Cell*, 142(3), pp. 387–397. doi: 10.1016/j.cell.2010.06.036.
- Jack, C. R., Knopman, D. S., Jagust, W. J., Petersen, R. C., Weiner, M. W., Aisen, P. S., Shaw, L. M., Vemuri, P., Wiste, H. J., Weigand, S. J., Lesnick, T. J., Pankratz, V. S., Donohue, M. C., Trojanowski, J. Q. (2013). 'Update on hypothetical model of Alzheimer's disease biomarkers'. *Lancet Neurology*, 12(2), pp. 207–216. doi: 10.1016/S1474-4422(12)70291-0
- Jacob, C. P., Koutsilieri, E., Bartl, J., Neuen-Jacob, E., Arzberger, T., Zander, N., Ravid, R., Roggendorf, W., Riederer, P., Grunblatt, E. and Grünblatt, E. (2007) 'Alterations in expression of glutamatergic transporters and receptors in sporadic Alzheimer's disease', *Journal of Alzheimers Disease*, 11(1), pp. 97–116.
- Jacobsen, J. S., Wu, C.-C., Redwine, J. M., Comery, T. A., Arias, R., Bowlby, M., Martone, R., Morrison, J. H., Pangalos, M. N., Reinhart, P. H. and Bloom, F. E. (2006) 'Early-onset behavioral and synaptic deficits in a mouse model of Alzheimer's disease.', *Proceedings of the National Academy of Sciences of the United States of America*, 103(13), pp. 5161–6. doi: 10.1073/pnas.0600948103.
- Jia, X., Kohn, A., (2011), 'Gamma Rhythms in the Brain', *PLoS Biol* 9(4) : e1001045
- Jin, S., Lee, Y. K., Lim, Y. C., Zheng, Z., Lin, X. M., Ng, D. P. Y., Holbrook, J. D., Law, H. Y., Kwek, K. Y. C., Yeo, G. S. H. and Ding, C. (2013) 'Global DNA Hypermethylation in Down Syndrome Placenta', *PLoS Genetics*, 9(6), p. e1003515. doi: 10.1371/journal.pgen.1003515.
- Jones, M. J., Farré, P., McEwen, L. M., Macisaac, J. L., Watt, K., Neumann, S. M., Emberly, E., Cynader, M. S., Virji-Babul, N. and Kobor, M. S. (2013) 'Distinct DNA methylation patterns of cognitive impairment and trisomy 21 in Down syndrome.', *BMC Medical Genomics*, 6(1), p. 58. doi: 10.1186/1755-8794-6-58.
- De Jonghe, C., Esselens, C., Kumar-Singh, S., Craessaerts, K., Serneels, S., Checler, F., Annaert, W., Van Broeckhoven, C. and De Strooper, B. (2001) 'Pathogenic APP mutations near the gamma-secretase cleavage site differentially affect Abeta secretion and APP C-terminal fragment stability.', *Human Molecular Genetics*, 10(16), pp. 1665–71. doi: 10.1093/hmg/10.16.1665.
- Jonsson, T., Atwal, J. K., Steinberg, S., Snaedal, J., Jonsson, P. V., Bjornsson, S., Stefansson, H., Sulem, P., Gudbjartsson, D., Maloney, J., Hoyte, K., Gustafson, A., Liu, Y., Lu, Y.,

- Bhangale, T., Graham, R. R., Huttenlocher, J., Bjornsdottir, G., Andreassen, O. A., Jönsson, E. G., Palotie, A., Behrens, T. W., Magnusson, O. T., Kong, A., Thorsteinsdottir, U., Watts, R. J. and Stefansson, K. (2012) 'A mutation in APP protects against Alzheimer's disease and age-related cognitive decline.', *Nature*, 488(7409), pp. 96–9. doi: 10.1038/nature11283.
- Jung, J. H., An, K., Kwon, O. Bin, Kim, H. S. and Kim, J.-H. H. (2011) 'Pathway-specific alteration of synaptic plasticity in Tg2576 mice', *Molecules and Cells*, 32(2), pp. 197–201. doi: 10.1007/s10059-011-0077-8.
- Kamenetz, F., Tomita, T., Hsieh, H., Seabrook, G., Borchelt, D., Iwatsubo, T., Sisodia, S. and Malinow, R. (2003) 'APP Processing and Synaptic Function', *Neuron*, 37(6), pp. 925–937. doi: 10.1016/S0896-6273(03)00124-7.
- Karmiloff-Smith, A., Al-Janabi, T., D'Souza, H., Groet, J., Massand, E., Mok, K., Startin, C., Fisher, E., Hardy, J., Nizetic, D., Tybulewicz, V. and Strydom, A. (2016) 'The importance of understanding individual differences in Down syndrome', *F1000Research*, 5, p. 389. doi: 10.12688/f1000research.7506.1.
- Karran, E., Mercken, M. and De Strooper, B. (2011) 'The amyloid cascade hypothesis for Alzheimer's disease: an appraisal for the development of therapeutics.', *Nature Reviews. Drug discovery*, 10(9), pp. 698–712. doi: 10.1038/nrd3505.
- Kasuga, K., Shimohata, T., Nishimura, A., Shiga, A., Mizuguchi, T., Tokunaga, J., Ohno, T., Miyashita, A., Kuwano, R., Matsumoto, N., Onodera, O., Nishizawa, M. and Ikeuchi, T. (2009) 'Identification of independent APP locus duplication in Japanese patients with early-onset Alzheimer disease.', *Journal of Neurology, Neurosurgery, and Psychiatry*, 80(9), pp. 1050–1052. doi: 10.1136/jnnp.2008.161703.
- Kimura, R. and Ohno, M. (2009) 'Impairments in remote memory stabilization precede hippocampal synaptic and cognitive failures in 5XFAD Alzheimer mouse model.', *Neurobiology of Disease*, 33(2), pp. 229–35. doi: 10.1016/j.nbd.2008.10.006.
- Kirson, E. D., Yaari, Y. and Perouansky, M. (1998) 'Presynaptic and postsynaptic actions of halothane at glutamatergic synapses in the mouse hippocampus.', *British Journal of Pharmacology*, 124(8), pp. 1607–1614. doi: 10.1038/sj.bjp.0701996.
- Kitazawa, M., Medeiros, R. and Laferla, F. M. (2012) 'Transgenic mouse models of Alzheimer disease: developing a better model as a tool for therapeutic interventions.', *Current Pharmaceutical Design*, 18(8), pp. 1131–47.
- Klein, B. P. and Mervis, C. B. (1999) 'Contrasting Patterns of Cognitive Abilities of 9- and 10-Year-Olds With Williams Syndrome or Down Syndrome', *Developmental Neuropsychology*, 16(2), pp. 177–196. doi: 10.1207/S15326942DN1602_3.
- Kleschevnikov, A. M., Belichenko, P. V., Gall, J., George, L., Nosheny, R., Maloney, M. T., Salehi, A. and Mobley, W. C. (2012) 'Increased efficiency of the GABAA and GABAB receptor-mediated neurotransmission in the Ts65Dn mouse model of Down

syndrome', *Neurobiology of Disease*, 45(2), pp. 683–691. doi: 10.1016/j.nbd.2011.10.009.

Kleschevnikov, A. M., Belichenko, P. V., Faizi, M., Jacobs, L. F., Htun, K., Shamloo, M. and Mobley, W. C. (2012) 'Deficits in cognition and synaptic plasticity in a mouse model of Down syndrome ameliorated by GABAB receptor antagonists.', *The Journal of Neuroscience*, 32(27), pp. 9217–27. doi: 10.1523/JNEUROSCI.1673-12.2012.

Kleschevnikov, A. M., Belichenko, P. V., Villar, A. J., Epstein, C. J., Malenka, R. C. and Mobley, W. C. (2004) 'Hippocampal long-term potentiation suppressed by increased inhibition in the Ts65Dn mouse, a genetic model of Down syndrome.', *The Journal of Neuroscience*, 24(37), pp. 8153–60. doi: 10.1523/JNEUROSCI.1766-04.2004.

Korenberg, J. R., Chen, X. N., Schipper, R., Sun, Z., Gonsky, R., Gerwehr, S., Carpenter, N., Daumer, C., Dignan, P. and Distèche, C. (1994) 'Down syndrome phenotypes: the consequences of chromosomal imbalance.', *Proceedings of the National Academy of Sciences of the United States of America*, 91(11), pp. 4997–5001. doi: 10.1073/pnas.91.23.11281a.

Korenberg, J. R., Kawashima, H., Pulst, S. M., Ikeuchi, T., Ogasawara, N., Yamamoto, K., Schonberg, S. A., West, R., Allen, L. and Magenis, E. (1990) 'Molecular definition of a region of chromosome 21 that causes features of the Down syndrome phenotype.', *American Journal of Human Genetics*, 47(2), pp. 236–246.

Korogod, N., Lou, X. and Schneggenburger, R. (2007) 'Posttetanic potentiation critically depends on an enhanced Ca(2+) sensitivity of vesicle fusion mediated by presynaptic PKC.', *Proceedings of the National Academy of Sciences of the United States of America*, 104(40), pp. 15923–15928. doi: 10.1073/pnas.0704603104.

Krinsky-McHale, S. J., Devenny, D. A., Gu, H., Jenkins, E. C., Kittler, P., Murty, V. V., Schupf, N., Scotto, L., Tycko, B., Urv, T. K., Ye, L., Zigman, W. B. and Silverman, W. (2008) 'Successful aging in a 70-year-old man with down syndrome: A case study', *Intellectual and Developmental Disabilities*, 46(3), pp. 215–228. doi: 10.1352/2008.46:215-228.

Kudo, W., Lee, H.-P., Zou, W.-Q., Wang, X., Perry, G., Zhu, X., Smith, M. A., Petersen, R. B. and Lee, H. (2012) 'Cellular prion protein is essential for oligomeric amyloid- β -induced neuronal cell death.', *Human Molecular Genetics*, 21(5), pp. 1138–44. doi: 10.1093/hmg/ddr542.

De la Torre, R., De Sola, S., Pons, M., Duchon, A., de Lagran, M. M., Farré, M., Fitó, M., Benejam, B., Langohr, K., Rodriguez, J., Pujadas, M., Bizot, J. C., Cuenca, A., Janel, N., Catuara, S., Covas, M. I., Blehaut, H., Hérault, Y., Delabar, J. M. and Dierssen, M. (2014) 'Epigallocatechin-3-gallate, a DYRK1A inhibitor, rescues cognitive deficits in Down syndrome mouse models and in humans', *Molecular Nutrition and Food Research*, 58(2), pp. 278–288. doi: 10.1002/mnfr.201300325.

- Lana-Elola, E., Watson-Scales, S. D., Fisher, E. M. C. and Tybulewicz, V. L. J. (2011) 'Down syndrome: searching for the genetic culprits.', *Disease models & mechanisms*, 4(5), pp. 586–95. doi: 10.1242/dmm.008078.
- Lana-Elola, E., Watson-Scales, S., Slender, A., Gibbins, D., Martineau, A., Douglas, C., Mohun, T., Fisher, E. M. and Tybulewicz, V. L. (2016) 'Genetic dissection of Down syndrome-associated congenital heart defects using a new mouse mapping panel.', *eLife*, 5(9), pp. 1689–1699. doi: 10.7554/eLife.11614.
- Lanfranchi, S., Cornoldi, C. and Vianello, R. (2004) 'Verbal and visuospatial working memory deficits in children with Down syndrome.', *American Journal of Mental Retardation*, 109(6), pp. 456–466. doi: 10.1352/0895-8017(2004)109<456:VAVWMD>2.0.CO;2.
- Lanfranchi, S., Jerman, O., Dal Pont, E., Alberti, A. and Vianello, R. (2010) 'Executive function in adolescents with Down Syndrome', *Journal of Intellectual Disability Research*, 54(4), pp. 308–319. doi: 10.1111/j.1365-2788.2010.01262.x.
- Larner, A. J. (2013) 'Presenilin-1 mutations in alzheimer's disease: An update on genotype-phenotype relationships', *Journal of Alzheimer's Disease*, pp. 653–659. doi: 10.3233/JAD-130746.
- Laurén, J., Gimbel, D. A., Nygaard, H. B., Gilbert, J. W. and Strittmatter, S. M. (2009) 'Cellular prion protein mediates impairment of synaptic plasticity by amyloid-beta oligomers.', *Nature*, 457(7233), pp. 1128–32. doi: 10.1038/nature07761.
- Lee, A., Westenbroek, R. E., Haeseleer, F., Palczewski, K., Scheuer, T. and Catterall, W. A. (2002) 'Differential modulation of CaV2.1 channels by calmodulin and Ca²⁺-binding protein 1', *Nature Neuroscience*, 5(3), pp. 210–217. doi: 10.1038/nn805.
- Lee, H. K., Barbarosie, M., Kameyama, K., Bear, M. F. and Huganir, R. L. (2000) 'Regulation of distinct AMPA receptor phosphorylation sites during bidirectional synaptic plasticity.', *Nature*, 405(6789), pp. 955–959. doi: 10.1038/35016089.
- Lee, J. S., Kim, M.-H., Ho, W.-K. and Lee, S.-H. (2008) 'Presynaptic release probability and readily releasable pool size are regulated by two independent mechanisms during posttetanic potentiation at the calyx of Held synapse.', *Journal of Neuroscience*, 28(32), pp. 7945–53. doi: 10.1523/JNEUROSCI.2165-08.2008.
- Lesne S. E., Sherman, M. A., Grant, M., Kuskowski, M., Schneider, J. A., Bennett, D. A., Ashe, K. H., (2013) 'Brain amyloid-beta oligomers in ageing and Alzheimer's disease'. *Brain*; 136 (5), pp. 1383–98. doi: 10.1093/brain/awt062
- Lejeune, J., Gauthier, M. and Turpin, R. (1959) 'Human chromosomes in tissue cultures', *C R Hebd Seances Acad Sci*, 248(4), pp. 602–603.
- Letourneau, A., Santoni, F. a, Bonilla, X., Sailani, M. R., Gonzalez, D., Kind, J., Chevalier, C., Thurman, R., Sandstrom, R. S., Hibaoui, Y., Garieri, M., Popadin, K., Falconnet, E., Gagnebin, M., Gehrig, C., Vannier, A., Guipponi, M., Farinelli, L., Robyr, D., Migliavacca,

E., Borel, C., Deutsch, S., Feki, A., Stamatoyannopoulos, J. a, Herault, Y., van Steensel, B., Guigo, R. and Antonarakis, S. E. (2014) 'Domains of genome-wide gene expression dysregulation in Down's syndrome.', *Nature*, 508(7496), pp. 345–50. doi: 10.1038/nature13200.

Lev-Ram, V., Wong, S. T., Storm, D. R. and Tsien, R. Y. (2002) 'A new form of cerebellar long-term potentiation is postsynaptic and depends on nitric oxide but not cAMP', *Proceedings of the National Academy of Sciences*, 99(12), pp. 8389–8393. doi: 10.1073/pnas.122206399.

Leverenz, J. B. and Raskind, M. A. (1998) 'Early amyloid deposition in the medial temporal lobe of young Down syndrome patients: a regional quantitative analysis.', *Experimental Neurology*, 150(2), pp. 296–304. doi: 10.1006/exnr.1997.6777.

Lewis, J., Dickson, D. W., Lin, W. L., Chisholm, L., Corral, A., Jones, G., Yen, S. H., Sahara, N., Skipper, L., Yager, D., Eckman, C., Hardy, J., Hutton, M., McGowan, E., Glenner, G. G., Wong, C. W., Masters, C. L., Wischik, C. M., Hardy, J., Allsop, D., Selkoe, D., Roses, A. D., Goate, A., Sherrington, R., Levy-Lahad, E., Scheuner, D., Borchelt, D. R., Citron, M., Mehta, N. D., Games, D., Hsiao, K., Duff, K., Borchelt, D. R., Holcomb, L., Lewis, J., Hutton, M., Lewis, J., Mullan, M., Lannfelt, L., Jicha, G. A., Bowser, R., Kazam, I. G., Davies, P., Jicha, G. A., Mikol, J., Brion, S., Guicharnaud, L., Waks, O., Callahan, M. J., Jorm, A. F., Korten, A. E., Henderson, A. S., Rocca, W. A., Gravina, S. A., Haugabook, S. J., Greenberg, S. G., Davies, P., Dickson, D. W., Vincent, I., Zheng, J. H., Dickson, D. W., Kress, Y., Davies, P., Hardy, J., Duff, K., Gwinn-Hardy, K., Perez-Tur, J., Hutton, M., Götz, J., Chen, F., Dorpe, J. van and Nitsch, R. M. (2001) 'Enhanced neurofibrillary degeneration in transgenic mice expressing mutant tau and APP.', *Science*, 293(5534), pp. 1487–91. doi: 10.1126/science.1058189.

Li, J.-M., Zeng, Y.-J., Peng, F., Li, L., Yang, T.-H., Hong, Z., Lei, D., Chen, Z. and Zhou, D. (2010) 'Aberrant glutamate receptor 5 expression in temporal lobe epilepsy lesions.', *Brain Research*, 1311, pp. 166–74. doi: 10.1016/j.brainres.2009.11.024.

Li, S., Hong, S., Shepardson, N. E., Walsh, D. M., Shankar, G. M. and Selkoe, D. (2009) 'Soluble Oligomers of Amyloid β Protein Facilitate Hippocampal Long-Term Depression by Disrupting Neuronal Glutamate Uptake', *Neuron*, 62(6), pp. 788–801. doi: 10.1016/j.neuron.2009.05.012.

Lie, A. A., Blümcke, I., Beck, H., Schramm, J., Wiestler, O. D. and Elger, C. E. (1998) 'Altered Patterns of Ca²⁺/Calmodulin-dependent Protein Kinase II and Calcineurin Immunoreactivity in the Hippocampus of Patients with Temporal Lobe Epilepsy', *Journal of Neuropathology & Experimental Neurology*, 57(11), pp. 1078-1088

Lisman, J. (1989) 'A mechanism for the Hebb and the anti-Hebb processes underlying learning and memory.', *Proceedings of the National Academy of Sciences of the United States of America*. *National Academy of Sciences*, 86(23), pp. 9574–8. Liu, W., Zhou, H., Liu, L., Zhao, C., Deng, Y., Chen, L., Wu, L., Mandrycky, N., McNabb, C. T., Peng, Y., Fuchs, P. N., Lu, J., Sheen, V., Qiu, M., Mao, M. and Lu, Q. R. (2015) 'Disruption of neurogenesis and cortical development in transgenic mice misexpressing Olig2, a gene in the Down

syndrome critical region.’, *Neurobiology of Disease*, 77, pp. 106–16. doi: 10.1016/j.nbd.2015.02.021.

Liu, Y. Y., Tan, L., Wang, H.-F. F., Liu, Y. Y., Hao, X.-K. K., Tan, C.-C. C., Jiang, T., Liu, B., Zhang, D.-Q. Q., Yu, J.-T. T. and Alzheimer’s Disease Neuroimaging Initiative (2016) ‘Multiple Effect of APOE Genotype on Clinical and Neuroimaging Biomarkers Across Alzheimer’s Disease Spectrum’, *Molecular Neurobiology*, 53(7), pp. 4539–4547. doi: 10.1007/s12035-015-9388-7.

Llorens-Martín, M. V., Rueda, N., Tejada, G. S., Flórez, J., Trejo, J. L. and Martínez-Cué, C. (2010) ‘Effects of voluntary physical exercise on adult hippocampal neurogenesis and behavior of Ts65Dn mice, a model of Down syndrome’, *Neuroscience*, 171(4), pp. 1228–1240. doi: 10.1016/j.neuroscience.2010.09.043.

Loane, M., Morris, J. K., Addor, M.-C., Arriola, L., Budd, J., Doray, B., Garne, E., Gatt, M., Haeusler, M., Khoshnood, B., Klungsøyr Melve, K., Latos-Bielenska, A., McDonnell, B., Mullaney, C., O’Mahony, M., Queisser-Wahrendorf, A., Rankin, J., Rissmann, A., Rounding, C., Salvador, J., Tucker, D., Wellesley, D., Yevtushok, L. and Dolk, H. (2013) ‘Twenty-year trends in the prevalence of Down syndrome and other trisomies in Europe: impact of maternal age and prenatal screening.’, *European Journal of Human Genetics*, 21(1), pp. 27–33. doi: 10.1038/ejhg.2012.94.

Lopes, C., Chettouh, Z., Delabar, J. M. and Rachidi, M. (2003) ‘The differentially expressed C21orf5 gene in the medial temporal-lobe system could play a role in mental retardation in Down syndrome and transgenic mice.’, *Biochemical and Biophysical Research Communications*, 305(4), pp. 915–24.

Lott, I. T. and Dierssen, M. (2010) ‘Cognitive deficits and associated neurological complications in individuals with Down’s syndrome’, *The Lancet Neurology*, 9(6), pp. 623–633. doi: 10.1016/S1474-4422(10)70112-5.

Lu, J., Esposito, G., Scuderi, C., Steardo, L., Delli-Bovi, L. C., Hecht, J. L., Dickinson, B. C., Chang, C. J., Mori, T. and Sheen, V. (2011) ‘S100B and APP promote a gliocentric shift and impaired neurogenesis in down syndrome neural progenitors’, *PLoS One*, 6(7), p. e22126. doi: 10.1371/journal.pone.0022126.

Lue, L.-F., Kuo, Y.-M., Roher, A. E., Brachova, L., Shen, Y., Sue, L., Beach, T., Kurth, J. H., Rydel, R. E., Rogers, J., Crystal, H., Dickson, D., Fuld, P., Masur, D., Scott, R., Mehler, M., Masdeu, J., Kawas, C., Aronson, M., Wolfson, L., Katzman, R., Terry, R., DeTeresa, R., Brown, T., Davis, P., Fuld, P., Renbing, X., Peck, A., Dickson, D., Crystal, H., Mattiace, L., Masur, D., Blau, A., Davies, P., Yen, S., Aronson, M., Arrigada, P., Marzloff, K., Hyman, B., Lue, L., Brachova, L., Civin, W., Rogers, J., Blessed, G., Tomlinson, B., Roth, M., Dekosky, S., Dickson, D., Ivanushkin, A., Heitner, J., Yen, S., Davies, P., Mirra, S., Hyman, A., McKeel, D., Sumi, S., Crain, B., Brownlee, L., Vogel, F., Hughes, J., Belle, G. van, Berg, L., neuropathologists, participating C., Braak, H., Braak, F., Scheff, S., DeKosky, S., Price, D., Terry, R., Masliah, E., Salmon, D., Butters, N., DeTeresa, R., Hill, R., Hansen, L., Katzman, R., Kuo, Y., Emmerling, M., Bisgaier, C., Essenburg, A., Lampert, H., Roher, A., Gowing, E., Roher, A., Woods, A., Cotter, R., Chaney, M., Little, S., Ball, M., Kuo, Y.,

Emmerling, M., Vigo-Pelfrey, C., Kasunic, T., Kirkpatrick, J., Murdoch, G., Ball, M., Roher, A., Galasko, D., Chang, L., Clark, C., Kaye, J., Knopman, D., Thomas, R., Kholodenko, D., Schenk, D., Lieberburg, I., Miller, B., Green, R., Basherad, R., Kertiles, L., Boss, M., Seubert, P., Wisniewski, H., Bancher, C., Barcikowska, M., Wen, G., Currie, J., Otvos, L., Feiner, L., Lang, E., Szendrei, G., Goedert, M., Lee, V., Su, J., Cummings, B., Cotman, C., Harrington, C., Louwagie, J., Rossau, R., Vanmechelen, E., Perry, R., Perry, E., Xuereb, J., Roth, M., Wischik, C., Hixson, J., Vernier, D., Sparks, D., Scheff, S., Liu, H., Landers, T., Danner, F., Coyne, C., Hunsaker, J., Joachim, C., Selkoe, D., Tagliavini, F., Giaccone, G., Frangione, B., Bugianin, O., Delaere, P., Duyckaerts, C., Masters, C., Beyreuther, K., Piette, F., Hauw, J., Teller, J., Russo, C., DeBusk, L., Angelini, G., Zaccheo, D., Dagna-Bricarelli, F., Scartezzini, P., Bertolini, S., Mann, D., Tabaton, M., Gambetti, P., Lambert, M., Barlow, A., Chromy, B., Edwards, C., Freed, R., Liosatos, M., Morgan, T., Rozovsky, I., Trommer, B., Viola, K., Wals, P., Zhang, C., Finch, C., Krafft, G., Klein, W., Oda, T., Wals, P., Osterburg, H., Johnson, S., Pasinetti, G., Morgan, T., Rozovsky, I., Stine, W., Snyder, S., Hozman, T., Finch, C., Roher, A., Lowenson, J., Clarke, S., Woods, A., Cotter, R., Gowing, E., Ball, M., Ishii, K., Tamaoka, A., Mizusawa, H., Shoji, S., Ohtake, T., Frazer, P., Takahashi, H., Tsuji, S., Gearing, M., Mizutani, T., Yamada, S., Kato, M., George-Hyslop, P. S., Mirra, S., Mori, H., Greenberg, S., Briggs, M., Hyman, B., Kokoris, G., Takis, C., Kanter, D., Kase, C., Pessin, M., Alonzo, N., Hyman, B., Rebeck, G., Greenberg, S., Olichney, J., Hansen, L., Galasko, D., Saitoh, T., Hofstetter, C., Katzman, R. and Thal, L. (1999) 'Soluble Amyloid β Peptide Concentration as a Predictor of Synaptic Change in Alzheimer's Disease', *The American Journal of Pathology*, 155(3), pp. 853–862. doi: 10.1016/S0002-9440(10)65184-X.

Lüscher, C. and Malenka, R. C. (2012) 'NMDA receptor-dependent long-term potentiation and long-term depression (LTP/LTD)', *Cold Spring Harbor Perspectives in Biology*, 4(6), pp. 1–15. doi: 10.1101/cshperspect.a005710.

Luthi, A., Di Paolo, G., Cremona, O., Daniell, L., De Camilli, P. and McCormick, D. A. (2001) 'Synaptojanin 1 contributes to maintaining the stability of GABAergic transmission in primary cultures of cortical neurons.', *The Journal of Neuroscience*, 21(23), pp. 9101–11. doi: 21/23/9101.

Lyle, R., Béna, F., Gagos, S., Gehrig, C., Lopez, G., Schinzel, A., Lespinasse, J., Bottani, A., Dahoun, S., Taine, L., Doco-Fenzy, M., Cornillet-Lefèbvre, P., Pelet, A., Lyonnet, S., Toutain, A., Colleaux, L., Horst, J., Sinet, M., Delabar, J. M., Antonarakis, S. E. and Lyle, R. (2009) 'Genotype–phenotype correlations in Down syndrome identified by array CGH in 30 cases of partial trisomy and partial monosomy chromosome 21', *European Journal of Human Genetics*, 17214(1710), pp. 454–466. doi: 10.1038/ejhg.2008.214.

Lynch, M., Sayin, Ü., Bownds, J., Janumpalli, S. and Sutula, T. (2000) 'Long-term consequences of early postnatal seizures on hippocampal learning and plasticity', *European Journal of Neuroscience*, 12(7), pp. 2252–2264. doi: 10.1046/j.1460-9568.2000.00117.x.

Macek, T. A., Winder, D. G., Gereau, R. W., Ladd, C. O. and Conn, P. J. (1996) 'Differential involvement of group II and group III mGluRs as autoreceptors at lateral and medial perforant path synapses.', *Journal of Neurophysiology*, 76(6), pp. 3798–806.

- Maejima, T., Hashimoto, K., Yoshida, T., Aiba, A. and Kano, M. (2001) 'Presynaptic Inhibition Caused by Retrograde Signal from Metabotropic Glutamate to Cannabinoid Receptors', *Neuron*, 31(3), pp. 463–475. doi: 10.1016/S0896-6273(01)00375-0.
- Malenka, R. C. and Bear, M. F. (2004) 'LTP and LTD: An Embarrassment of Riches', *Neuron*, 44(1), pp. 5–21. doi: 10.1016/j.neuron.2004.09.012.
- Mann, D. M. A., Yates, P. O., Marcyniuk, B. and Ravindara, C. R. (1986) 'The Topography of Plaques and Tangles in Down's Syndrome Patients of Different Ages', *Neuropathology and Applied Neurobiology*, 12(5), pp. 447–457. doi: 10.1111/j.1365-2990.1986.tb00053.x.
- Marin-Padilla, M. (1976) 'Pyramidal cell abnormalities in the motor cortex of a child with Down's syndrome. A Golgi study.', *The Journal of Comparative Neurology*, 167(1), pp. 63–81. doi: 10.1002/cne.901670105.
- Martin, K. R., Corlett, A., Dubach, D., Mustafa, T., Coleman, H. A., Parkington, H. C., Merson, T. D., Bourne, J. A., Porta, S., Arbonés, M. L., Finkelstein, D. I. and Pritchard, M. A. (2012) 'Over-expression of RCAN1 causes down syndrome-like hippocampal deficits that alter learning and memory', *Human Molecular Genetics*, 21(13), pp. 3025–3041. doi: 10.1093/hmg/ddc134.
- Masliyah, E., Alford, M., DeTeresa, R., Mallory, M. and Hansen, L. (1996) 'Deficient glutamate transport is associated with neurodegeneration in Alzheimer's disease.', *Annals of Neurology*, 40(5), pp. 759–66. doi: 10.1002/ana.410400512.
- Massey, C. A., Sowers, L. P., Dlouhy, B. J. and Richerson, G. B. (2014) 'Mechanisms of sudden unexpected death in epilepsy: the pathway to prevention.', *Nature Reviews. Neurology*, 10(5), pp. 271–82. doi: 10.1038/nrneurol.2014.64.
- Mayeux, R. and Stern, Y. (2012) 'Epidemiology of Alzheimer disease', *Cold Spring Harbor Perspectives in Medicine*, 2(8), pp. a006239–a006239. doi: 10.1101/cshperspect.a006239.
- Mccarron, M., Mccallion, P., Reilly, E. and Mulryan, N. (2014) 'A prospective 14-year longitudinal follow-up of dementia in persons with Down syndrome', *Journal of Intellectual Disability Research*, 58(1), pp. 61–70. doi: 10.1111/jir.12074.
- McGeer, P.L., Rogers, J., McGeer, E.G., 'Inflammation, Antiinflammatory Agents, and Alzheimer's Disease: The Last 22 Years', *Journal of Alzheimers Disease*. 4;54(3): pp. 853-857. doi: 10.3233/JAD-160488
- McKhann, G. M., Wenzel, H. J., Robbins, C. A., Sosunov, A. A. and Schwartzkroin, P. A. (2003) 'Mouse strain differences in kainic acid sensitivity, seizure behavior, mortality, and hippocampal pathology', *Neuroscience*, 122(2), pp. 551–561. doi: 10.1016/S0306-4522(03)00562-1.

McNaughton, B. L. L. (1980) 'Evidence for two physiologically distinct perforant pathways to the fascia dentata', *Brain Research*, 199(1), pp. 1–19. doi: 10.1016/0006-8993(80)90226-7.

Menasha, J., Levy, B., Hirschhorn, K. and Kardon, N. B. (2005) 'Incidence and spectrum of chromosome abnormalities in spontaneous abortions: new insights from a 12-year study.', *Genetics in Medicine*, 7(4), pp. 251–263. doi: 10.1097/01.GIM.0000160075.96707.04.

Menéndez, M. (2005) 'Down syndrome, Alzheimer's disease and seizures.', *Brain & Development*, 27(4), pp. 246–52. doi: 10.1016/j.braindev.2004.07.008.

Meng, X., Peng, B., Shi, J., Zheng, Y., Chen, H., Zhang, J., Li, L. and Zhang, C. (2006) 'Effects of overexpression of Sim2 on spatial memory and expression of synapsin I in rat hippocampus', *Cell Biology International*, 30(10), pp. 841–847. doi: 10.1016/j.cellbi.2006.07.003.

Menghini, D., Costanzo, F. and Vicari, S. (2011) 'Relationship between brain and cognitive processes in down syndrome', *Behavior Genetics*, 41(3), pp. 381–393. doi: 10.1007/s10519-011-9448-3.

Meyer, D., Bonhoeffer, T. and Scheuss, V. (2014) 'Balance and stability of synaptic structures during synaptic plasticity.', *Neuron*, 82(2), pp. 430–43. doi: 10.1016/j.neuron.2014.02.031.

Minkeviciene, R., Rheims, S., Dobszay, M. B., Zilberter, M., Hartikainen, J., Fülöp, L., Penke, B., Zilberter, Y., Harkany, T., Pitkänen, A. and Tanila, H. (2009) 'Amyloid beta-induced neuronal hyperexcitability triggers progressive epilepsy.', *The Journal of Neuroscience*, 29(11), pp. 3453–62. doi: 10.1523/JNEUROSCI.5215-08.2009.

Mishizen-Eberz, A. J., Rissman, R. A., Carter, T. L., Ikonovic, M. D., Wolfe, B. B. and Armstrong, D. M. (2004) 'Biochemical and molecular studies of NMDA receptor subunits NR1/2A/2B in hippocampal subregions throughout progression of Alzheimer's disease pathology', *Neurobiology of Disease*, 15(1), pp. 80–92. doi: 10.1016/j.nbd.2003.09.016.

Möller, J. C., Hamer, H. M., Oertel, W. H. and Rosenow, F. (2002) 'Late-onset myoclonic epilepsy in Down's syndrome (LOMEDS)', *Seizure*, 11(SUPPL. A), pp. 303–305. doi: 10.1053/seiz.2001.0648.

Moretti, D. V., Babiloni, C., Binetti, G., Cassetta, E., Dal Forno, G., Ferreris, F., Ferri, R., Lanuzza, B., Miniussi, C., Nobili, F., Rodriguez, G., Salinari, S., Rossini, P. M. (2004). 'Individual analysis of EEG frequency and band power in mild Alzheimer's disease', *Clinical Neurophysiology*, 115(2), pp. 299–308

Mori, T., Koyama, N., Arendash, G. W., Horikoshi-Sakuraba, Y., Tan, J. and Town, T. (2010) 'Overexpression of human S100B exacerbates cerebral amyloidosis and gliosis

in the Tg2576 mouse model of Alzheimer's disease', *GLIA*, 58(3), pp. 300–314. doi: 10.1002/glia.20924.

Morice, E., Andrae, L. C., Cooke, S. F., Vanes, L., Fisher, E. M. C., Tybulewicz, V. L. J. and Bliss, T. V. P. (2008) 'Preservation of long-term memory and synaptic plasticity despite short-term impairments in the Tc1 mouse model of Down syndrome.', *Learning & Memory*, 15(7), pp. 492–500. doi: 10.1101/lm.969608.

Morris, J. K. and Alberman, E. (2009) 'Trends in Down's syndrome live births and antenatal diagnoses in England and Wales from 1989 to 2008: analysis of data from the National Down Syndrome Cytogenetic Register', *British Medical Journal*, 339(3), pp. 3794–3794. doi: 10.1136/bmj.b3794.

Morris, R. G. (1989) 'Synaptic plasticity and learning: selective impairment of learning rats and blockade of long-term potentiation in vivo by the N-methyl-D-aspartate receptor antagonist AP5.', *The Journal of neuroscience : the official journal of the Society for Neuroscience*. Society for Neuroscience, 9(9), pp. 3040–3057.

Moser, M. B. and Moser, E. I. (1998) 'Functional differentiation in the hippocampus', *Hippocampus*, pp. 608–619. doi: 10.1002/(SICI)1098-1063(1998)8:6<608::AID-HIPO3>3.0.CO;2-7.

Moshé, S. L. and Albala, B. J. (1983) 'Maturation changes in postictal refractoriness and seizure susceptibility in developing rats', *Annals of Neurology*, 13(5), pp. 552–557. doi: 10.1002/ana.410130514.

Mucke, L., Masliah, E., Yu, G. Q., Mallory, M., Rockenstein, E. M., Tatsuno, G., Hu, K., Kholodenko, D., Johnson-Wood, K. and McConlogue, L. (2000) 'High-level neuronal expression of abeta 1-42 in wild-type human amyloid protein precursor transgenic mice: synaptotoxicity without plaque formation.', *The Journal of Neuroscience*, 20(11), pp. 4050–8.

Müller, U. C. and Zheng, H. (2012) 'Physiological functions of APP family proteins', *Cold Spring Harbor Perspectives in Medicine*, 2(2), p. a006288. doi: 10.1101/cshperspect.a006288.

Myhrer, T. (1988) 'The role of medial and lateral hippocampal perforant path lesions and object distinctiveness in rats' reaction to novelty', *Physiology and Behavior*, 42(4), pp. 371–377. doi: 10.1016/0031-9384(88)90279-X.

Nabavi, S., Fox, R., Proulx, C. D., Lin, J. Y., Tsien, R. Y. and Malinow, R. (2014) 'Engineering a memory with LTD and LTP.', *Nature*, 511(7509), pp. 348–352. doi: 10.1038/nature13294.

Naie, K., Tsanov, M. and Manahan-Vaughan, D. (2007) 'Group I metabotropic glutamate receptors enable two distinct forms of long-term depression in the rat dentate gyrus in vivo', *European Journal of Neuroscience*, 25(11), pp. 3264–3275. doi: 10.1111/j.1460-9568.2007.05583.x.

Nguyen, P. V, Abel, T., Kandel, E. R. and Bourtschouladze, R. (2000) 'Strain-dependent differences in LTP and hippocampus-dependent memory in inbred mice.', *Learning & Memory*, 7(3), pp. 170–9. doi: 10.1101/lm.7.3.170.

Nguyen, P. V and Kandel, E. R. (1996) 'A macromolecular synthesis-dependent late phase of long-term potentiation requiring cAMP in the medial perforant pathway of rat hippocampal slices.', *The Journal Neuroscience*, 16(10), pp. 3189–98. Nishiyama, H., Knopfel, T., Endo, S. and Itohara, S. (2002) 'Glial protein S100B modulates long-term neuronal synaptic plasticity.', *Proceedings of the National Academy of Sciences of the United States of America*, 99(6), pp. 4037–42. doi: 10.1073/pnas.052020999.

Nisticò, R., Dargan, S., Fitzjohn, S. M., Lodge, D., Jane, D. E., Collingridge, G. L. and Bortolotto, Z. A. (2009) 'GLUK1 receptor antagonists and hippocampal mossy fiber function.', *International Review of Neurobiology*, 85, pp. 13–27. doi: 10.1016/S0074-7742(09)85002-2.

Noebels, J. (2011) 'A perfect storm: Converging paths of epilepsy and Alzheimer's dementia intersect in the hippocampal formation', *Epilepsia*, 52(SUPPL. 1), pp. 39–46. doi: 10.1111/j.1528-1167.2010.02909.x.

Nosheny, R. L., Belichenko, P. V., Busse, B. L., Weissmiller, A. M., Dang, V., Das, D., Fahimi, A., Salehi, A., Smith, S. J. and Mobley, W. C. (2015) 'Increased cortical synaptic activation of TrkB and downstream signaling markers in a mouse model of Down Syndrome', *Neurobiology of Disease*, 77, pp. 173–190. doi: 10.1016/j.nbd.2015.02.022.

O'Doherty, A., Ruf, S., Mulligan, C., Hildreth, V., Errington, M. L., Cooke, S., Sesay, A., Modino, S., Vanes, L., Hernandez, D., Linehan, J. M., Sharpe, P. T., Brandner, S., Bliss, T. V. P., Henderson, D. J., Nizetic, D., Tybulewicz, V. L. J. and Fisher, E. M. C. (2005) 'An aneuploid mouse strain carrying human chromosome 21 with Down syndrome phenotypes.', *Science*, 309(5743), pp. 2033–7. doi: 10.1126/science.1114535.

O'Leary, D. M., Cassidy, E. M. and O'Connor, J. J. (1997) 'Group II and III metabotropic glutamate receptors modulate paired pulse depression in the rat dentate gyrus in vitro', *European Journal of Pharmacology*, 340(1), pp. 35–44. doi: 10.1016/S0014-2999(97)01405-2.

Oakley, H., Cole, S. L., Logan, S., Maus, E., Shao, P., Craft, J., Guillozet-Bongaarts, A., Ohno, M., Disterhoft, J., Van Eldik, L., Berry, R. and Vassar, R. (2006) 'Intraneuronal beta-amyloid aggregates, neurodegeneration, and neuron loss in transgenic mice with five familial Alzheimer's disease mutations: potential factors in amyloid plaque formation.', *The Journal of Neuroscience*, 26(40), pp. 10129–40. doi: 10.1523/JNEUROSCI.1202-06.2006.

Oddo, S., Caccamo, A., Shepherd, J. D., Murphy, M. P., Golde, T. E., Kaye, R., Metherate, R., Mattson, M. P., Akbari, Y., LaFerla, F. M., Bliss, T. P., Collingridge, G. L., Caroni, P., Chapman, P. F., White, G. L., Jones, M. W., Cooper-Blacketer, D., Marshall, V. J., Irazarry, M., Younkin, L., Good, M. W., Bliss, T. P., Hyman, B. T., et al., Chui, D., Tanahashi, H., Ozawa, K.,

Ikeda, S., Checler, F., Ueda, O., Suzuki, H., Araki, W., Inoue, H., Shirotani, K., al., et, DeKosky, S., Scheff, S., Dickson, D., Crystal, H., Bevona, C., Honer, W., Vincent, I., Davies, P., Fitzjohn, S., Morton, R., Kuenzi, F., Rosahl, T., Shearman, M., Lewis, H., Smith, D., Reynolds, D., Davies, C., Collingridge, G., al., et, Flood, D., Coleman, P., Gotz, J., Chen, F., Barmettler, R., Nitsch, R., Gotz, J., Chen, F., Dorpe, J. van, Nitsch, R., Gouras, G., Tsai, J., Naslund, J., Vincent, B., Edgar, M., Checler, F., Greenfield, J., Haroutunian, V., Buxbaum, J., Xu, H., al., et, Grundke-Iqbal, I., Iqbal, K., George, L., Tung, Y., Kim, K., Wisniewski, H., Guo, Q., Fu, W., Sopher, B., Miller, M., Ware, C., Martin, G., Mattson, M., Gyure, K., Durham, R., Stewart, W., Smialek, J., Troncoso, J., Hardy, J., Selkoe, D., Higuchi, M., Ishihara, T., Zhang, B., Hong, M., Andreadis, A., Trojanowski, J., Lee, V., Hsia, A., Masliah, E., McConlogue, L., Yu, G., Tatsuno, G., Hu, K., Kholodenko, D., Malenka, R., Nicoll, R., Mucke, L., Kamenetz, F., Tomita, T., Hsieh, H., Seabrook, G., Borchelt, D., Iwatsubo, T., Sisodia, S., Malinow, R., Kaye, R., Head, E., Thompson, J., McIntire, T., Milton, S., Cotman, C., Glabe, C., Kuo, Y., Beach, T., Sue, L., Scott, S., Layne, K., Kokjohn, T., Kalback, W., Luehrs, D., Vishnivetskaya, T., Abramowski, D., al., et, LaFerla, F., LaFerla, F., Tinkle, B., Bieberich, C., Haudenschild, C., Jay, G., LaFerla, F., Troncoso, J., Strickland, D., Kawas, C., Jay, G., Leissring, M., Akbari, Y., Fanger, C., Cahalan, M., Mattson, M., LaFerla, F., Lewis, J., McGowan, E., Rockwood, J., Melrose, H., Nacharaju, P., Slegtenhorst, M. Van, Gwinn-Hardy, K., Murphy, M. P., Baker, M., Yu, X., al., et, Lewis, J., Dickson, D., Lin, W., Chisholm, L., Corral, A., Jones, G., Yen, S., Sahara, N., Skipper, L., Yager, D., al., et, Li, Q., Maynard, C., Cappai, R., McLean, C., Cherny, R., Lynch, T., Culvenor, J., Trevisan, J., Tanner, J., Bailey, K., al., et, Masliah, E., Mallory, M., Alford, M., DeTeresa, R., Hansen, L., McKeel, D., Morris, J., Mendell, J., Sahenk, Z., Gales, T., Paul, L., Mesulam, M., Mesulam, M., Moechars, D., Dewachter, I., Lorent, K., Reverse, D., Baekelandt, V., Naidu, A., Tesseur, I., Spittaels, K., Haute, C., Checler, F., al., et, Parent, A., Linden, D., Sisodia, S., Borchelt, D., Scheff, S., Scott, S., DeKosky, S., Schwab, C., McGeer, P., Selkoe, D., Selkoe, D., Sugarman, M., Yamasaki, T., Oddo, S., Echevoyen, J., Murphy, M., Golde, T., Jannatipour, M., Leissring, M., LaFerla, F., Suzuki, N., Cheung, T., Cai, X., Odaka, A., Otvos, L., Eckman, C., Golde, T., Younkin, S., Sze, C., Troncoso, J., Kawas, C., Mouton, P., Price, D., Martin, L., Takahashi, R., Milner, T., Li, F., Nam, E., Edgar, M., Yamaguchi, H., Beal, M., Xu, H., Greengard, P., Gouras, G., Terry, R., Masliah, E., Salmon, D., Butters, N., DeTeresa, R., Hill, R., Hansen, L., Katzman, R., Thomson, A., Walsh, D., Klyubin, I., Fadeeva, J., Cullen, W., Anwyl, R., Wolfe, M., Rowan, M., Selkoe, D., Wirths, O., Multhaup, G., Czech, C., Blanchard, V., Moussaoui, S., Tremp, G., Pradier, L., Beyreuther, K., Bayer, T., Wong, P., Cai, H., Borchelt, D., Price, D., Zhang, Y., McLaughlin, R., Goodyer, C., LeBlanc, A., Zucker, R. and Regehr, W. (2003) 'Triple-transgenic model of Alzheimer's disease with plaques and tangles: intracellular Abeta and synaptic dysfunction.', *Neuron*, 39(3), pp. 409–21. doi: 10.1016/S0896-6273(03)00434-3.

Olofsdotter, K., Lindvall, O. and Asztély, F. (2000) 'Increased synaptic inhibition in dentate gyrus of mice with reduced levels of endogenous brain-derived neurotrophic factor', *Neuroscience*, 101(3), pp. 531–539. doi: 10.1016/S0306-4522(00)00428-0.

Olson, L. E., Roper, R. J., Baxter, L. L., Carlson, E. J., Epstein, C. J. and Reeves, R. H. (2004) 'Down syndrome mouse models Ts65Dn, Ts1Cje, and Ms1Cje/Ts65Dn exhibit variable

severity of cerebellar phenotypes.’, *Developmental Dynamics: an official publication of the American Association of Anatomists*, 230(3), pp. 581–9. doi: 10.1002/dvdy.20079.

Olson, L. E., Roper, R. J., Sengstaken, C. L., Peterson, E. A., Aquino, V., Galdzicki, Z., Siarey, R., Pletnikov, M., Moran, T. H. and Reeves, R. H. (2007) ‘Trisomy for the Down syndrome “critical region” is necessary but not sufficient for brain phenotypes of trisomic mice’, *Human Molecular Genetics*, 16(7), pp. 774–782. doi: 10.1093/hmg/ddm022.

Otmakhov, N., Tao-Cheng, J.-H., Carpenter, S., Asrican, B., Dosemeci, A., Reese, T. S. and Lisman, J. (2004) ‘Persistent accumulation of calcium/calmodulin-dependent protein kinase II in dendritic spines after induction of NMDA receptor-dependent chemical long-term potentiation.’, *The Journal of Neuroscience*, 24(42), pp. 9324–31. doi: 10.1523/JNEUROSCI.2350-04.2004.

Owens, J. R., Harris, F., Walker, S., McAllister, E. and West, L. (1983) ‘The incidence of Down’s syndrome over a 19-year period with special reference to maternal age.’, *Journal of Medical Genetics*, 20(2), pp. 90–3.

Pakkenberg, B., Pelvig, D., Marner, L., Bundgaard, M. J., Gundersen, H. J. G., Nyengaard, J. R. and Regeur, L. (2003) ‘Aging and the human neocortex’, in *Experimental Gerontology*, pp. 95–99. doi: 10.1016/S0531-5565(02)00151-1.

Palop, J. J., Chin, J., Roberson, E. D., Wang, J., Thwin, M. T., Bien-Ly, N., Yoo, J., Ho, K. O., Yu, G.-Q. Q., Kreitzer, A., Finkbeiner, S., Noebels, J. L. and Mucke, L. (2007) ‘Aberrant Excitatory Neuronal Activity and Compensatory Remodeling of Inhibitory Hippocampal Circuits in Mouse Models of Alzheimer’s Disease’, *Neuron*, 55(5), pp. 697–711. doi: 10.1016/j.neuron.2007.07.025.

Palop, J. J., Jones, B., Kekoni, L., Chin, J., Yu, G.-Q., Raber, J., Masliah, E. and Mucke, L. (2003) ‘Neuronal depletion of calcium-dependent proteins in the dentate gyrus is tightly linked to Alzheimer’s disease-related cognitive deficits.’, *Proceedings of the National Academy of Sciences of the United States of America*, 100(16), pp. 9572–7. doi: 10.1073/pnas.1133381100.

Palop, J. J. and Mucke, L. (2009) ‘Epilepsy and Cognitive Impairments in Alzheimer Disease’, *Archives of Neurology*, 66(4), pp. 435–440.

Pang, P. T. and Lu, B. (2004) ‘Regulation of late-phase LTP and long-term memory in normal and aging hippocampus: role of secreted proteins tPA and BDNF’, *Ageing Research Reviews*, 3(4), pp. 407–430. doi: 10.1016/j.arr.2004.07.002.

Park, J., Song, W.-J., Chung, K. C., Kwang, A. and Chung, C. (2009) ‘Function and regulation of Dyrk1A: towards understanding Down syndrome’, *Cellular and Molecular Life Sciences*. SP Birkhäuser Verlag Basel, 66(20), pp. 3235–3240. doi: 10.1007/s00018-009-0123-2.

- Pelleri, M. C., Cicchini, E., Locatelli, C., Vitale, L., Caracausi, M., Piovesan, A., Rocca, A., Poletti, G., Seri, M., Strippoli, P. and Cocchi, G. (2016) 'Systematic reanalysis of partial trisomy 21 cases with or without Down syndrome suggests a small region on 21q22.13 as critical to the phenotype', *Human Molecular Genetics*. doi: 10.1093/hmg/ddw116.
- Pennington, B. F., Moon, J., Edgin, J., Stedron, J. and Nadel, L. (2013) 'The neuropsychology of Down syndrome: evidence for hippocampal dysfunction.', *Child Development*, 74(1), pp. 75–93.
- Pereira, P. L., Magnol, L., Sahún, I., Brault, V., Duchon, A., Prandini, P., Gruart, A., Bizot, J.-C., Chadeaux-Vekemans, B., Deutsch, S., Trovero, F., Delgado-García, J. M., Antonarakis, S. E., Dierssen, M. and Herault, Y. (2009) 'A new mouse model for the trisomy of the *Abcg1-U2af1* region reveals the complexity of the combinatorial genetic code of down syndrome.', *Human Molecular Genetics*, 18(24), pp. 4756–69. doi: 10.1093/hmg/ddp438.
- Perez, Y., Chapman, C. A., Woodhall, G., Robitaille, R. and Lacaille, J.-C. (1999) 'Differential induction of long-lasting potentiation of inhibitory postsynaptic potentials by theta patterned stimulation versus 100-Hz tetanization in hippocampal pyramidal cells in vitro', *Neuroscience*, 90(3), pp. 747–757. doi: 10.1016/S0306-4522(98)00531-4.
- Petralia, R. S. and Petralia, R. S. (2012) 'Distribution of Extrasynaptic NMDA Receptors on Neurons', *The Scientific World Journal*, 2012, pp. 1–11. doi: 10.1100/2012/267120.
- Pinter, J. D., Brown, W. E., Eliez, S., Schmitt, J. E., Capone, G. T. and Reiss, A. L. (2001) 'Amygdala and hippocampal volumes in children with Down syndrome : A high-resolution MRI study', *Neurology*, 56(May 2001), pp. 972–974. doi: 10.1212/WNL.56.7.972.
- de Pittà, M., Volman, V., Berry, H. and Ben-Jacob, E. (2011) 'A tale of two stories: Astrocyte regulation of synaptic depression and facilitation', *PLoS Computational Biology*, 7(12), p. e1002293. doi: 10.1371/journal.pcbi.1002293.
- Pogribna, M., Melnyk, S., Pogribny, I., Chango, A., Yi, P. and James, S. J. (2001) 'Homocysteine metabolism in children with Down syndrome: in vitro modulation.', *American Journal of Human Genetics*, 69(1), pp. 88–95. doi: 10.1086/321262.
- Politoff A.L., Stadter, R.P., Monson, N., Hass. P., (1996) 'Cognition-Related EEG Abnormalities in Nondemented Down Syndrome Subjects', *Dement Geriatr Cogn Disord*, 7, pp69–75
- Pöschel, B. and Manahan-Vaughan, D. (2007) 'Persistent (>24h) long-term depression in the dentate gyrus of freely moving rats is not dependent on activation of NMDA receptors, L-type voltage-gated calcium channels or protein synthesis', *Neuropharmacology*, 52(1), pp. 46–54. doi: 10.1016/j.neuropharm.2006.07.019.

- Pöschel, B., Wroblewska, B., Heinemann, U. and Manahan-Vaughan, D. (2005) 'The metabotropic glutamate receptor mGluR3 is critically required for hippocampal long-term depression and modulates long-term potentiation in the dentate gyrus of freely moving rats.', *Cerebral Cortex*, 15(9), pp. 1414–23. doi: 10.1093/cercor/bhi022.
- Prandini, P., Deutsch, S., Lyle, R., Gagnebin, M., Delucinge Vivier, C., Delorenzi, M., Gehrig, C., Descombes, P., Sherman, S., Dagna Bricarelli, F., Baldo, C., Novelli, A., Dallapiccola, B. and Antonarakis, S. E. (2007) 'Natural gene-expression variation in Down syndrome modulates the outcome of gene-dosage imbalance.', *American Journal of Human Genetics*, 81(2), pp. 252–63. doi: 10.1086/519248.
- Prasher, V. P., Farrer, M. J., Kessling, a M., Fisher, E. M., West, R. J., Barber, P. C. and Butler, a C. (1998) 'Molecular mapping of Alzheimer-type dementia in Down's syndrome.', *Annals of neurology*, 43(3), pp. 380–3. doi: 10.1002/ana.410430316.
- Pucharcós, C., Fuentes, J. J., Casas, C., de la Luna, S., Alcántara, S., Arbonés, M. L., Soriano, E., Estivill, X. and Pritchard, M. (1999) 'Alu-splice cloning of human Intersectin (ITSN), a putative multivalent binding protein expressed in proliferating and differentiating neurons and overexpressed in Down syndrome.', *European Journal of Human Genetics*, 7(6), pp. 704–12. doi: 10.1038/sj.ejhg.5200356.
- Pueschel, S. M., Louis, S. and McKnight, P. (1991) 'Seizure disorders in Down syndrome.', *Archives of Neurology*, 48(3), pp. 318–320. doi: 10.1001/archneur.1991.00530150088024.
- Rachidi, M., Delezoide, A.-L. L., Delabar, J.-M. M. and Lopes, C. (2009) 'A quantitative assessment of gene expression (QAGE) reveals differential overexpression of DOPEY2, a candidate gene for mental retardation, in Down syndrome brain regions', *International Journal of Developmental Neuroscience*, 27(4), pp. 393–8. doi: 10.1016/j.ijdevneu.2009.02.001.
- Rachidi, M., Lopes, C., Charron, G., Delezoide, A.-L., Paly, E., Bloch, B. and Delabar, J.-M. (2005) 'Spatial and temporal localization during embryonic and fetal human development of the transcription factor SIM2 in brain regions altered in Down syndrome.', *International Journal of Developmental Neuroscience*, 23(5), pp. 475–84. doi: 10.1016/j.ijdevneu.2005.05.004.
- Rachidi, M., Lopes, C., Costantine, M. and Delabar, J.-M. M. (2005) 'C21orf5, a new member of Dopey family involved in morphogenesis, could participate in neurological alterations and mental retardation in Down syndrome', *DNA Research*, 12(3), pp. 203–210. doi: 10.1093/dnares/dsi004.
- Rahmani, Z., Blouin, J., CREAU-GOLDBERGt, N., WATKINSt, P. C., Ois Mattei, J., Poissonnier, M., Prieurii, M., CHETrouH, Z., Nicole, A., Aurias, A., Sinet, P. and Delabar, J. (1989) 'Critical role of the D21S55 region on chromosome 21 in the pathogenesis of Down syndrome', *Medical Sciences*, 86, pp. 5958–5. doi: 10.1073/pnas.86.15.5958.

- Ram, G. and Chinen, J. (2011) 'Infections and immunodeficiency in Down syndrome.', *Clinical and Experimental Immunology*, 164(1), pp. 9–16. doi: 10.1111/j.1365-2249.2011.04335.x.
- Raser, J. M. and O'Shea, E. K. (2005) 'Noise in gene expression: origins, consequences, and control.', *Science*, 309(5743), pp. 2010–2013. doi: 10.1126/science.1105891.
- Rayner, G., Jackson, G. D. and Wilson, S. J. (2016) 'Mechanisms of memory impairment in epilepsy depend on age at disease onset.', *Neurology*. doi: 10.1212/WNL.0000000000003231.
- Reeves, R. H., Irving, N. G., Moran, T. H. H., Wohn, A., Kitt, C., Sisodia, S. S., Schmidt, C., Bronson, R. T. and Davisson, M. M. T. (1995) 'A mouse model for Down syndrome exhibits learning and behaviour', *Nature Genetics*, 11(2), pp. 177–184. doi: 10.1038/ng0595-111.
- Regehr, W. G. (2012) 'Short-term presynaptic plasticity', *Cold Spring Harbor Perspectives in Biology*, 4(7), pp. 1–19. doi: 10.1101/cshperspect.a005702.
- Reid, I. C. and Stewart, C. A. (1997) 'Seizures, memory and synaptic plasticity', *Seizure*, 6(5), pp. 351–359. doi: 10.1016/S1059-1311(97)80034-9.
- Renner, M., Lacor, P. N., Velasco, P. T., Xu, J., Contractor, A., Klein, W. L. and Triller, A. (2010) 'Deleterious Effects of Amyloid β Oligomers Acting as an Extracellular Scaffold for mGluR5', *Neuron*, 66(5), pp. 739–754. doi: 10.1016/j.neuron.2010.04.029.
- Resta, R. G. (2005) 'Changing demographics of Advanced Maternal Age (AMA) and the impact on the predicted incidence of down syndrome in the United States: Implications for prenatal screening and genetic counseling', *American Journal of Medical Genetics*, 133 A(1), pp. 31–36. doi: 10.1002/ajmg.a.30553.
- Reisel, D., Bannerman, D.M., Schmitt, W.B., Deacon, R.M., Flint, J., Borchardt, T., Seeburg, P.H. and Rawlins, J.N.P., (2002) 'Spatial memory dissociations in mice lacking GluR1', *Nature neuroscience*, 5(9), pp.868-873
- Roberson, E. D., Scarce-Lavie, K., Palop, J. J., Yan, F., Cheng, I. H., Wu, T., Gerstein, H., Yu, G.-Q. and Mucke, L. (2007) 'Reducing endogenous tau ameliorates amyloid beta-induced deficits in an Alzheimer's disease mouse model.', *Science*. American Association for the Advancement of Science, 316(5825), pp. 750–4. doi: 10.1126/science.1141736.
- Roberts, J. E., Price, J. and Malkin, C. (2007) 'Language and communication development in Down syndrome', *Mental Retardation and Developmental Disabilities Research Reviews*, pp. 26–35. doi: 10.1002/mrdd.20136.
- Roberts, L. V. and Richmond, J. L. (2015) 'Preschoolers with Down syndrome do not yet show the learning and memory impairments seen in adults with Down syndrome', *Developmental Science*, 18(3), pp. 404–419. doi: 10.1111/desc.12225.

Roder, J. K., Roder, J. C. and Gerlai, R. (1996) 'Conspecific exploration in the T-maze: Abnormalities in S100 β transgenic mice', *Physiology and Behavior*, 60(1), pp. 31–36. doi: 10.1016/0031-9384(95)02247-3.

Rodrigues, S. M., Schafe, G. E. and Ledoux, J. E. (2004) 'Molecular mechanisms underlying emotional learning and memory in the lateral amygdala', *Neuron*, pp. 75–91. doi: 10.1016/j.neuron.2004.09.014.

Rogaeva, E., Meng, Y., Lee, J. H., Gu, Y., Kawarai, T., Zou, F., Katayama, T., Baldwin, C. T., Cheng, R., Hasegawa, H., Chen, F., Shibata, N., Lunetta, K. L., Pardossi-Piquard, R., Bohm, C., Wakutani, Y., Cupples, L. A., Cuenco, K. T., Green, R. C., Pinessi, L., Rainero, I., Sorbi, S., Bruni, A., Duara, R., Friedland, R. P., Inzelberg, R., Hampe, W., Bujo, H., Song, Y.-Q., Andersen, O. M., Willnow, T. E., Graff-Radford, N., Petersen, R. C., Dickson, D., Der, S. D., Fraser, P. E., Schmitt-Ulms, G., Younkin, S., Mayeux, R., Farrer, L. A. and St George-Hyslop, P. (2007) 'The neuronal sortilin-related receptor SORL1 is genetically associated with Alzheimer disease.', *Nature Genetics*, 39(2), pp. 168–77. doi: 10.1038/ng1943.

Rogawski, M. A., Gryder, D., Castaneda, D., Yonekawa, W., Banks, M. K. and Lia, H. (2003) 'GluR5 kainate receptors, seizures, and the amygdala.', *Annals of the New York Academy of Sciences*, 985, pp. 150–62.

Roper, R. J. and Reeves, R. H. (2006) 'Understanding the basis for Down syndrome phenotypes.', *PLoS Genetics*, 2(3), p. e50. doi: 10.1371/journal.pgen.0020050.

Rovelet-Lecrux, A., Frebourg, T., Tuominen, H., Majamaa, K., Campion, D. and Remes, A. M. (2007) 'APP locus duplication in a Finnish family with dementia and intracerebral haemorrhage', *Journal of Neurology, Neurosurgery & Psychiatry*, 78(10), pp. 1158–1159. doi: 10.1136/jnnp.2006.113514.

Rueda, N., Flórez, J. and Martínez-Cué, C. (2013) 'Apoptosis in Down's syndrome: lessons from studies of human and mouse models.', *Apoptosis : an international journal on programmed cell death*, 18(2), pp. 121–34. doi: 10.1007/s10495-012-0785-3.

Ryoo, S. R., Hey, K. J., Radnaabazar, C., Yoo, J. J., Cho, H. J., Lee, H. W., Kim, I. S., Cheon, Y. H., Young, S. A., Chung, S. H. and Song, W. J. (2007) 'DYRK1A-mediated hyperphosphorylation of Tau: A functional link between down syndrome and Alzheimer disease', *Journal of Biological Chemistry*, 282(48), pp. 34850–34857. doi: 10.1074/jbc.M707358200.

Saganich, M. J., Schroeder, B. E., Galvan, V., Bredesen, D. E., Koo, E. H. and Heinemann, S. F. (2006) 'Deficits in synaptic transmission and learning in amyloid precursor protein (APP) transgenic mice require C-terminal cleavage of APP.', *The Journal of Neuroscience*, 26(52), pp. 13428–13436. doi: 10.1523/JNEUROSCI.4180-06.2006.

Sago, H., Carlson, E. J., Smith, D. J., Kilbridge, J., Rubin, E. M., Mobley, W. C., Epstein, C. J. and Huang, T. T. (1998) 'Ts1Cje, a partial trisomy 16 mouse model for Down

syndrome, exhibits learning and behavioral abnormalities.’, *Proceedings of the National Academy of Sciences of the United States of America*, 95(11), pp. 6256–6261. doi: 10.1073/pnas.95.11.6256.

Sago, H., Carlson, E. J., Smith, D. J., Rubin, E. M., Crnic, L. S., Huang, T. T. and Epstein, C. J. (2000) ‘Genetic dissection of region associated with behavioral abnormalities in mouse models for Down syndrome.’, *Pediatric Research*, 48(5), pp. 606–13. doi: 10.1203/00006450-200011000-00009.

Saito, T., Matsuba, Y., Mihira, N., Takano, J., Nilsson, P., Itohara, S., Iwata, N. and Saido, T. C. (2014) ‘Single App knock-in mouse models of Alzheimer’s disease’, *Nature Neuroscience*, 17(5), pp. 661–663. doi: 10.1038/nn.3697.

Santaguida, S. and Amon, A. (2015) ‘Short- and long-term effects of chromosome mis-segregation and aneuploidy’, *Nature Reviews Molecular Cell Biology*, 16(August), pp. 473–485. doi: 10.1038/nrm4025.

Sasaki, A., Yamaguchi, H., Ogawa, A., Sugihara, S. and Nakazato, Y. (1997) ‘Microglial activation in early stages of amyloid- β protein deposition’, *Acta Neuropathologica*, 94(4), pp. 316–322. doi: 10.1007/s004010050713.

Sathe, K., Maetzler, W., Lang, J. D., Mounsey, R. B., Fleckenstein, C., Martin, H. L., Schulte, C., Mustafa, S., Synofzik, M., Vukovic, Z., Itohara, S., Berg, D. and Teismann, P. (2012) ‘S100B is increased in Parkinson’s disease and ablation protects against MPTP-induced toxicity through the RAGE and TNF- α pathway.’, *Brain*, 135(Pt 11), pp. 3336–47. doi: 10.1093/brain/aws250.

Scharfman, H. E. (2002) ‘Epilepsy as an example of neural plasticity.’, *The Neuroscientist: a review journal bringing neurobiology, neurology and psychiatry*. NIH Public Access, 8(2), pp. 154–73.

Schmitz, C., Rutten, B. P. F., Pielen, A., Schäfer, S., Wirths, O., Tremp, G., Czech, C., Blanchard, V., Multhaup, G., Rezaie, P., Korr, H., Steinbusch, H. W. M., Pradier, L. and Bayer, T. A. (2004) ‘Hippocampal neuron loss exceeds amyloid plaque load in a transgenic mouse model of Alzheimer’s disease.’, *The American Journal of Pathology*, 164(4), pp. 1495–502. doi: 10.1016/S0002-9440(10)63235-X.

Schubert, M., Siegmund, H., Pape, H. C. and Albrecht, D. (2005) ‘Kindling-induced changes in plasticity of the rat amygdala and hippocampus’, *Learning & Memory*, 12(1072–0502 (Print)), pp. 520–526. doi: 10.1101/lm.4205.

Scott-McKean, J. J. and Costa, A. C. S. (2011) ‘Exaggerated NMDA mediated LTD in a mouse model of Down syndrome and pharmacological rescuing by memantine.’, *Learning & Memory*, 18(12), pp. 774–8. doi: 10.1101/lm.024182.111.

Seidl, R., Cairns, N., Singewald, N., Kaehler, S. T. and Lubec, G. (2001) ‘Differences between GABA levels in Alzheimer’s disease and Down syndrome with Alzheimer-like

neuropathology', *Naunyn-Schmiedeberg's Archives of Pharmacology*, 363(2), pp. 139–145. doi: 10.1007/s002100000346.

Selkoe, D. J., Morris, J. C., Petersen, R. C., Lewis, J., Davies, P., Maloney, A. J., Whitehouse, P. J., Small, D. H., Mok, S. S., Bornstein, J. C., Davies, C. A., Mann, D. M., Sumpter, P. Q., Yates, P. O., Terry, R. D., Dickson, D. W., Sze, C. I., Masliah, E., Hsia, A. Y., Mucke, L., Naslund, J., Kuo, Y.-M., McLean, C. A., Lue, L. F., Bookheimer, S. Y., Reiman, E. M., Polvikoski, T., Selkoe, D. J., Chen, G., Larson, J., Lynch, G., Games, D., Seubert, P., Moechars, D., Chapman, P. F., Fitzjohn, S. M., Johnson-Wood, K., Gravina, S. A., Walsh, D., Lambert, M. P., Hartley, D., Stephan, A., Laroche, S., Davis, S., Dewachter, I. and Dodart, J. C. (2002) 'Alzheimer's disease is a synaptic failure.', *Science*, 298(5594), pp. 789–91. doi: 10.1126/science.1074069.

Sgobio, C., Ghiglieri, V., Costa, C., Bagetta, V., Siliquini, S., Barone, I., Di Filippo, M., Gardoni, F., Gundelfinger, E. D., Di Luca, M., Picconi, B. and Calabresi, P. (2010) 'Hippocampal Synaptic Plasticity, Memory, and Epilepsy: Effects of Long-Term Valproic Acid Treatment', *Biological Psychiatry*, 67(6), pp. 567–574. doi: 10.1016/j.biopsych.2009.11.008.

Shankar, G. M., Li, S., Mehta, T. H., Garcia-Munoz, A., Shepardson, N. E., Smith, I., Brett, F. M., Farrell, M. A., Rowan, M. J., Lemere, C. A., Regan, C. M., Walsh, D. M., Sabatini, B. L. and Selkoe, D. J. (2008) 'Amyloid-beta protein dimers isolated directly from Alzheimer's brains impair synaptic plasticity and memory.', *Nature Medicine*, 14(8), pp. 837–42. doi: 10.1038/nm1782.

Shi, J., Zhang, T., Zhou, C., Chohan, M. O., Gu, X., Wegiel, J., Zhou, J., Hwang, Y. W., Iqbal, K., Grundke-Iqbal, I., Gong, C. X. and Liu, F. (2008) 'Increased dosage of Dyrk1A alters alternative splicing factor (ASF)-regulated alternative splicing of tau in down syndrome', *Journal of Biological Chemistry*, 283(42), pp. 28660–28669. doi: 10.1074/jbc.M802645200.

Shi, S.-H. H., Hayashi, Y., Esteban, J. A. and Malinow, R. (2001) 'Subunit-specific rules governing AMPA receptor trafficking to synapses in hippocampal pyramidal neurons', *Cell*, 105(3), pp. 331–343. doi: 10.1016/S0092-8674(01)00321-X.

Shipton, O. A., Leitz, J. R., Dworzak, J., Acton, C. E. J., Tunbridge, E. M., Denk, F., Dawson, H. N., Vitek, M. P., Wade-Martins, R., Paulsen, O. and Vargas-Caballero, M. (2011) 'Tau Protein Is Required for Amyloid β -Induced Impairment of Hippocampal Long-Term Potentiation', *The Journal of Neuroscience*, 31(5), pp. 1688–1692. doi: 10.1523/JNEUROSCI.2610-10.2011.

Siarey, R. J., Carlson, E. J., Epstein, C. J., Balbo, A., Rapoport, S. I. and Galdzicki, Z. (1999) 'Increased synaptic depression in the Ts65Dn mouse, a model for mental retardation in Down syndrome', *Neuropharmacology*, 38(12), pp. 1917–1920. doi: 10.1016/S0028-3908(99)00083-0.

Siarey, R. J., Stoll, J., Rapoport, S. I. and Galdzicki, Z. (1997) 'Altered long-term potentiation in the young and old Ts65Dn mouse, a model for Down Syndrome',

Neuropharmacology, 36(11-12), pp. 1549-1554. doi: 10.1016/S0028-3908(97)00157-3.

Siarey, R. J., Villar, A. J., Epstein, C. J. and Galdzicki, Z. (2005) 'Abnormal synaptic plasticity in the Ts1Cje segmental trisomy 16 mouse model of Down syndrome.', *Neuropharmacology*, 49(1), pp. 122-8. doi: 10.1016/j.neuropharm.2005.02.012.

De Simone, R., Daquin, G. and Genton, P. (2006) 'Senile myoclonic epilepsy in Down syndrome: A video and EEG presentation of two cases', *Epileptic Disorders*, 8(3), pp. 223-227.

De Simone, R., Puig, X. S., Gélisse, P., Crespel, A. and Genton, P. (2010) 'Senile myoclonic epilepsy: delineation of a common condition associated with Alzheimer's disease in Down syndrome.', *Seizure*, 19(7), pp. 383-9. doi: 10.1016/j.seizure.2010.04.008.

Sinet, P. M., Théophile, D., Rahmani, Z., Chettouh, Z., Blouin, J. L., Prieur, M., Noel, B. and Delabar, J. M. (1994) 'Mapping of the down syndrome phenotype on chromosome 21 at the molecular level', *Biomedicine and Pharmacotherapy*, 48(5-6), pp. 247-252. doi: 10.1016/0753-3322(94)90140-6.

Skotko, B. G., Levine, S. P. and Goldstein, R. (2011) 'Self-perceptions from people with Down syndrome', *American Journal of Medical Genetics, Part A*, 155(10), pp. 2360-2369. doi: 10.1002/ajmg.a.34235.

Slegers, K., Brouwers, N., Gijssels, I., Theuns, J., Goossens, D., Wauters, J., Del-Favero, J., Cruts, M., Duijn, C. M. van and Broeckhoven, C. Van (2006) 'APP duplication is sufficient to cause early onset Alzheimer's dementia with cerebral amyloid angiopathy', *Brain*, 129(11), pp. 2977-2983.

Slegers, K. and van Duijn, C. M. (2001) 'Alzheimer's Disease: Genes, Pathogenesis and Risk Prediction', *Community Genetics*, 4(4), pp. 197-203. doi: 10.1159/000064193.

Sleigh, J., Harvey, M., Voss, L. and Denny, B. (2014) 'Ketamine - more mechanisms of action than just NMDA blockade', *Trends in Anaesthesia and Critical Care*, pp. 76-81. doi: 10.1016/j.tacc.2014.03.002.

Śmigielska-Kuzia, J., Boćkowski, L., Sobaniec, W., Kułak, W. and Sendrowski, K. (2010) 'Amino acid metabolic processes in the temporal lobes assessed by proton magnetic resonance spectroscopy (1H MRS) in children with Down syndrome', *Pharmacological Reports*, 62(6), pp. 1070-1077.

Smith, G. K., Kesner, R. P. and Korenberg, J. R. (2014) 'Dentate gyrus mediates cognitive function in the Ts65Dn/DnJ mouse model of down syndrome', *Hippocampus. NIH Public Access*, 24(3), pp. 354-362. doi: 10.1002/hipo.22229.

Snyder, E. M., Nong, Y., Almeida, C. G., Paul, S., Moran, T., Choi, E. Y., Nairn, A. C., Salter, M. W., Lombroso, P. J., Gouras, G. K. and Greengard, P. (2005) 'Regulation of NMDA

receptor trafficking by amyloid-beta.', *Nature neuroscience*. Nature Publishing Group, 8(8), pp. 1051–8. doi: 10.1038/nn1503.

So, E. L. (2010) 'Interictal epileptiform discharges in persons without a history of seizures: what do they mean?', *Journal of clinical neurophysiology : official publication of the American Electroencephalographic Society*, 27(4), pp. 229–238. doi: 10.1097/WNP.0b013e3181ea42a4.

Souchet, B., Guedj, F., Penke-Verdier, Z., Daubigney, F., Duchon, A., Herault, Y., Bizot, J.-C., Janel, N., Créau, N., Delatour, B. and Delabar, J. M. (2015) 'Pharmacological correction of excitation/inhibition imbalance in Down syndrome mouse models', *Frontiers in Behavioral Neuroscience*, 9(October), p. 267. doi: 10.3389/fnbeh.2015.00267.

Souchet, B., Guedj, F., Sahún, I., Duchon, A., Daubigney, F., Badel, A., Yanagawa, Y., Barallobre, M. J., Dierssen, M., Yu, E., Herault, Y., Arbones, M., Janel, N., Créau, N. and Delabar, J. M. (2014) 'Excitation/inhibition balance and learning are modified by Dyrk1a gene dosage', *Neurobiology of Disease*, 69, pp. 65–75. doi: 10.1016/j.nbd.2014.04.016.

Stasko, M. R. and Costa, A. C. S. (2004) 'Experimental parameters affecting the Morris water maze performance of a mouse model of Down syndrome', *Behavioural Brain Research*, 154(1), pp. 1–17. doi: 10.1016/j.bbr.2004.01.012.

Stäubli, U., Scafidi, J. and Chun, D. (1999) 'GABAB receptor antagonism: facilitatory effects on memory parallel those on LTP induced by TBS but not HFS.', *The Journal of neuroscience : the official journal of the Society for Neuroscience*, 19(11), pp. 4609–15.

Steinbach, J. P., Müller, U., Leist, M., Li, Z. W., Nicotera, P. and Aguzzi, A. (1998) 'Hypersensitivity to seizures in beta-amyloid precursor protein deficient mice.', *Cell Death and Differentiation*, 5(10), pp. 858–66. doi: 10.1038/sj.cdd.4400391.

Stover, K. R., Campbell, M. A., Van Winssen, C. M. and Brown, R. E. (2015) 'Early detection of cognitive deficits in the 3xTg-AD mouse model of Alzheimer's disease.', *Behavioural brain research*, 289, pp. 29–38. doi: 10.1016/j.bbr.2015.04.012.

De Strooper, B. (2014) 'Lessons from a failed γ -secretase Alzheimer trial', *Cell*, pp. 721–726. doi: 10.1016/j.cell.2014.10.016.

Strydom, A., Shooshtari, S., Lee, L., Raykar, V., Torr, J., Tsiouris, J., Jokinen, N., Courtenay, K., Bass, N., Sinnema, M. and Maaskant, M. (2010) 'Dementia in older adults with intellectual disabilities - epidemiology, presentation, and diagnosis', *Journal of Policy and Practice in Intellectual Disabilities*, pp. 96–110. doi: 10.1111/j.1741-1130.2010.00253.x.

Suárez, L. M., Cid, E., Gal, B., Inostroza, M., Brotons-Mas, J. R., Gómez-Domínguez, D., de la Prida, L. M. and Solís, J. M. (2012) 'Systemic Injection of Kainic Acid Differently

Affects LTP Magnitude Depending on its Epileptogenic Efficiency', *PLoS One*, 7(10), p. e48128. doi: 10.1371/journal.pone.0048128.

Suetsugu, M. and Mehraein, P. (1980) 'Spine distribution along the apical dendrites of the pyramidal neurons in Down's syndrome - A quantitative golgi study', *Acta Neuropathologica*, 50(3), pp. 207–210. doi: 10.1007/BF00688755.

Sumarsono, S. H., Wilson, T. J., Tymms, M. J., Venter, D. J., Corrick, C. M., Kola, R., Lahoud, M. H., Papas, T. S., Seth, A. and Kola, I. (1996) 'Down's syndrome-like skeletal abnormalities in Ets2 transgenic mice.', *Nature*, 379(6565), pp. 534–7. doi: 10.1038/379534a0.

Tarawneh, R. and Holtzman, D. M. (2012) 'The clinical problem of symptomatic Alzheimer disease and mild cognitive impairment', *Cold Spring Harbor Perspectives in Medicine*, 2(5). doi: 10.1101/cshperspect.a006148.

Terry, R., Masliah, E., Salmon, D., Butters, N., DeTeresa, R., Hill, R., Hansen, L. and Katzman, R. (1991) 'Physical basis of cognitive alterations in Alzheimer's disease: synapse loss is the major correlate of cognitive impairment.', *Annals of Neurology*, 30(4), pp. 572–580. doi: 10.1002/ana.410300410.

Texidó, L., Martín-Satué, M., Alberdi, E., Solsona, C. and Matute, C. (2011) 'Amyloid β peptide oligomers directly activate NMDA receptors', *Cell Calcium*, 49(3), pp. 184–190. doi: 10.1016/j.ceca.2011.02.001.

Ting, J. T., Daigle, T. L., Chen, Q. and Feng, G. (2014) 'Acute brain slice methods for adult and aging animals: application of targeted patch clamp analysis and optogenetics.', *Methods in Molecular Biology*, 1183, pp. 221–42. doi: 10.1007/978-1-4939-1096-0_14.

Tomic, J. L., Pensalfini, A., Head, E. and Glabe, C. G. (2009) 'Soluble fibrillar oligomer levels are elevated in Alzheimer's disease brain and correlate with cognitive dysfunction', *Neurobiology of Disease*, 35(3), pp. 352–358. doi: 10.1016/j.nbd.2009.05.024.

Townsend, M., Shankar, G. M., Mehta, T., Walsh, D. M. and Selkoe, D. J. (2006) 'Effects of secreted oligomers of amyloid beta-protein on hippocampal synaptic plasticity: a potent role for trimers.', *The Journal of Physiology*, 572(Pt 2), pp. 477–92. doi: 10.1113/jphysiol.2005.103754.

Trazzi, S., Mitrugno, V. M., Valli, E., Fuchs, C., Rizzi, S., Guidi, S., Perini, G., Bartesaghi, R. and Ciani, E. (2011) 'APP-dependent up-regulation of Ptch1 underlies proliferation impairment of neural precursors in Down syndrome', *Human Molecular Genetics*, 20(8), pp. 1560–1573. doi: 10.1093/hmg/ddr033.

Troca-Marín, J. A., Alves-Sampaio, A. and Montesinos, M. L. (2011) 'An increase in basal BDNF provokes hyperactivation of the Akt-mammalian target of rapamycin pathway and deregulation of local dendritic translation in a mouse model of Down's

syndrome.’, *The Journal of Neuroscience*, 31(26), pp. 9445–55. doi: 10.1523/JNEUROSCI.0011-11.2011.

Truett, G. E., Heeger, P., Mynatt, R. L., Truett, A. A., Walker, J. A. and Warman, M. L. (2000) ‘Preparation of PCR-quality mouse genomic DNA with hot sodium hydroxide and tris (HotSHOT).’, *BioTechniques*, 29(1), pp. 52, 54.

Vicari, S., Bellucci, S. and Carlesimo, G. A. (2000) ‘Implicit and explicit memory: A functional dissociation in persons with Down syndrome’, *Neuropsychologia*, 38(3), pp. 240–251. doi: 10.1016/S0028-3932(99)00081-0.

Voronov, S. V., Frere, S. G., Giovedi, S., Pollina, E. A., Borel, C., Zhang, H., Schmidt, C., Akeson, E. C., Wenk, M. R., Cimasoni, L., Arancio, O., Davisson, M. T., Antonarakis, S. E., Gardiner, K., De Camilli, P. and Di Paolo, G. (2008) ‘Synaptojanin 1-linked phosphoinositide dyshomeostasis and cognitive deficits in mouse models of Down’s syndrome.’, *Proceedings of the National Academy of Sciences of the United States of America*, 105(27), pp. 9415–20. doi: 10.1073/pnas.0803756105.

Vossel, K. A., Tartaglia, M. C., Nygaard, H. B., Zeman, A. Z., Miller, B. L., (2017) ‘Epileptic activity in Alzheimer’s disease: causes and clinical relevance’, *The Lancet Neurology*, 16(4), pp. 311–322. doi: 10.1016/S1474-4422(17)30044-3

Wang, H. W., Pasternak, J. F., Kuo, H., Ristic, H., Lambert, M. P., Chromy, B., Viola, K. L., Klein, W. L., Stine, W. B., Krafft, G. A. and Trommer, B. L. (2002) ‘Soluble oligomers of β amyloid (1-42) inhibit long-term potentiation but not long-term depression in rat dentate gyrus’, *Brain Research*, 924(2), pp. 133–140. doi: 10.1016/S0006-8993(01)03058-X.

Wang, H. Y., Lee, D. H., Davis, C. B. and Shank, R. P. (2000) ‘Amyloid peptide A β (1-42) binds selectively and with picomolar affinity to α 7 nicotinic acetylcholine receptors.’, *Journal of Neurochemistry*, 75(3), pp. 1155–61.

Wang, P. P. and Bellugi, U. (1994) ‘Evidence from two genetic syndromes for a dissociation between verbal and visual-spatial short-term memory’, *Journal of Clinical and Experimental Neuropsychology*, 16(2), pp. 317–322. doi: 10.1080/01688639408402641.

Wang, X., Huang, T., Zhao, Y., Zheng, Q., Thompson, R. C., Bu, G., Zhang, Y., Hong, W. and Xu, H. (2014) ‘Sorting nexin 27 regulates A β production through modulating γ -secretase activity.’, *Cell Reports*, 9(3), pp. 1023–33. doi: 10.1016/j.celrep.2014.09.037.

Wang, X., Zhao, Y., Zhang, X., Badie, H., Zhou, Y., Mu, Y., Loo, L. S., Cai, L., Thompson, R. C., Yang, B., Chen, Y., Johnson, P. F., Wu, C., Bu, G., Mobley, W. C., Zhang, D., Gage, F. H., Ranscht, B., Zhang, Y., Lipton, S. a, Hong, W. and Xu, H. (2013) ‘Loss of sorting nexin 27 contributes to excitatory synaptic dysfunction by modulating glutamate receptor recycling in Down’s syndrome.’, *Nature Medicine*, 19(4), pp. 473–80. doi: 10.1038/nm.3117.

- Wang, Y., Wang, Y., Zhang, H., Gao, Y., Huang, C., Zhou, A., Zhou, Y. and Li, Y. (2016) 'Sequential posttranslational modifications regulate PKC degradation.', *Molecular Biology of the Cell*, 27(2), pp. 410–20. doi: 10.1091/mbc.E15-09-0624.
- Wang, Z.X., Tan, L., Liu, K. and Yu, J.T. (2016) 'The Essential Role of Soluble A β Oligomers in Alzheimer's Disease.', *Molecular Neurobiology*, 53(3) pp. 1905–24. doi: 10.1007/s12035-015-9143-0
- Weitzdoerfer, R., Dierssen, M., Fountoulakis, M. and Lubec, G. (2001) 'Fetal life in Down syndrome starts with normal neuronal density but impaired dendritic spines and synaptosomal structure.', *Journal of Neural Transmission. Supplementum*, (61), pp. 59–70.
- Westmark, C. J., Westmark, P. R. and Malter, J. S. (2010) 'Alzheimer's disease and Down syndrome rodent models exhibit audiogenic seizures.', *Journal of Alzheimer's Disease*, 20(4), pp. 1009–13. doi: 10.3233/JAD-2010-100087.
- White, N. S., Alkire, M. T. and Haier, R. J. (2003) 'A voxel-based morphometric study of nondemented adults with Down Syndrome', *NeuroImage*, 20(1), pp. 393–403. doi: 10.1016/S1053-8119(03)00273-8.
- Whittle, N., Sartori, S. B., Dierssen, M., Lubec, G. and Singewald, N. (2007) 'Fetal Down syndrome brains exhibit aberrant levels of neurotransmitters critical for normal brain development.', *Pediatrics*, 120(6), pp. e1465-71. doi: 10.1542/peds.2006-3448.
- Winocur, G., Roder, J. and Lobaugh, N. (2001) 'Learning and memory in S100-beta transgenic mice: an analysis of impaired and preserved function.', *Neurobiology of Learning and Memory*, 75(2), pp. 230–43. doi: 10.1006/nlme.2000.3961.
- Wirrell, E. C. (2010) 'Prognostic significance of interictal epileptiform discharges in newly diagnosed seizure disorders.', *Journal of Clinical Neurophysiology*, 27(4), pp. 239–48. doi: 10.1097/WNP.0b013e3181ea4288.
- Wiseman, F. K., Al-Janabi, T., Hardy, J., Karmiloff-Smith, A., Nizetic, D., Tybulewicz, V. L. J., Fisher, E. M. C. and Strydom, A. (2015) 'A genetic cause of Alzheimer disease: mechanistic insights from Down syndrome.', *Nature Reviews. Neuroscience*, 16(9), pp. 564–74. doi: 10.1038/nrn3983.
- Wisniewski, K. E., Dalton, A. J., Mclachlan, D. R. C., Wen, G. Y. and Wisniewski, H. M. (1985) 'Alzheimer's disease in Down's syndrome: Clinicopathologic studies', *Neurology*, 35(7), pp. 957–961. doi: 10.1212/WNL.35.7.957.
- Witton, J., Padmashri, R., Zinyuk, L. E., Popov, V. I., Kraev, I., Line, S. J., Jensen, T. P., Tedoldi, A., Cummings, D. M., Tybulewicz, V. L. J., Fisher, E. M. C., Bannerman, D. M., Randall, A. D., Brown, J. T., Edwards, F. A., Rusakov, D. A., Stewart, M. G. and Jones, M. W. (2015) 'Hippocampal circuit dysfunction in the Tc1 mouse model of Down syndrome', *Nature Neuroscience*, 18(9), pp. 1291–1298. doi: 10.1038/nn.4072.

- Wolfer, D. P. and Lipp, H. P. (2000) 'Dissecting the behaviour of transgenic mice: is it the mutation, the genetic background, or the environment?', *Experimental Physiology*, 85(6), pp. 627–34. doi: 10.1111/j.1469-445X.2000.02095.x.
- Wolvetang, E. J., Wilson, T. J., Sanij, E., Busciglio, J., Hatzistavrou, T., Seth, A., Hertzog, P. J. and Kola, I. (2003) 'ETS2 overexpression in transgenic models and in Down syndrome predisposes to apoptosis via the p53 pathway', *Human Molecular Genetics*, pp. 247–255. doi: 10.1093/hmg/ddg015.
- Wood, A. J. J., Campagna, J. A., Miller, K. W. and Forman, S. A. (2003) 'Mechanisms of Actions of Inhaled Anesthetics', *New England Journal of Medicine*, 348(21), pp. 2110–2124. doi: 10.1056/NEJMra021261.
- Wright, A. L., Zinn, R., Hohensinn, B., Konen, L. M., Beynon, S. B., Tan, R. P., Clark, I. a., Abdipranoto, A. and Vissel, B. (2013) 'Neuroinflammation and Neuronal Loss Precede A β Plaque Deposition in the hAPP-J20 Mouse Model of Alzheimer's Disease', *PLoS One*, 8(4), p. e59586. doi: 10.1371/journal.pone.0059586.
- Xiao, Q., Gil, S. C., Yan, P., Wang, Y., Han, S., Gonzales, E., Perez, R., Cirrito, J. R. and Lee, J. M. (2012) 'Role of Phosphatidylinositol Clathrin Assembly Lymphoid-Myeloid Leukemia (PICALM) in intracellular Amyloid Precursor Protein (APP) processing and amyloid plaque pathogenesis', *Journal of Biological Chemistry*, 287(25), pp. 21279–21289. doi: 10.1074/jbc.M111.338376.
- Xie, L., Helmerhorst, E., Taddei, K., Plewright, B., Van Bronswijk, W. and Martins, R. (2002) 'Alzheimer's beta-amyloid peptides compete for insulin binding to the insulin receptor.', *The Journal of Neuroscience*, 22(10), p. RC221. doi: 20026383.
- Xu, J. and Wu, L. G. (2005) 'The decrease in the presynaptic calcium current is a major cause of short-term depression at a calyx-type synapse', *Neuron*, 46(4), pp. 633–645. doi: 10.1016/j.neuron.2005.03.024.
- Xu, Z., Chen, R.Q., Gu, Q.H., Yan, J.Z., Wang, S.H., Liu, S.Y., and Lu, W. (2009) 'Metaplastic regulation of long-term potentiation/long-term depression threshold by activity-dependent changes of NR2A/NR2B ratio', *The Journal of Neuroscience*, Jul 8;29(27):8764-73. doi: 10.1523/JNEUROSCI.1014-09.2009.
- Yaar, M., Zhai, S., Pilch, P. F., Doyle, S. M., Eisenhauer, P. B., Fine, R. E. and Gilchrist, B. A. (1997) 'Binding of beta-amyloid to the p75 neurotrophin receptor induces apoptosis. A possible mechanism for Alzheimer's disease.', *The Journal of Clinical Investigation*, 100(9), pp. 2333–40. doi: 10.1172/JCI119772.
- Yamakawa, K. (2012) 'Towards the understanding of Down syndrome using mouse models', *Congenital Anomalies*, 52(2), pp. 67–71. doi: 10.1111/j.1741-4520.2012.00367.x.
- Yang, D. S., Stavrides, P., Mohan, P. S., Kaushik, S., Kumar, A., Ohno, M., Schmidt, S. D., Wesson, D., Bandyopadhyay, U., Jiang, Y., Pawlik, M., Peterhoff, C. M., Yang, A. J., Wilson,

D. A., St George-Hyslop, P., Westaway, D., Mathews, P. M., Levy, E., Cuervo, A. M. and Nixon, R. A. (2011) 'Reversal of autophagy dysfunction in the TgCRND8 mouse model of Alzheimer's disease ameliorates amyloid pathologies and memory deficits', *Brain*, 134(1), pp. 258–277. doi: 10.1093/brain/awq341.

Yu, T., Li, Z., Jia, Z., Clapcote, S. J., Liu, C., Li, S., Asrar, S., Pao, A., Chen, R., Fan, N., Carattini-Rivera, S., Bechard, A. R., Spring, S., Henkelman, R. M., Stoica, G., Matsui, S.-I. I., Nowak, N. J., Roder, J. C., Chen, C., Bradley, A. and Yu, Y. E. (2010) 'A mouse model of Down syndrome trisomic for all human chromosome 21 syntenic regions', *Human Molecular Genetics*, 19(14), pp. 2780–2791. doi: 10.1093/hmg/ddq179.

Yu, T., Liu, C., Belichenko, P., Clapcote, S. J., Li, S., Pao, A., Kleschevnikov, A., Bechard, A. R., Asrar, S., Chen, R., Fan, N., Zhou, Z., Jia, Z., Chen, C., Roder, J. C., Liu, B., Baldini, A., Mobley, W. C. and Yu, Y. E. (2010) 'Effects of individual segmental trisomies of human chromosome 21 syntenic regions on hippocampal long-term potentiation and cognitive behaviors in mice.', *Brain Research*, 1366, pp. 162–71. doi: 10.1016/j.brainres.2010.09.107.

Zhang, L., Kirschstein, T., Sommersberg, B., Merkens, M., Manahan-Vaughan, D., Elgersma, Y. and Beck, H. (2005) 'Hippocampal synaptic metaplasticity requires inhibitory autophosphorylation of Ca²⁺/calmodulin-dependent kinase II.', *The Journal of Neuroscience*, 25(33), pp. 7697–707. doi: 10.1523/JNEUROSCI.2086-05.2005.

Zhang, L., Meng, K., Jiang, X., Liu, C., Pao, A., Belichenko, P. V., Kleschevnikov, A. M., Josselyn, S., Liang, P., Ye, P., Mobley, W. C. and Yu, Y. E. (2014) 'Human chromosome 21 orthologous region on mouse chromosome 17 is a major determinant of down syndrome-related developmental cognitive deficits', *Human Molecular Genetics*, 23(3), pp. 578–589. doi: 10.1093/hmg/ddt446.

Zhao, W.-Q. and Alkon, D. L. (2001) 'Role of insulin and insulin receptor in learning and memory', *Molecular and Cellular Endocrinology*, 177(1–2), pp. 125–134. doi: 10.1016/S0303-7207(01)00455-5.

Zhao, W.-Q., De Felice, F. G., Fernandez, S., Chen, H., Lambert, M. P., Quon, M. J., Krafft, G. A., Klein, W. L., Felice, F. G. De, Fernandez, S., Chen, H., Lambert, M. P., Quon, M. J., Krafft, G. A. and Klein, W. L. (2008) 'Amyloid beta oligomers induce impairment of neuronal insulin receptors', *The FASEB Journal*, 22(1), pp. 246–260.

Zhao, W. Q., Santini, F., Breese, R., Ross, D., Zhang, X. D., Stone, D. J., Ferrer, M., Townsend, M., Wolfe, A. L., Seager, M. A., Kinney, G. G., Shughrue, P. J. and Ray, W. J. (2010) 'Inhibition of calcineurin-mediated endocytosis and α -amino-3-hydroxy-5-methyl-4-isoxazolepropionic acid (AMPA) receptors prevents amyloid β oligomer-induced synaptic disruption', *Journal of Biological Chemistry*, 285(10), pp. 7619–7632. doi: 10.1074/jbc.M109.057182.

Annex A

```
# Event Classification Processor, ECP16, 07-APR-15
#
# Event Types and Colors: see classifier_types at top.
# Metric Names: see classifier_metrics at top.
# Interval Measure Calculation: see the call to lwdaq_metrics.
# Interval Metric Calculation: see bottom, adjust offset and range of metrics.
# Configuration of Coherence and Rhythm: see threshold values.
# Control of Displays and Diagnostics: see the show and diagnostic parameters.
# Code that Displays Intermittency Measure: one-third down in show_intermittency.
# Code that Displays Minor Peaks and Valleys: half-way down in show_coherence.
# Code that Displays Major Peaks and Valleys: two-thirds down in show_rhythm.
#

# Define event type names and color codes for the Event Classifier.
set config(classifier_types) "Ictal red \
    IctalSpikes purple \
    Hiss blue \
    Spindle orange \
    Artifact green \
    Depression cyan \
    Baseline gray"

# Define metric names for the Event Classifier.
set config(classifier_metrics) "power\
    coastline\
    intermittency\
    coherence\
    asymmetry\
    rhythm"

# Configure the processor diagnostic displays.
set show_intermittency 0
set show_coherence 0
set show_rhythm 0
set show_frequency 0
set note_glitches 0
set metric_diagnostics 0

# The coherence threshold produces the minor peaks and valleys, which we use to
# measure the coherence of the interval, and also to stabilize the rhythm measure.
set coherence_threshold 0.1

# The rhythm threshold produces the major peaks and valleys, which we use to
# measure the rhythm of the interval.
set rhythm_threshold 0.3

# We use the baseline power value for this channel as a scaling factor
# for our power metric calculation. We do not set the baseline power
# in this processor, so we must make sure we set it in the Neuroarchiver's
# calibration window.
upvar #0 Neuroarchiver_info(bp_${info(channel_num)}) baseline_pwr
```

```

# We begin this channel's section of the characteristics line with the
# channel number.
append result "$info(channel_num) "

# If we have too much signal loss, we ignore this interval.
set max_loss 20.0

# We won't be using the fourier transform to calculate metrics, so
# we instruct the Neuroarchiver to calculate the transform only if
# the user wants to plot it in the a-f display.
set config(af_calculate) 0

# The following code, when enabled, plots the coastline progress, derivative
# of coastline, and a list of derivative values sorted into decreasing order
# so as to show on the value versus time plot the fraction of the coastline
# that is generated by the 10% points of greatest derivative. This fraction
# is the area under the first 10% of the sorted derivative plot, divided by
# the total area under the sorted derivative plot.
if {$show_intermittency} {
    set values [lwdaq glitch_filter $config(glitch_threshold) $info(values)]
    set cp [lwdaq coastline_x_progress $values]
    lwdaq_graph $cp $info(vt_image) -y_only 1 -color 9
    set coastline [lindex $cp end]
    set dcp ""
    set max 0.0
    foreach c $cp {
        if {$dcp == ""} {set cc $c}
        append dcp "[expr abs($c - $cc)] "
        set cc $c
    }
    set dcp [lsort -decreasing -real $dcp]
    lwdaq_graph $dcp $info(vt_image) -y_only 1 -y_min 0 -color 5
}

# Coherence peak and valley display. When enabled, peaks are marked with a
# short downward mark at the top of the display, valleys by a short upward
# mark at the bottom of the display.
if {$show_coherence} {
    set values [lwdaq glitch_filter $config(glitch_threshold) $info(values)]
    scan [lwdaq ave_stdev $values] %f%f%f%f%f ave stdev max min mad
    set range [expr $max-$min]
    set max [lindex $values 0]
    set min $max
    set vv $max
    set state "0 "
    set i 0
    set min_i 0
    set max_i 0
    set state "none"
    set maxima "0 1 "
    set minima "0 -1 "
    foreach v $values {
        if {$v>$max} {

```

```

        set max $v
        set max_i $i
    }
    if {$v<$min} {
        set min $v
        set min_i $i
    }
    if {(abs($v-$min)/$range>$coherence_threshold) &&
($state!="min")} {
        append minima "$min_i -1.0 $min_i 0 $min_i -1.0 "
        set max $v
        set max_i $i
        set min $v
        set min_i $i
        set state "min"
    } elseif {(abs($v-$max)/$range>$coherence_threshold) &&
($state!="max")} {
        append maxima "$max_i +1.0 $max_i 0 $max_i +1.0 "
        set max $v
        set max_i $i
        set min $v
        set min_i $i
        set state "max"
    }
    incr i
    set vv $v
}
if {$state=="max"} {
    append minima "$min_i -1.0 $min_i 0 $min_i -1.0 "
}
if {$state=="min"} {
    append maxima "$max_i +1.0 $max_i 0 $max_i +1.0 "
}
append minima "$i -1.0"
append maxima "$i +1.0"
lwdaq_graph $maxima $info(vt_image) -color 9 \
    -y_max 1.0 -y_min -20 \
    -x_min 0.0 -x_max [expr [llength $values]-1]
lwdaq_graph $minima $info(vt_image) -color 9 \
    -y_max 20 -y_min -1.0 \
    -x_min 0.0 -x_max [expr [llength $values]-1]
}

```

Rhythm peak and valley display. When enabled, peaks are marked with a
long downward mark at the top of the display, valleys by a long upward
mark at the bottom of the display.

```

if {$show_rhythm} {
    set values [lwdaq glitch_filter $config(glitch_threshold) $info(values)]
    scan [lwdaq ave_stdev $values] %f%f%f%f%f ave stdev max min mad
    set range [expr $max-$min]
    set max [lindex $values 0]
    set min $max
    set vv $max
    set state "0 "
}

```

```

set i 0
set min_i 0
set max_i 0
set state "none"
set maxima "0 1 "
set minima "0 -1 "
foreach v $values {
    if {$v>$max} {
        set max $v
        set max_i $i
    }
    if {$v<$min} {
        set min $v
        set min_i $i
    }
    if {(abs($v-$min)/$range>$rhythm_threshold) && ($state!="min")} {
        append minima "$min_i -1.0 $min_i +0.9 $min_i -1.0 "
        set max $v
        set max_i $i
        set min $v
        set min_i $i
        set state "min"
    } elseif {(abs($v-$max)/$range>$rhythm_threshold) &&
($state!="max")} {
        append maxima "$max_i +1.0 $max_i -0.9 $max_i +1.0 "
        set max $v
        set max_i $i
        set min $v
        set min_i $i
        set state "max"
    }
    incr i
    set vv $v
}
if {$state=="max"} {
    append minima "$min_i -1.0 $min_i +0.9 $min_i -1.0 "
}
if {$state=="min"} {
    append maxima "$max_i +1.0 $max_i -0.9 $max_i +1.0 "
}
append minima "$i -1.0"
append maxima "$i +1.0"
lwdaq_graph $maxima $info(vt_image) -color 9 \
    -y_max 1.0 -y_min -20 \
    -x_min 0.0 -x_max [expr [llength $values]-1]
lwdaq_graph $minima $info(vt_image) -color 9 \
    -y_max 20 -y_min -1.0 \
    -x_min 0.0 -x_max [expr [llength $values]-1]
}

```

We add a single-letter code that indicates the type of the interval, so
far as this processor can deduce it. We have L for loss, U for unclassified
and N for no event.

```
if {($info(loss)<$max_loss)} {
```

```

        append result "U "
    } else {
        append result "L "
    }

    # We calculate metrics using a library routine. We select which routine with
    # a letter code. After the letter we pass numeric parameters that direct the
    # metric calculation. We check the metric result for errors, and if we find
    # them, we print the error message to the Neuroarchiver text window, and set
    # the metric string to all zeros. So that we can see diagnostic printing from
    # the metric calculator, we direct the lwdaq library to print in the Neuroarchiver
    # text window with the lwdaq_config command.
    if {($info(loss)<$max_loss)} {
        lwdaq_config -text_name $info(text)
        set metrics [lwdaq_metrics $info(values) "C \
            $config(glitch_threshold) \
            $coherence_threshold \
            $rhythm_threshold \
            $metric_diagnostics"]
        if {[LWDAQ_is_error_result $metrics]} {
            Neuroarchiver_print $metrics
            set metrics "0 0 0 0 0 0 0"
        }
    } else {
        set metrics "0 0 0 0 0 0 0"
    }

    # We write our baseline power to the characteristics line. This is the signal
    # amplitude for which the power metric should be 0.5. Note that different metric
    # calculations may use different measures of amplitude, such as standard deviation
    # or mean absolute deviation. Whatever measure the metric calculator uses, when
    # this measure is equal to our power center value, the power metric will be 0.5.
    append result "[format %.1f $baseline_pwr] "

    # Scan the metrics string for the metric values.
    scan $metrics %f%f%f%f%f%f%f%d \
        power coastline intermittency coherence asymmetry rhythm frequency
    glitches

    # Frequency marking. We mark the metric calculation's best guess at the frequency
    # in the amplitude versus frequency display with a vertical black line. The black line
    # starts at the bottom of the display and ascends to a height proportional to the
    # rhythm metric.
    if {$show_frequency} {
        set fHz [expr $frequency/$config(play_interval)]
        set marks "$fHz 0.0 $fHz $rhythm"
        lwdaq_graph $marks $info(af_image) -color 9 \
            -y_min 0.0 -y_max 1.0 \
            -x_min $config(f_min) -x_max $config(f_max)
    }

    # Glitch counting and notification
    set config(glitch_count) [expr $config(glitch_count) + $glitches]
    if {$note_glitches} {

```

```

        if {$glitches>0} {
            Neuroarchiver_print "NOTE: Removed $glitches glitches from
channel $info(channel_num)."
        }
    }

# We calculate the metric values from the various interval measures. The metrics
# are bounded zero to one. We use Neuroclassifier_sigmoidal to transform the
# measures,
# which are all greater than zero, into bounded metric values. We pass to the
# sigmoidal
# routine the value of the measure, a centering value, which is the value of the
# measure
# for which the metric will be one half, and an exponent, which determines how sharp
# the
# sigmoidal function is at the center. The larger the exponent, smaller the range of
# measure
# values about the center that will appear near one half.
lappend result [Neuroclassifier_sigmoidal $power $baseline_pwr 1.0]
lappend result [Neuroclassifier_sigmoidal $coastline 20 2.0]
lappend result [Neuroclassifier_sigmoidal $intermittency 0.4 4.0]
lappend result [Neuroclassifier_sigmoidal $coherence 0.4 3.0]
lappend result [Neuroclassifier_sigmoidal $asymmetry 1.0 2.0]
lappend result [Neuroclassifier_sigmoidal $rhythm 0.4 2.0]
append result " "

```

Annex B

```
append result "$info(channel_num) [format %.2f [expr 100.0 - $info(loss)]] "  
foreach {lo hi} {1 3.99 4 7.99 8 11.99 12 29.99 30 49.99 50 69.99 70  
119.99 120 160} {  
  if {$info(loss) <= 20} {  
    set bp [expr 0.001 * [Neuroarchiver_band_power $lo $hi 0]]  
  } {  
    set bp 0.0  
  }  
  append result "[format %.2f $bp] "  
}
```

```

import matplotlib.pyplot as plt
import numpy as np
import csv
import itertools
import pandas as pd
import numpy.ma as ma
import os

os.chdir('[file path]')

def EEGpower(infile):
    mydata = pd.read_csv(infile, sep=' ', header=None, error_bad_lines=False,
warn_bad_lines=False)
    global powerall
    if len(mydata.columns) == 103:

        df1 = (mydata.iloc[:,2:12])
        df1.columns = ["trans_id", "reception", "1_4Hz", "4_8Hz", "8_12Hz", "12_30Hz",
"30_50Hz", "50_70Hz", "70_120Hz", "120_160Hz"]
        df2 = (mydata.iloc[:,12:22])
        df2.columns = ["trans_id", "reception", "1_4Hz", "4_8Hz", "8_12Hz", "12_30Hz",
"30_50Hz", "50_70Hz", "70_120Hz", "120_160Hz"]
        df3 = (mydata.iloc[:,22:32])
        df3.columns = ["trans_id", "reception", "1_4Hz", "4_8Hz", "8_12Hz", "12_30Hz",
"30_50Hz", "50_70Hz", "70_120Hz", "120_160Hz"]
        df4 = (mydata.iloc[:,32:42])
        df4.columns = ["trans_id", "reception", "1_4Hz", "4_8Hz", "8_12Hz", "12_30Hz",
"30_50Hz", "50_70Hz", "70_120Hz", "120_160Hz"]
        df5 = (mydata.iloc[:,42:52])
        df5.columns = ["trans_id", "reception", "1_4Hz", "4_8Hz", "8_12Hz", "12_30Hz",
"30_50Hz", "50_70Hz", "70_120Hz", "120_160Hz"]
        df6 = (mydata.iloc[:,52:62])
        df6.columns = ["trans_id", "reception", "1_4Hz", "4_8Hz", "8_12Hz", "12_30Hz",
"30_50Hz", "50_70Hz", "70_120Hz", "120_160Hz"]
        df7 = (mydata.iloc[:,62:72])
        df7.columns = ["trans_id", "reception", "1_4Hz", "4_8Hz", "8_12Hz", "12_30Hz",
"30_50Hz", "50_70Hz", "70_120Hz", "120_160Hz"]
        df8 = (mydata.iloc[:,72:82])
        df8.columns = ["trans_id", "reception", "1_4Hz", "4_8Hz", "8_12Hz", "12_30Hz",
"30_50Hz", "50_70Hz", "70_120Hz", "120_160Hz"]
        df9 = (mydata.iloc[:,82:92])
        df9.columns = ["trans_id", "reception", "1_4Hz", "4_8Hz", "8_12Hz", "12_30Hz",
"30_50Hz", "50_70Hz", "70_120Hz", "120_160Hz"]
        df10 = (mydata.iloc[:,92:102])
        df10.columns = ["trans_id", "reception", "1_4Hz", "4_8Hz", "8_12Hz", "12_30Hz",
"30_50Hz", "50_70Hz", "70_120Hz", "120_160Hz"]
        df10 = (mydata.iloc[:,92:102])
        df10.columns = ["trans_id", "reception", "1_4Hz", "4_8Hz", "8_12Hz", "12_30Hz",
"30_50Hz", "50_70Hz", "70_120Hz", "120_160Hz"]

        alldata = df1.append([df2, df3, df4, df5, df6, df7, df8, df9, df10], ignore_index =
True)

```

```

trans1 = (alldata[alldata.trans_id == 1]).mean(axis=0)
trans2 = (alldata[alldata.trans_id == 2]).mean(axis=0)
trans3 = (alldata[alldata.trans_id == 3]).mean(axis=0)
trans4 = (alldata[alldata.trans_id == 4]).mean(axis=0)
trans5 = (alldata[alldata.trans_id == 5]).mean(axis=0)
trans6 = (alldata[alldata.trans_id == 6]).mean(axis=0)
trans7 = (alldata[alldata.trans_id == 7]).mean(axis=0)
trans8 = (alldata[alldata.trans_id == 8]).mean(axis=0)
trans9 = (alldata[alldata.trans_id == 9]).mean(axis=0)
trans10 = (alldata[alldata.trans_id == 10]).mean(axis=0)
trans11 = (alldata[alldata.trans_id == 11]).mean(axis=0)
trans12 = (alldata[alldata.trans_id == 12]).mean(axis=0)
trans14 = (alldata[alldata.trans_id == 14]).mean(axis=0)

wt = pd.concat([trans2,trans5],axis=1).mean(axis=1)
tc1 = pd.concat([trans4,trans7],axis=1).mean(axis=1)
j20 = pd.concat([trans8,trans12],axis=1).mean(axis=1)
tc1j20 = pd.concat([trans10,trans11],axis=1).mean(axis=1)

powerall = pd.concat([wt, tc1, j20, tc1j20], axis=1)
powerall.columns = ["wt","tc1","j20", "tc1j20",]

elif len(mydata.columns) == 93:

    df1 = (mydata.iloc[:,2:12])
    df1.columns = ["trans_id", "reception", "1_4Hz", "4_8Hz", "8_12Hz", "12_30Hz",
"30_50Hz", "50_70Hz", "70_120Hz", "120_160Hz"]
    df2 = (mydata.iloc[:,12:22])
    df2.columns = ["trans_id", "reception", "1_4Hz", "4_8Hz", "8_12Hz", "12_30Hz",
"30_50Hz", "50_70Hz", "70_120Hz", "120_160Hz"]
    df3 = (mydata.iloc[:,22:32])
    df3.columns = ["trans_id", "reception", "1_4Hz", "4_8Hz", "8_12Hz", "12_30Hz",
"30_50Hz", "50_70Hz", "70_120Hz", "120_160Hz"]
    df4 = (mydata.iloc[:,32:42])
    df4.columns = ["trans_id", "reception", "1_4Hz", "4_8Hz", "8_12Hz", "12_30Hz",
"30_50Hz", "50_70Hz", "70_120Hz", "120_160Hz"]
    df5 = (mydata.iloc[:,42:52])
    df5.columns = ["trans_id", "reception", "1_4Hz", "4_8Hz", "8_12Hz", "12_30Hz",
"30_50Hz", "50_70Hz", "70_120Hz", "120_160Hz"]
    df6 = (mydata.iloc[:,52:62])
    df6.columns = ["trans_id", "reception", "1_4Hz", "4_8Hz", "8_12Hz", "12_30Hz",
"30_50Hz", "50_70Hz", "70_120Hz", "120_160Hz"]
    df7 = (mydata.iloc[:,62:72])
    df7.columns = ["trans_id", "reception", "1_4Hz", "4_8Hz", "8_12Hz", "12_30Hz",
"30_50Hz", "50_70Hz", "70_120Hz", "120_160Hz"]
    df8 = (mydata.iloc[:,72:82])
    df8.columns = ["trans_id", "reception", "1_4Hz", "4_8Hz", "8_12Hz", "12_30Hz",
"30_50Hz", "50_70Hz", "70_120Hz", "120_160Hz"]
    df9 = (mydata.iloc[:,82:92])
    df9.columns = ["trans_id", "reception", "1_4Hz", "4_8Hz", "8_12Hz", "12_30Hz",
"30_50Hz", "50_70Hz", "70_120Hz", "120_160Hz"]

    alldata = df1.append([df2, df3, df4, df5, df6, df7, df8, df9], ignore_index = True)

```

```

trans1 = (alldata[alldata.trans_id == 1]).mean(axis=0)
trans2 = (alldata[alldata.trans_id == 2]).mean(axis=0)
trans3 = (alldata[alldata.trans_id == 3]).mean(axis=0)
trans4 = (alldata[alldata.trans_id == 4]).mean(axis=0)
trans5 = (alldata[alldata.trans_id == 5]).mean(axis=0)
trans6 = (alldata[alldata.trans_id == 6]).mean(axis=0)
trans7 = (alldata[alldata.trans_id == 7]).mean(axis=0)
trans8 = (alldata[alldata.trans_id == 8]).mean(axis=0)
trans9 = (alldata[alldata.trans_id == 9]).mean(axis=0)
trans10 = (alldata[alldata.trans_id == 10]).mean(axis=0)
trans11 = (alldata[alldata.trans_id == 11]).mean(axis=0)
trans12 = (alldata[alldata.trans_id == 12]).mean(axis=0)
trans14 = (alldata[alldata.trans_id == 14]).mean(axis=0)

wt = pd.concat([trans2,trans5],axis=1).mean(axis=1)
tc1 = pd.concat([trans4,trans7],axis=1).mean(axis=1)
j20 = pd.concat([trans8,trans12],axis=1).mean(axis=1)
tc1j20 = pd.concat([trans10,trans11],axis=1).mean(axis=1)

powerall = pd.concat([wt, tc1, j20, tc1j20], axis=1)
powerall.columns = ["wt","tc1","j20", "tc1j20", ]

elif len(mydata.columns) == 83:

    df1 = (mydata.iloc[:,2:12])
    df1.columns = ["trans_id", "reception", "1_4Hz", "4_8Hz", "8_12Hz", "12_30Hz",
"30_50Hz", "50_70Hz", "70_120Hz", "120_160Hz"]
    df2 = (mydata.iloc[:,12:22])
    df2.columns = ["trans_id", "reception", "1_4Hz", "4_8Hz", "8_12Hz", "12_30Hz",
"30_50Hz", "50_70Hz", "70_120Hz", "120_160Hz"]
    df3 = (mydata.iloc[:,22:32])
    df3.columns = ["trans_id", "reception", "1_4Hz", "4_8Hz", "8_12Hz", "12_30Hz",
"30_50Hz", "50_70Hz", "70_120Hz", "120_160Hz"]
    df4 = (mydata.iloc[:,32:42])
    df4.columns = ["trans_id", "reception", "1_4Hz", "4_8Hz", "8_12Hz", "12_30Hz",
"30_50Hz", "50_70Hz", "70_120Hz", "120_160Hz"]
    df5 = (mydata.iloc[:,42:52])
    df5.columns = ["trans_id", "reception", "1_4Hz", "4_8Hz", "8_12Hz", "12_30Hz",
"30_50Hz", "50_70Hz", "70_120Hz", "120_160Hz"]
    df6 = (mydata.iloc[:,52:62])
    df6.columns = ["trans_id", "reception", "1_4Hz", "4_8Hz", "8_12Hz", "12_30Hz",
"30_50Hz", "50_70Hz", "70_120Hz", "120_160Hz"]
    df7 = (mydata.iloc[:,62:72])
    df7.columns = ["trans_id", "reception", "1_4Hz", "4_8Hz", "8_12Hz", "12_30Hz",
"30_50Hz", "50_70Hz", "70_120Hz", "120_160Hz"]
    df8 = (mydata.iloc[:,72:82])
    df8.columns = ["trans_id", "reception", "1_4Hz", "4_8Hz", "8_12Hz", "12_30Hz",
"30_50Hz", "50_70Hz", "70_120Hz", "120_160Hz"]

    alldata = df1.append([df2, df3, df4, df5, df6, df7, df8], ignore_index = True)

    trans1 = (alldata[alldata.trans_id == 1]).mean(axis=0)
    trans2 = (alldata[alldata.trans_id == 2]).mean(axis=0)
    trans3 = (alldata[alldata.trans_id == 3]).mean(axis=0)

```

```

trans4 = (alldata[alldata.trans_id == 4]).mean(axis=0)
trans5 = (alldata[alldata.trans_id == 5]).mean(axis=0)
trans6 = (alldata[alldata.trans_id == 6]).mean(axis=0)
trans7 = (alldata[alldata.trans_id == 7]).mean(axis=0)
trans8 = (alldata[alldata.trans_id == 8]).mean(axis=0)
trans9 = (alldata[alldata.trans_id == 9]).mean(axis=0)
trans10 = (alldata[alldata.trans_id == 10]).mean(axis=0)
trans11 = (alldata[alldata.trans_id == 11]).mean(axis=0)
trans12 = (alldata[alldata.trans_id == 12]).mean(axis=0)
trans14 = (alldata[alldata.trans_id == 14]).mean(axis=0)

wt = pd.concat([trans2,trans5],axis=1).mean(axis=1)
tc1 = pd.concat([trans4,trans7],axis=1).mean(axis=1)
j20 = pd.concat([trans8,trans12],axis=1).mean(axis=1)
tc1j20 = pd.concat([trans10,trans11],axis=1).mean(axis=1)

powerall = pd.concat([wt, tc1, j20, tc1j20], axis=1)
powerall.columns = ["wt","tc1","j20", "tc1j20", ]

elif len(mydata.columns) == 73:

    df1 = (mydata.iloc[:,2:12])
    df1.columns = ["trans_id", "reception", "1_4Hz", "4_8Hz", "8_12Hz", "12_30Hz",
"30_50Hz","50_70Hz", "70_120Hz", "120_160Hz"]
    df2 = (mydata.iloc[:,12:22])
    df2.columns = ["trans_id", "reception", "1_4Hz", "4_8Hz", "8_12Hz", "12_30Hz",
"30_50Hz","50_70Hz", "70_120Hz", "120_160Hz"]
    df3 = (mydata.iloc[:,22:32])
    df3.columns = ["trans_id", "reception", "1_4Hz", "4_8Hz", "8_12Hz", "12_30Hz",
"30_50Hz","50_70Hz", "70_120Hz", "120_160Hz"]
    df4 = (mydata.iloc[:,32:42])
    df4.columns = ["trans_id", "reception", "1_4Hz", "4_8Hz", "8_12Hz", "12_30Hz",
"30_50Hz","50_70Hz", "70_120Hz", "120_160Hz"]
    df5 = (mydata.iloc[:,42:52])
    df5.columns = ["trans_id", "reception", "1_4Hz", "4_8Hz", "8_12Hz", "12_30Hz",
"30_50Hz","50_70Hz", "70_120Hz", "120_160Hz"]
    df6 = (mydata.iloc[:,52:62])
    df6.columns = ["trans_id", "reception", "1_4Hz", "4_8Hz", "8_12Hz", "12_30Hz",
"30_50Hz","50_70Hz", "70_120Hz", "120_160Hz"]
    df7 = (mydata.iloc[:,62:72])
    df7.columns = ["trans_id", "reception", "1_4Hz", "4_8Hz", "8_12Hz", "12_30Hz",
"30_50Hz","50_70Hz", "70_120Hz", "120_160Hz"]

    alldata = df1.append([df2, df3, df4, df5, df6, df7], ignore_index = True)

    trans1 = (alldata[alldata.trans_id == 1]).mean(axis=0)
    trans2 = (alldata[alldata.trans_id == 2]).mean(axis=0)
    trans3 = (alldata[alldata.trans_id == 3]).mean(axis=0)
    trans4 = (alldata[alldata.trans_id == 4]).mean(axis=0)
    trans5 = (alldata[alldata.trans_id == 5]).mean(axis=0)
    trans6 = (alldata[alldata.trans_id == 6]).mean(axis=0)
    trans7 = (alldata[alldata.trans_id == 7]).mean(axis=0)
    trans8 = (alldata[alldata.trans_id == 8]).mean(axis=0)
    trans9 = (alldata[alldata.trans_id == 9]).mean(axis=0)

```

```

trans10 = (alldata[alldata.trans_id == 10]).mean(axis=0)
trans11 = (alldata[alldata.trans_id == 11]).mean(axis=0)
trans12 = (alldata[alldata.trans_id == 12]).mean(axis=0)
trans14 = (alldata[alldata.trans_id == 14]).mean(axis=0)

wt = pd.concat([trans2,trans5],axis=1).mean(axis=1)
tc1 = pd.concat([trans4,trans7],axis=1).mean(axis=1)
j20 = pd.concat([trans8,trans12],axis=1).mean(axis=1)
tc1j20 = pd.concat([trans10,trans11],axis=1).mean(axis=1)

elif len(mydata.columns) == 63:

    df1 = (mydata.iloc[:,2:12])
    df1.columns = ["trans_id", "reception", "1_4Hz", "4_8Hz", "8_12Hz", "12_30Hz",
"30_50Hz", "50_70Hz", "70_120Hz", "120_160Hz"]
    df2 = (mydata.iloc[:,12:22])
    df2.columns = ["trans_id", "reception", "1_4Hz", "4_8Hz", "8_12Hz", "12_30Hz",
"30_50Hz", "50_70Hz", "70_120Hz", "120_160Hz"]
    df3 = (mydata.iloc[:,22:32])
    df3.columns = ["trans_id", "reception", "1_4Hz", "4_8Hz", "8_12Hz", "12_30Hz",
"30_50Hz", "50_70Hz", "70_120Hz", "120_160Hz"]
    df4 = (mydata.iloc[:,32:42])
    df4.columns = ["trans_id", "reception", "1_4Hz", "4_8Hz", "8_12Hz", "12_30Hz",
"30_50Hz", "50_70Hz", "70_120Hz", "120_160Hz"]
    df5 = (mydata.iloc[:,42:52])
    df5.columns = ["trans_id", "reception", "1_4Hz", "4_8Hz", "8_12Hz", "12_30Hz",
"30_50Hz", "50_70Hz", "70_120Hz", "120_160Hz"]
    df6 = (mydata.iloc[:,52:62])
    df6.columns = ["trans_id", "reception", "1_4Hz", "4_8Hz", "8_12Hz", "12_30Hz",
"30_50Hz", "50_70Hz", "70_120Hz", "120_160Hz"]

    alldata = df1.append([df2, df3, df4, df5, df6], ignore_index = True)

    trans1 = (alldata[alldata.trans_id == 1]).mean(axis=0)
    trans2 = (alldata[alldata.trans_id == 2]).mean(axis=0)
    trans3 = (alldata[alldata.trans_id == 3]).mean(axis=0)
    trans4 = (alldata[alldata.trans_id == 4]).mean(axis=0)
    trans5 = (alldata[alldata.trans_id == 5]).mean(axis=0)
    trans6 = (alldata[alldata.trans_id == 6]).mean(axis=0)
    trans7 = (alldata[alldata.trans_id == 7]).mean(axis=0)
    trans8 = (alldata[alldata.trans_id == 8]).mean(axis=0)
    trans9 = (alldata[alldata.trans_id == 9]).mean(axis=0)
    trans10 = (alldata[alldata.trans_id == 10]).mean(axis=0)
    trans11 = (alldata[alldata.trans_id == 11]).mean(axis=0)
    trans12 = (alldata[alldata.trans_id == 12]).mean(axis=0)
    trans14 = (alldata[alldata.trans_id == 14]).mean(axis=0)

    wt = pd.concat([trans2,trans5],axis=1).mean(axis=1)
    tc1 = pd.concat([trans4,trans7],axis=1).mean(axis=1)
    j20 = pd.concat([trans8,trans12],axis=1).mean(axis=1)
    tc1j20 = pd.concat([trans10,trans11],axis=1).mean(axis=1)

    powerall = pd.concat([wt, tc1, j20, tc1j20], axis=1)
    powerall.columns = ["wt", "tc1", "j20", "tc1j20", ]

```

```

elif len(mydata.columns) == 53:

    df1 = (mydata.iloc[:,2:12])
    df1.columns = ["trans_id", "reception", "1_4Hz", "4_8Hz", "8_12Hz", "12_30Hz",
"30_50Hz", "50_70Hz", "70_120Hz", "120_160Hz"]
    df2 = (mydata.iloc[:,12:22])
    df2.columns = ["trans_id", "reception", "1_4Hz", "4_8Hz", "8_12Hz", "12_30Hz",
"30_50Hz", "50_70Hz", "70_120Hz", "120_160Hz"]
    df3 = (mydata.iloc[:,22:32])
    df3.columns = ["trans_id", "reception", "1_4Hz", "4_8Hz", "8_12Hz", "12_30Hz",
"30_50Hz", "50_70Hz", "70_120Hz", "120_160Hz"]
    df4 = (mydata.iloc[:,32:42])
    df4.columns = ["trans_id", "reception", "1_4Hz", "4_8Hz", "8_12Hz", "12_30Hz",
"30_50Hz", "50_70Hz", "70_120Hz", "120_160Hz"]
    df5 = (mydata.iloc[:,42:52])
    df5.columns = ["trans_id", "reception", "1_4Hz", "4_8Hz", "8_12Hz", "12_30Hz",
"30_50Hz", "50_70Hz", "70_120Hz", "120_160Hz"]

    alldata = df1.append([df2, df3, df4, df5], ignore_index = True)

    trans1 = (alldata[alldata.trans_id == 1]).mean(axis=0)
    trans2 = (alldata[alldata.trans_id == 2]).mean(axis=0)
    trans3 = (alldata[alldata.trans_id == 3]).mean(axis=0)
    trans4 = (alldata[alldata.trans_id == 4]).mean(axis=0)
    trans5 = (alldata[alldata.trans_id == 5]).mean(axis=0)
    trans6 = (alldata[alldata.trans_id == 6]).mean(axis=0)
    trans7 = (alldata[alldata.trans_id == 7]).mean(axis=0)
    trans8 = (alldata[alldata.trans_id == 8]).mean(axis=0)
    trans9 = (alldata[alldata.trans_id == 9]).mean(axis=0)
    trans10 = (alldata[alldata.trans_id == 10]).mean(axis=0)
    trans11 = (alldata[alldata.trans_id == 11]).mean(axis=0)
    trans12 = (alldata[alldata.trans_id == 12]).mean(axis=0)
    trans14 = (alldata[alldata.trans_id == 14]).mean(axis=0)

    wt = pd.concat([trans2,trans5],axis=1).mean(axis=1)
    tc1 = pd.concat([trans4,trans7],axis=1).mean(axis=1)
    j20 = pd.concat([trans8,trans12],axis=1).mean(axis=1)
    tc1j20 = pd.concat([trans10,trans11],axis=1).mean(axis=1)

    powerall = pd.concat([wt, tc1, j20, tc1j20], axis=1)
    powerall.columns = ["wt","tc1","j20", "tc1j20", ]

elif len(mydata.columns) == 43:

    df1 = (mydata.iloc[:,2:12])
    df1.columns = ["trans_id", "reception", "1_4Hz", "4_8Hz", "8_12Hz", "12_30Hz",
"30_50Hz", "50_70Hz", "70_120Hz", "120_160Hz"]
    df2 = (mydata.iloc[:,12:22])
    df2.columns = ["trans_id", "reception", "1_4Hz", "4_8Hz", "8_12Hz", "12_30Hz",
"30_50Hz", "50_70Hz", "70_120Hz", "120_160Hz"]
    df3 = (mydata.iloc[:,22:32])
    df3.columns = ["trans_id", "reception", "1_4Hz", "4_8Hz", "8_12Hz", "12_30Hz",
"30_50Hz", "50_70Hz", "70_120Hz", "120_160Hz"]

```

```

df4 = (mydata.iloc[:,32:42])
df4.columns = ["trans_id", "reception", "1_4Hz", "4_8Hz", "8_12Hz", "12_30Hz",
"30_50Hz", "50_70Hz", "70_120Hz", "120_160Hz"]

```

```

alldata = df1.append([df2, df3, df4], ignore_index = True)

```

```

trans1 = (alldata[alldata.trans_id == 1]).mean(axis=0)
trans2 = (alldata[alldata.trans_id == 2]).mean(axis=0)
trans3 = (alldata[alldata.trans_id == 3]).mean(axis=0)
trans4 = (alldata[alldata.trans_id == 4]).mean(axis=0)
trans5 = (alldata[alldata.trans_id == 5]).mean(axis=0)
trans6 = (alldata[alldata.trans_id == 6]).mean(axis=0)
trans7 = (alldata[alldata.trans_id == 7]).mean(axis=0)
trans8 = (alldata[alldata.trans_id == 8]).mean(axis=0)
trans9 = (alldata[alldata.trans_id == 9]).mean(axis=0)
trans10 = (alldata[alldata.trans_id == 10]).mean(axis=0)
trans11 = (alldata[alldata.trans_id == 11]).mean(axis=0)
trans12 = (alldata[alldata.trans_id == 12]).mean(axis=0)
trans14 = (alldata[alldata.trans_id == 14]).mean(axis=0)

```

```

wt = pd.concat([trans2,trans5],axis=1).mean(axis=1)
tc1 = pd.concat([trans4,trans7],axis=1).mean(axis=1)
j20 = pd.concat([trans8,trans12],axis=1).mean(axis=1)
tc1j20 = pd.concat([trans10,trans11],axis=1).mean(axis=1)

```

```

powerall = pd.concat([wt, tc1, j20, tc1j20], axis=1)
powerall.columns = ["wt", "tc1", "j20", "tc1j20", ]

```

```

elif len(mydata.columns) ==33:

```

```

df1 = (mydata.iloc[:,2:12])
df1.columns = ["trans_id", "reception", "1_4Hz", "4_8Hz", "8_12Hz", "12_30Hz",
"30_50Hz", "50_70Hz", "70_120Hz", "120_160Hz"]

```

```

df2 = (mydata.iloc[:,12:22])
df2.columns = ["trans_id", "reception", "1_4Hz", "4_8Hz", "8_12Hz", "12_30Hz",
"30_50Hz", "50_70Hz", "70_120Hz", "120_160Hz"]

```

```

df3 = (mydata.iloc[:,22:32])
df3.columns = ["trans_id", "reception", "1_4Hz", "4_8Hz", "8_12Hz", "12_30Hz",
"30_50Hz", "50_70Hz", "70_120Hz", "120_160Hz"]

```

```

alldata = df1.append([df2, df3], ignore_index = True)

```

```

trans1 = (alldata[alldata.trans_id == 1]).mean(axis=0)
trans2 = (alldata[alldata.trans_id == 2]).mean(axis=0)
trans3 = (alldata[alldata.trans_id == 3]).mean(axis=0)
trans4 = (alldata[alldata.trans_id == 4]).mean(axis=0)
trans5 = (alldata[alldata.trans_id == 5]).mean(axis=0)
trans6 = (alldata[alldata.trans_id == 6]).mean(axis=0)
trans7 = (alldata[alldata.trans_id == 7]).mean(axis=0)
trans8 = (alldata[alldata.trans_id == 8]).mean(axis=0)
trans9 = (alldata[alldata.trans_id == 9]).mean(axis=0)
trans10 = (alldata[alldata.trans_id == 10]).mean(axis=0)
trans11 = (alldata[alldata.trans_id == 11]).mean(axis=0)
trans12 = (alldata[alldata.trans_id == 12]).mean(axis=0)

```

```

trans14 = (alldata[alldata.trans_id == 14]).mean(axis=0)

wt = pd.concat([trans2,trans5],axis=1).mean(axis=1)
tc1 = pd.concat([trans4,trans7],axis=1).mean(axis=1)
j20 = pd.concat([trans8,trans12],axis=1).mean(axis=1)
tc1j20 = pd.concat([trans10,trans11],axis=1).mean(axis=1)

powerall = pd.concat([wt, tc1, j20, tc1j20], axis=1)
powerall.columns = ["wt","tc1","j20", "tc1j20", ]

elif len(mydata.columns) ==23:

    df1 = (mydata.iloc[:,2:12])
    df1.columns = ["trans_id", "reception", "1_4Hz", "4_8Hz", "8_12Hz", "12_30Hz",
"30_50Hz", "50_70Hz", "70_120Hz", "120_160Hz"]
    df2 = (mydata.iloc[:,12:22])
    df2.columns = ["trans_id", "reception", "1_4Hz", "4_8Hz", "8_12Hz", "12_30Hz",
"30_50Hz", "50_70Hz", "70_120Hz", "120_160Hz"]
    alldata = df1.append([df2], ignore_index = True)

    trans1 = (alldata[alldata.trans_id == 1]).mean(axis=0)
    trans2 = (alldata[alldata.trans_id == 2]).mean(axis=0)
    trans3 = (alldata[alldata.trans_id == 3]).mean(axis=0)
    trans4 = (alldata[alldata.trans_id == 4]).mean(axis=0)
    trans5 = (alldata[alldata.trans_id == 5]).mean(axis=0)
    trans6 = (alldata[alldata.trans_id == 6]).mean(axis=0)
    trans7 = (alldata[alldata.trans_id == 7]).mean(axis=0)
    trans8 = (alldata[alldata.trans_id == 8]).mean(axis=0)
    trans9 = (alldata[alldata.trans_id == 9]).mean(axis=0)
    trans10 = (alldata[alldata.trans_id == 10]).mean(axis=0)
    trans11 = (alldata[alldata.trans_id == 11]).mean(axis=0)
    trans12 = (alldata[alldata.trans_id == 12]).mean(axis=0)
    trans14 = (alldata[alldata.trans_id == 14]).mean(axis=0)

    wt = pd.concat([trans2,trans5],axis=1).mean(axis=1)
    tc1 = pd.concat([trans4,trans7],axis=1).mean(axis=1)
    j20 = pd.concat([trans8,trans12],axis=1).mean(axis=1)
    tc1j20 = pd.concat([trans10,trans11],axis=1).mean(axis=1)

    powerall = pd.concat([wt, tc1, j20, tc1j20], axis=1)
    powerall.columns = ["wt","tc1","j20", "tc1j20", ]

elif len(mydata.columns) ==13:

    df1 = (mydata.iloc[:,2:12])
    df1.columns = ["trans_id", "reception", "1_4Hz", "4_8Hz", "8_12Hz", "12_30Hz",
"30_50Hz", "50_70Hz", "70_120Hz", "120_160Hz"]
    alldata = df1

    trans1 = (alldata[alldata.trans_id == 1]).mean(axis=0)
    trans2 = (alldata[alldata.trans_id == 2]).mean(axis=0)
    trans3 = (alldata[alldata.trans_id == 3]).mean(axis=0)
    trans4 = (alldata[alldata.trans_id == 4]).mean(axis=0)
    trans5 = (alldata[alldata.trans_id == 5]).mean(axis=0)

```

```

trans6 = (alldata[alldata.trans_id == 6]).mean(axis=0)
trans7 = (alldata[alldata.trans_id == 7]).mean(axis=0)
trans8 = (alldata[alldata.trans_id == 8]).mean(axis=0)
trans9 = (alldata[alldata.trans_id == 9]).mean(axis=0)
trans10 = (alldata[alldata.trans_id == 10]).mean(axis=0)
trans11 = (alldata[alldata.trans_id == 11]).mean(axis=0)
trans12 = (alldata[alldata.trans_id == 12]).mean(axis=0)
trans14 = (alldata[alldata.trans_id == 14]).mean(axis=0)

wt = pd.concat([trans2,trans5],axis=1).mean(axis=1)
tc1 = pd.concat([trans4,trans7],axis=1).mean(axis=1)
j20 = pd.concat([trans8,trans12],axis=1).mean(axis=1)
tc1j20 = pd.concat([trans10,trans11],axis=1).mean(axis=1)

powerall = pd.concat([wt, tc1, j20, tc1j20], axis=1)
powerall.columns = ["wt","tc1","j20", "tc1j20", ]

else:

    powerall = "error " + str(infile)

return powerall

for infile in os.listdir([file path]):
    powerall = EEGpower(infile)
    path = '[file path]'
    filename = 'analysis2_' + str(infile)
    fullpath = os.path.join(path, filename)
    if isinstance(powerall, pd.DataFrame):
        powerall.to_csv(fullpath, sep=',', encoding='utf-8')
        print ("done " + str(infile))
    else:
        print (powerall)
import csv
import pandas as pd
import os
datetimelist = pd.read_csv("[file path]", sep=',', header=None, )
os.chdir('[file path]')
powerfilepath = '[file path]'
for infile4 in os.listdir(powerfilepath):
    for x in range(510):
        datex = str(datetimelist.iloc[x,0])
        timex = str(datetimelist.iloc[x,1])
        datetimerow = (datetimelist.iloc[x,:])
        datetimekey = (str(datetimerow[2]))
        stringfilename = (str(infile4)).replace(str(powerfilepath),
        "").replace("_powerspectrum.txt", "").replace("analysis2_", "")
        datetimekey = (str(datetimerow[2]))
        dateandtime = str(datex) + "," + str(timex)
        if (datetimekey.find(stringfilename)>=0):
            mydata3 = pd.read_csv(infile4, sep=',')
            mydata4 = (mydata3.iloc[2:10,:])
            mydata4['date'] =(datex, datex, datex, datex, datex, datex, datex, datex)
            mydata4['time'] =(timex, timex, timex, timex, timex, timex, timex, timex)

```

```

        mydata4['file']=(stringfilename, stringfilename, stringfilename, stringfilename,
stringfilename, stringfilename, stringfilename, stringfilename)
        newpath = 'C:\\Users\\anick\\Dropbox\\PhD\\DATA\\EEG\\Power April
2015\\power analysis 2\\datetime'
        newfullpath = os.path.join(newpath, stringfilename)
        mydata4.to_csv(newfullpath, sep=',', encoding='utf-8')
        print (datetimekey,stringfilename,dateandtime)
import csv
import pandas as pd
import os

OutputFilename = '[output file]'
InputPath = '[input file path]'
OutputPath = '[output file path]'
InputPath = os.path.normpath(InputPath)
OutputPath = os.path.normpath(OutputPath)
filename = os.path.join(OutputPath,OutputFilename)
file_out = open(filename, 'w')
print ("Output file opened")
for file in os.listdir(InputPath):
    filename = os.path.join(InputPath,file)
    if os.path.isfile(filename):
        print (" Adding :" + file)
        file_in = open(filename, 'r')
        content = file_in.read()
        file_out.write(content)
file_in.close()
file_out.close()

```